COMPOUND-SPECIFIC CARBON ISOTOPE GEOCHEMISTRY OF POLYCYCLIC AROMATIC HYDROCARBONS IN EASTERN NEWFOUNDLAND ESTUARIES

VINCENT PATRICK O'MALLEY

Compound-Specific Carbon Isotope Geochemistry of Polycyclic Aromatic Hydrocarbons in Eastern Newfoundland Estuaries

by

© Vincent Patrick O'Malley, B.Sc(Hon), M.Sc.

A thesis submitted to the School of Graduate Studies in partial fulfilment of requirements for the degree of Doctor of Philosophy

Department of Earth Science

Memorial University of Newfoundland

1994

St. John's Newfoundland

ISBN 0-315-91646-X

Abstract

Compound-specific carbon isotope analysis (CSIA) was performed on individual polycyclic (or polynuclear) aromatic hydrocarbons (PAH) isolated from a diverse range of environmental samples. These measurements were undertaken to determine whether CSIA could provide additional or complementary information to molecular signatures for quantitatively apportioning inputs of PAH to depositional environments. PAH extraction and purification methods suitable for CSIA were developed, and the isotopic integrity of the $\delta^{13}C$ values of standard PAH taken through these work-up procedures and when exposed to a range of weathering reactions was assessed. The molecular and isotopic signatures of prominent primary and secondary sources of PAH were then characterized and quantitatively compared to the corresponding signatures isolated from St. John's Harbour and Conception Bay sediment samples.

No significant isotopic fractionations were observed in a range of 3, 4 and 5-ring PAH taken through the sample work-up procedures. The $\delta^{13}C$ values of a similar range of standard compounds was also unaffected when exposed to a series of volatilization, photolytic and microbial degradation studies.

The molecular signatures of the prominent primary combustion sources in eastern Newfoundland (fire and car soots) were characterized by the presence of 3, 4 and 5-ring parental PAH, whereas petroleum-related sources including crankcase oil were dominated by 2 and 3-ring parental and methylated PAH. The trend observed in the $\delta^{13}C$ values of the 3, 4 and 5-ring PAH in the two combustion sources was postulated to be jointly controlled by precursor compounds in the original source

material and a series of secondary reactions that occur during pyrolysis and pyrosynthesis (e.g., wood burning and car engine combustion). The significantly $\delta^{13}C$-depleted compounds observed in crankcase oil compared to the combustion sources, particularly phenanthrene and pyrene, was attributed to thermally-induced aromatization reactions of natural compounds in the oil. The aromatization of cyclic precursors (e.g., terpenoids) commonly found in virgin crankcase oil results in the production of some 3 and 4-ring PAH.

Secondary source molecular signatures (road sweeps, untreated sewage and roadside snow) were comparable, and indicated PAH mainly of combustion origin. The application of two component (combustion vs. crankcase oil) mixing calculations using both the $\delta^{13}C$ and the normalized molecular abundances indicated that PAH in the open-road sweeps and snow samples were influenced by approximately 30% inputs of crankcase oil while crankcase oil inputs to sewage were around 20%.

PAH of combustion, petroleum and diagenetic origin were identified from the molecular characterization ofSt. John's Harbour sediments. From the two-component mixing calculations, approximately 70% of the overall input of PAH was identified to be of combustion origin, with vehicle emissions apparently being the dominant input source. Crankcase oil inputs account for the remaining 30% of the PAH in these sediments. However, intersample isotopic and molecular variations indicated a range of combustion contributions ranging from 50% to 90%.

The molecular signatures of Conception Bay sediments were characterized by combustion and diagenetically-derived PAH. The observed $\delta^{13}C$ variations in the 3, 4 and 5-ring compounds also indicated that the PAH were derived from a combination

of at least two primary sources. However, the $\delta^{13}C$-depleted component is quite unlike crankcase oil and PAH contributions from other petroleum-related source or diagenetic origin are suggested as suitable candidates for this unknown component.

CSIA of individual PAH was found to be highly complementary to molecular signatures in elucidating primary source inputs to depositional environments. Additionally, CSIA allows for a more quantitative approach to apportionment using the individual $\delta^{13}C$ alone or in combination with the molecular abundance data and mass-balance models.

Acknowledgments

During the course of a PhD dissertation, one comes in contact with many people who valuably contribute in some way or other to the final completed document. I wish to extend my sincerest thanks and appreciation to the following individuals who contributed enormously to this work.

I will be forever grateful to my supervisor, Dr. Jun Abrajano, who initially introduced me to "Isotope Biogeochemistry" and who kindly allowed me the opportunity to work in his laboratories. More fundamentally, his critical and quantitative approach to science is exemplary and it helped me immensely during the latter stages of my work. I would also like to thank him for providing some financial support, and particularly for his patience and encouragement to complete this study.

This work would not have been possible without the invaluable intervention of Dr. Jocelyne Hellou, who provided both laboratory facilities and access to instrumentation at the Toxicology Section, Department of Fisheries and Oceans (DFO), Newfoundland. Her advice and useful discussions, particularly on compound identification were most informative. I also wish to acknowledge the efforts of Dr. Jerry Payne (DFO) who generously provided some baseline data to help in some of the interpretations and who feels that one should emulate the efforts of Bernard Shaw who produced seven drafts of his initial works before they were finally accepted. My heartfelt thanks go to Linda Fancey, Catherine Upshall, George Sheppard, Howard Hodder and Dr. Emmanuel Gentil for their technical assistance and for accommodating me in their respective laboratories. I also extend a special thanks to the DFO Library staff who patiently tracked down some important reference material

with great efficiency.

I am indebted to Drs. Christopher Pereira (Mines and Energy) and Joe Kicenuik (DFO) who generously shared their boat time on board the CSS Hudson and Karl and Jackie II, respectively. The efforts of Mark Hawryluk (DFO) and Dr. Bill Scott (C-CORE) who provided the sampling devices is also appreciated.

Drs. Eric Barnsley, Tacor Patel and Steven Armstrong (Microbiology, MUN) were most helpful in their discussions in designing and providing the laboratory facilities to undertake the microbial degradation studies. I extend a special thanks to Drs Eric Barnsley (MUN) and Jim Mueller (EPA, Florida) who kindly donated the pure bacterial strains necessary to undertake these studies.

Dr. Paul Eakin (VG Isotech, UK) willingly provided some analyses of preliminary samples and standards during the initial design stage of the work.

Dr. Jeffery Santrock (General Motors, Michigan) provided some invaluable discussion on car engine design and operation.

I would like to extend my gratitude to the School of Graduate Studies and to the Department of Earth Sciences for the financial support and for the cooperation and help provided by the faculty and staff. In particular, the efforts of Dr. Mark Wilson for his extensive professional and social knowledge and for allowing me access to his laboratory facilities. The ever humorous Pat Browne for his efficiency in resolving any administration difficulties encountered. Linda Winsor for her meticulous care and attention in running the GC/C/IRMS facility.

To my thesis committee, Drs. Moire Wadleigh and Robert Helleur for their comprehensive reviews of the work and helpful comments. Also a special thanks to

my examination board Drs. Nathaniel E. Ostrom, Paris Georghiou and Mark Wilson.

The staff at Kingsbridge Motors and Virginia Park Ultramar Service Stations who patiently collected vehicle mufflers with great caution. I am also indebted to the people of St. John's who allowed me access to their domains to collect fire soot samples.

Dr. Jack Lawson for providing office space during the writing stage and for introducing me to a number of his sea-loving mammalian friends. Drs. Anne Mathieu and John Brattey for taking the time to review some earlier sections of this dissertation and to Tilman Bieger, Alan Stark and Gary Thompson for some of the late night or early morning discussions. A special thanks to my running partner, Timothy Fowler who accompanied me on many a taught provoking lunchtime excursion around the lake during the writing stages.

I will be forever grateful for the love and support that I have received from my parents, sister and brothers. Also a special thanks to my friends in Europe, particularly Fr. Patrick Nolan, Thierry Mathieu, Seonad Dason and all the Still family for their support and words of encouragement. Finally, and by no means least Ruth Still for her loving support and conviction in me to complete this dissertation. Her patience, courage and commitment can only be admired and it helped me to maintain a perspective on this work.

Table of Contents

List of Tables

List of Figures

List of Appendices

List of Abbreviations

A = Anthracene

Ace = Acenaphthene

Anthant = Anthanthrene

Ay = Acenaphthylene

BaA = Benz(a)anthracene

BaP = Benzo(a)pyrene

BbF = Benzo(b)fluoranthene

BeP = Benzo(e)pyrene

BFl = Benzofluoranthenes

BkF = Benzo(k)fluoranthene

B(ghi)Fl =Benzo(ghi)fluoranthene

B(ghi)Pery = Benzo(ghi)perylene

Chy = Chrysene

CP(cd)Py = Cyclopenta(cd)pyrene

CSIA = Compound-specific isotope analysis

DBT = Dibenzothiophene

DB(a,h)A = Dibenz(a,h)anthracene

DDBT = Dimethyl dibenzothiophene

DNa = Dimethyl naphthalene

DPa = Dimethyl phenanthrene

F = Fluorene

Fl = Fluoranthene

Fur = Furnace

GC/C/IRMS = Gas chromatograph/combustion/isotope ratio mass spectrometer

GC-FID = Gas chromatography flame ionization detection

GC-MS = Gas chromatography mass spectrometry

Ind = Indeno(123 cd)pyrene

IP = Indeno(1,2,3-cd)pyrene

IS = Internal standard

MDBT = Methyl dibenzothiophene

MFl-Py = Methyl fluoranthene-pyrene

MNa = Methyl naphthalene

MPa = Methylphenanthrene

Na = Naphthalene

Pa = Phenanthrene

PAH = Polycyclic aromatic hydrocarbons

PGS = Power generating station

PNa = Phenyl naphthalene

Pery = Perylene

Py = Pyrene

R = Retene

TDBT = Trimethyl dibenzothiophene

TIC = Total ion chromatogram

TNa = Trimethyl naphthalene

TPA = Trimethyl phenanthrene

UCM = Unresolved complex mixture

1.0 INTRODUCTION

1.1 General statement:

Polycyclic (or polynuclear) aromatic hydrocarbons (PAH) are a group of hydrocarbons containing two or more fused benzene rings (Figure 1; Neff, 1979; McElroy et al., 1985). These compounds are ubiquitous environmental contaminants and many have toxic properties including an association with mutagenesis and carcinogenesis (Cerniglia, 1991). The World Health Organization (WHO) and the U.S. Environmental Protection Agency (USEPA) have recommended sixteen parental (unsubstituted rings) PAH as priority pollutants (Figure 1). Although several sources of PAH have been identified, anthropogenic emissions contribute the greatest proportion of PAH to modern estuarine and coastal environments (Bjorseth and Ramdahl, 1983). PAH can enter such environments as a result of direct discharges from petroleum spills, natural oil seepage and offshore production activities, or indirectly from natural and anthropogenic terrestrial sources. Evaluation of the impact of PAH on coastal and estuarine environments requires the assessment of concentrations, binding and transformations, and recognition of sources (Canton and Grimalt, 1992). Since PAH are hydrophobic and lipophilic, they tend to adsorb to fine particulates and accumulate in sediments. Sediments are recognised to be the largest repository for and potential source of organic contaminants in the marine environment. Thus they offer the potential for evaluating the relative importance of PAH contributions from various sources as a function of space and time.

Source apportionment generally refers to the quantitative assignment of a combination of distinct sources for a particular group of compounds introduced into a

Figure 1. The 16 PAH recommended by the World Health Organisation (WHO) and U.S. Environmental Protection Agency (USEPA) to be listed as priority pollutants. Na = Naphthalene, Ay = Acenaphthylene Ae = Acenaphthene, F = Fluorene, Pa = Phenanthrene, A = Anthracene, Fl = Fluoranthene, Py = Pyrene, BaA = Benz(a)anthracene, Chy = Chrysene, Benzo(k)fluoranthene, BbF = Benzo(b)fluoranthene, BaP = Benzo(a)pyrene, IP = Indeno(1,2,3-cd)pyrene, B(ghi)Pery = Benzo(ghi)perylene and DB(a,h)A = Dibenz(a,h)anthracene. Also included is an example of a methylated compound with a methyl substitution at the 9 carbon position (9-Methylphenanthrene) MPa = Methylphenanthrene.

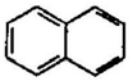

Na (128)

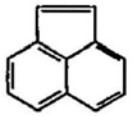

Ay (152)

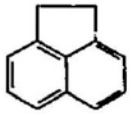

Ae (154)

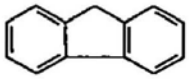

F (166)

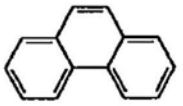

Pa (178)

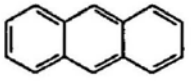

A (178)

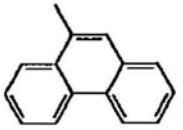

MPa (192)

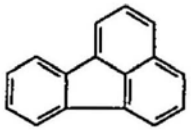

FL (202)

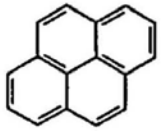

Py (202)

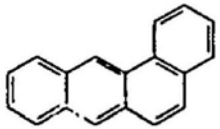

BaA (228)

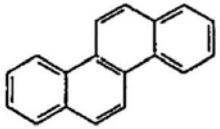

Chy (228)

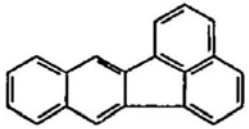

BkF (252)

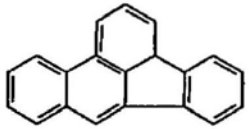

BbF (252)

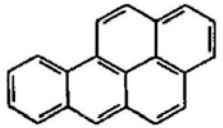

BaP (252)

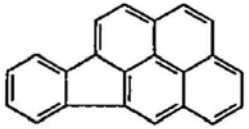

IP (276)

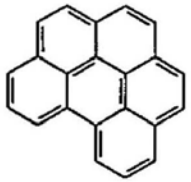

B(ghi)Pery (276)

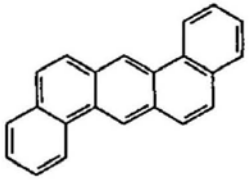

DB(ah)A (278)

system. Presently, source apportionment studies of fluxes and deposition of PAH in coastal and inshore marine sediments rely on PAH distribution patterns as well as on the use of molecular markers characteristic of certain source emissions to distinguish between and among natural and anthropogenic inputs (Dastillung and Albrecht, 1976; Lake et al., 1979; Sporstol et al., 1983; Simoneit, 1986; Kennicutt II et al., 1991; Canton and Grimalt 1992; Brown and Maher, 1992; Steinhauer and Boehm, 1992). Molecular parameters have been used with varying success to constrain specific inputs of PAH to sediments.

PAH can undergo physical, chemical and biological weathering when they are suspended in the atmosphere and water column, and during deposition at the sediment water interface. These transformations, together with the initial non-uniqueness of molecular characteristics for many potential sources, make molecular signatures inadequate for determining specific PAH sources. For example, Wakeham et al. (1980a) isolated very similar concentrations of alkylated and non-alkylated compounds from different sources and Grimmer et al. (1983a) noted that very similar parental PAH profiles were produced during the combustion of different materials. These characteristics make it difficult to perform quantitative apportionment using molecular signatures alone. It is for these reasons that complementary or even alternative source apportionment techniques need to be evaluated. Compound-specific isotope analysis (CSIA) of carbon is one such technique that may provide independent constraints for elucidating inputs of anthropogenic PAH to depositional environments, such as sediments. The measurement of $^{13}C/^{12}C$ ratios in individual compounds is accomplished using a modified conventional stable isotope ratio mass spectrometer following initial separation by gas chromatography and carbon

conversion to CO_2 by combustion. The instrument used to perform such measurements is known as a gas chromatograph/combustion/isotope ratio mass spectrometer (GC/C/IRMS) (Sano et al., 1976; Matthews and Hayes, 1978; Freedman et al., 1988). Apart from the preliminary results we have published (e.g., Abrajano et al., 1993; O'Malley et al., 1994) the measurement of the carbon isotope ratios of individual PAH deposited in modern sediments have not been reported. However, Freeman et al. (1990) demonstrated that the carbon isotope ratio of individual aromatic hydrocarbons can be used to establish the relationship between diagenetically altered hydrocarbons and their source material, while Chung et al. (1992) and Clayton (1992) have reported individual $\delta^{13}C$ values for methylated PAH extracted from a suite of crude oils.

The ability to source apportion PAH deposited in sediments using CSIA requires that: (a) input sources be isotopically distinct to a greater degree than instrument precision and natural variability in the isotopic composition of the source, (b) initial isotopic signatures be preserved during transportation, sedimentation and biodegradation, and (c) suitable procedures of separation and purification of fractions can be developed so that they do not alter the isotopic composition of individual compounds.

The primary aim of the following study is to determine whether CSIA can provide complementary information to existing trace sourcing techniques (molecular signatures) in elucidating prominent source contributions of PAH. St. John's Harbour (high PAH levels) and Conception Bay (low PAH levels), both from eastern Newfoundland, were used as "model" study sites. The elevated PAH concentrations in the Harbour sediments are mainly due to a number of input sources such as sewage and boat traffic as well as

the relatively enclosed configuration of the depositional basin. In contrast, Conception Bay is situated away from notable urban perturbation where PAH inputs are limited to a small number of potential point sources. The following objectives were targeted to accomplish the overall aim of this research:

(1) adopt suitable PAH extraction and purification methods to minimise coelution and background effects that are normally associated with environmental samples.

(2) assess the ability of the adopted extraction and purification procedures to maintain the isotopic integrity of PAH standards.

(3) assess the isotopic stability of standard PAH in *in-vitro* volatilization, photolytic and microbial degradation studies.

(4) define the chemical and isotopic signatures of PAH from potential primary and secondary sources in eastern Newfoundland.

(5) define the chemical and isotopic characteristics of PAH in sediments from St. John's Harbour and Conception Bay, and

(6) quantitatively compare the molecular and isotopic signatures of the sediment PAH to those of the potential sources.

For the purpose of the present study, primary sources refer to the exact origin of PAH while secondary sources correspond to intermediate reservoirs of PAH in the environment. The primary sources of PAH studied were combustion by-products from domestic fireplaces, woodstoves and oil-fired furnaces (#2 fuel oil), vehicle exhaust emissions, crankcase oil and emissions from an oil-fired power generating station (Bunker C fuel oil) close to the Conception Bay site. Secondary sources included road surface

particulates, sewage effluents, snow and atmospheric particulates.

1.2 Physical and chemical properties of PAH:

The stability of PAH prior to deposition in sedimentary environments is influenced by a variety of important removal mechanisms, such as volatilization, sedimentation, chemical oxidation and reduction, photodecomposition and microbial degradation (Cerniglia, 1991). The degree to which a PAH will be affected by these processes is predominantly related to the physical and chemical properties of the individual compounds (Lee et al., 1981; Zander, 1983).

PAH are homocyclic species containing only carbon and hydrogen atoms (Vo-Dinh, 1989) while heterocyclic compounds contain nitrogen, sulphur and oxygen. In contrast to alkylated PAH that are characterized by varying degrees of substitution, parental PAH have no substituents. This study predominantly targets homocyclic species but certain characteristics of the substituted compounds will also be addressed. The PAH of primary environmental concern range from naphthalene, molecular weight (MW) 128 to coronene, MW 300 (Neff, 1979).

The extent to which PAH are altered prior to deposition depends on their physical and chemical properties, which generally vary with molecular weight (Afghan and Chau, 1989). PAH can be divided into kata-annellated and peri-condensed systems. In kata-annellated PAH, the tertiary carbon atoms are centres of two interlinked rings (e.g. anthracene. Figure 1) whereas in peri-condensed PAH some of the tertiary carbon atoms are centres of three interlinked rings (e.g. pyrene Figure 1). The fusion of benzene rings

to produce PAH gives rise to a phenomenon known as annellation (ring fusion) (Clar, 1964) where some rings give up part of their aromaticity to adjacent rings. PAH stability is thus dependent on the number of benzenoid rings within a structure. PAH with shared rings have a greater degree of reactivity than PAH with rings that maintain their benzenoid structure. For example, anthracene with its linear annellated structure has only one benzenoid ring and the mobility of the two pi-electrons is indicated by the direction of the arrow in Figure 2. However, if the ring was arranged angularly as for phenanthrene, the third ring would now contain three double bonds or six pi-electrons which are necessary to form a benzenoid ring (B2). Therefore, phenanthrene molecules are more stable than anthracene molecules. PAH reactivity is also affected by varying bond lengths and bond localization energies around individual rings (Figure 2 and 3). This is highlighted in Figure 2 where the hydrogen of the 9,10 double bond in phenanthrene undergoes an addition reaction with bromine (B3). This increased reactivity of the 9,10 bond in phenanthrene and anthracene and at position 1 of naphthalene can be explained by the electronegativity of these carbons. Structurally, PAH can also be described as "alternant" (six membered ring only) and "nonalternant" (combination of five and six membered rings). Since the first ionization potential (the energy required to remove an electron from the double-occupied highest occupied molecular orbital) is greater for the nonalternant PAH, it is postulated that these compounds will generally be more stable in the natural environment (Zander, 1983).

The solubility of PAH in aqueous environments can have a significant effect on their metabolic transformations and on the quantity deposited in bottom sediments. The

Figure 2. Linear and angular structures of anthracene (A) and phenanthrene (B1). Note the double bond at the 9,10 position of phenanthrene (B2) undergoes an addition reaction with bromine (B3). Circle inside the ring indicates benzenoid structure (Clar, 1964).

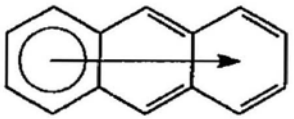

(A)

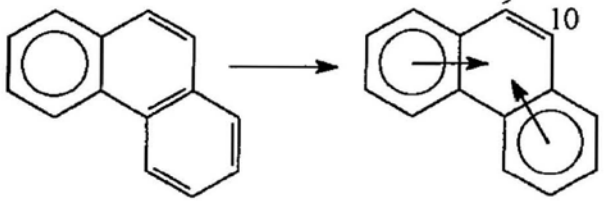

(B1) **(B2)**

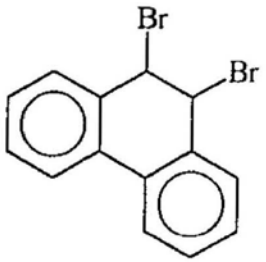

(B3)

Figure 3. Bond localization energies for single sites on the rings of naphthalene, anthracene, phenanthrene and benz(a)Anthracene. Note position 1 on naphthalene and positions 9,10 on phenanthrene (as modified from Zander, 1983).

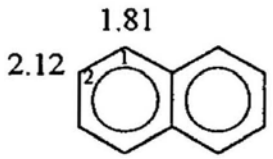

Naphthalene

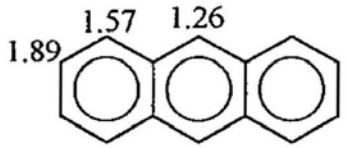

Anthracene

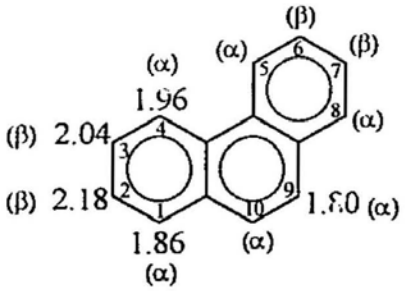

Phenanthrene

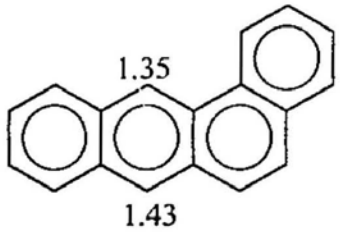

Benz(a)anthracene

high molecular weight and aromaticity of PAH as well as the absence of polar substituents give these compounds their hydrophobic properties. These properties together with their lipophilic characteristics and low vapour pressure explain why PAH exhibit such a strong adsorption affinity for solid surfaces. These compounds thus tend to be associated with suspended particulate matter in both atmospheric and aquatic environments, especially on lipid-rich particle surfaces. PAH have a wide range of solubilities (Table 1) and the solubility trends can be summarized as follows (May et al., 1978; Readman et al., 1982; Means and Wijayaratne, 1982; Whitehouse, 1984):

- water solubility of PAH decreases with increasing molecular weight,
- linear fused PAH such as naphthalene and anthracene are less soluble than angular or pericondensed structures such as phenanthrene and pyrene,
- alkyl substitutions decreases water solubility, and
- solubility increases with increasing temperature.

The vapour pressure of a PAH dictates whether the compound will exist in the particle or gaseous phase. The partitioning between these phases can influence the range of compounds deposited in sediments. PAH tightly bound to the particulate phase are less likely to be altered during transportation (Korfmacher et al., 1980; Baek et al., 1991a; Killops and Massoud, 1992). Temperature increases result in more particle phase PAH in the vapour phase, while temperature decreases result in more vapour phase PAH appearing in the particle phase (Yamasaki et al., 1982; Van Vaeck and Van Cauwenberghe, 1985; Lane 1989). Thus, PAH deposition could theoretically be greater during colder periods.

Table 1. Solubility coefficients of low, high and methylated PAH at 25°C (as modified from Afghan and Chau, 1989).

Compound	Solubility (µg/l)
Fluorene	800.0
Anthracene	59.0
Phenanthrene	435.0
2-Methylanthracene	21.3
9-Methylphenanthrene	261.0
1-methylphenanthrene	269.0
Fluoranthene	260.0
Pyrene	133.0
9,10-Dimethylanthracene	56.0
Benzo(a)fluorene	45.0
Benzo(b)fluorene	29.6
Benzo(a)anthracene	11.0
Chrysene	1.9
Triphenylene	43.0
Benzo[b]fluoranthene	2.4
Benzo[j]fluoranthene	2.4
Benzo[a]pyrene	3.8
Benzo[e]pyrene	2.4
Perylene	2.4
Benzo(ghi)fluoranthene	0.5
Benzo[ghi]perylene	0.3
Coronene	0.1

1.3 Formation and sources:

PAH found in recently deposited sediments are derived from a complex mixture of diverse natural and anthropogenic sources (Table 2) (Youngblood and Blumer, 1975; Laflamme and Hites, 1978; Wakeham et al, 1980ab; Sporstol et al., 1983; Colombo et al., 1989; Kennicutt II et al., 1991; Lipiatou and Saliot, 1991; Canton and Grimalt 1992; Brown and Maher, 1992; Steinhauer and Boehm, 1992). Sedimentary PAH distributions show some common features (Table 3). The dominance of 4 and 5-ring PAH (Fl, Py, BaA, Chy, BeP and BaP), Pa/A ratio between 2 and 6, high Pa/MPa ratio and Fl/Py ratio close to unity are usually associated with high temperature combustion of natural sources (forest fires) and fossil fuels (Youngblood and Blumer, 1975; Laflamme and Hites, 1978; Lake et al, 1979; Barrick and Prahl, 1987; Killops and Howell, 1988). Common characteristics related to petroleum are a series of 2 and 3-ring parental and alkylated compounds (Na, MNa, Pa, and MPa), low Pa/MPa and Fl/Py ratios and an unresolved complex mixture (UCM) (Boehm and Farrington, 1984; Socha and Carpenter, 1987; Kennicutt II et al., 1991; Kennicutt II et al., 1992; Volkman et al., 1992). Individual markers such as perylene and retene, which are thought to be formed by the diagenetic alteration of biogenic compounds are also typical of recently deposited sediments (Wakeham et al, 1980a; Venkatesan, 1988; Lipiatou and Saliot, 1992).

The three main proposed mechanisms responsible for the formation of PAH that can eventually be deposited in sediments are:

(1) Biosynthesis.

(2) Diagenesis of sedimentary organic matter

Table 2. Summary of natural and anthropogenic sources of PAH and industrial and domestic processes that generate and emit PAH.

Source	Source Type	Process
Natural	- Volcanoes & Geothermal Sources	
	- Forest fires	
	- Biosynthesis	
	- Diagenesis	
	- Petroleum seeps	
Anthropogenic	- Fossil Fuels	- Coal, Petroleum & Wood.
	- Industrial	- Acetylene preparation from natural gas
		- Pyrolysis of kerogen to form benzene
		- Wood pyrolysis to form charcoal, tars.
		- Coke production
		- Gas production from petroleum
		- Coal gasification
		- Production of synthetic alcohol
		- Oil refinery operations
		- Al electrolyte manufacture
	- Domestic heating	- Wood stoves, space heating.
	- Incineration	- Industrial and domestic wastes
	- Power generation	- Fossil fuels
	- Vehicle exhaust emissions	
	- Crankcase oil	
	- Runoff	
	- Sewage outfalls	

Table 3. Characteristic molecular signatures and markers used to identify inputs of combustion and petroleum-derived PAH to sediments and other depositional environments (Bohem and Farrington, 1984; Killops and Howell, 1988; Steinhauer and Boehm, 1992; Canton and Grimalt, 1992). UCM = Unresolved Complex Mixture.

Molecular Signature		Definition
Naphthalenes	-	The naphthalene homologous series are associated with unweathered petroleum and are rarely found in "clean" sediments at detectable levels.
Phenanthrene/ Anthracene (Pa/A)	-	Low Pa/A ratio indicative of combustion High (Pa/A) indicative of petroleum.
Alkylated/Parental	-	Alkylated species are abundant in petroleum while parental are associated with combustion.
Σ Phenanthrenes	-	Sum of the unsubstituted and alkyl-substituted phenanthrenes have petroleum, combustion and diagenetic sources but the presence of more highly alkylated species is usually indicative of petroleum.
Σ Dibenzothiophenes	-	Sum of the unsubstituted three-ring heterocyclic parent and alkyl-substituted dibenzothiophene are distinct compounds of many crude oils.
Σ 4,5-ring PAH	-	Dominance of 4,5-ring PAH (Fl, Py, BaA,Chy, BFl, BaP BeP) indicates combustion.
Σ PAH	-	Sum of 2 to 5-ring petrogenic and digenetic PAH when used in conjunction with the 4,5-ring parameter, the relative contribution of petrogenic and pyrogenic sources can be determined.
Naphthalene/ Phenanthrene (N/P)	-	The N/P > 1 indicates fresh inputs of phenanthrene petroleum and N/P < 1 is indicative of clean sediments.
Chrysene/ Benz(a)anthracene	-	The dominance of chrysene is indicative of petroleum inputs.
Cyclopenta(c,d)pyrene		Predominantly vehicular origin
Pyrene/Perylene Py/Peryl	-	High Py/Pery ratio indicative of anthropogenic origin, low Py/Pery ratio indicative of diagenetic origin
Retene	-	Thermal degradation of wood resins
UCM	-	Biodegraded petroleum

(3) High temperature pyrolysis of organic materials

1.3.1 Biosynthesis:

Extensive discussions exist in the literature regarding the biosynthesis of PAH. For example, Borneff et al. (1968) claimed that 3,4-benzopyrene, 11,12-benzofluoranthene, 1,2,3-indenopyrene, benzo(ghi)perylene, 3,4-benzofluoranthene, 1,2 benzanthracene and fluoranthene were produced by the fresh-water algae *Chlorella vulgaris*. Lima-Zanghi (1968) reported the synthesis of benzo(a)pyrene by the anaerobic *Clostridium putride* and Niaussat et al. (1970) observed that *Bacillus badius* synthesised benzo(a)pyrene and perylene. However, Hase and Hites (1976) concluded from a series of experiments that bacteria do not produce PAH but rather bioaccumulate them from the growth medium. Similar observations were reported by Grimmer and Duevel (1970) using more rigorously designed experiments. Therefore, it is generally accepted that direct biosynthetic contributions to the aqueous and sediment phases are insignificant in comparison to non-biosynthesized sources.

1.3.2 Diagenesis of sedimentary organic materials:

The early diagenesis of sedimentary organic matter can lead to the formation of a number of PAH. Examples of reactions are: diagenetic production of phenanthrene and chrysene derivatives from aromatization of pentacyclic triterpenoids originating from terrestrial plants, early diagenesis of abietic acids to produce retene, and in-situ generation of perylene from perylene quinones (Youngblood and Blumer, 1975; Laflamme and Hites, 1978; Wakeham et al., 1980b; Tan and Heit, 1981; Simoneit and Mazurek, 1982; Tissier and Saliot, 1983; Venkatesan, 1988; Lipiatou and Saliot, 1992). Perylene and retene are

the two most prominent diagenetic PAH found in recently deposited sediments (Colombo et al., 1989). The origin of perylene has been linked to terrestrial precursors (4,9-dihydroxyperylene-3,10-quinone, the possible candidate), marine precursors and anthropogenic inputs (Blumer, 1977; Laflamme and Hites, 1978; Prahl and Carpenter, 1979; Venkatesan and Kaplan, 1982; Tissier and Saliot, 1983; Venkatesan, 1988; Colombo et al., 1989; Lipiatou and Saliot, 1991). The diagenetic pathway for retene is well constrained (Figure 4), (Wakeham et al., 1980b; Lipiatou and Saliot, 1992) but it can also be produced from wood combustion (Ramdahl, 1983a).

Further diagenesis and catagenesis of sedimentary organic matter results eventually in the formation of petroleum. PAH formation during oil generation is attributed to both the aromatization of multi-ring biological compounds (e.g., sterols) and to the fusion of smaller hydrocarbon fragments into new aromatic structures (Radke, 1987). Steroids are probably the most well understood in terms of biological origin and geological fate, and a simplification of the proposed pathways of sterol diagenesis and catagenesis is summarized in Figure 5 (Mackenzie, 1984). Crude oils, usually formed at temperatures below 150°C have a predominance of substituted over parental PAH.

1.3.3 High temperature pyrolysis of organic material:

PAH are predominantly the by-products of incomplete combustion (i.e., pyrolysis) of organic material. The mechanisms by which these processes occur are complex and have been widely studied over the last 30 years (Badger et al., 1964; Crittenden and Long, 1976; Schmeltz and Hoffman, 1976; Howard and Longwell, 1983; Colket and Hall, 1992). Synthesis is generally believed to occur through a free radical pathway wherein

Figure 4. The proposed hypothetical degradation scheme of abietic acid leading to the formation of retene (modified from Wakeham et al., 1980a).

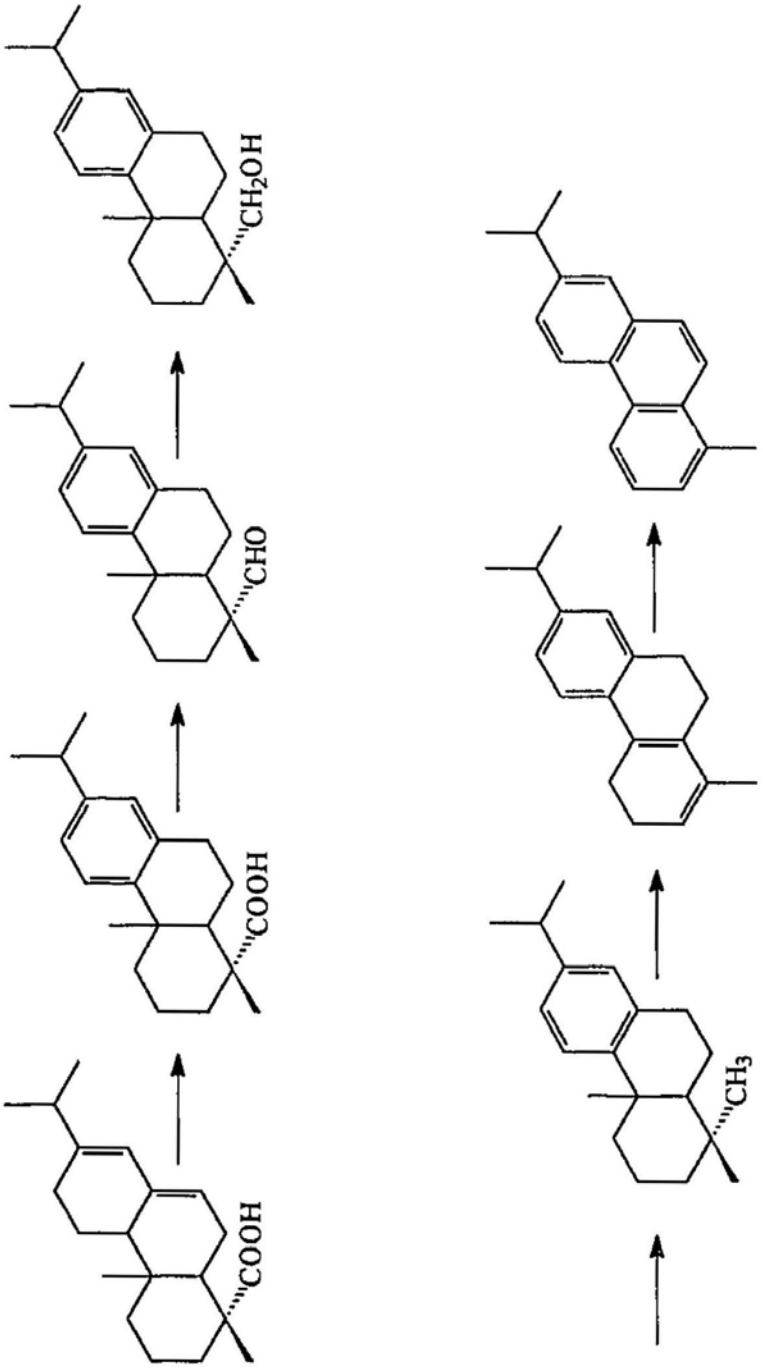
CH2OH
CHO
COOH
COOH
CH3

Figure 5. Simplified reaction scheme to show the conversion of a sterol (I) to various aromatic hydrocarbons during diagenesis. M implies that the reaction occurs in more than one step and R represents aromatization of the A ring while L represents aromatization of the B ring. Compounds II, V and VI appear during diagenesis but are further aromatized to triaromatic steroids (modified from Mackenzie, 1984).

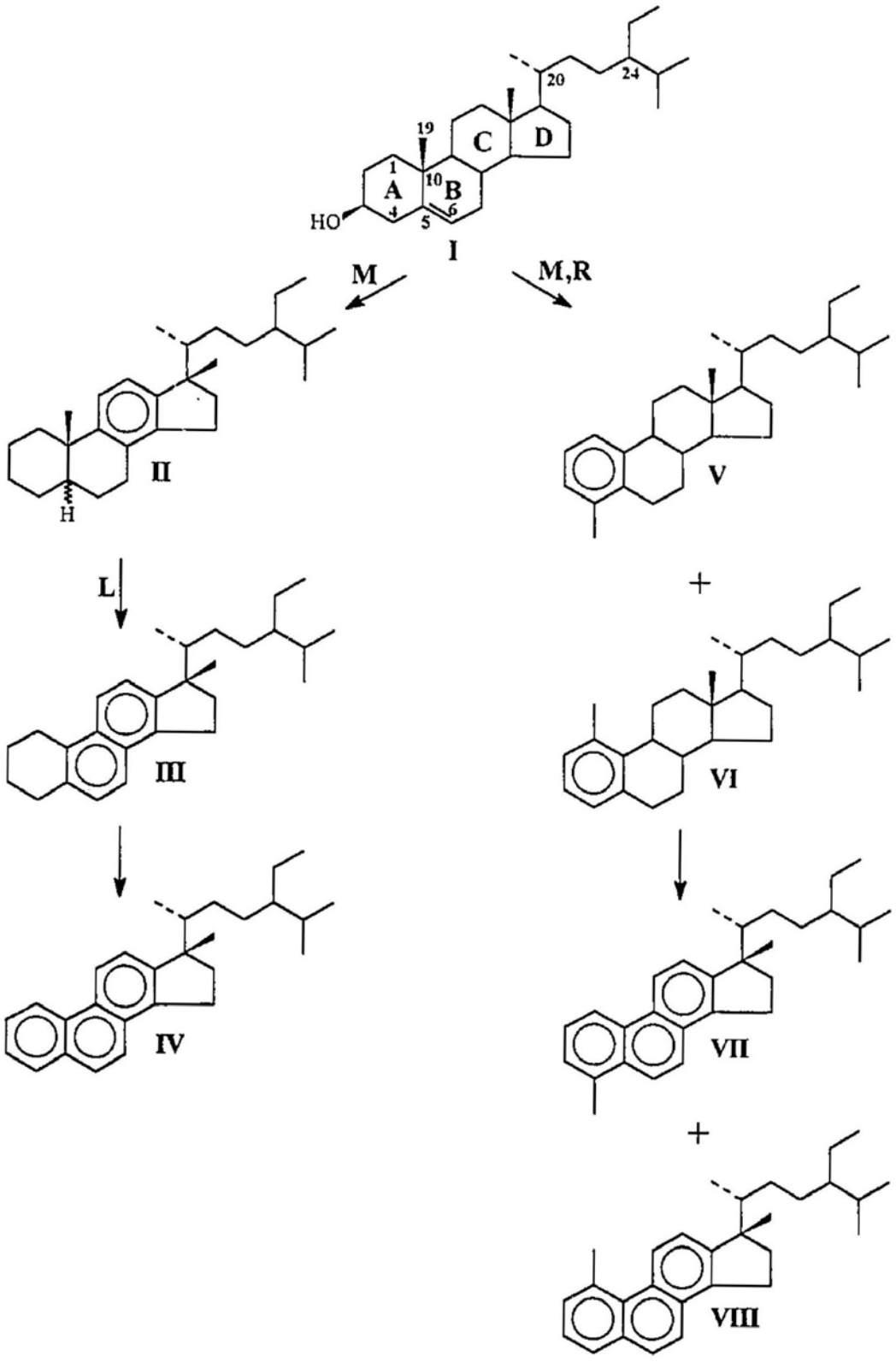
HO
I
M
M,R
II
V
L
III
VI
IV
VII
VIII

radicals of various molecular weights can combine to yield a series of different hydrocarbon products. Therefore, the formation of PAH is thought to occur in two distinct reaction steps: pyrolysis and pyrosynthesis (Lee et al., 1981). In pyrolysis, organic compounds are partially cracked to smaller unstable molecules at high temperatures. This is followed by pyrosynthesis or fusion of fragments into larger and relatively more stable aromatic structures. Badger et al. (1960) was the first to propose this stepwise synthesis using BaP (Figure 6). Compounds identified in studies by Crittenden and Long (1976) suggest that the C_2 species react to form C_4, C_6 and C_8 species, and confirmed the mechanisms proposed by Badger et al. (1960; Figure 6). Despite the large quantities of different PAH formed during primary reactions, only a limited number enter the environment. This is because initially-formed PAH themselves can be destroyed during combustion as a result of secondary reactions that lead to the formation of either higher condensed structures or oxidized carbon (Schmeltz and Hoffman, 1976). For example, the pyrolysis of naphthalene can yield a range of higher molecular weight species such as perylene and the benzofluoranthenes, possibly as a result of cyclodehydrogenation of the binaphthyls (e.g., Figure 7; Lang et al., 1963). This may be particularly important for compounds that are deposited on the walls of open fireplaces along with soot particulates close to the hot zone of the flame.

While the aromaticity of the combustion material can influence PAH emission (Hangebrauck et al., 1967; Gross, 1974), combustion characteristics such as temperature and fuel to air ratio are considered to be the most important factors contributing to PAH yield (Begeman and Burgan, 1970; Jensen and Hites, 1983; Fangmark et al., 1993).

Figure 6. Stepwise reaction scheme proposed by Badger et al. (1964) to account for PAH formation. In this particular example, benzo(a)pyrene (7) is formed as a result of a recombination of free radicals starting with acetylene (1). Compound (2) is a four carbon unit such as vinylacetylene or 1,3-butadiene and species (3) is styrene or ethylbenzene (Crittenden and Long 1976).

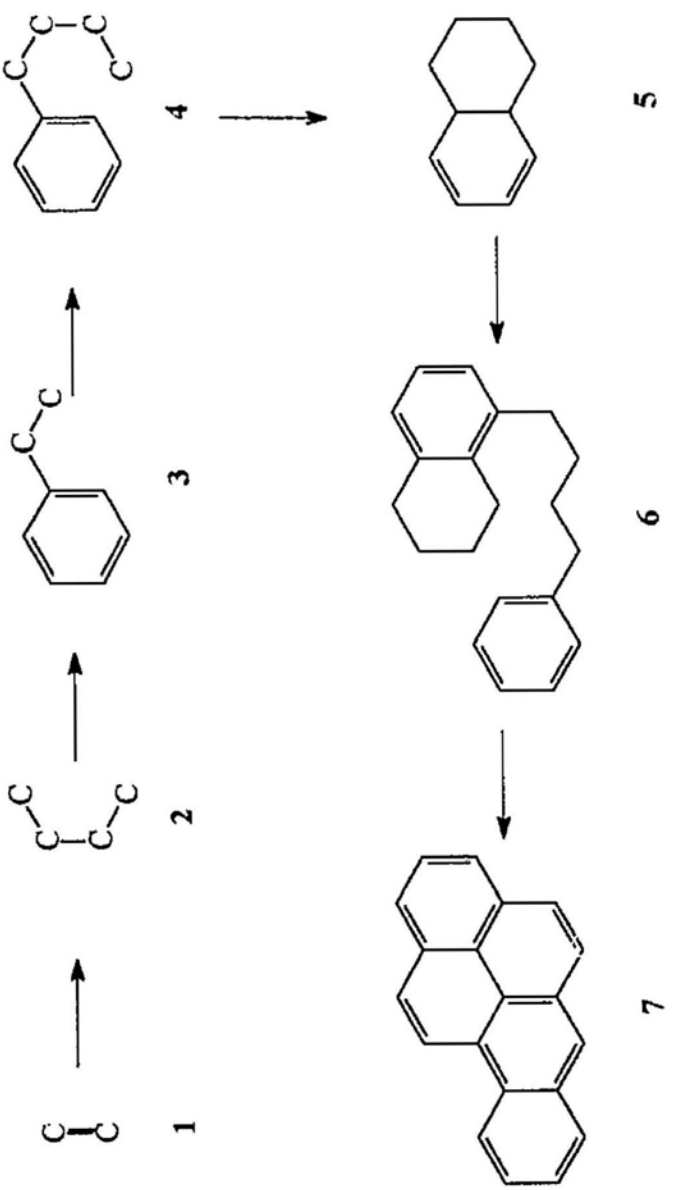
1
2
3
4
5
6
7

Figure 7. Examples of some higher molecular weight PAH produced as a result of secondary reactions of naphthalene during pyrolysis. Perylene and the benzofluoranthenes are thought to be formed from the cyclodehydrogenation of the intermediate binaphthyls (modified from Lang et al., 1963).

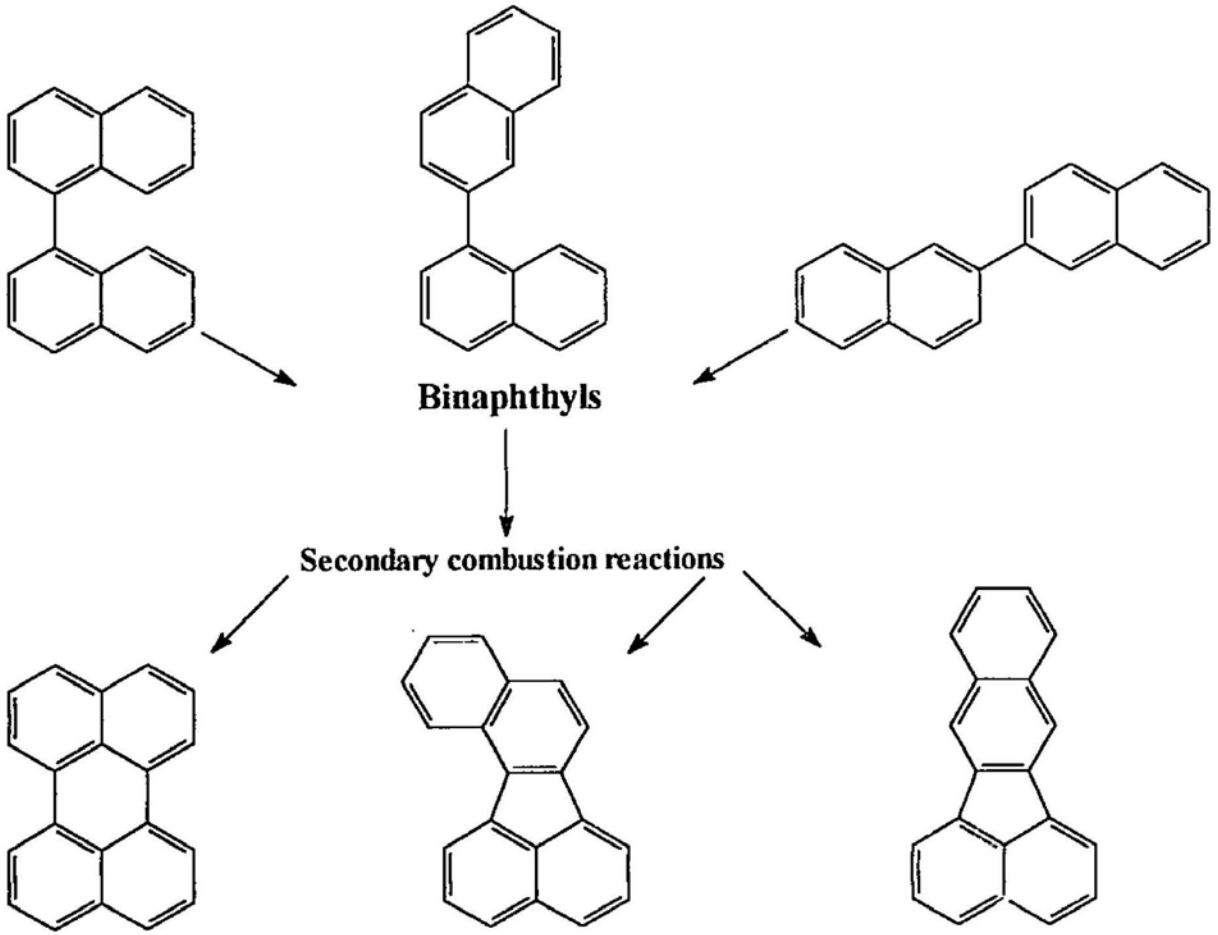
Binaphthyls
Secondary combustion reactions
Perylene
Benzofluoranthenes

Maximum yields of PAH ranging in molecular weight from naphthalene to coronene, were produced during the combustion of hydrocarbons at 780°C, decreasing at higher and lower temperatures (Commins, 1969). High temperature combustion tends to favour the simpler unsubstituted 4 and 5-ring aromatics (e.g., fluoranthene and pyrene) whereas lower temperatures of 150 - 200° preserve a greater degree of alkylation (e.g., methylated naphthalenes)(Neff, 1979). This observation is consistent with the abundance of highly alkylated PAH assemblages observed in crude oils. Open flame temperatures (200-800°C) favour significant quantities of both parental and substituted PAH. The fact that lower temperatures tend to favour the more alkylated PAH, suggests that these compounds may be possible precursors to their corresponding non-alkylated analogues. It is generally accepted that as fuel:air ratios increase, the concentration of 4 and 5-ring PAH also increases (Fangmark et al., 1993), while the concentration of higher molecular weight compounds decreases since the temperatures are below the optimum required for formation of these compounds (Commins, 1969; Guerin, 1979; Uthe, 1991). The composition of unsubstituted PAH produced during pyrolysis at defined temperatures appears to be independent of the type of combustion material (Laflamme and Hites, 1978; Lake et al., 1979; Grimmer et al., 1983a).

In general, all organic compounds containing carbon and hydrogen may serve as precursors of PAH during combustion (Neff, 1979; Lee et al., 1981). However, carbohydrates (highly oxidized) are relatively poor PAH precursors compared to more highly reduced compounds, such as lipids, especially paraffinic waxes (Neff, 1979). Other precursors such as lignin and cellulose also produce PAH during combustion

(Liverovskii et al., 1972; Maja, 1986). Schmeltz and Hoffmann (1976) reported that sterols were excellent precursors for Na, A, Pa, Chy and BaP. Combustion of petroleum aromatic hydrocarbons produce similar variation in yields of PAH (Brunnemann and Hoffmann, 1976) while aliphatic hydrocarbons were determined to be relatively poor PAH precursors.

Other important potential sources of PAH identified in sedimentary environments are asphalt, tire and brake wear and crankcase oils (Wakeham et al, 1980a; Spies et al., 1987; Broman et al, 1988; Takada et al., 1990; Latimer et al., 1990).

1.4 Pathways and sinks:

PAH enter coastal and estuarine environments directly or indirectly from:

(1) Domestic and industrial effluents and urban runoff

(2) Deposition of airborne particulates, and

(3) Direct spillage of petroleum and petroleum products

1.4.1 Domestic and industrial effluents and urban runoff:

PAH in domestic sewage are predominantly a mixture of aerially deposited compounds produced from domestic fuel combustion and industrial and vehicle emissions, combined with PAH from road surfaces that have been flushed into sewage systems (Wild and Jones, 1993). Road surface PAH are derived primarily from crankcase oil, asphalt and tire and brake wear (Wakeham et al, 1980a; Ostman and Colmsjo, 1988; Broman et al., 1988; Takada et al., 1990). Some PAH are removed from sewage during treatment; for example, studies by Petrasek et al. (1983) showed that a mean of 64% total PAH was

removed from sewage effluents by primary treatment (sedimentation). Not all urban runoff enters the sewer system and even some sewer designs allow runoff to be independently discharged to aquatic systems without primary treatment. The quantity of runoff from an urban environment is generally governed by the fraction of paved area within a catchment and the annual precipitation. During periods of continued rainfall, road surfaces are continually washed and the contributions of PAH to watersheds are generally low. However, significant episodic contributions to aquatic systems can occur after prolonged dry periods or during spring snow melt (Hoffman et al., 1985; Pham, 1993).

The distribution and quantity of PAH in industrial effluents depends on the nature of the operation and on the degree of treatment prior to discharge. In some urban areas, industrial effluents are combined with domestic effluents prior to treatment or they are independently treated before being discharged to sewer systems.

1.4.2 Deposition of airborne particulates:

It is generally accepted that virtually all PAH emitted to the atmosphere are associated with airborne particulates (Suess, 1976; Mc Veety and Hites, 1988; Baek et al., 1991ab). PAH are initially generated in the gas phase, and then as the vapour cools, they are adsorbed onto particulates (Van Vaeck and Van Cauwenberghe, 1985). The highest concentrations of PAH in airborne particulates occurs in the less than 5 μm particle size range (Pierce and Katz, 1975; Vaeck et al., 1979; Van Cauwenberghe, 1983; Sicre et al., 1987). PAH distribution between the gas and particulate phase is generally influenced by the following factors: vapour pressure as a function of ambient temperature,

availability of fine particulate material and the affinity of individual PAH for the particulate organic matrix (Van Vaeck et al., 1979; Yamasaki et al., 1982; Tuominen et al., 1988; Coutant et al., 1988; Baek et al., 1991b). Atmospheric concentrations of PAH are normally high in winter and low during the summer months (Pierce and Katz, 1975; Gordon, 1976; Brun et al., 1991). These variations are mainly attributed to increased rates of photochemical activity during the summer and increased consumption of fossil fuels during the winter period. Residence times of particulate PAH in the atmosphere and their dispersal by wind are determined predominantly by particle size, atmospheric physics and meteorological conditions. The main processes governing the deposition of airborne PAH include wet and dry deposition and to a smaller extent, vapour phase deposition onto surfaces. Particles between 5-10 μm are generally removed rapidly by sedimentation and by wet and dry deposition (Baek et al., 1991ab). However, PAH associated with fine particulates (2-3 μm) can remain suspended in the atmosphere for a sufficiently long time to allow dispersal over hundreds or thousands of kilometres (McVeety and Hites, 1988; Baek et al., 1991a). Fine particles are also known not to be efficiently removed by wet deposition (Grover et al., 1977). The concentration of PAH in persistent atmospheric particulate matter may be reduced by the desorption of some of the constituents from the particle to the gas phase, the so called "aerodynamic dilution" effect (De Wiest and Della-Fiorentina, 1975). The PAH signature and concentrations of the most persistent fraction can also be altered by the chemical reactions described in section 1.5.1.

1.4.3 Spillage of petroleum and petroleum products:

PAH from petroleum and petroleum products can enter aquatic systems directly by spillage, accidental release and natural oil seeps, or indirectly through sewers, urban and highway run-off. Although PAH only constitute a small fraction of known petroleum hydrocarbons, the National Research Council (1985) estimated that between 1.7-8.8 million tons of petroleum hydrocarbons are entering the marine environment annually. Crankcase oils or used engine lubricating oils are an important source of PAH in urban environments and have been shown to contain elevated levels of PAH. The world production of crankcase oil is estimated to be approximately 40 million tons per annum and 4.4% of that is estimated to reach aquatic environments (GESAMP, 1993). As well as combustion-derived PAH, crankcase oil also consists of PAH from uncombusted fuel (Pruell and Quinn, 1988; Vazquez-Duhalt, 1989).

Worldwide annual inputs of PAH to coastal and estuarine environments are very difficult to estimate due to the diffuse nature of the potential sources described. Once PAH enter aquatic environments they become rapidly associated with particulate matter and are deposited in bottom sediments (Gearing et al., 1980). Physical factors, such as turbulence, deep water currents, surface waves and upwelling influence the length of time they remain suspended in the water column. The rate at which PAH are incorporated into bottom sediments is controlled by sedimentation rate, bioturbation and bottom sediment-water column exchanges (Officer and Lynch, 1989; Kirso et al., 1990; Santschi et al., 1990).

1.5 Physical, chemical and biological transformations:

The degree and type of PAH incorporated in bottom sediments as particulates depends not only on the nature and magnitude of various source contributions, but also on the susceptibility of the PAH to various physical, chemical and microbial degradation reactions. If these reactions alter molecular signatures or involve isotopic fractionation they may complicate efforts to apportion sources of PAH in environmental samples. The following section outlines the potential reactions PAH may undergo in atmospheric and aqueous environments prior to eventual deposition in bottom sediments.

1.5.1 Physical and chemical transformations:

Laboratory experiments have shown that PAH are photoreactive in the atmosphere (Zafiriou, 1977; Butler and Crossley, 1981; Atkinson, 1990; Bunce and Dryfhout, 1992) and in the photic zone of the water column (Zepp and Scholtzhauer, 1979; Payne and Phillips, 1985; Paalme et al., 1990; Ehrhardt et al., 1992). PAH are also degraded by reactions with oxygen, ozone, nitrogen and sulphur producing oxygenated, nitro and sulphur containing compounds including carcinogenic quinones (Butler and Crossley, 1981; Atkinson and Aschmann, 1984; Arey et al., 1986; Nielsen and Ramdahl, 1986). The reactivity of PAH under *in-situ* atmospheric conditions is difficult to predict from laboratory experiments. However, there is potential for chemical transformation of PAH by gas-particle interactions in emission plumes, exhaust systems or during atmospheric transport, particularly in more polluted urban environments. Photochemical transformations are generally considered to be the most important mode of atmospheric decomposition of PAH in both the particle and gaseous phases (Masclet et al., 1986;

Kamens et al., 1990; Bunce and Dryfhout, 1992). The existence of PAH oxidation products in atmospheric particulate matter, indicates that PAH react with oxygen or ozone (singlet molecular oxygen) in the atmosphere (Khan et al., 1967; Pitts et al., 1969). Since singlet molecular oxygen is not produced by the direct adsorption of sunlight and the oxygen produced from the photolysis of ozone has a short lifetime (0.57 sec) in the atmosphere, it is expected to have an insignificant role in the atmospheric decomposition of PAH (Lane, 1989). Atmospheric reactions of PAH with sulphur and nitrogen are also expected to be negligible. Butler and Crossley (1981) and Grosjean et al. (1983) have shown that SO_2 appears to be totally unreactive with PAH at concentrations typical of those found in the atmosphere of a polluted city even after 99 days of exposure. The reaction of hydroxyl radicals (OH) with organic molecules during daylight conditions is considered to be the major reaction of these molecules leading to their removal from the atmosphere (Nielsen, 1984; Atkinson, 1990). There is great variation in the reported half-lives of various PAH due to photolysis, largely because of the differences in the nature of the substrate on which the PAH are adsorbed and the degree to which they are bound .(Valerio and Lazzarotto, 1985; Behymer and Hites, 1988; Coutant et al., 1988; Paalme et al., 1990). For example, Korfmacher et al. (1980) reported greater stability for PAH adsorbed on coal fly-ash than for pure or dissolved forms, as well as for those adsorbed on silica gel, alumina or coated on glass surfaces. Several studies have concluded that the carbon content and the colour of substrates are important factors in controlling PAH reactivity (Kamens et al, 1986; Behymer and Hites, 1988; Wortham et al., 1993). The suppression of photochemical degradation of PAH adsorbed on soot and fly-ash has been tentatively attributed to physical factors, such as particle size and colour. Darker

substrates absorb more light and thereby protect PAH from photolytic degradation reactions (Behymer and Hites, 1988). Transition metal ions present on particle surfaces can stabilize the ground state or quench the excited state of PAH, and may also be important in protecting reactive compounds (Korfmacher et al., 1980; Van Cauwenberghe, 1983; Dunstan et al., 1989).

Photooxidation by singlet oxygen appears to be the dominant chemical degradation process of PAH in aquatic systems (Lee et al., 1978; Hinga, 1984; Payne and Phillips, 1985). The degree to which PAH are oxidised in an aqueous system depends on PAH type and structure, water column characteristics (such as oxygen availability), temperature and depth of light penetration, and residence time in the photic zone (Payne and Phillips, 1985; Paalme et al., 1990). Paalme et al. (1990) have shown that the rate of photochemical degradation of different PAH in aqueous solutions can differ by a factor of >140 depending on their chemical structure, with perylene, benzo(b)fluoranthene and coronene showing the greater stability. Alkyl PAH are reported to be more sensitive to photooxidation reactions than parental PAH (Radding et al., 1976; Ehrhardt et al., 1992). This preferential degradation is most likely due to benzyl hydrogen activation (Ehrhardt and Petrick, 1984; Rontani et al., 1987). Payne and Phillips. (1985) reported that benz(a)anthracene and benzo(a)pyrene are photolytically degraded 2.7 times faster in summer than in winter. Once deposited in sediments, photoxidation reactions are generally significantly reduced due to the presence of more anoxic conditions and limited light penetration (Mille et al., 1988). PAH residence time in sediments depends on the extent of physical, chemical and biological reactions occurring at the sediment-water interface, as well as the intensity of bottom currents (Hinga, 1984).

Finally, volatilization also plays a key role in the environmental persistence of PAH (Hallett and Brecher, 1984). Volatilization rates decrease by a factor of 3-10 with each additional benzene ring. With the exception of Na, the rates of photolysis of dissolved PAH are higher than the rates of volatilization, although once bound to particulates, the effects of these two processes is rendered negligible.

1.5.2 Biodegradation:

PAH in the atmosphere and open waters may undergo volatilization and photodecomposition, but microbial degradation is believed to be the dominant sink below the photic zone. Microbial degradation has also been recognized as the most prominent mechanism for removing PAH from contaminated environments (Bossert et al., 1984). Microbial adaptations may result from chronic exposure to elevated concentrations as shown by the higher biodegradation rates in PAH-contaminated sediments than in pristine environments (Shiaris, 1989). Nevertheless, it is also known that preferential degradation of PAH will not occur in contaminated environments where there are more accessible forms of carbon (Shiaris, 1989). A summary of the turnover times for naphthalene, phenanthrene and BaP in water and sediment is shown in Table 4.

The ability of microorganisms to degrade fused aromatic rings is determined by their combined enzymatic capability which can be affected by several environmental factors (McElroy et al., 1985; Cerniglia and Heitkamp, 1989; Cerniglia, 1991). The most rapid biodegradation of PAH occurs at the water/sediment interface (Shiaris, 1989; Cerniglia, 1991) and no degradation was detected by Mille et al. (1988) in suboxic conditions (dissolved oxygen, 0.2-0.3 ppm and redox potential between 180-200 mv). Prokaryotic microorganisms metabolize PAH by an initial dioxygenase attack to

Table 4. Summary of the estimated turnover times (days) of naphthalene, phenanthrene and benzo(a)pyrene in water, sediments and soils at various temperatures (Shiaris, 1989).

PAH and Environment	Temp °C	Time (days)	Reference
Naphthalene:			
Estuarine water	13	500	*Lee & Ryan (1976)*
Estuarine water	24	30-79	*Lee & Ryan (1976)*
Estuarine water	10	1-30	*Readman et al. (1982)*
Seawater	24	330	*Lee & Ryan (1976)*
Seawater	12	15-800	*Lee & Anderson (1977)*
Estuarine sediment	25	21	*Bauer & Capone (1985)*
Estuarine sediment		287	*Pruell & Quinn (1985)*
Estuarine sediment	22	34	*Heitkamp & Cerniglia (1987)*
Estuarine sediment	30	15-20	*Hambrick et al. (1980)*
Estuarine sediment	2-22	13-20	*Shiaris (1989)*
Stream sediment	12	>42	*Herbes & Schwall (1978)*
Stream sediment	12	0.3	*Herbes & Schwall (1978)*
Reservoir sediment	22	62	*Heitkamp & Cerniglia (1987)*
Reservoir sediment	22	45	*Heitkamp & Cerniglia (1987)*
Phenanthrene:			
Estuarine sediment	25	56	*Heitkamp & Cerniglia (1987)*
Estuarine sediment	2-22	8-20	*Shiaris (1989)*
Reservoir sediment	22	252	*Heitkamp & Cerniglia (1987)*
Reservoir sediment	22	112	*Heitkamp & Cerniglia (1987)*
Sludge-treated soil	20	282	*Bossert et al. (1984)*
Benzo(a)pyrene:			
Estuarine water	10	2-9000	*Readman et al. (1982)*
Estuarine sediment	22	>2800	*Heitkamp & Cerniglia (1987)*
Estuarine sediment	2-22	54-82	*Shiaris (1989)*
Stream sediment	12	>20800	*Herbes & Schwall (1978)*
Stream sediment	12	>1250	*Herbes & Schwall (1978)*
Reservoir sediment	22	>4200	*Heitkamp & Cerniglia (1987)*
Sludge-treated soil	20	>2900	*Bossert et al. (1984)*

yield cis-dihydrodiols and finally catechol (Figure 8). Biodegradation and utilization of lower molecular weight PAH by a diverse group of bacteria, fungi and algae has been demonstrated (Table 5; Cerniglia and Heitkamp, 1989). The degradation pathways of higher molecular weight PAH, such as pyrene, benzo(e)pyrene and benzo(a)pyrene are less well understood, but since these compounds are more resistant to microbial degradation processes, they tend to persist in contaminated environments. However, the degradation of fluoranthene, pyrene and benzo(a)pyrene has been reported in laboratory conditions (Barnsley, 1983; Wesseinfelds et al., 1990; Mueller et al., 1988), and Mueller et al. (1990) have isolated a Pseudomonas species (*Pseudomonas paucimobilus*) that is capable of degrading and utilizing fluoranthene as a sole carbon source. It is generally recognised that PAH with three or more condensed rings do not normally serve as substrates for microbial growth, but may be the subject of cometabolic transformations. Cometabolic reactions of pyrene, 1,2 benzanthracene, 3,4 benzopyrene and phenanthrene can be stimulated in the presence of either naphthalene or phenanthrene (Bauer and Capone, 1988; Smith et al., 1991). Nevertheless, the degradation of PAH by cometabolic reactions is expected to be insignificant because of the extremely slow rates of these reactions in natural ecosystems (Smith, 1990). In addition to cometabolism, bacterial inhibition in the presence of compound mixtures was also shown to occur (McCarty et al., 1984; Smith et al., 1991). Elevated temperatures increase the rate of biotransformation reactions in vitro, for example, laboratory studies have shown a 50% loss of phenanthrene after 180 days at 8°C in water compared to 75% loss in 28 days at 25°C (Sherrill and Sayler, 1981; Lee, 1981). Based on these observations,

Figure 8. Typical dioxygenase (bacteria) mediated oxidation of PAH by microorganisms leading to the formation of Cis-Dihydrodiol and Catechol, respectively (modified from Cerniglia and Heitkamp, 1989).

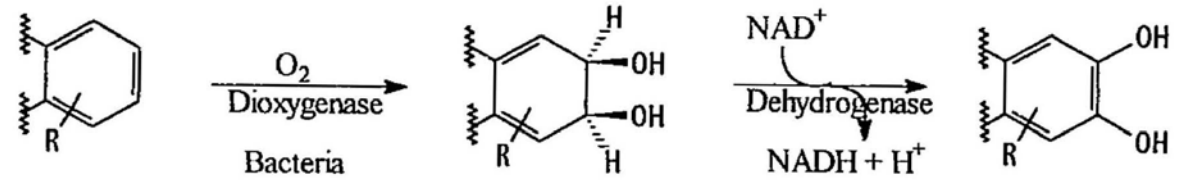

Polycyclic Aromatic Hydrocarbon

<u>Cis</u>-Dihydrodiol

Catechol

Table 5. Summary of bacterial and fungal species capable of oxidizing and utilizing some low and high molecular weight PAH.

Organism	Substrate	Reference
Pseudomonas sp.	Naphthalene	Davies and Evans (1964)
		Jeffrey et al. (1975)
		Barnsley (1975)
	Phenanthrene	Jerina et al. (1976)
		Evans et al. (1977)
		Barnsley (1983)
	Anthracene	Jerina et al. (1976)
	Fluoranthene	Mueller et al. (1990)
		Weissenfels et al. (1990)
	Pyrene	Barnsely (1983)
		Weissenfels et al. (1990)
Flavobacteria sp.	Phenanthrene	Colla et al. (1959)
	Anthracene	Colla et al. (1959)
Alcaligenes sp.	Phenanthrene	Kiyohara et al. (1982)
Aeromonas sp.	Naphthalene	Kiyohara & Nagao (1978)
	Phenanthrene	Kiyohara et al. (1982)
Beijerenckia sp.	Phenanthrene	Jerina et al. (1976)
	Anthracene	Jerina et al. (1976)
	Benz(a)anthracene	Gibson et al. (1976)
	Benzo(a)pyrene	Gibson et al. (1976)
Bacillus sp.	Naphthalene	Cerniglia (1984)
Cunninghamella sp.	Naphthalene	Cerniglia (1978)
	Phenanthrene	Cerniglia & Yang (1984)
	Benzo(a)pyrene	Cerniglia & Gibson (1979)
Micrococcus sp.	Phenanthrene	Ghosh & Mishra (1983)
Mycobacterium sp.	Phenanthrene	Guerin and Jones (1988)
	Phenanthrene	Boldrin et al. (1993)
	Fluorene	Boldrin et al. (1993)
	Fluoranthene	Boldrin et al. (1993)
	Pyrene	Boldrin et al. (1993)

biodegradation rates of PAH are likely to be low in sediments of the cold-water systems under investigation.

1.6 δ ^{13}C of PAH[1]:

The isotopic signature imparted on individual PAH during formation is determined by both the isotopic composition of the original precursor material and by the formation conditions. Since these two factors can vary widely, the potential exists for PAH produced from different sources and from a variety of processes to have characteristic isotopic signatures. Isotopic characterization of bulk organic and aromatic fractions has been performed for many years (e.g. Deines, 1980; Sofer, 1984; Conkright, 1989) but it is only in recent years, with the introduction of GC/C/IRMS that isotopic characterization of individual organic compounds has been attempted. Before the present work, isotopic characterization of individual PAH had not been conducted on extracts from environmental samples. Nevertheless, Freeman (1991) analyzed individual aromatic compounds in an ancient system (Eocene Messel Shale) and demonstrated the general tendency of aromatic compounds to be consistently enriched in ^{13}C compared to the aliphatic fraction. This pattern is consistent with diagenetic effects associated with aromatization of geolipids (Stahl, 1980; Sofer 1984; Conkright, 1989). Several examples of diagenetically produced PAH (substituted Pa, Chy, retene and perylene) have been reported, mainly from the aromatization of natural products such as pentacyclic triterpenoids (Wakeham et al., 1980b, Tan and Heit, 1981; Mackenzie, 1984). The

---

[1] $\delta^{13}C = 1000(R_s/R_{std} - 1)$ Eq. 1
where R represents the abundance ratio of $^{13}C/^{12}C$ and the subscripts s and PDB refer to sample and standard Pee Dee Belemnite, respectively.

aromatization of natural compounds to produce PAH is not expected to result in significant isotopic alterations. This contention is supported by the successful use of compound-specific carbon isotope signatures to trace precursor-product relationships in diagenetic systems (e.g., Hayes et al., 1989; Freeman, 1991). It is notable, however, that the range of $\delta^{13}C$ values to be expected from potential precursors (e.g., triterpenoids) remains to be fully defined at present.

Prior to the present work, the only isotopic values reported for individual PAH were from crude petroleum extracts. Chung (1992) recently reported a 7.9 and 7.0‰ depletion in two methylated naphthalene homologues compared to their corresponding parental compound which had a $\delta^{13}C$ value of -29.2‰. Isotopic values for tetrahydronaphthalene (-34.1‰) and decahydronaphthalene (-49.9‰) were also reported. These values are inconsistent with the common presumption of increasing enrichment in ^{13}C with increased aromatization. The $\delta^{13}C$ depleted isotopic values observed in these petroleum-associated PAH may be dictated by the similarly depleted nature of the precursor compounds. However, unlike Chung, Clayton (1992) found identical $\delta^{13}C$ values for phenanthrenes and methylated phenanthrene isomers isolated from a suite of four North Sea oils. Presently, published $\delta^{13}C$ values of petroleum-associated PAH are limited (see above), and it is more than likely that further analysis will reveal more variations that would reflect the isotopic composition of precursor compounds and the nature and degree of diagenetic reactions.

The specific mechanisms governing the isotopic signatures of individual combustion-PAH are poorly understood. It is expected that the combustion of isotopically distinct materials would result in PAH with different isotopic signatures. Although the

specific isotopic values of PAH during combustion have not been studied, laboratory combustion studies have shown that temperature dependent carbon isotope fractionations occur between 400-500°C (Sackett, 1978; Arneth and Matzigkeit, 1986ab). Holt and Abrajano (1991) also observed using stepped combustion analysis that alteration of original components at low temperatures may result in products having an isotopic value which does not reflect the nature of the original source. Due to the nature of PAH formation pathways previously discussed, the $\delta^{13}C$ of combustion-derived compounds may be dictated by a series of primary and secondary reactions that initial and intermediate precursors undergo prior to the formation of the final PAH. The isotopic effects associated with ring cleavage reactions of intermediate precursors (low molecular weight compounds) may result in ^{13}C enriched higher molecular weight species formed by the fusion of these reduced species. Variations in the $\delta^{13}C$ of the higher molecular weight condensed compounds may therefore depend on the $\delta^{13}C$ of the precursor radical. In the absence of pyrosynthetic recombination reactions, combustion produced PAH isotopic compositions are largely dictated by those of the original precursor compounds. Finally, alkylation or dealkylation reactions at specific sites of a parent molecule will alter the isotopic composition of that compound only to the extent that the alkyl branch is isotopically different from the substrate PAH.

Once PAH are emitted to the environment, the extent of alteration of the isotopic signature during transformation reactions depends on the nature of the carbon branching pathways involved in the reaction. Isotopic fractionation as a result of kinetic mass-dependent reactions (volatilization or diffusion) are unlikely to be significant because the

differences in the translational velocities between the light and heavy carbon in these high molecular weight compounds are small. Substitution reactions, resulting in the maintenance of ring aromaticity are also anticipated not to significantly alter the isotopic signature of the substrate molecule, although it is possible that the extent of substitution could result in isotope effects.

1.7 Field sites:

St. John's Harbour and Conception Bay are situated, respectively, on the north east and north coast of the Avalon Peninsula, Newfoundland (Figure 9). The location and characteristics of these study areas are ideal for the present study, because:

(1) Previous studies of St. John's Harbour sediments (Payne, pers. comm.) revealed elevated PAH levels surpassed only by the Sydney Harbour (Nova Scotia) in the whole of Canada. St. John's Harbour is a repository of all major outputs of watersheds from the city area, and is an important shipping port in eastern Canada. Conception Bay, in contrast is situated away from major urban developments.

(2) Both sites are characterized as cold ocean systems where temperatures are conducive to the preservation of original PAH signatures.

(3) Meteorological conditions, with mean annual rainfall of 1157 mm, favour rapid deposition of atmospheric PAH without extensive alteration and frequent inputs due to urban runoff. Also, low temperatures (mean annual max 9°C, min -1°C) and low mean annual sunshine hours (1497) also serves to limit PAH degradation rates in transit to sediment.

Figure 9. Location of field sites, St. John's Harbour and Conception Bay, Newfoundland, which were used as "model" study sites in the present study.

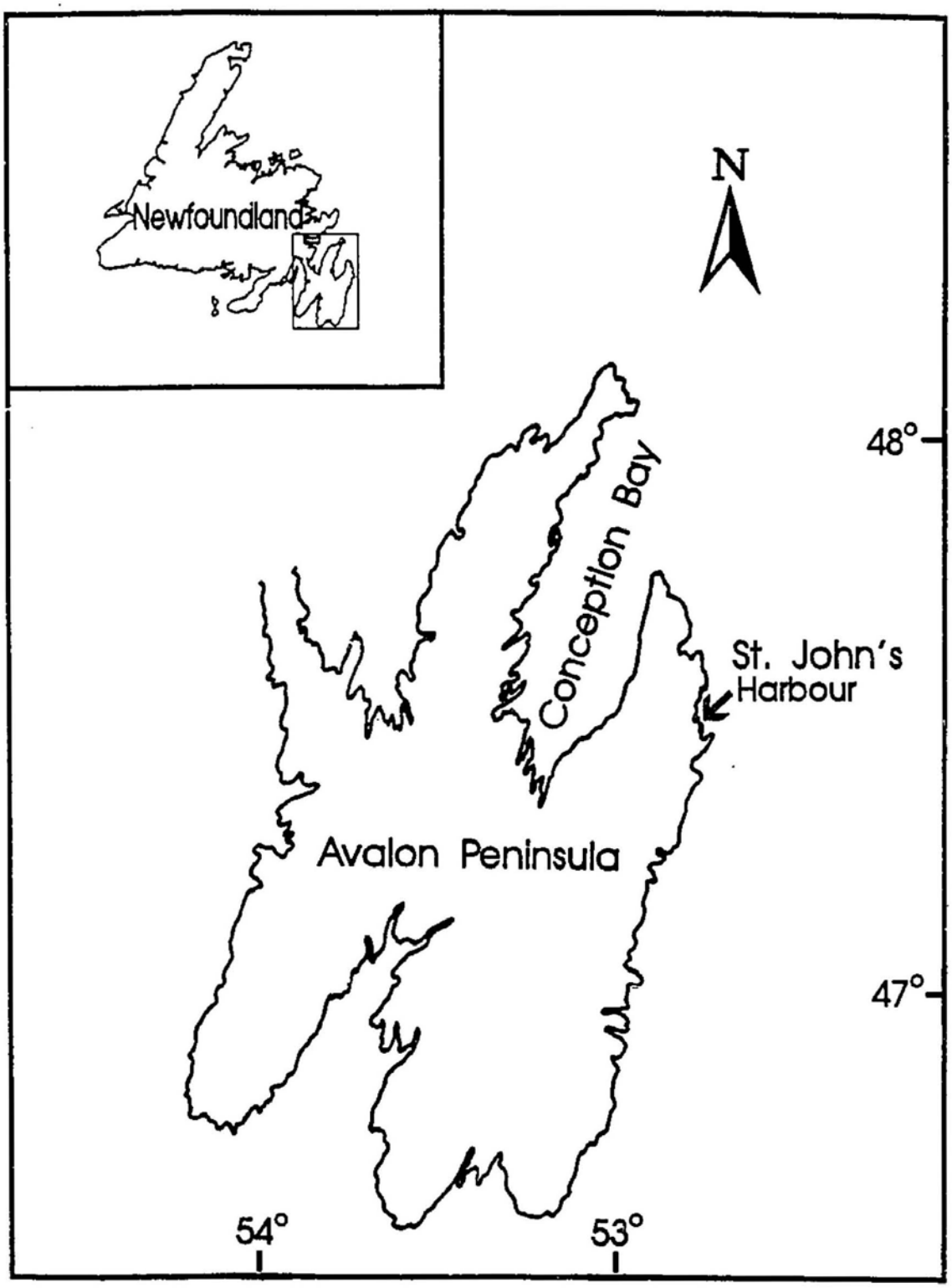
Newfoundland
N
48°
Conception Bay
St. John's
Harbour
Avalon Peninsula
47°
54°
53°

St John's Harbour has a small basin approximately 2 km long, 0.4-0.6 km wide and is surrounded by steeply rising topography except at the western end. The depth of the basin varies between a maximum of 30 m and a sill depth of 14 m at the entrance. The approach is approximately 1 km long, from 0.1 to 0.3 km wide and does not significantly obstruct shallow water exchange with the open ocean. The Harbour has served the city of St. John's as an important shipping route and raw sewage disposal site since its inception back in the 1500's. The location of freshwater and sewage inputs are shown in Figure 10 with a mean input of raw sewage being approximately 82,000 m^3 per year (Newfoundland Design Associates Ltd., 1987-1988). The sewer system in the older parts of the city, in the immediate vicinity of the Harbour allows for the co-disposal of storm sewer and sewage effluents. Urban development, consisting mainly of residential and commercial properties, is concentrated on the north side of the Harbour.

Sediments and organic matter are primarily derived from raw sewage inputs, urban runoff, riverine inputs and snow dumping. The potential primary PAH sources identified in the watershed are fireplace and heating stove wood combustion, domestic heating furnaces, vehicle exhaust emissions, petroleum spillage, crankcase oil, asphalt, tire and brake wear. The pathways (e.g., secondary source contributions) by which these primary sources reach the estuarine sediments are largely the same as the sediments themselves, although they may be augmented to varying degrees by direct discharges (e.g., from shipping) as well as wet and dry aerial deposition. Existing road clearing practices indicate that roadside snow may be an important medium for concentrating various PAH prior to deposition.

Figure 10. Location of sampling sites and sewage and freshwater discharges to St. John's Harbour.

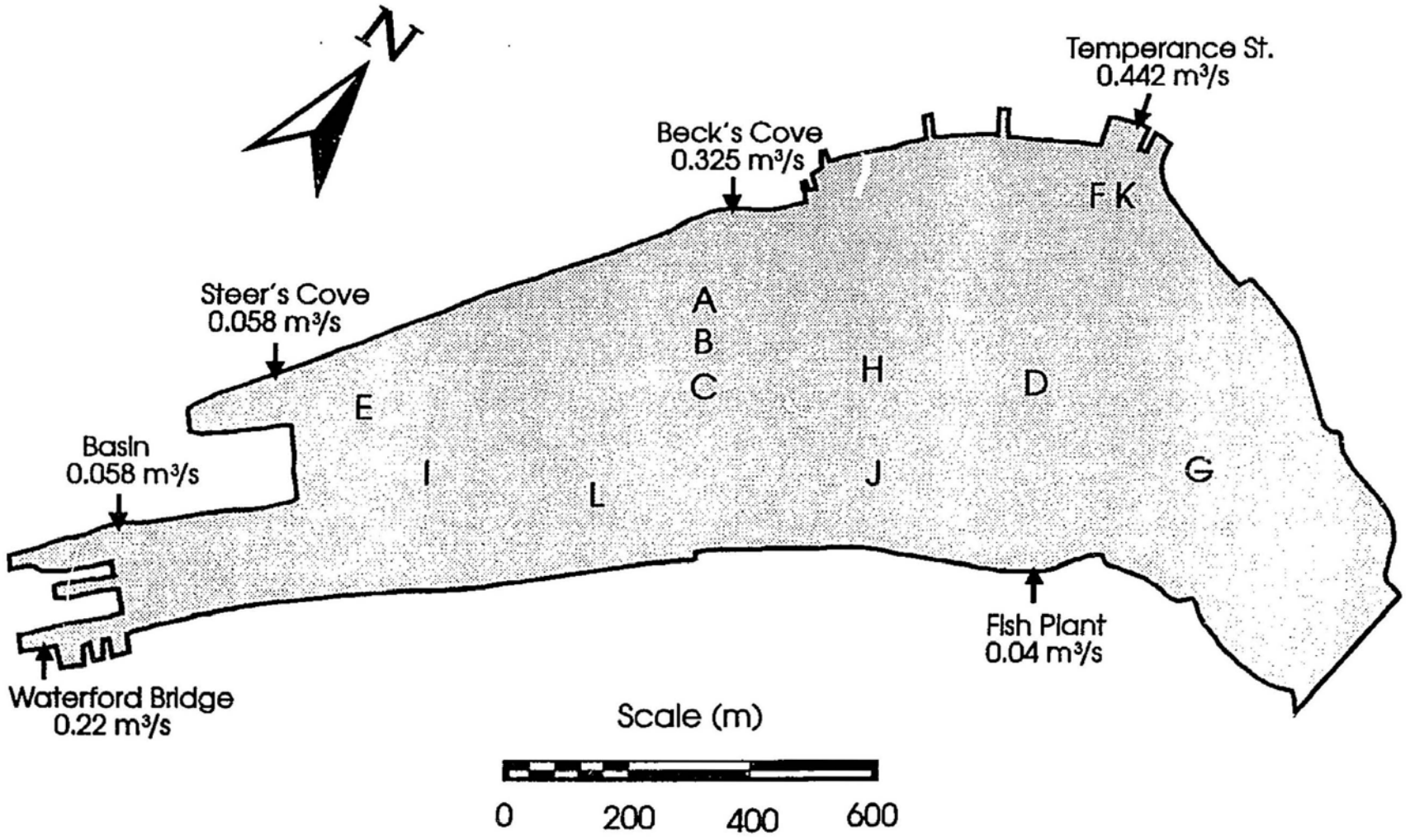
N
Temperance St.
0.442 m³/s
Beck's Cove
0.325 m³/s
Steer's Cove
0.058 m³/s
Basin
0.058 m³/s
Waterford Bridge
0.22 m³/s
Fish Plant
0.04 m³/s
A
B
C
D
E
F
G
H
I
J
K
L
Scale (m)
0
200
400
600

Water column characteristics are varied with mean summer temperatures ranging between 7-11°C and depletions in dissolved oxygen concentrations of up to 70% have been recorded at a number of sites at depths of 10 to 12 metres. It has been suggested that the assimilative capacity (ability to degrade organic matter) of the water column has been reached in the Harbour (Newfoundland Design Ltd., 1987-1988), and this is expected to enhance the preservation of PAH in the water column and sediments.

Conception Bay, is approximately 1440 km^2 in size and is surrounded on three sides by undulating sparsely populated terrain. The Bay is characterized by a central deep sill where depths approach 300 m and a 170 m deep sill at the mouth of the bay (Ostrom, 1992). Approximately twelve small freshwater rivers and tributaries drain into the Bay carrying various concentrations of organic and inorganic substances that are dominated by degradation products of terrestrial vegetation. From a reconnaissance study, a number of local anthropogenic point sources that can contribute to the pollution burden of the Bay have been identified. The most prominent potential point source is an oil-fired power generating station on the southern tip of the Bay, which utilizes Bunker C fuel for power generation. Frequent sooting out practices may result in the release of PAH-rich soot materials, and under suitable atmospheric and meteorological conditions, these could eventually be deposited in the sediments. Other potential point sources are two small petrol storage facilities on the southern and western sides of the Bay. These sources together with highway runoff, sewage, out-board boat motors and atmospheric deposition (e.g., wood burning) are the likely contributors of PAH to the Bay.

The most notable water column activity is the development of a spring

phytoplankton bloom in May normally terminated by thermal stratification and a weaker fall bloom in September. Unlike St. John's Harbour, the year round deep water temperature in Conception Bay ranges between -1.5 and 0°C which may be too low to support substantial microbial activity (Pomeroy et al., 1991). Significant preservation of PAH and other organic material in the sediments may therefore be expected.

1.8 Study summary:

Since the precision and accuracy of CSIA measurements could depend on the purity and yield of the sample, this study initially concentrated on the adoption of effective extraction and purification methods for the isolation of PAH from environmental samples. The suitability of these methodologies was then assessed by spiking exhaustively extracted sediments with pure PAH standards and evaluating the carbon isotope signature of the individual compounds before and after sample processing. Accuracy and precision of CSIA measurements, using numerous repeat analysis of standard PAH mixture and field samples were determined. Isotopic effects during evaporation, photolytic decomposition and microbial alteration were experimentally assessed using standard compounds in *in-vitro* studies. Finally, the potential of CSIA for tracing PAH sources was evaluated by comparing the molecular and isotopic signatures of prominent primary and secondary sources to those isolated from St. John's Harbour and Conception Bay sediments.

2.0 EXPERIMENTAL METHODS

2.1 Principle of operation of the GC/C/IRMS.

The earliest development of a gas chromatographic (GC) interface to an isotope-ratio mass spectrometer (IRMS) can be attributed to Sano et al. (1976). The initial system design was improved upon by Matthews and Hayes (1978) who reported better sensitivity and measurement precision. Further instrumental developments, capabilities and limitations have been discussed in detail elsewhere (Barrie et al., 1984; Freedman et al., 1988; Hayes et al., 1989; Eakin et al., 1992; Goodman and Brenna, 1992). An example of the instrument configuration used in the present work (Isochrom series II, developed by VG Isogas) is shown in Figure 11. Individual components of an organic mixture are separated using a capillary column. As the individual components emerge from the column, they are directed to the micro combustion furnace where they are quantitatively converted to CO_2, H_2O and other by-products in the presence of copper oxide wires at 800 to 900°C. The effluent from the furnace is then directed through a cryogenic trap (-100°C) to remove the water and other condensibles before being sent to the mass spectrometer. The $\delta^{13}C$ value of CO_2 produced for each individual compound, (compared to the standard reference gas) is calculated and reported in conventional delta (δ) notation in parts per thousand ($^{o}/_{oo}$) relative to PDB. (see Eq. 1, p 48)

Compound-specific carbon isotope analysis (CSIA) has been performed on a wide variety of standard and natural organic mixtures with reported precisions of between 0.3

Figure 11. Configuration of the Isochrom series II (GC/C/IRMS), at Memorial University of Newfoundland. C/O = Change over valve, RG = Referance gas valve, He = Helium gas, VSOS = Variable split open split, FID = Flame ionisation detector.

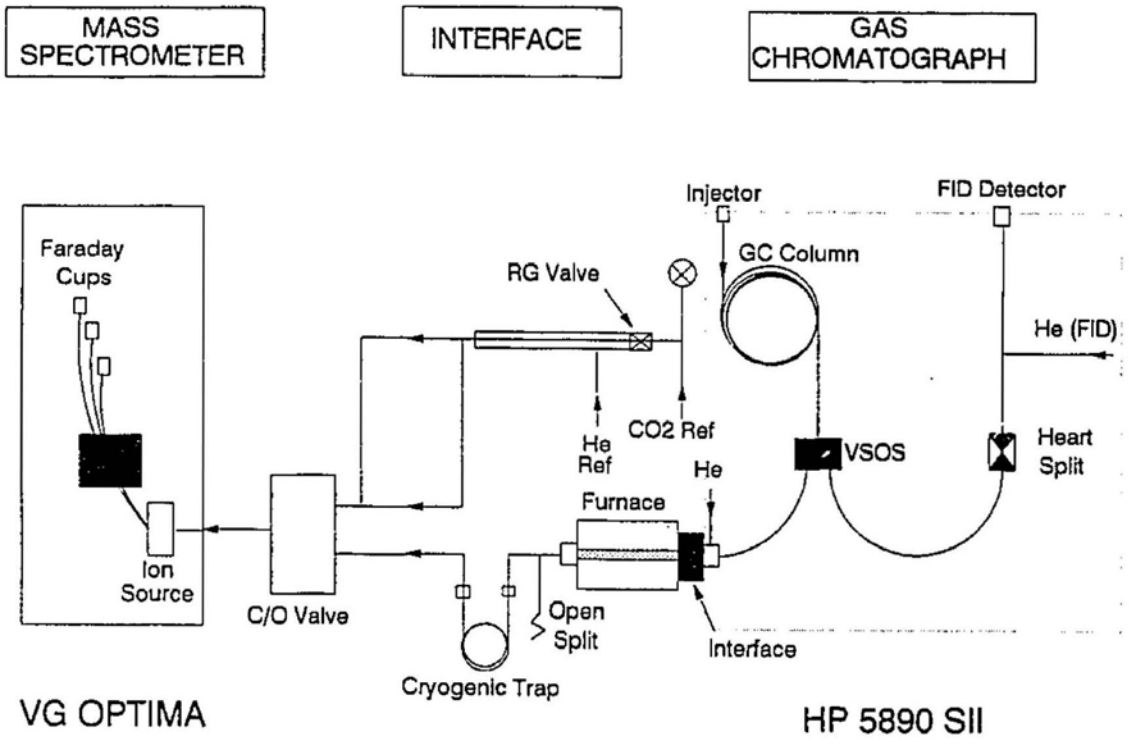
MASS SPECTROMETER
INTERFACE
GAS CHROMATOGRAPH
Injector
FID Detector
Faraday Cups
GC Column
RG Valve
He (FID)
He Ref
CO2 Ref
VSOS
Heart Split
He
Furnace
Ion Source
C/O Valve
Open Split
Interface
Cryogenic Trap
VG OPTIMA
HP 5890 SII

and 1‰ (e.g., Hayes et al., 1989; Freeman et al., 1990; Rieley et al., 1991; Abrajano and Holt, 1992, Eakin et al., 1992; Macko et al., 1992; Guo et al., 1993, Goni et al., 1993). The precision and accuracy of these measurements were predominantly affected by matrix characteristics (e.g., backgrounds, peak overlap or poor resolution and coelution) and performance of the instrumentation (Hayes et al., 1989; Freeman, 1990; Eakin et al., 1992; Merritt et al., 1992; Goodman and Brenna, 1992; Guo et al, 1993). The present software for $\delta^{13}C$ calculations has routines which perform background and peak overlap corrections (e.g., VG Isotech application note No. 19) but manual refinements of correction procedures are required for complex matrices. Unlike standard organic mixtures, the molecular signature of extracts from contaminated environmental samples (e.g., St. John's Harbour) are characterized by the presence of variably separated compounds and a hump known as the unresolved complex mixture (UCM). The magnitude of the background generated by the UCM has the potential to influence the precision and accuracy of the background correction calculations, particularly for small peaks where the isotopic compositions of peak and background are dramatically different. Ostrom and Bakel (1992) showed a 0.3‰ shift in the isotopic ratio of a standard mixture of n-alkanes when a high background was deliberately introduced. Therefore, it is necessary to adopt sample purification methods that can minimize the presence of the UCM without affecting the isotopic compositions of peaks of interest. When peaks overlap (identified by multiple inflections in the 44/45 ratio trace; Figure 11), the isotopically light end of the first peak is overrun by the isotopically heavy front of the second peak thereby complicating the

correction procedure. Isotopic fractionations within individual peaks are related to vapour-pressure isotope effects (Van Hook, 1969) in which ^{13}C containing molecules elute faster than ^{12}C molecules during GC separation (Hayes et al., 1989). This phenomenon is of particular concern for example, for the isotopic determination of PAH isomeric compounds with similar retention times (e.g., Pa/A, BaA/Chy and BeP/BaP). The degree to which these compounds can be separated prior to CSIA analysis is dictated by GC operating conditions and type of capillary column. Isotopic contributions due to co-elution are difficult to determine but their effects can sometimes be preempted by meticulous sample preparation and purification prior to injection, as well as careful selection of GC conditions.

Important sources of instrumental error influencing CSIA precision include linearity effects and peak broadening or tailing. In contrast to conventional IRMS, the major ion beams of the sample and reference gas are imbalanced, and may give rise to linearity effects. Since most complex organic mixtures consist of compounds with varying concentrations, sample/reference beam balancing is not possible for all compounds. Eakin et al. (1992) addressed sample/reference imbalance effects and concluded that the observed deviations were not associated with linearity effects but to some other instrumental effect associated with small sample analysis or ion source contamination. We have extensively tested the linear range (1E-9 to 1E-8 Amps) of our isotopic measurements, and all standards and samples were diluted so that the peaks were within this range. A potentially important source of error is peak broadening which is mainly a function of chromatography. Under chromatographic conditions used in the

present study, peak broadening resulted in a loss of precision in isotopic values for compounds at higher retention times. Peak tailing, associated with leaks or dead volume in the interface can also significantly reduce the precision obtained in isotopic measurements.

It is evident from the description of sensitivity requirements of the GC/C/IRMS that efficient methods are necessary for extracting and purifying individual PAH from environmental samples in sufficient quantities for isotope measurements. An important additional prerequisite of the extraction and isolation methods, is that they do not fractionate (i.e to preferentially enrich or deplete the compounds of interest in ^{13}C) the carbon isotopes at any stage during processing. In general, the steps followed prior to GC/C/IRMS of environmental samples include:

(1) extraction and isolation from a sample matrix

(2) purification and separation of the compounds or compound fractions of interest from the matrix, and

(3) detection, identification and quantitation of the purified compounds.

PAH analysis of environmental samples can therefore be cumbersome and require many steps. Since there are many steps involved in the separation and purification procedures, it is imperative that great care be exercised to avoid contamination during sampling and processing. Unlike most other quantitative organic analysis, authentic isotope PAH standards are not available. Hence one of the initial objectives of this study was to develop a set of PAH isotopic standards for routine instrument calibration and other tests. Various extraction and purification methods were investigated and the adopted methods

were tested for maintenance of isotopic integrity.

The following describes the materials and methods used initially to perform various preliminary investigations followed by a description of the procedures adopted for the collection, extraction and purification of individual PAH from environmental samples. Finally, instrument procedures for GC, GC-MS, and GC/C/IRMS analyses are outlined.

2.2 Materials:

(a) All glassware were washed in hot water with detergent and rinsed in triplicate with distilled water. They were then fired at 350°C overnight and finally solvent washed with equal volumes of methanol, acetone and dichloromethane.

(b) Cellulose thimbles, Whatman single layer (33 x 80 mm), were pre-extracted in Soxhlet units using 5% methanol-dichloromethane, 1% methanol-dichloromethane and pure dichloromethane for 3 hr at five cycles per hour.

(c) Glass distilled solvents (Anachemia) were redistilled and checked for purity by concentrating 200 ml to 20 µl and injecting 1 µl on a GC-FID and GC-MS using the same temperature program: 35 to 250°C at 4°C/min and from 250 to 280°C at 10°C/min.

(d) Copper powder (250 µm) was activated by stirring in concentrated hydrochloric acid and allowed to settle for five minutes. The copper was then washed under vacuum with distilled water followed by methanol and distilled dichloromethane. Copper remained active for up to three weeks when stored at -20°C, in dichloromethane.

(e) Standards and pre- and post-extracted samples were stored at -20°C.

(f) All column chromatography (purification) was performed using 50 cm x 1.0 cm columns with sintered glass filters, except where otherwise specified.

2.3 Preparation of the pure PAH isotopic standard:

PAH solid standards (> 99% purity) were purchased from Supelco, Inc. (Bellefonte, PA) and stored at -20°C. The carbon isotope ratio of each compound was initially determined using conventional isotope ratio mass spectrometry following a modification of a technique described by Sofer (1980). Pyrex tubing 6 mm I.D. was cut into 20 cm lengths, sealed at one end and fired in a muffle furnace at 570°C. After cooling, 2 mg of each compound in triplicate was weighed into these cleaned tubes together with about 1.5 g of pre-fired copper oxide. Distilled dichloromethane was used to transfer some of the high molecular weight compounds whenever difficulties were experienced in transferring the pure standard quantitatively into a combustion tube. Prior to sealing each tube, the solvent was evaporated using a stream of dry nitrogen in a darkened fumehood. The individual tubes were then evacuated using a high vacuum line and sealed. Before combustion the tubes were hand shaken to thoroughly mix the sample and copper wire for more complete combustion. The tubes were then loaded in a stainless steel block and combusted at 570°C, overnight and allowed to cool slowly inside the oven. Following combustion, the resultant carbon dioxide was purified cryogenically on a high vacuum line using a tube cracking system similar to that described by DesMarais and Hayes (1976). The quantity of purified CO_2 produced was measured manometrically and collected into pre-evacuated sample holders. Determination of isotope ratios was performed using a Finnigan-Matt 252 or a VG Optima stable isotope ratio mass spectrometer.

To test for complete combustion at 550°C, a subset of standards (Pa, A, Fl, Py,

BaA, BbF and BaP) was taken through the above procedure, with the exception that pyrex tubes were replaced with silica glass tubes and combustion was performed at 850°C overnight. For GC/C/IRMS standardization and calibration, a solution of 14 PAH, with nominal concentrations of 560 ng/µl was prepared by weighing approximately 2.8 mg of each compound and dissolving them in 5 ml of distilled hexane.

2.4 Isotope fractionation due to sample work-up:

Isotopic fractionation as a result of sample loss during Soxhlet extraction and chromatographic purification was investigated using two separate solutions of pure PAH standards (Solution I = F, Pa, BaA and BbF, Solution II = Pa, A, Fl and Py). Three to four mg of each compound was weighed into precleaned 10 ml volumetric flasks and dissolved in distilled hexane. Ten µl of the prepared mixtures were added to 15 g portions of sterile sediments that had been exhaustively extracted with distilled dichloromethane. These spiked sediments were then extracted and purified using the procedures outlined in Figure 12. The recovery of each compound was determined using calibration curves constructed on the GC-FID and GC-MS using a range of concentrations of standard PAH.

2.5 Effects of volatilization and photolysis on the $\delta^{13}C$ of PAH:

Isotopic fractionation due to volatilization was investigated by evaporating mixtures of individual PAH under nitrogen at 25°C. Possible isotopic alterations due to volatilization were also assessed in a high temperature water bath at 100 and 150°C

Figure 12. Extraction and purification procedures adopted for the isolation of PAH from sediment and source samples which were also shown to maintain the isotopic integrity of pure PAH standards.

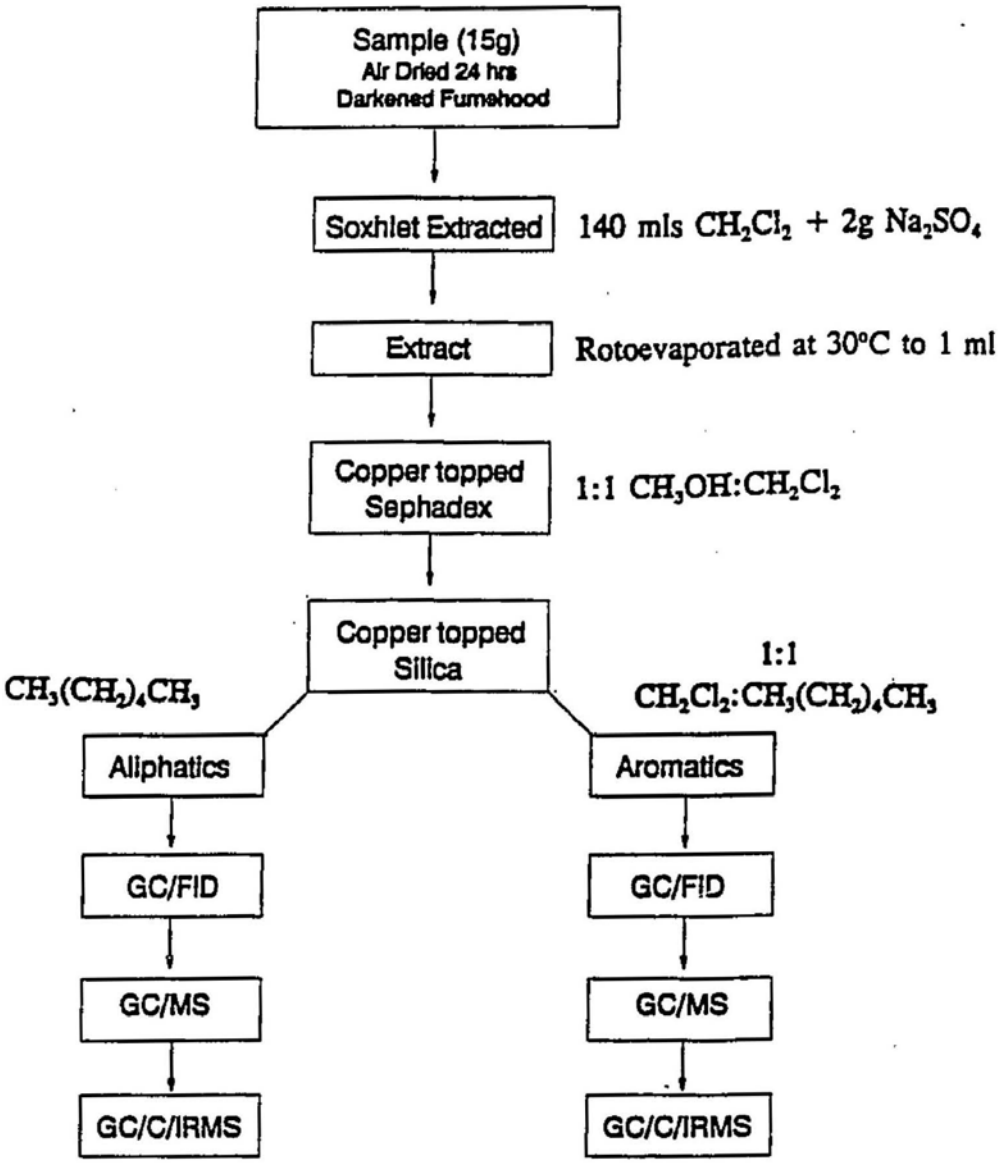
Sample (15g)
Air Dried 24 hrs
Darkened Fumehood
Soxhlet Extracted
140 mls CH_2Cl_2 + 2g Na_2SO_4
Extract
Rotoevaporated at 30°C to 1 ml
Copper topped Sephadex
1:1 $CH_3OH:CH_2Cl_2$
Copper topped Silica
$CH_3(CH_2)_4CH_3$
1:1
$CH_2Cl_2:CH_3(CH_2)_4CH_3$
Aliphatics
Aromatics
GC/FID
GC/FID
GC/MS
GC/MS
GC/C/IRMS
GC/C/IRMS

respectively for 30 minutes.

Similarly, the isotopic effect during photolytic oxidation of residual PAH was evaluated in a number of separate experiments. First, 2-4 mg of five preselected solid PAH (Na, Ace, Pa, Py and BaP) were exposed separately to sunlight and air for 30 hours at 27°C. At the end of this experiment, the PAH were mixed and taken up in 10 ml of dichloromethane for analysis. Further extended photolytic experiments were performed with a mixture containing 3 mg of A, Fl, Py and BbF, dissolved in 5 ml of cyclohexane. This mixture was divided into 12 equal portions and duplicate solutions were exposed to direct sunlight for 0, 4, 8, 24, 36 and 48 hr, at temperatures between 12 and 14°C. Another mixture, containing 3-4 mg of Na, F, Ace, Pa, A, Fl, Py, and BaA was dissolved in 10 ml of dichloromethane. Ten 200 µl aliquots of this solution were then transferred to 2 ml clear air tight glass vials. The vials were sealed and exposed in duplicate for 2, 4, 6, 8 and 10 hr, to direct sunlight at temperatures between 24-27°C. Duplicate unexposed controls were kept at -20°C in the dark. Anthracene is known to be highly sensitive to photolytic degradation reactions and any isotopic anomalies associated with such degradation processes should be reflected in experiments using this compound (Bjorseth and Ramdahl, 1983). Several tests were also conducted in which anthracene, dissolved in hexane, cyclohexane and in the absence of a solvent substrate was exposed (in duplicate) to direct sunlight for 0, 2, 4, 6, and 8 hr, at temperatures between 24-26°C.

2.6 Isotopic alterations due to microbial degradation:

The isotopic effects associated with the microbial degradation of two pure PAH were assessed using compound specific pure *Pseudomonas* species. Naphthalene degradation and utilization was investigated using *Pseudomonas putida*, Biotype B ATCC

17484 using a modification of procedures described previously (Barnsely, 1975; Weissenfels et al., 1990). A minimal salts medium (MSM) containing 6.5 g/l $CaCl_2.2H_2O$, 0.01 g/l $ZnSO_4.7H_2O$, 0.04 g/l $CuSO_4.5H_2O$, 0.04 g/l $CoCl_2.6H_2O$, 0.05 g/l $NaMoO_4.2H_2O$, 0.25 g of yeast extract and 1 ml of trace element solution was prepared and sterilized at 121°C, for 15 minutes. After cooling, 20 ml of this solution was transferred into eight sterilized 100 ml conical flasks together with an 20 mg/l solution of pure naphthalene dissolved in dichloromethane. These flasks were plugged with sterilized foam plugs and allowed to stand at room temperature until the solvent evaporated. Prior to inoculation the plugs were replaced and any residual solvent was removed under pure nitrogen. The flasks, with the exception of the control samples, were then inoculated with a suspension of pure *Pseudomonas putida*, and grown in the presence of naphthalene, as a sole carbon source, giving an initial optical density (OD) of 0.025. The samples were then incubated in duplicate at 25°C, on a orbital shaker, in the dark, for 0, 6, 12, and 24 hr together with two controls each containing 20 ml of the MSM and naphthalene. Bacterial growth was recorded by measuring the OD at 600 nm, at the end of each sampling period. Growth was terminated by the addition of distilled dichloromethane. The residual naphthalene was recovered by repeated washing with equal volumes of distilled dichloromethane in a separation flask. The extract was then concentrated and purified on a silica column. Following purification, the sample was concentrated to 20 µl for GC/C/IRMS determination. Because rapid growth occurred during this initial experiment, the above procedure was repeated by incubating samples at 0, 2, 4, 6, and 8 hr with 120 mg/l of naphthalene as a sole carbon source.

Degradation and utilization of fluoranthene was studied using *Pseudomonas paucimobilis* strain EPA 505 developed by Mueller et al (1990). The procedures adopted were similar to the naphthalene study except on this occasion, 30 ml of a Bushnell-Hass MSM (Mueller pers. comm.) was added to a flask containing 196 mg/l of pure fluoranthene which had been dissolved in acetone. The contents were sonicated for two minutes prior to inoculation. The samples were incubated at 30°C in the dark and growth was again monitored by measuring the OD at 600 nm. The degradation and utilization of fluoranthene was accompanied by the appearance of a bright orange colour which was attributed to the fluoranthene metabolites. Growth was terminated by the addition of dichloromethane and the residual fluoranthene was recovered using the methods previously described for naphthalene.

2.7 Sample collection:

2.7.1 Sediments:

Sediments were collected in Conception Bay using the Department of Fisheries and Oceans Marinus and FRV Shamook, while samples from the St. John's Harbour were obtained using the CSS Hudson from the Department of Fisheries and Oceans and the Karl & Jackie from Memorial University of Newfoundland. During the summer 1992, cores were collected from various sites located along the deep central basin of Conception Bay (Figure 13) using a box coring device with a 30 cm x 12 cm ID solvent rinsed metal core barrel. Immediately after siphoning off surface water above the sediment, some of the cores were extruded, sub-sampled into 2 cm sections, and stored in precleaned brown

Figure 13. Location of the sampling sites in Conception Bay.

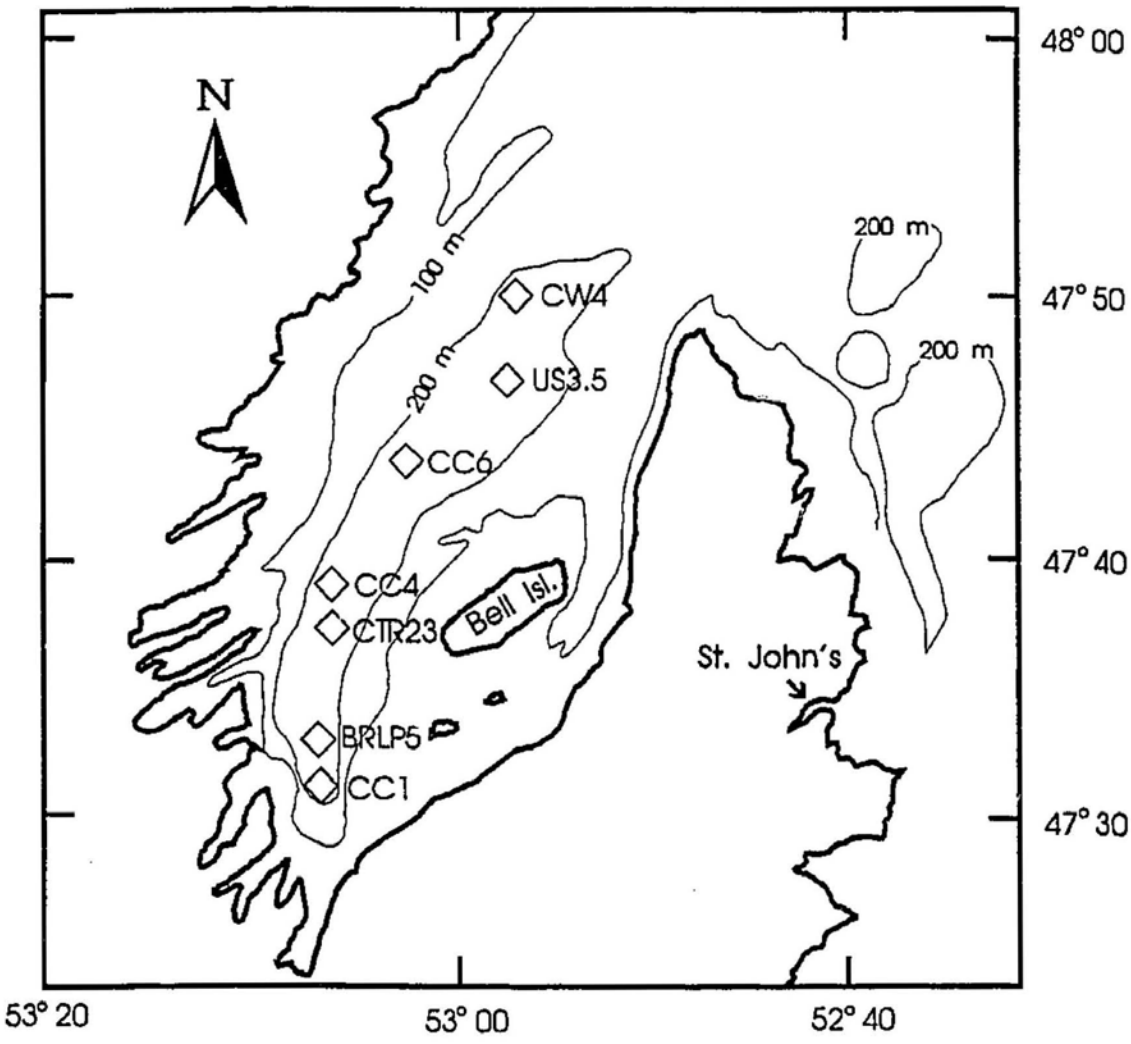
N
100 m
200 m
200 m
200 m
CW4
US3.5
CC6
CC4
CTR23
Bell Isl.
BRLP5
CC1
St. John's
48° 00
47° 50
47° 40
47° 30
53° 20
53° 00
52° 40

glass bottles. Selected cores were stored intact in PVC sleeves in an upright position. Grab samples representing the top few centimetres of sediment were also collected using a precleaned lead weighted shipex grab sampler. These samples were split into two equal sections and stored in pre-fired aluminum foil. All samples and cores were kept on dry ice until returned to the laboratory where they were stored at -20°C, until ready for processing.

Sediment sampling in St. John's Harbour was performed initially in the Fall of 1992 at four sites using a solvent washed Van Veen grab sampler (Figure 10). Samples, representing the top few centimetres of sediment, were obtained from the deep portion in the middle of the Harbour and close to input sources, particularly sewage outfalls and the landfill leachate plume at Robin Hood Bay. A 3.34 m piston core was also obtained from a location adjacent to the sewage outfall at Ouidi Vidi Road. The piston core was initially split into two equal sections and one section was archived at -20°C. The remaining section was sub-sampled at 10 cm intervals for the first 2 m and every 20 cm for the remaining portion of the core. Five additional Van Veen grab samples were obtained from similar sites within the Harbour and one from outside the Harbour close to Freshwater Bay during the summer of 1993.

2.7.2 Sources:

Source apportionment of PAH in sediments relies on constraining the isotopic signature of the primary input sources in the vicinity of the study sites. Pathways by which PAH reach the sediments can be similarly elucidated by constraining the isotopic signature of secondary source contributions such as road runoff, sewage and atmospheric

particulates. These secondary sources, are postulated to consist of a mixture of primary source inputs, although it is possible that only one of the primary sources could dominate in a secondary source. Table 6, lists the potential primary and secondary source contributors sampled during this study. Initially, individual spot sampling was performed to assess isotopic variation within the individual sources. Soots, predominantly representing wood burning sources, were scraped from the inside wall of open fireplaces and inside the stack of wood burning stoves onto precleaned aluminium foil using a solvent washed spatula. A large composite sample was prepared containing 0.5 g each of 26 individual soots collected from open fireplaces and stoves, from the immediate vicinity of St.John's Harbour and Conception Bay. These individual samples were initially weighed and then crushed in a mortar and pestle to produce uniform particle sizes. Vehicle emission soots were obtained by sampling old muffler systems. Thirty mufflers were collected that had obvious soot build-up and a number of individual and composite samples were prepared. Domestic heating furnaces burning #2 fuel oil represent another primary combustion source. Bulk soot samples were collected from the stack interior of these furnaces during servicing and stored in precleaned aluminum foil. Soot sampling from the power generating station in Conception Bay was undertaken by trained personnel from the plant, previously instructed on the various sampling protocols. Six bulk samples, 40 g each, were obtained from various locations inside the hopper system. A composite sample of these soots was prepared by crushing 10 g of each individual sample and pooling to form a homogenous mixture of uniform particle size. All soot samples were later transferred to pre-cleaned glass vials lined with aluminum.

Table 6. The primary and secondary sources identified that may be important contributors of PAH to the sediments of the two study sites. See Appendix G for sample location of some of the fire soots, roadsweeps and snow samples and Appendix H for number of samples collected.

PRIMARY SOURCES	SECONDARY SOURCES
Vehicle muffler soots	Open-road surfaces
Open domestic fireplace soots	Enclosed car park
Wood stove soot	Untreated sewage effluents
Domestic heating furnaces	Roadside snow
Crankcase oil	Atmospheric particulates
Two-stroke outboard motor engines	
Power generating station (PGS)	
Other petroleum products	

The predominant primary petroleum input source identified was used crankcase oil and 10 individual spot samples were directly sampled from car engines using long Pasteur pipettes. Further composite samples (8) were obtained by sampling the waste oil sump of garages in the St. John's area. The isotopic signature of PAH contributions from outboard two-stroke motors were assessed by sampling water from the engines test tanks in outboard motor repair garages. These tanks were initially stirred to mix settled particulates and 500 ml was sampled in pre-cleaned 500 ml mason jars. The isotopic signature of both crude oil and uncombusted #2 fuel oil were also assessed to compare to the signatures of the other petroleum products investigated.

Road sweep samples were obtained by sweeping approximately 1 m^2 of open road surfaces with a solvent washed brush into an aluminum lined dust pan. Prior to transferring to a clean glass vial, unwanted materials such as stones and twigs were removed with tweezers. Surface sweepings from underground car parks with asphalt and cement paved surfaces were also obtained to assess the effects of weathering on open road systems. Isotopic signatures associated with sewage inputs were assessed by grab sampling sewage close to the main sewage outfall in the Harbour. Accumulated roadside snow samples from the winter of 1992-1993 were collected in precleaned 500 ml mason jars. The snow was allowed to melt and dry in open jars at room temperature in a darkened fumehood. The residues were then scraped from the inside of the jars using a solvent washed spatula and transferred to pre-cleaned aluminum foil and mixed homogenously before sieving through a 250 μm sieve.

2.8 PAH extraction and purification:

2.8.1 Extraction:

A number of different solvent extraction methods are available for the extraction of PAH from environmental samples. No standard method exists, but favourable results are obtained for Soxhlet extraction using a range of sediments and solvent ratios (Farrington and Tripp, 1975; Hilpert et al., 1978; Wong and Williams, 1980; Lake et al., 1980; Brown et al., 1980; Macleod et al., 1982; Grimalt et al, 1984; Lichtenthaler et al., 1986; MacLeod et al., 1988). Although comparable results were obtained for some tests using sonication, Soxhlet extraction was adopted in this study, because it is a widely recognised reference extraction method and exhaustive extractions can be achieved for a wider variety of samples when appropriate solvents, sediment:solvent ratios and sample sizes are utilized. However, a number of the intercomparison studies concluded that solvent choice seemed more important than the choice of extraction method (Farrington and Tripp, 1975; Grimalt et al., 1984; Ehrhardt et al., 1991). Initially benzene, alone or in a solvent mixture was the most commonly used extraction solvent, but it has now been replaced by toluene or dichloromethane. Giger and Schaffner (1978) reported good PAH recovery using dichloromethane in a 6 hr Soxhlet extraction period while Grimalt et al. (1984) also obtained comparable results using 2:1 dichloromethane:methanol.

A series of initial experiments were conducted to determine appropriate sample sizes to produce sufficient PAH concentration for GC/C/IRMS analysis and optimize extraction efficiencies. Initially 35 g of partially air dried Conception Bay sediment and road sweep samples were extracted with 160 ml of dichloromethane together with 5 g of

sodium sulfate. Subsequent extraction of the same sample showed that residual PAH remained after the initial 24 hr extraction period. Sample extraction efficiency was evaluated by repeated extraction experiments using crushed and well dried sediments. It was noted that more exhaustive extraction was accomplished when the sediment was stirred in the thimble after 12 hr of extraction. This mixing prevented sample compaction and exposed/unexposed particle surfaces particularly when larger samples were required (i.e., lower concentrations).

The procedure adopted in this study was to air dry 30 g of sediment for 24 hr at ambient temperatures in a darkened fumehood to constant weight. The sample was then crushed in a precleaned mortar and pestle to break up compacted clumps and to produce a homogenous sample. Particle sizing was not performed at this stage in order to prevent unnecessary contact with surfaces that could potentially contaminate the sample and to avoid loss of very fine PAH containing particulates. A sub-sample, 15-17 g for Conception Bay samples and 4-5 g for St. John's Harbour samples, was Soxhlet extracted with 2 g of precleaned sodium sulfate, using 140 ml of dichloromethane, for 24 hr at three cycles per hour in precleaned extraction thimbles. Following extraction, the extracts were concentrated to 1 ml in a Buchii rotary evaporator at 30°C. The weight of the extract was determined by drying the sample to constant weight under nitrogen. Similar procedures were used for the extraction of PAH from fireplace soots, car soots and road sweep materials. Separate particle size fractions (<63 μm, <125 μm and <250 μm) of the road sweep material were extracted in order to determine the PAH concentration of the various size fractions. Five gram portions of soot materials were normally extracted and

diluted when necessary prior to column chromatography.

2.8.2 Purification:

PAH purification was carried out following a modification of gel permeation and adsorption chromatographic procedures described previously (Youngblood and Blumer, 1975; Giger and Schaffner, 1978; Pruell et al., 1984; Cretney et al., 1987). Various combinations of these chromatographic separations were extensively tested for optimum sample purification before adopting the procedure outlined in Figure 12. Initially extracts were purified using a combination of alumina and silica columns. The resultant aromatic fraction, when injected on the GC, showed significant interference of the PAH by a range of presumably biogenic compounds. This problem is especially severe for the Conception Bay sediments. Giger and Schaffner (1978) demonstrated that these interfering materials can be eliminated by the use of Sephadex LH-20 in a simple coarse prefractionation technique. LH-20 is a methylated cross linked dextran which has the ability to separate aromatic compounds by ring size exclusion (Talarico et al., 1965; Streuli, 1971). A 1:1 mixture of dichloromethane:methanol was found to be a suitable alternative to the 1:1 benzene:methanol used by Giger and Schaffner (1978). After Sephadex and silica chromatography, road sweep extracts remained highly pigmented and contained very few resolved PAH. Extracts were dominated by the presence of a UCM, which is attributed to the presence of multi-branched compounds. Further purification steps to separate the UCM and improve peak resolution were attempted with little improvement (e.g., Ramos and Prohaska, 1981). Alumina chromatography (7.5% deactivated, hexane) was also performed which successfully removed the pigments, but there was no significant

improvement in the resolution of the compounds of interest.

The following general procedures were adopted for the purification of sediments, fireplace soots, car soots and road sweep samples. Sephadex columns were prepared by conditioning 5 g of Sephadex LH-20, 25-100 mesh in 30 ml of 1:1 methanol:dichloromethane overnight (the degree of swelling is affected by the solvent choice). This was then transferred to a column containing 0.5 g of acid washed sand, previously rinsed with dichloromethane. Purification of the Sephadex was carried out using 3 x 30 ml volumes of 1:1 dichloromethane:methanol and the purity of the Sephadex was verified by fluorometry (310/360 nm, excitation/emission wavelengths) using the final 3 ml eluted from the column. Sample extracts were taken up in 0.5 ml of 1:1 methanol:dichloromethane and added to the column (and rinsed with two further 0.5 ml portions). Concentrated samples were diluted prior to column chromatography to prevent column overload. Elution of the aromatic fraction was traced by collecting 3 ml fractions of the eluent and reading the fluorescence at 310/360 nm excitation/emission wavelengths. Since fluorescence was detected only in the fifth fraction, the initial 12 ml eluent were discarded. The next twenty 3 ml fractions containing the aromatic hydrocarbons were collected at an elution rate of 1.5-2.0 ml/min. Ring size elution was traced using synchronous fluorescence (Wakeham et al., 1977) on certain fractions from 275/300 nm to 450/475 nm excitation/emission to obtain the maximum fluorescence for each ring size. The mono-aromatics show a maximum excitation at 280-290 nm, 2-ring at 310-320 nm, 3-4-rings at 340-380 nm, while maximums for 5-ring compounds occur at >400 nm. These fractions were then combined and concentrated to near dryness at 30°C. The

remaining methanol:dichloromethane was displaced by hexane by evaporating under nitrogen flow. The reproducibility of this procedure was tested using a diverse range of environmental samples with varying PAH concentrations.

Silica gel columns were prepared by adding 10 g (14 g for road sweep) of silica gel (Aldrich 100-200 mesh) to 50 ml of dichloromethane. The dichloromethane was eluted and displaced by an equal bed volume of hexane. Column background was again checked by fluorometry. The total hydrocarbon fraction was taken up in 0.5 ml of hexane (and rinsed with two further 0.5 ml portions) and added to the column. The aliphatics were eluted with 30 ml of hexane and the aromatics with 60 ml of 1:1 dichloromethane:hexane. Larger volumes of dichloromethane:hexane (80 ml) were used for more concentrated samples. Tests, using pentane and toluene to separate the aliphatic and aromatic fractions were also conducted and, although comparable separation efficiencies were achieved, the use of hexane:dichloromethane was preferred because of the relatively higher boiling point of toluene. Similar to the gel permeation chromatography, the elution of the aromatics was traced using fluorescence at 310/360 nm (excitation/emission). Again, fractions showing fluorescence were combined and concentrated to dryness. The sequence of the Sephadex and silica column chromatography can be alternated with no significant difference in the efficiency of the purification. Prior to GC and GC-MS injection, appropriate volumes of hexane containing 40 ng/µl of phenyl hexane (internal standard) were added to each sample.

Elemental sulphur present in large quantities in Conception Bay sediments was removed by the addition of 5 g of activated copper powder to the top of the Sephadex and

silica columns. Sulphur removal is important, since it can lead to erroneous results in GC-MS analyses (Blumer, 1957). Initially, a separate copper column containing 20 g of copper granules activated by the addition of 0.25 N or concentrated HCl proved inadequate for the removal of elemental sulphur. This incomplete removal was attributed to the short contact time and small surface area between the copper granules and sample extract. Tests have shown that elemental sulphur can also be effectively removed by adding similar quantities of activated copper powder to the extraction flask after initial sample reduction. A procedural blanks in which 2 g of sodium sulfate were Soxhlet extracted and purified by column chromatography was run with every 10 samples. The efficiency of the adopted extraction and purification methods at recovering mixtures of pure PAH was assessed using the procedures described in section 2.4.

The aromatic fraction of crankcase oil was purified using a two-step column chromatographic procedure (silica gel and Sephadex). Approximately 50-60 mg of crankcase oil was dissolved in 0.5 ml of hexane. This was then carefully added to a 350 mm x 16 mm ID chromatographic column containing 35 g of silica gel. The aliphatic fraction was initially eluted with 160 ml of hexane and the aromatic fraction was collected with 180 ml of 1:1 dichloromethane:hexane. The aromatic fraction was then concentrated to 2 ml by rotary evaporation and the remaining hexane:dichloromethane was replaced with 0.5 ml of dichloromethane:methanol under nitrogen. The extract was then added to a Sephadex column, identical to the column used for previous purification studies. The aromatics were fractionated into 3 ml portions with UV light detection. The aromatic fraction can be clearly separated into three pigmented fluorescent bands with varying

intensity. The first intensely pigmented band was eluted in two 3 ml fractions, while the second band with less pigmentation was eluted in a single 3 ml volume. The final fluorescent band was eluted in 4 x 3 ml and after GC-MS analysis these latter four fractions were combined and concentrated. Subsequent gas chromatography-mass spectrometry (GC-MS) analysis indicated that the first band consisted predominantly of a significant UCM with poor peak resolution, while the second was made up of a mixture of well resolved low molecular weight PAH and a UCM. The third band consisted of well separated PAH ranging from two to five ring compounds (Figure 14). Repeated analysis of individual crankcase oil samples indicated that the separation and thickness of these individual bands was dependent on oil exposure time within engines. Older oils tended to produce well separated bands and normally had higher concentrations of parental PAH. The isolation and purification of the aromatic fractions from crude oils and #2 fuel oil was also carried out using the procedures just outlined.

The PAH were extracted from the outboard two-stroke engine water sample by extracting 500 ml of the sample in a separatory funnel with three 150 ml portions of dichloromethane. The extract was then concentrated to 2 ml and purified using the technique described above for crankcase oils.

2.9 Sample analyses by GC-FID, GC-MS and GC/C/IRMS:

2.9.1 Sample analyses by GC-FID and GC-MS:

Prominent PAH compounds were initially separated, identified and quantified using a Perkin Elmer 8310 gas chromatograph equipped with a flame ionization detector and a 30 m x 0.25 mm ID and 0.25 μm film thickness SPB-5 [Supelco] capillary column.

Figure 14. The total ion chromatograms (TIC) of the crankcase oil PAH fractions separated using Sephadex LH-20.

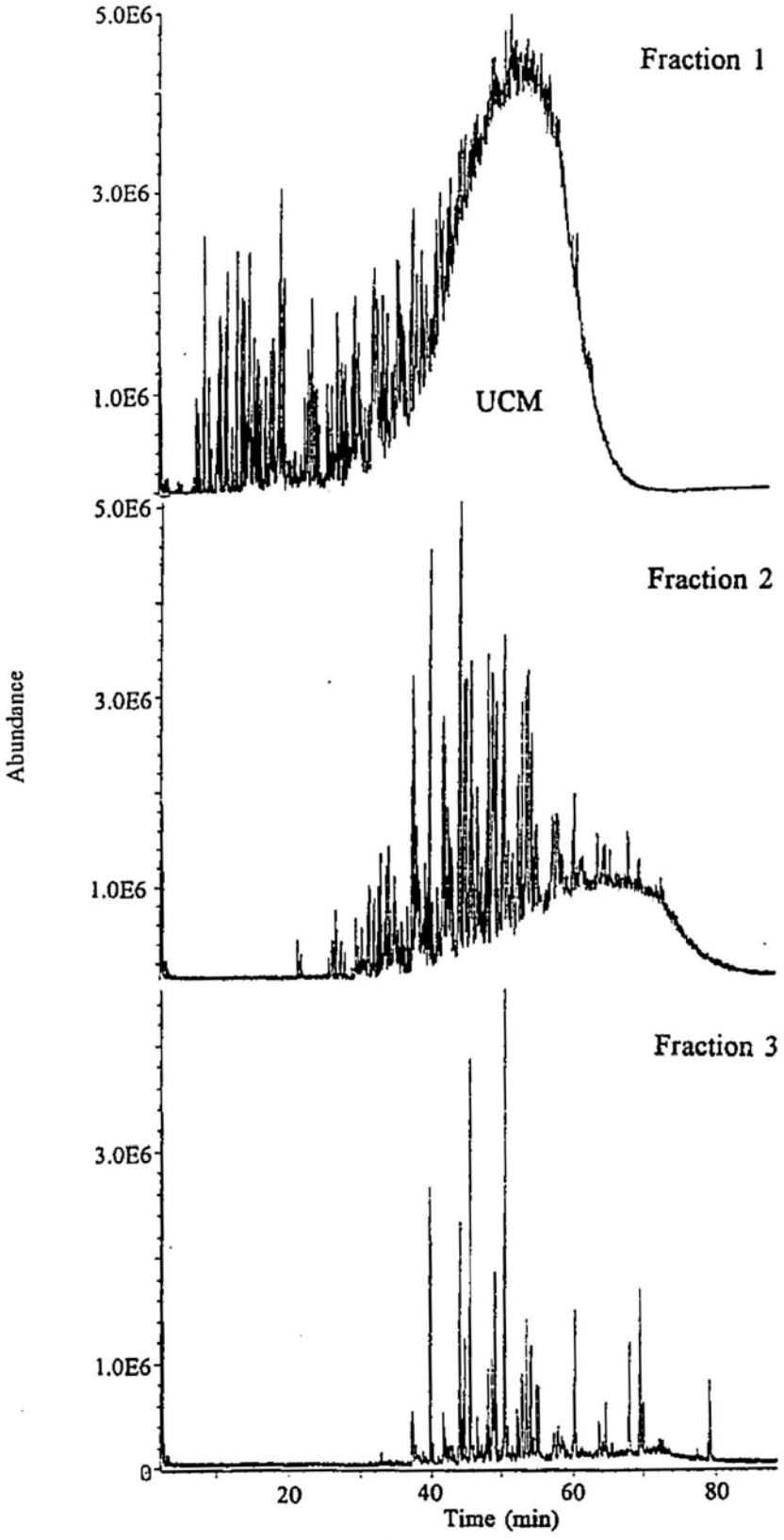
5.0E6
3.0E6
1.0E6
Fraction 1
UCM
5.0E6
3.0E6
1.0E6
Fraction 2
Abundance
3.0E6
1.0E6
0
Fraction 3
20
40
60
80
Time (min)

A 1 µl sample was injected splitless (50 sec) into a heated (285°C) split/splitless injector and the oven was programmed from 35 to 250°C at 4°C/min and from 250 to 280°C at 10°C/min. The flame ionisation detector (FID) was heated to a temperature of 300°C. Subsequent tests using the sediment samples demonstrated that the best resolution was achieved using a 30 m x 0.25 mm ID and 0.12 µm film thickness CPSil-5 capillary column (Chrompak). Individual PAH quantification in sediments and source samples was performed using external calibration curves constructed using a range of concentrations of pure PAH standards injected on the GC and GC-MS. The performance of the FID was assessed using an internal phenyl hexane spike. A 5.6% standard deviation was obtained in FID response with repeated injections (20 x 1µl) of this internal standard. Parental PAH were initially identified using NBS 1647(a) and confirmed by GC-MS using a Hewlett Packard model 5890B mass selective detector (MSD) and a 25 m x 0.25 mm ID and 0.12 µm film thickness CPSil 5 column (Hellou et al. 1992). Methylated compounds were identified by injecting individual methyl standards and their presence was confirmed using GC-MS. The identification of retene and other unknown compounds where authentic standards are not available were carried out by comparison of the spectra with literature spectra.

2.9.2 Sample analyses by GC/C/IRMS:

The GC/C/IRMS was tested using a wide variety of "reference" standards that included the previously prepared pure PAH mixtures (Section 2.2). The CO_2 reference gas was calibrated relative to PDB using primary standards NBS 22-graphite and NBS 19-TS limestone, and a secondary carbonate standard provided by Dr. M. Wilson, Memorial University of Newfoundland. As previously described, the capability of the GC column to resolve individual compounds is an important requirement in performing reliable isotopic measurements. Compared to OV-1 and SPB-5 capillary columns, superior

separation and sensitivity was achieved using a CPSil-5 capillary column (30 m x 0.25 mm ID and 0.12 mm film thickness). As a matter of routine procedure, FID traces were first obtained before performing GC/C/IRMS analysis. The initial FID measurement enabled the determination of optimum injection volumes and retention time range of the compounds of interest (i.e., the sampling window). Eluates were directed by the heart split valve to the FID before and after the selected window. During this time (i.e., before and after sample window) a series of CO_2 reference gas pulses were allowed into the mass spectrometer at 30 second intervals. For the samples of interest, the corresponding CO_2 eluates (the CO_2 produced as a result of combusting the individual compounds in the combustion interface) are diverted to the mass spectrometer where the ion currents of masses 44, 45 and 46 were measured simultaneously by three fixed Faraday cups with matched time constants (Figure 11). A variety of temperature programs, normally terminating with a 10 minute column clean-up period at 280°C were used to isolate the compounds of interest. Optimum separation (to minimise co-elution effects) for 3 and 4-ring compounds was achieved using 10°C/min between 35-150°C, and 4°C between 150-280°C/min for 10 minutes. However, due to peak broadening, separation of higher molecular weight 5-ring compounds was best achieved using temperature programs with rapid initial ramp rates. The mass spectrometer was tuned to give optimal sensitivity and reference gas pulse injections were set to produce a major ion beam response of between 5.5-6.5 E-9 Amps for the reference gas pulse injections. Prior to injection, samples with complex backgrounds were taken up in appropriate volumes of a solution containing one aromatic (acenaphthalene) and two aliphatic (C_{21} and C_{25}) internal standards whose isotopic values had been previously determined using conventional isotope techniques and GC/C/IRMS. These internal standards were strategically selected to appear as close as possible at the beginning, middle and end of the chromatographic run and so as not to

interfere with the compounds under investigation. The addition of these internal standards enabled instrument performance and reliability of background substraction to be independently assessed in complex sample matrices. Significant error in reported values can result if the sample peak is small and the background is large, especially if the $\delta^{13}C$ of the background is dramatically different from that of the sample peak of interest. Elevated backgrounds were particularly prevalent in the crankcase oil samples, but the effects of these backgrounds were reduced using the column purification procedures described in section 2.8.2. An automatic background correction on samples with significant backgrounds can be carried out using procedures described elsewhere (e.g., VG Isotech application note No. 19). This procedure involves calculating background 45/44 and 46/44 ratios by selecting specific background ratio points along the chromatogram and fitting them to polynomial curves. These ratios together with the measured mass 44 background area are used to estimate the corresponding 45 and 46 background areas. The resultant three background areas are used to estimate the total peak areas calculated from the 44, 45 and 46 traces. However an initial investigation of this "automatic" procedure revealed that, in some cases the true $\delta^{13}C$ values of the three internal standards could not be simultaneously recovered. This is true even when the internal standards are not coeluting with any compound. Manual background correction was performed in these cases. This was undertaken in two stages, the first stage entailed manual selection of new background points between the first two internal standards (17 - 50 minutes) and then fitting a new polynomial background trace (45/44 and 46/44) until the $\delta^{13}C$ of the two internal standards were as close as possible to their "true" values. The $\delta^{13}C$ of the compounds of interest adjacent and between these two internal standards were then reported. The $\delta^{13}C$ of the samples peaks on the second portion of the chromatogram (portion containing the second and third internal standards 40 - 70 minutes) were obtained

using the same procedure described above except that the latter two standards were used to verify the validity of the background trace.

Problems of co-elution were reduced by optimizing sample purification and chromatographic conditions. However, co-elution was found to occur in some complex samples and whenever the peaks of interest could not be clearly elucidated, the $\delta^{13}C$ of these compounds were not reported. In general, the dilution factor was such that a 1 µl injection of sample or standard contained 10 nanomoles of the most abundant PAH. With a splitless injection, the most abundant compound in a 1 µl injection yielded a major ion beam (i.e., mass 44) signal of approximately 1E-8 Amp.

2.10 Bulk δ13C, total organic carbon, metal and grain size analysis of sediments:

The following additional analyses were performed on the Conception Bay sediments in order to help constrain important primary input sources. Total organic carbon (TOC) and bulk $\delta^{13}C$ of the organic fraction were determined using conventional isotope measurement techniques. Carbonates were removed from air dried sediment (2.0-2.5 g) by the addition of 20% HCl solution overnight. Following decarbonation, samples were repetitively washed to neutrality with deionized water and dried overnight at 20°C. For TOC analysis 100-150 mg was taken through the procedure outlined in section 2.3. The quantity of CO_2 produced by combustion of sediments was measured manometrically. Trace metal analysis using X-Ray Fluorescence spectroscopy (XRF) on 5 g of homogenously mixed sediment (<63 µm) pressed into pellets was also performed. Sediment particle size determinations were carried out using approximately 30 g of post extracted sediments. Sieves ranging in size from >1000 µm to <63 µm were stacked and shaken on a mechanical shaker for 15 minutes. The quantity retained by each sieve was carefully weighed and calculated as a percentage of the total weight recovered.

3.0 RESULTS

3.1 Accuracy and precision of CSIA determinations using standard and field samples:

The mean and standard deviation* of repeated isotopic measurements of PAH standards using conventional IRMS and GC/C/IRMS analyses are summarized in Figure 15. Replicate measurements with conventional IRMS showed a precision ranging between 0.03 and 0.10‰, while the precision for thirty four repeated injections using GC/C/IRMS ranged between 0.25 and 0.39‰ (Table 7). Taking the isotopic values of the conventional IRMS measurements to be the "actual" or "true values" of the standard PAH, the accuracy+ of the GC/C/IRMS determinations for Pa, A, Fl, Py, BaA and BbF ranged between 0.01 and 0.30‰; Na, Ace, F and BaP analyses have accuracies that ranged between 0.41 and 0.57‰.

The precision of GC/C/IRMS analyses of individual PAH extracted from field samples was determined using a Harbour sediment sample, open fireplace soot and a car muffler soot. The mean and standard deviation of 10 x 1 µl replicate injections of these samples run under similar operating conditions along with internal standards are shown in Figures 16, 17 and 18 and summarized in Table 7. $\delta^{13}C$ values of the individual compounds were manually as well as automatically background corrected. The variation in the $\delta^{13}C$ precision of the individual PAH in the sediment sample ranged between 0.40

---

* All reported precisions are 2σ standard deviations unless otherwise specified.
+Accuracy is reported as the mean deviation per mil (‰) of the GC/C/IRMS values from the conventional values for the pure PAH.

Figure 15. A comparison of the mean $\delta^{13}C$ values obtained for the PAH pure standards using conventional methods of analysis and GC/C/IRMS. Error bars = standard deviation (2σ; 95% CI). Na = Naphthalene, Ace = Acenaphthene, F = Fluorene, Pa = Phenanthrene, A = Anthracene, Fl = Fluoranthene, Py = Pyrene, BaA = Benz(a)anthracene, BbF = Benzo(b)fluoranthene, BaP = Benzo(a)pyrene.

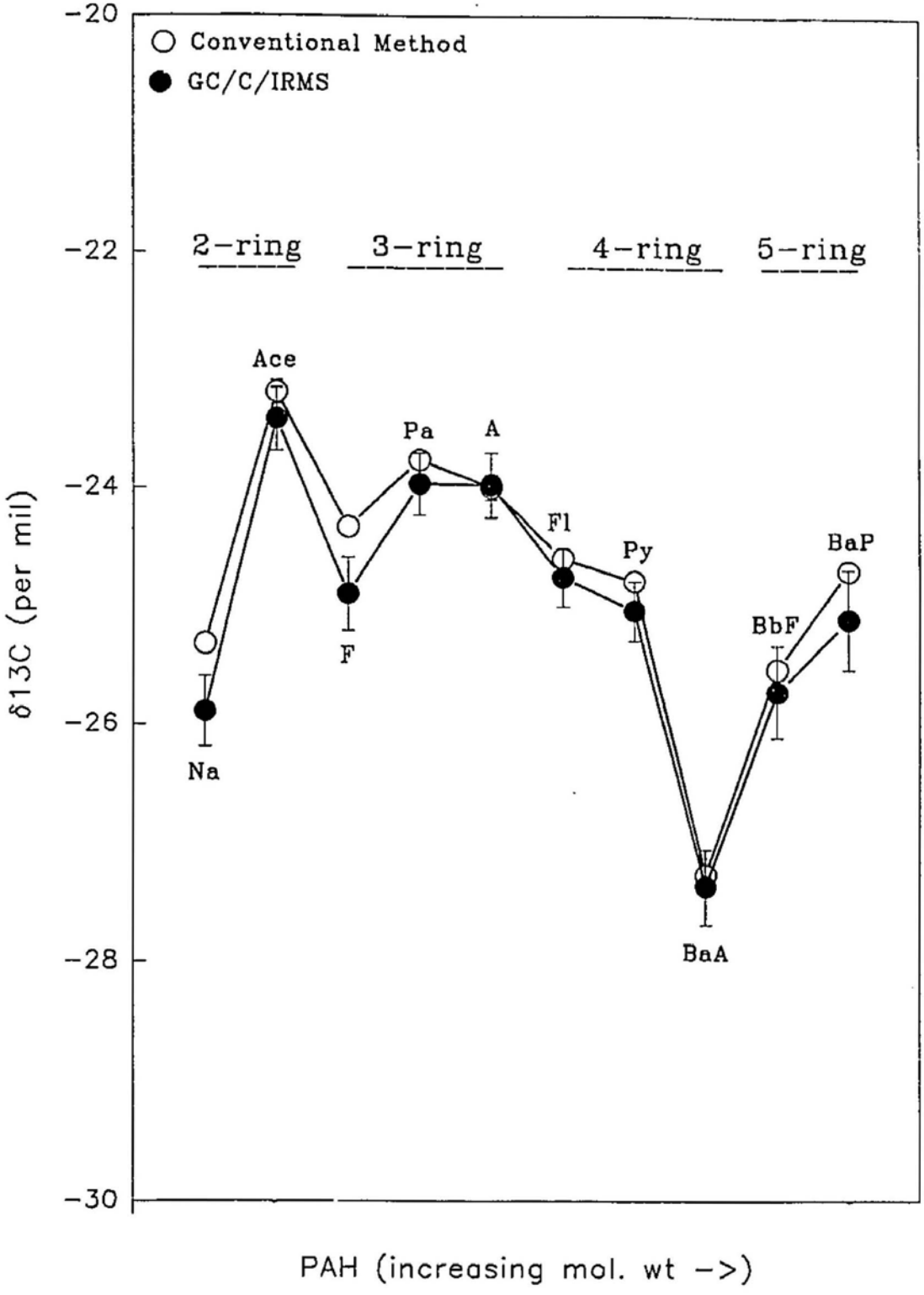
Conventional Method
GC/C/IRMS
2-ring
3-ring
4-ring
5-ring
Ace
Pa
A
Fl
Py
BaP
BbF
F
Na
BaA
-20
-22
-24
-26
-28
-30
δ13C (per mil)
PAH (increasing mol. wt ->)

Table 7. Summary of precision and accuracy ranges observed for GC/C/IRMS measurements of PAH from standard and field samples

Sample	Precision Range (‰)*	Internal Standard Accuracy (‰)**	Accuracy (‰)**
PAH standard:	0.25 to 0.39	0.11 to 0.20	0.01 to 0.57
Field samples:			
Sediment	0.40 to 0.51	0.16 to 0.21	
Fireplace soot	0.13 to 0.64	0.07 to 0.23	
Car soot	0.26 to 0.85	0.30 to 0.80	
Acenaphthalene	0.16 to 0.19		
C_{21}	0.13 to 0.80		
C_{25}	0.22 to 0.24		
Recovery expt.:	0.07 to 0.38		
Photolysis:			
Fl, Py and BbF in cyclohexane:	0.01 to 0.26	0.05 to 0.16	
Anthracene in cyclohexane:	0.06 to 0.25		
F, Pa, Fl and Py in dichloromethane:	0.01 to 0.34	0.01 to 0.18	
Acenaphthalene in dichloromethane:	0.11 to 0.31		
Repeat Anthracene in:			
hexane	0.07 to 0.23		
cyclohexane	0.06 to 0.20		
solid	0.07 to 0.37		
Microbial:			
Naphthalene		0.01 to 0.09	
Fluoranthene		0.01 to 0.11	

* = precision is 2σ standard deviation

** = relative to their respective conventional IRMS values

Figure 16. Mean and standard deviation (2σ) of 10 x 1µl replicate injections of 3, 4 and 5-ring PAH isolated from a Harbour sediment sample, along with internal standards (IS) used to test the reproducibility of the GC/C/IRMS at measuring the $\delta^{13}C$ of field samples. Ace = Acenaphthene, Pa = Phenanthrene, A = Anthracene, Fl = Fluoranthene, Py = Pyrene, MFl-Py = Methyl Fluoranthene-Pyrene, BaA = Benz(a)anthracene, Chy = Chrysene, BFl = Benzofluoranthenes and BaP = Benzo(a)pyrene.

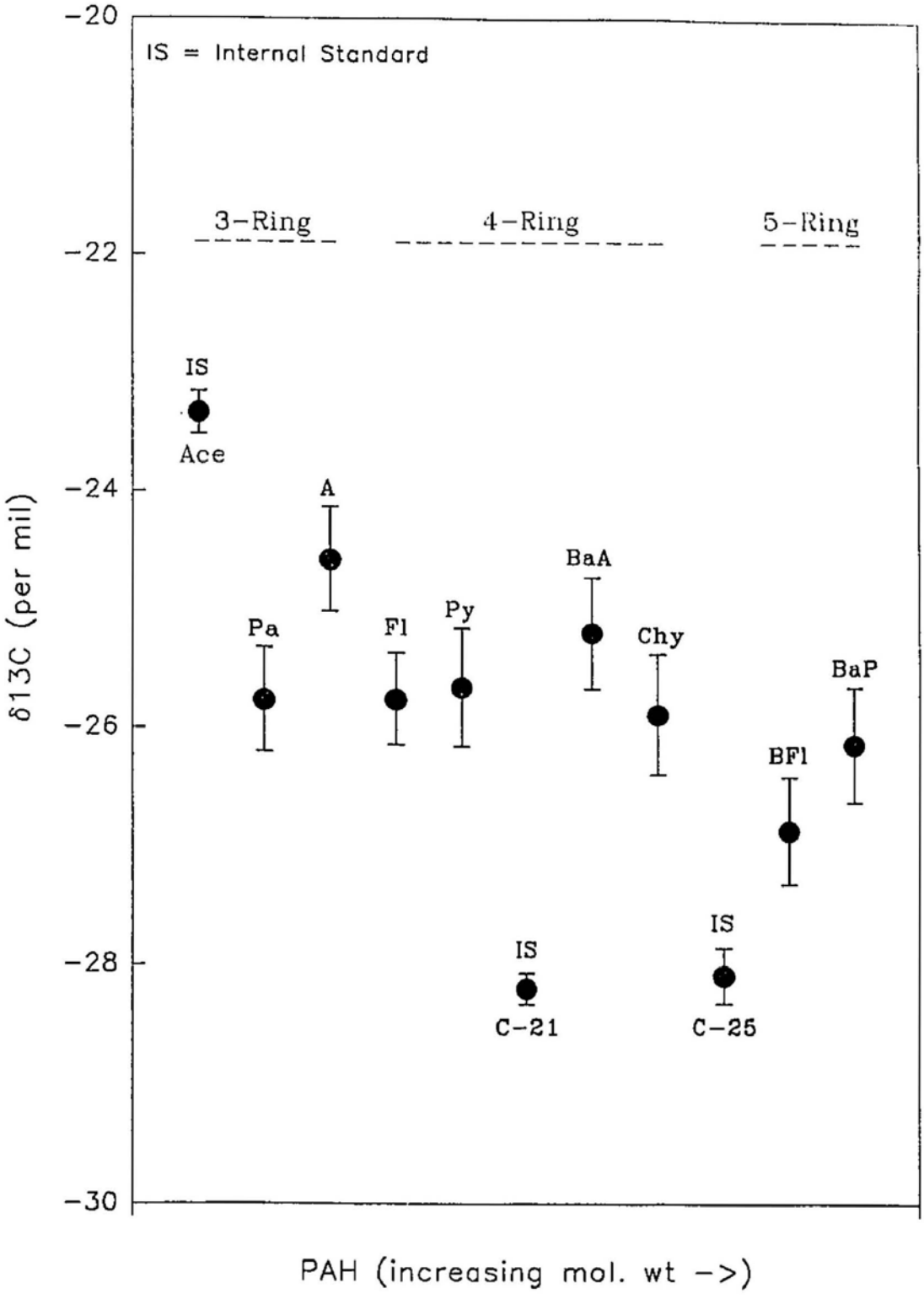
IS = Internal Standard
3-Ring
4-Ring
5-Ring
−20
−22
−24
−26
−28
−30
δ13C (per mil)
IS
Ace
A
Pa
Fl
Py
BaA
Chy
BaP
BFl
IS
C-21
IS
C-25
PAH (increasing mol. wt ->)

Figure 17 Mean and standard deviation (2σ) of 10 x 1µl replicate injections of 3, 4 and 5-ring PAH isolated from a fireplace soot sample, along with internal standards (IS) used to test the reproducibility of the GC/C/IRMS at measuring the $\delta^{13}C$ of field samples. Ace = Acenaphthene, Pa = Phenanthrene, A = Anthracene, MPa = Methyl Phenanthrene, PNa = Phenyl Naphthalene, Fl = Fluoranthene, Py = Pyrene, MFl-Py = Methyl Fluoranthene-Pyrene, BaA = Benz(a)anthracene, Chy = Chrysene, BFl = Benzofluoranthenes, BeP = Benzo(e)pyrene and BaP = Benzo(a)pyrene.

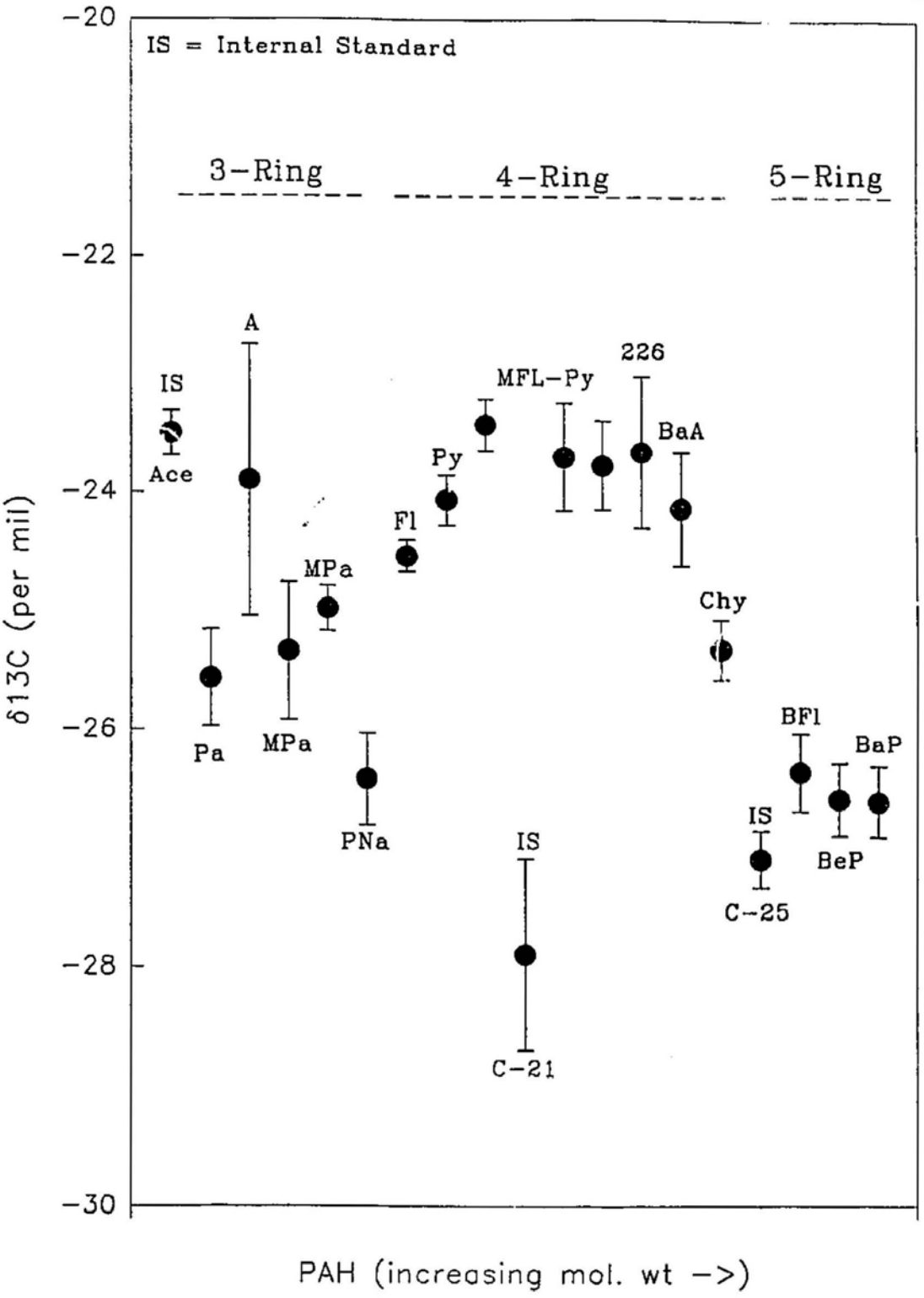
IS = Internal Standard
3-Ring
4-Ring
5-Ring
−20
−22
−24
−26
−28
−30
δ13C (per mil)
IS
Ace
A
Pa
MPa
MPa
PNa
Fl
Py
MFL-Py
IS
C-21
226
BaA
Chy
IS
C-25
BFl
BeP
BaP
PAH (increasing mol. wt ->)

Figure 18. Mean and standard deviation (2σ) of 10 x 1µl replicate injections of 2, 3, 4 and 5-ring PAH isolated from a car soot sample, along with internal standards (IS) used to test the reproducibility of the GC/C/IRMS at measuring the $\delta^{13}C$ of field samples. Na = Naphthalene, Ace = Acenaphthene, Pa = Phenanthrene, A = Anthracene, Fl = Fluoranthene, BaA = Benz(a)anthracene, Chy = Chrysene, BFl = Benzofluoranthenes, BeP = Benzo(e)pyrene and BaP = Benzo(a)pyrene.

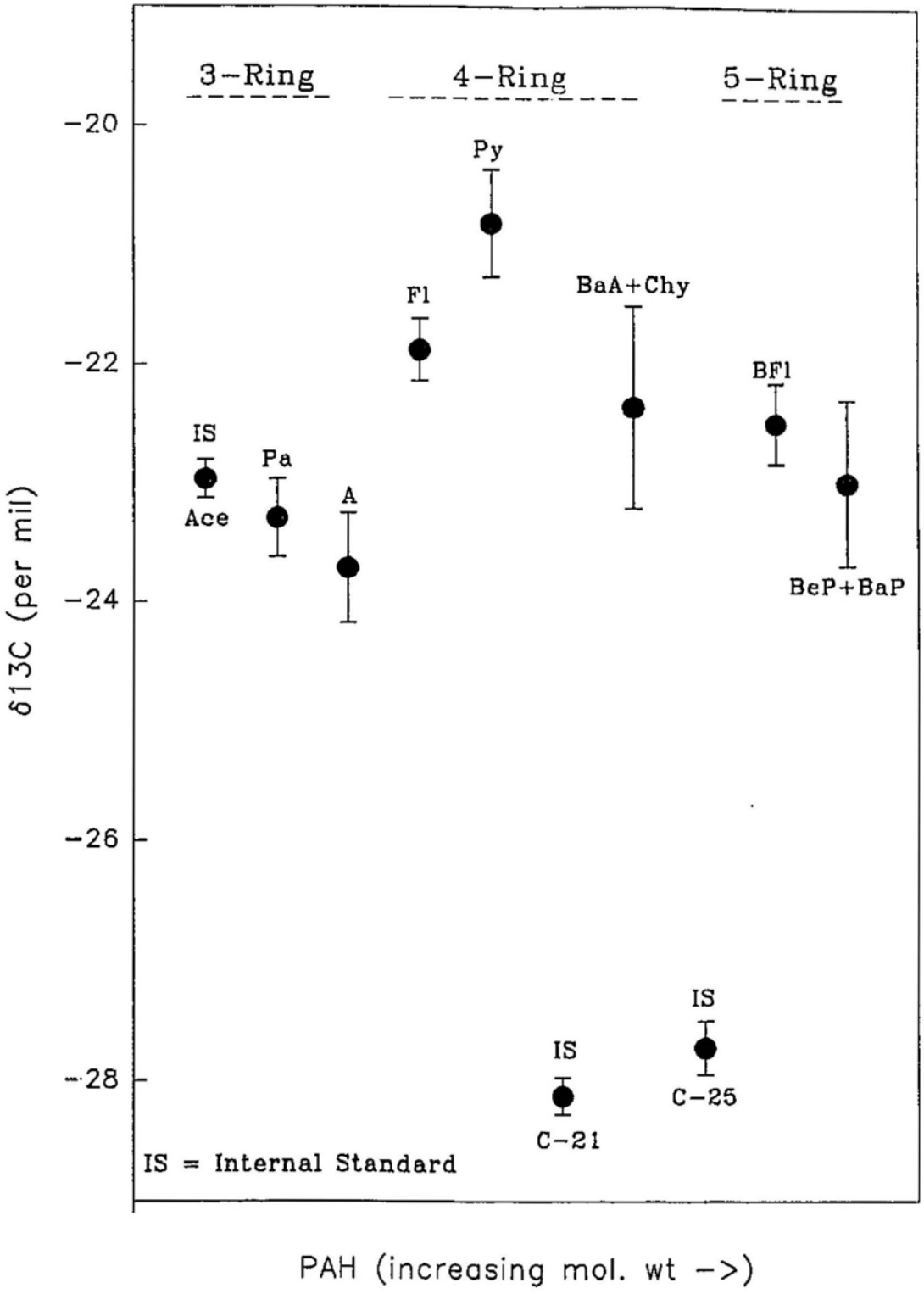
3-Ring
4-Ring
5-Ring
-20
-22
-24
-26
-28
δ13C (per mil)
IS
Ace
Pa
A
Fl
Py
BaA+Chy
BFl
BeP+BaP
IS
C-21
IS
C-25
IS = Internal Standard
PAH (increasing mol. wt ->)

and 0.51‰ and the $\delta^{13}C$ of internal standards was recovered to within 0.10 and 0.21‰ of their conventional values. Precision for the repeated measurements of the individual compounds in the fire soot sample ranged between 0.13 and 1.15‰, and internal standards were recovered to within 0.07 and 0.23‰ of their original value. Excluding the anomalously high anthracene variation, the precision ranged between 0.12 and 0.64‰. The precision for car soot PAH varied between 0.26 and 0.85‰ and recovery for the internal standards was within 0.30 and 0.80‰. Precision for the internal standards in the three samples varied: Ace ranged between 0.16‰ and 0.19‰, C_{21} between 0.13‰ and 0.80‰ and C_{25} between 0.22‰ and 0.24‰ (Table 7). The mean isotopic values of the UCM (sum of the isotopic values of the area under each individual peak) for the sediment sample, fireplace and car soots were -25.4‰, -25.5‰ and -26.7‰, respectively.

Percent recoveries and associated isotopic values of selected PAH standards taken through the sample extraction and purification procedures are summarized in Figure 19. With the exception of the mean recovery rate of 45% for F, recoveries for the remaining higher molecular weight PAH were generally better than 70%. The precision for the repeated isotopic measurements ranged between 0.07‰ and 0.38‰ and there is no correlation between the precision, accuracy and yields.

Figure 19. The mean $\delta^{13}C$ values and concentrations of standard PAH recovered from the PAH free spiked sediment samples (processed) using the adopted extraction and purification procedures. F = Fluorene, Pa = Phenanthrene, A = Anthracene, Fl = Fluoranthene, Py = Pyrene, BaA = Benz(a)anthracene, BbF = Benzo(b)fluoranthene.

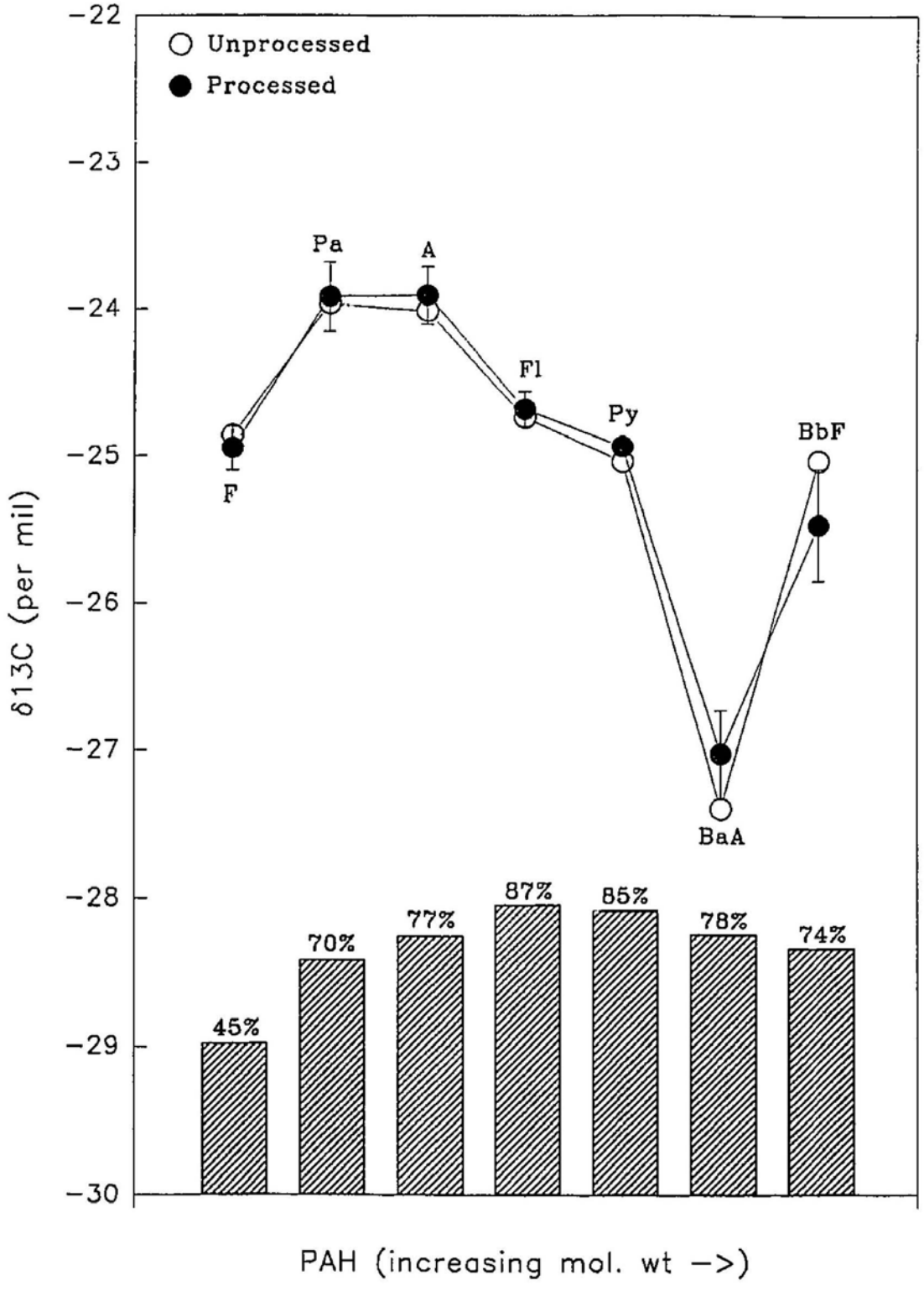
Unprocessed
Processed
δ13C (per mil)
−22
−23
−24
−25
−26
−27
−28
−29
−30
F
Pa
A
Fl
Py
BaA
BbF
45%
70%
77%
87%
85%
78%
74%
PAH (increasing mol. wt −>)

3.2 Isotopic effects due to photolysis:

Figures 20 and 21 summarize the mean isotopic values and the mean recovered yields of the standard PAH exposed to natural sunlight. There was no significant alteration from the initial isotopic values of three (Fl, Py and BbF) of the four parental compounds exposed to sunlight for 48 hr in cyclohexane at 12-14°C (Figure 20). Fl, Py and BbF concentrations gradually decreased, with the greatest reduction (35%) occurring in the pyrene concentration. In constrast to the apparent stability of Fl, Py and BbF, the isotopic value of anthracene in this set of experiments was altered by up to 2°/$_{oo}$ during the first 8 hr exposure. This enrichment was also accompanied by a simultaneous 57% decrease in the concentration during this time. Attempts to duplicate this isotopic shift using repeated experiments with anthracene dissolved in hexane, cyclohexane and in the absence of a solvent substrate and exposed to sunlight at 24 to 26°C were unsuccessful. The precision of the repeated measurements of anthracene in the hexane solution ranged between 0.07°/$_{oo}$ and 0.23°/$_{oo}$. Cyclohexane precision ranged between 0.22°/$_{oo}$ and 0.53°/$_{oo}$, while in the absence of a solvent substrate, precision ranged between 0.07°/$_{oo}$ and 0.37°/$_{oo}$ (Figure 22; Table 7).

The mean and precision in the isotopic values of pure PAH, exposed to sunlight, at 27°C, in dichloromethane, are shown in Figure 21. While the isotopic values of F, Pa, Fl and Py remained unaltered, Ace became progressively enriched as the concentration simultaneously decreased. In contrast to the overall 85% reduction in the Ace concentration, the decrease in F, Pa, Fl and Py concentrations ranged between 20 and 40%

Figure 20. Measured mean $\delta^{13}C$ values (2σ) and recovered concentrations of pure PAH exposed to natural sunlight for 4, 8, 24, 36 and 48 hrs at 12 - 14°C in cyclohexane.

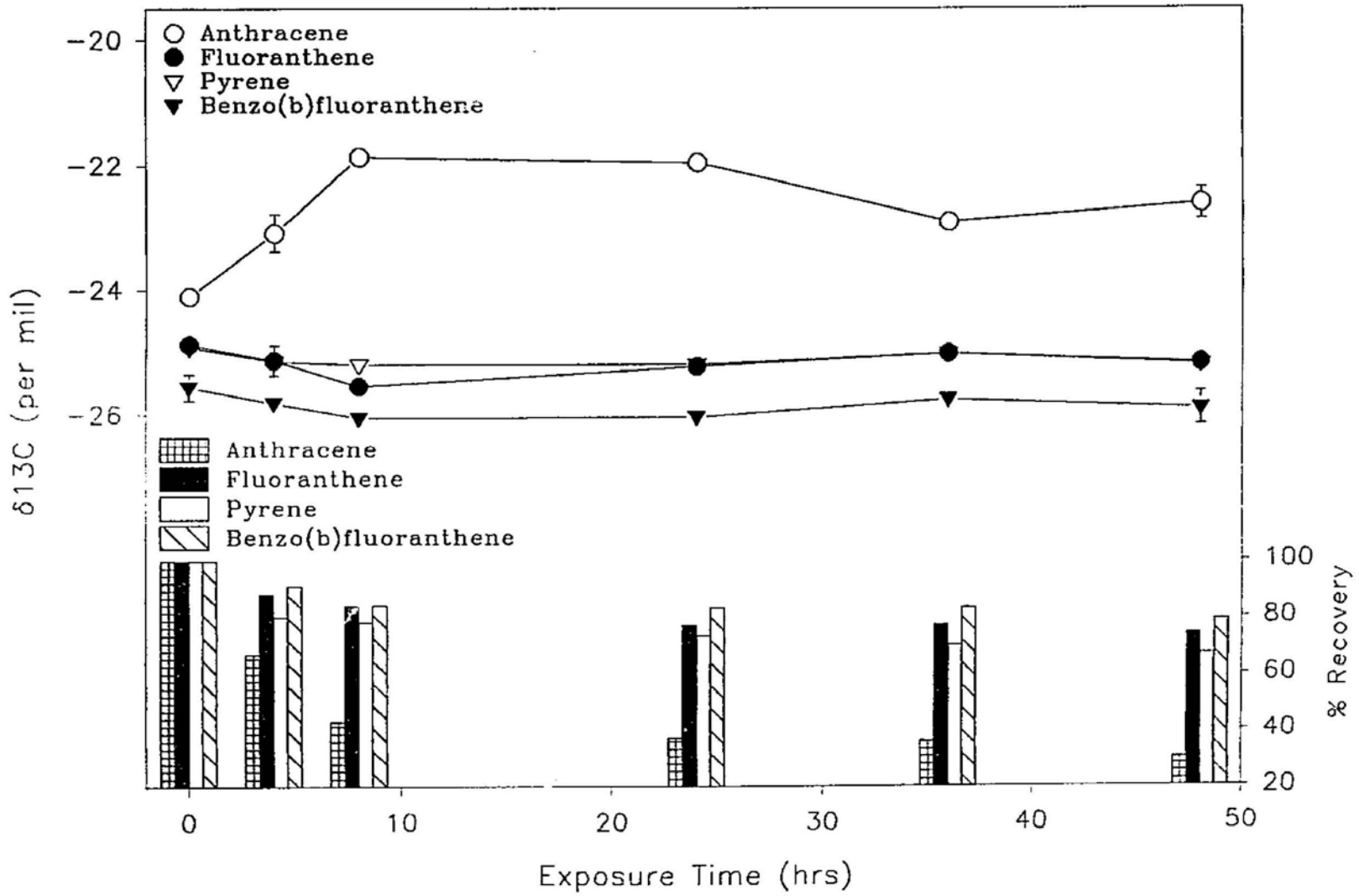
Anthracene
Fluoranthene
Pyrene
Benzo(b)fluoranthene
−20
−22
−24
−26
δ13C (per mil)
Anthracene
Fluoranthene
Pyrene
Benzo(b)fluoranthene
100
80
60
40
20
% Recovery
0
10
20
30
40
50
Exposure Time (hrs)

Figure 21. Measured mean $\delta^{13}C$ values (2σ) and recovered concentrations of pure PAH exposed to natural sunlight for 2, 4, 6, 8, and 10 hrs at 27°C in dichloromethane.

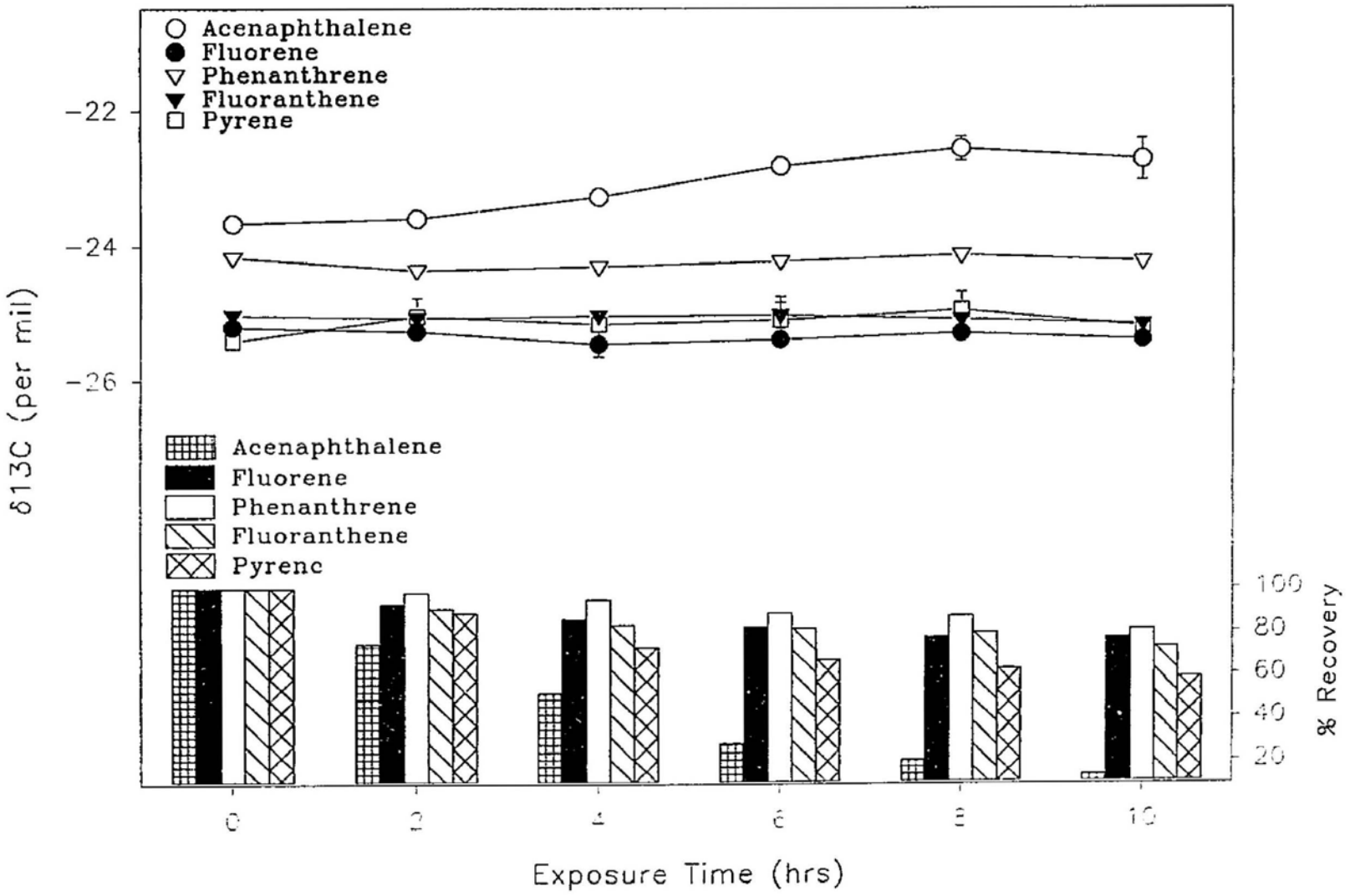
Acenaphthalene
Fluorene
Phenanthrene
Fluoranthene
Pyrene
−22
−24
−26
δ13C (per mil)
Acenaphthalene
Fluorene
Phenanthrene
Fluoranthene
Pyrene
100
80
60
40
20
% Recovery
0
2
4
6
8
10
Exposure Time (hrs)

Figure 22. Mean $\delta^{13}C$ (2σ) of repeated anthracene photolysis experiments using hexane and cyclohexane and in the absence of a solvent substrate (solid) at 24-26°C.

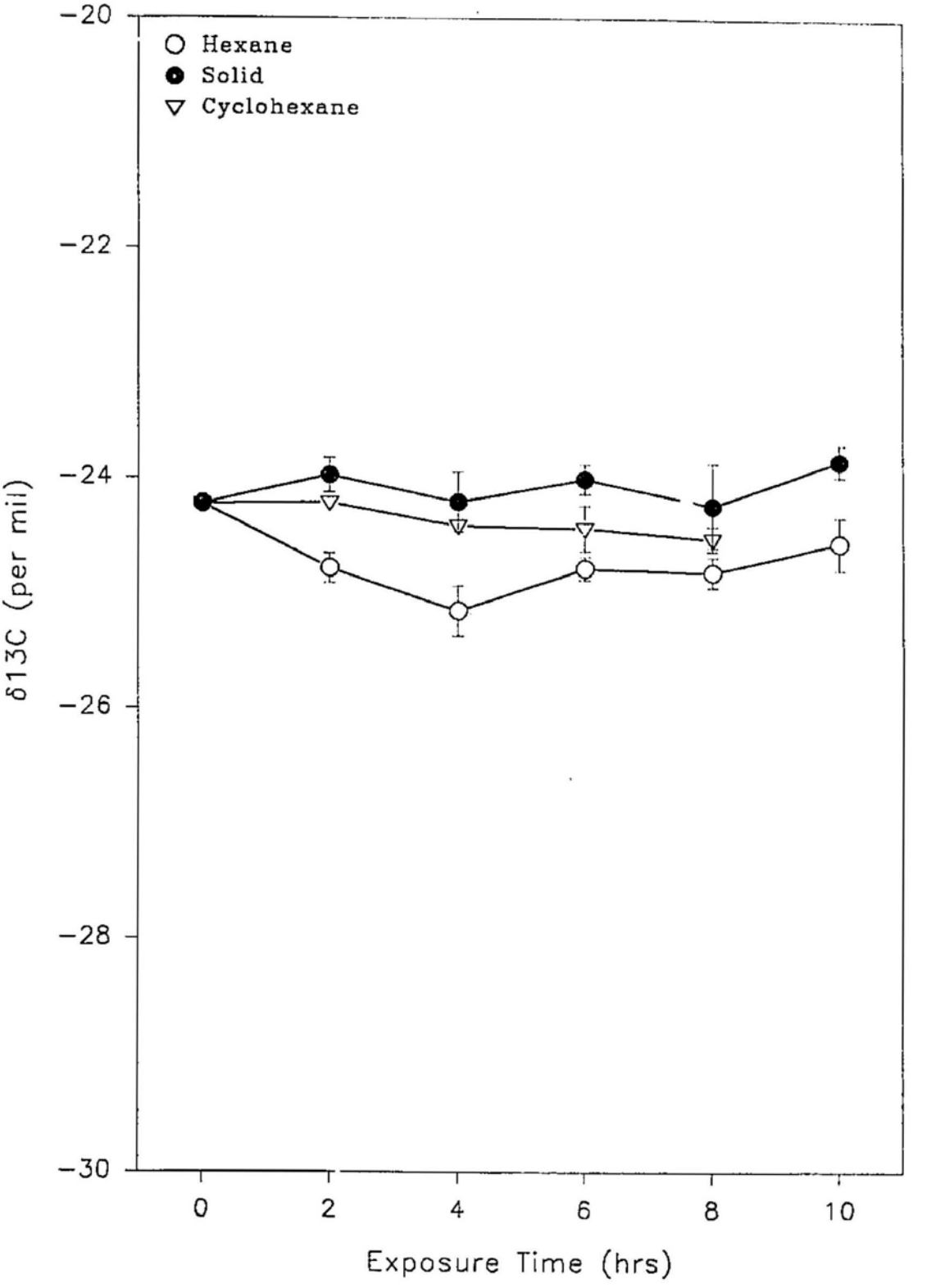
Hexane
Solid
Cyclohexane
−20
−22
−24
−26
−28
−30
δ13C (per mil)
0
2
4
6
8
10
Exposure Time (hrs)

of the original amounts with the greatest reduction recorded in pyrene.

Figure 23, shows an example of a plot of $\ln(C_o/C_t)$ against time for the dichloromethane study, where C_o is the initial concentration and C_t is the concentration at time t. All PAH exhibit more or less straight line fits passing through the origin indicating first-order kinetics which was also observed for the PAH exposed in cyclohexane. Rate constants (k in $time^{-1}$) and the half-lives ($t_{1/2}$) were calculated from: $t_{1/2}=\ln 2/k$ and are summarized in Table 8. The rate constants for Fl and Py were significantly greater in dichlorometane than in hexane.

3.3 Isotopic effects due to microbial degradation:

The microbial degradation of Na (Figure 24) and Fl (Figure 25) indicates that there is no significant alteration in their isotopic values (with all recovered values within $0.5‰$ of the original isotopic values) when these PAH are used as a sole carbon source. Rapid growth occurred in the Na experiments and up to 95% of the concentration was reduced after 6 hr of exposure. Similar reductions over the same time period were observed, even when higher initial concentrations were utilized. Since isotopic effects are predominantly manifested in reduced substrate concentrations, the Fl experiment was extended, despite the notable decay in bacterial growth (Figure 25). The concentration of Fl was reduced by 63% after 60 hr of exposure to an active bacterial population. There was no change in the isotopic values of Fl in the duplicate controls and no bacterial growth was recorded in these samples.

Figure 23. First-order photolytic degradation of pure PAH when exposed to natural sunlight at 27°C in dichloromethane. r = correlation coefficient

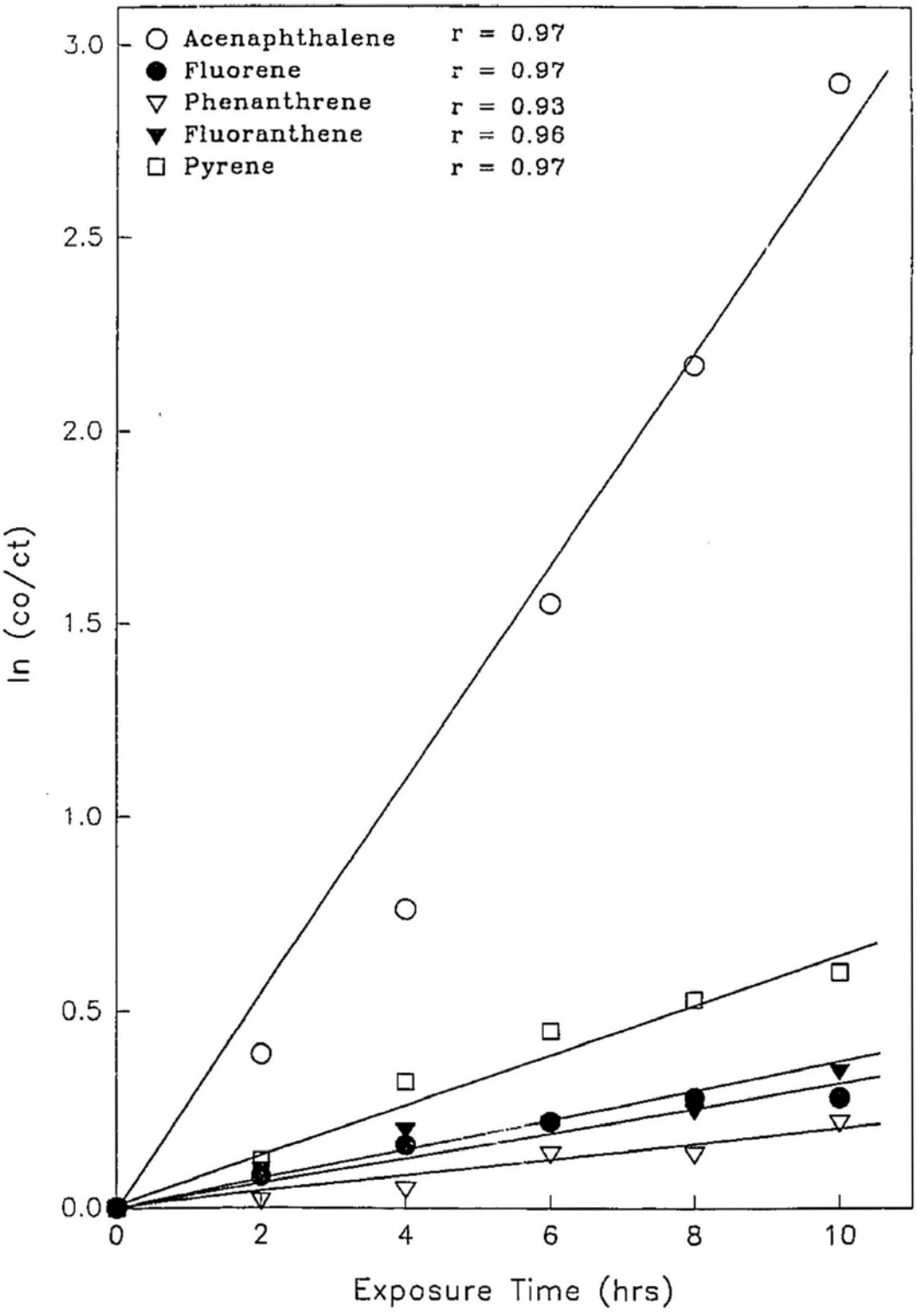
Acenaphthalene r = 0.97
Fluorene r = 0.97
Phenanthrene r = 0.93
Fluoranthene r = 0.96
Pyrene r = 0.97
3.0
2.5
2.0
1.5
1.0
0.5
0.0
ln (co/ct)
0
2
4
6
8
10
Exposure Time (hrs)

Table 8. Calculated first order rate constants (k/hr) and derived half-lives ($t_{1/2}$) for standard PAH exposed to natural sunlight in dichloromethane and cyclohexane. Ace = Acenaphthene, BbF = Benzo(b)fluoranthene.

PAH	Rate Constant k/hr	Half Life $t_{1/2}$ (h)				
			Other Published Data			
10 hr Exposure in Dichloromethane at 27°C						
Ace	0.35	2				
Fluorene	0.02	23	*		**	***
Phenanthrene	0.02	31	0.05	14	136	<10% loss after 9.5 hr*
Fluoranthene	0.03	23	0.01	48	270	<10% loss after 9.5 hr
Pyrene	0.06	11	0.10	7	136	~90% loss after 7.5 hr
48 hr Exposure in Cyclohexane at 12-14° C						
Anthracene	0.03	21	0.36	2	23	~65% loss after 2.5 hr
Fluoranthene	0.006	122	0.01	48	270	<10% loss after 9.5 hr
Pyrene	0.006	122	0.10	7	136	~90% loss after 7.5 hr
B(b)F	0.004	160		0.04	19	

*Sanders et al. (1993) Rate constants and half-lives of PAH irradiated in acetonitrile with 450 W mercury lamp

**Behymer and Hites (1988) Half-lives of PAH adsorbed onto coal fly ash with carbon composition of 0.1%

***Korfmacher et al. (1980) PAH irradiated in cyclohexanone with 150 W xenon lamp

Figure 24. The isotopic effects associated with the degradation of pure naphthalene using naphthalene degrading *Pseudomonas putida*, ATCC 17484. Inset, change in naphthalene concentrations over the first six hours of exposure in the duplicate experiments.

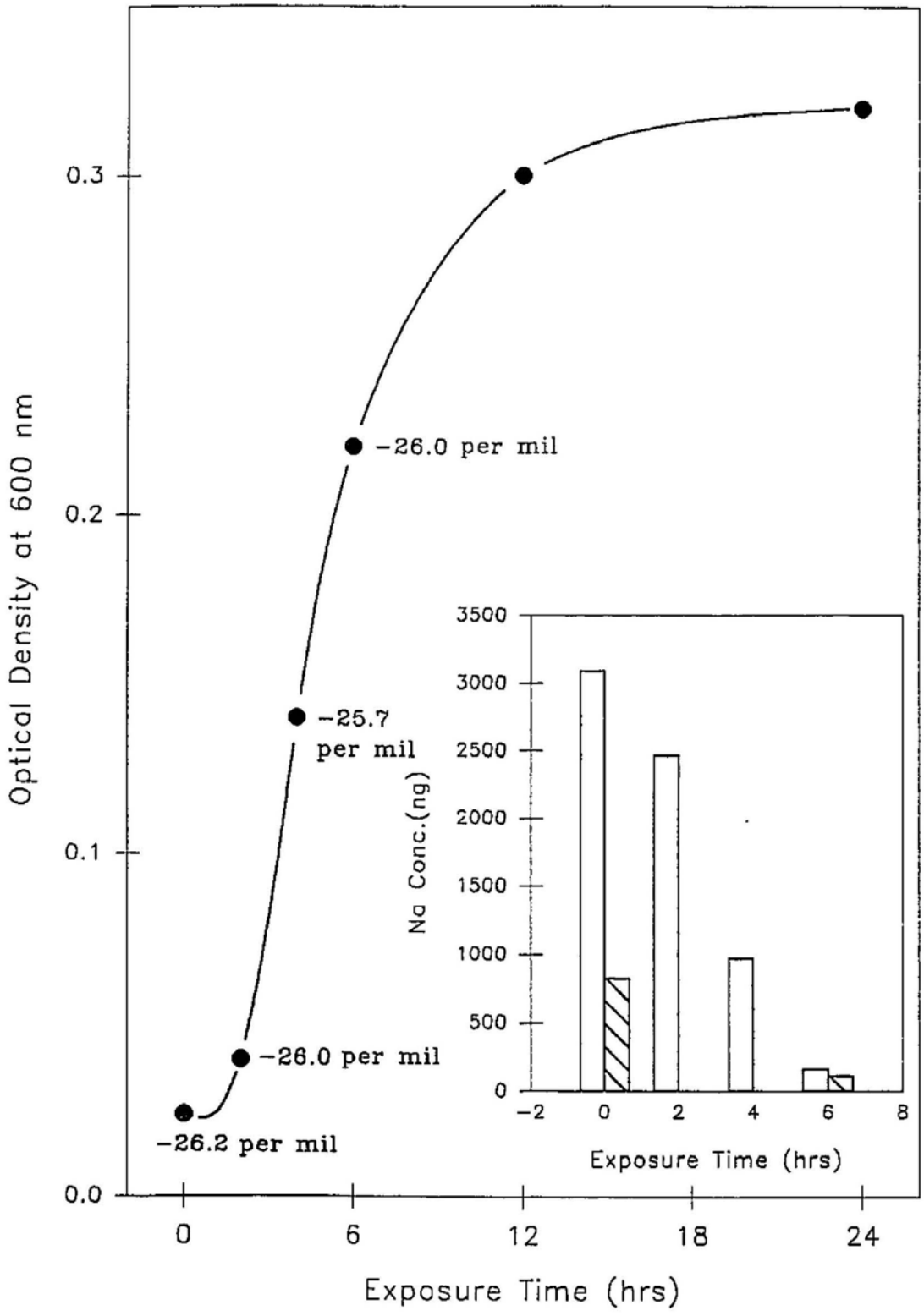
Optical Density at 600 nm
0.0
0.1
0.2
0.3
0
6
12
18
24
Exposure Time (hrs)
−26.2 per mil
−26.0 per mil
−25.7
per mil
−26.0 per mil
Na Conc.(ng)
0
500
1000
1500
2000
2500
3000
3500
−2
0
2
4
6
8
Exposure Time (hrs)

Figure 25. The isotopic effects associated with the degradation of pure fluoranthene using fluoranthene degrading *Pseudomonas paucimobilis*, EPA 505. Inset, change in Fl concentrations during the exposure period.

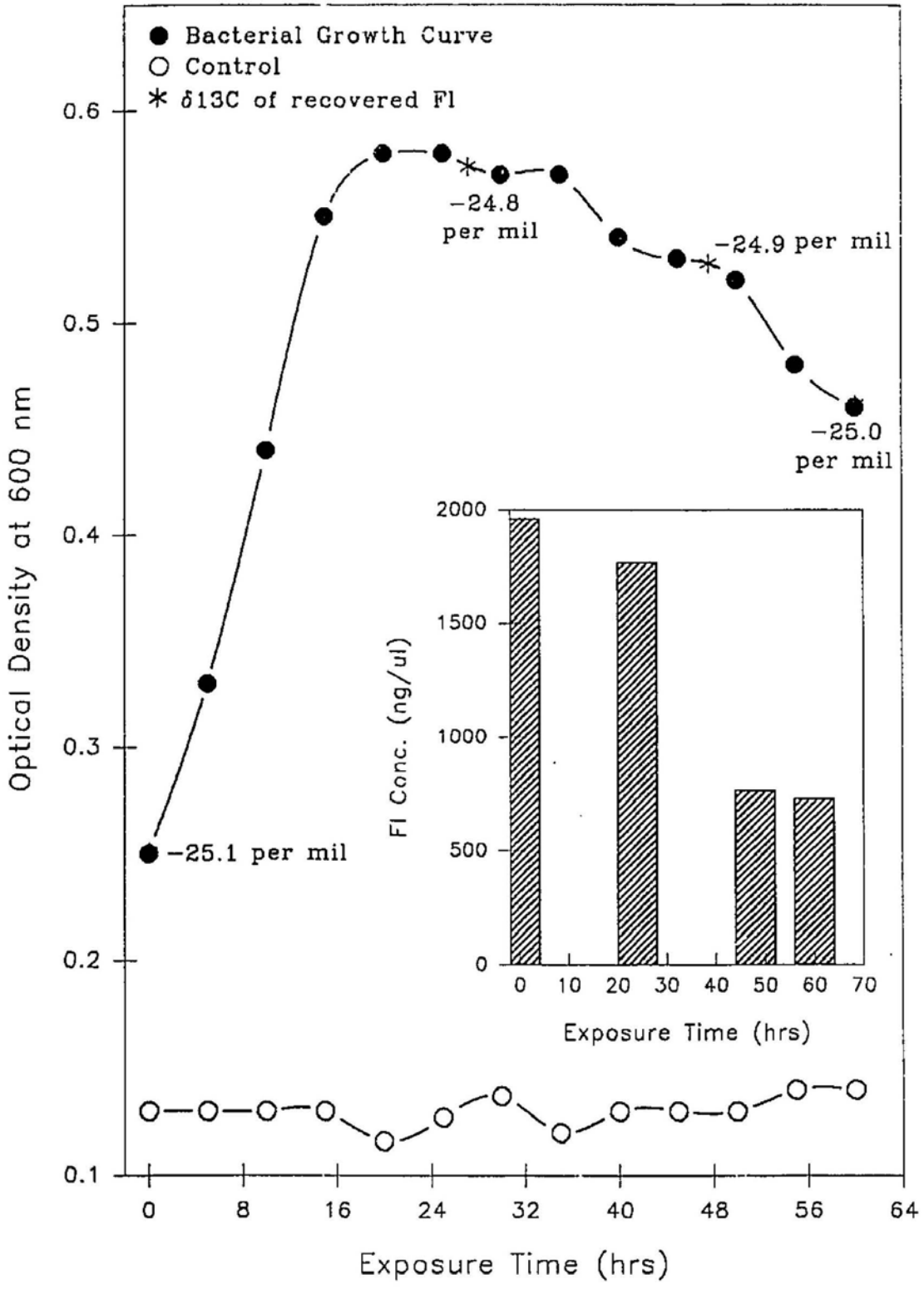
Bacterial Growth Curve
Control
* δ13C of recovered Fl
-24.8 per mil
-24.9 per mil
-25.0 per mil
-25.1 per mil
Optical Density at 600 nm
0.6
0.5
0.4
0.3
0.2
0.1
0
8
16
24
32
40
48
56
64
Exposure Time (hrs)
Fl Conc. (ng/ul)
2000
1500
1000
500
0
0 10 20 30 40 50 60 70
Exposure Time (hrs)

3.4 Molecular and carbon isotope signatures of the primary sources:

3.4.1 Fireplace soot:

3.4.1.1 Molecular signature:

The prominent PAH identified in the single and composite fireplace soot samples ranged from kata-annellated 3-ring to peri-condensed 6-ring compounds (Table 9; Appendix F1). Generally, the molecular signature is characterized by the dominance of 3, 4 and 5-ring parental PAH with some methylated 3 and 4-ring compounds. Other prominent compounds tentatively identified by GC-MS were isomers of a $C_{17}H_{14}$, m/z = 218 amu compound ([2]RI 2030), previously postulated to be 16,17-dihydro-15H-cyclopenta(a)phenanthrene (Killops and Howell, 1988) and a $C_{18}H_{18}$ hydrocarbon, retene (1-methyl-7-isopropylphenanthrene) also present in several samples. The presence of a $C_{18}H_{10}$, m/z = 226 amu compound (RI 2270), tentatively identified as benzo(ghi)fluoranthene or cyclopenta(cd)pyrene and the presence of a prominent UCM extending from 34 to 80 minutes (RI = 1570-3100) was also characteristic of these samples (Appendix F1). The absolute concentrations of prominent PAH varied significantly from sample to sample. Therefore individual concentrations were normalized to the total quantified PAH content in each sample. These normalized concentrations exhibit a dominance of Fl, Py and Chy in the 4-ring and the combined benzofluoranthenes in the 5-ring PAH (Figure 26).

---

[2] RI = Kovats index, where the first two numbers represent the closest n-alkane and the last two numbers is the ratio of the relative retention times between the two closest n-alkanes.

Table 9. The range of PAH isolated from the single open fireplace (Sing) and composite (Comp) soot samples. (++ = most abundant compounds that were isotopically measurable; + = detected but not isotopically analyzed). B(ghi)Fl =Benzo(ghi)fluoranthene, CP(cd)Py = Cyclopenta(cd)pyrene, Ind = Indeno(123 cd) pyrene, B(ghi)Per = Benzo(ghi)perylene, Anthant = Anthanthrene.

No	PAH	Mol Wt	Sing 1	Sing 2	Sing 3	Sing 4	Sing 5	Sing 6	Sing 7	Sing 8	Sing 9	Sing 10	Comp	Comp Repeat
1	Ace	154	+	+	+	+	+	+	+	+	+	+	+	+
2	Dibenzofuran	168	+	+	+	+	+	+	+	+	+	+	+	+
3	F	166	+	+	+	+	+	+	+	+	+	+	+	+
4	Methyl-F*	180	+	+	+	+	+	+	+	+	+	+	+	+
5	Pa	178	++	++	++	++	++	++	++	++	++	++	++	++
6	A	178	++	++	++	++	++	++	++	++	++	++	++	++
7	Methyl-Pa	192	++	++	++	++	++	++	++	++	++	++	++	++
8	Methylene Pa/A	190	++	++	++	++	++	++	++	++	++	++	++	++
9	Methyl-Pa	192	++	++	++	++	++	++	++	++	++	++	++	++
10	Phenyl-Na	204	++	++	++	++	++	++	++	++	++	++	++	++
11	Dimethyl-Pa	206	++	++	++	++	++	++	++	++	++	++	++	++
12	Fl	202	++	++	++	++	++	++	++	++	++	++	++	++
13	Py	202	++	++	++	++	++	++	++	++	++	++	++	++
14	Unknown	218	++	++	++	++	++	++	++	++	++	++	++	++
15	Unknown	218	+	+	+	+	+	+	+	+	+	+	+	+
16	Trimethyl-Pa	220	+	+	+	+	+	+	+	+	+	+	+	+
17	Methyl-Fl/Py*	216	++	++	++	++	++	++	++	++	++	++	++	++
18	Methyl-Fl/Py*	216	++	++	++	++	++	++	++	++	++	++	++	++
19	Methyl-Fl/Py*	216	++	++	++	++	++	++	++	++	++	++	++	++
20	Retene*	234			+	+			+	+			+	+
21	Dimethyl-Fl/Py*	230	+	+	+	+	+	+	+	+	+	+	+	+
22	B(ghi)Fl/CP(cd)Py*	226	++	++	++	++	++	++	++	++	++	++	++	++
23	BaA	228	++	++	++	++	++	++	++	++	++	++	++	++
24	Chy	228	++	++	++	++	++	++	++	++	++	++	++	++
25	Methyl-BaA/Chy*	242	++	++	++	++	++	++	++	++	++	++	++	++
26	BFl	252	++	++	++	++	++	++	++	++	++	++	++	++
27	BeP	252	++	++	++	++	++	++	++	++	++	++	++	++
28	BaP	252	++	++	++	++	++	++	++	++	++	++	++	++
29	Perylene	252												
30	Ind/B(ghi)Per/Anthant*	276	+	+	+	+	+	+	+	+	+	+	+	+
31	Ind/B(ghi)Per/Anthant*	276	+	+	+	+	+	+	+	+	+	+	+	+

* = Tentatively identified by GC-MS

Figure 26. Mean normalized concentrations of the 3, 4 and 5-ring PAH in the single and composite fire soot samples. Pa = Phenanthrene, A = Anthracene, MPa = Methyl Phenanthrene, Fl = Fluoranthene, Py = Pyrene, BaA = Benz(a)anthracene, Chy = Chrysene, BFl = Benzofluoranthenes, BeP = Benzo(e)pyrene and BaP = Benzo(a)pyrene.

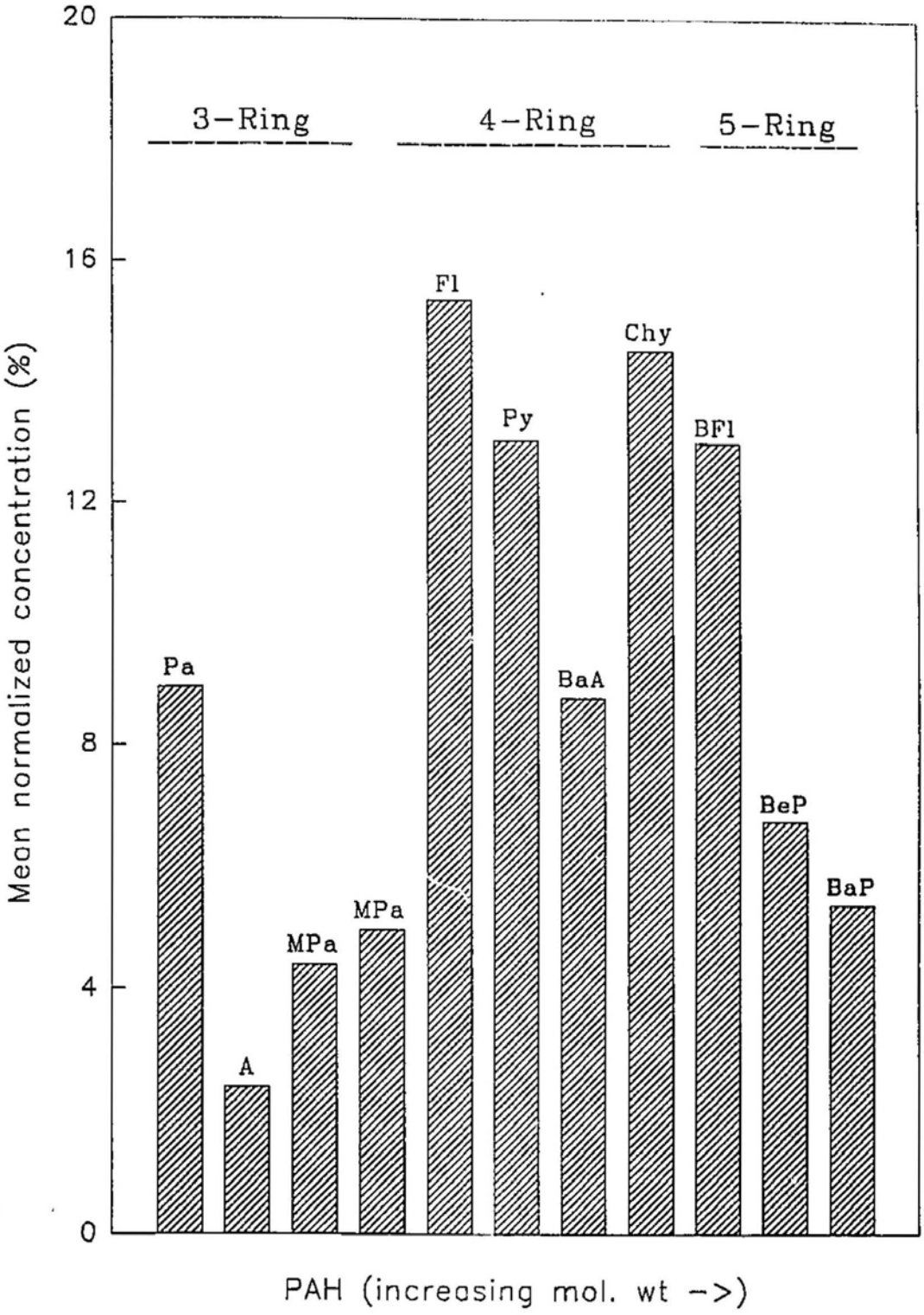
20
16
12
8
4
0
3-Ring
4-Ring
5-Ring
Mean normalized concentration (%)
Pa
A
MPa
MPa
Fl
Py
BaA
Chy
BFl
BeP
BaP
PAH (increasing mol. wt ->)

3.4.1.2 Carbon isotopes:

A summary of the mean and standard deviations of the $\delta^{13}C$ values for PAH isolated from single fireplace soot samples are shown in Figure 27. Mean $\delta^{13}C$ values for each compound ranged between -26.8°/$_{oo}$ and -24.3°/$_{oo}$, and sample to sample variations ranged between 0.58 and 1.60°/$_{oo}$ (Table 10). The isotopic value of the parental compounds ranged between -26.4°/$_{oo}$ and -24.3°/$_{oo}$, with variations between 0.69 and 1.60°/$_{oo}$, while their methylated homologues ranged between -26.9°/$_{oo}$ and -24.6°/$_{oo}$ with variations ranging between 0.58 and 1.20°/$_{oo}$. In general, $\delta^{13}C$ measured for Pa and its methylated derivatives were more depleted in ^{13}C than the higher molecular weight PAH. Collectively, the isotopic values of the 3-ring compounds (Pa, A, methyl and dimethyl Pa and phenyl Na) fluctuated between -27.5°/$_{oo}$ and -24.3°/$_{oo}$ with significantly enriched A compared to Pa and depleted phenyl Na. Pa was equally or more enriched than its methylated derivatives. With the possible exception of trimethyl Pa, the $\delta^{13}C$ values of Py and methylated Fl-Py became gradually enriched with increasing molecular weight between Fl (-25.7°/$_{oo}$) and the 226 species (-24.9°/$_{oo}$). In contrast to methyl Fl-Py, for example, parental Fl and Py are depleted. PAH between the 4-ring BaA (-25.2°/$_{oo}$) and the 5-ring BaP (-27.7°/$_{oo}$) became progressively depleted with increasing molecular weight. To futher assess the nature and trend of the sample to sample $\delta^{13}C$ variations, the isotopic signature of the PAH in the composite soot are compared to a number of single soot samples (Figure 28). All samples have very similar trends, but the triaromatic compounds (A, Pa and MPa) of the composite sample seem to be marginally more depleted than most of the single samples investigated. Retene in amounts that can be

Figure 27. Mean and range (standard deviation; 2σ) of the $\delta^{13}C$ of the individual 3, 4 and 5-ring parental and methylated PAH isolated from the single and composite fire soot samples. Pa = Phenanthrene, A = Anthracene, MPa = Methyl Phenanthrene, PNa = Phenyl Naphthalene, DPa = Dimethyl Phenanthrene, Fl = Fluoranthene, Py = Pyrene, MFl-Py = Methyl Fluoranthene-Pyrene, Trimethyl Phenanthrene, BaA = Benz(a)anthracene, Chy = Chrysene, BFl = Benzofluoranthenes, BeP = Benzo(e)pyrene and BaP = Benzo(a)pyrene.

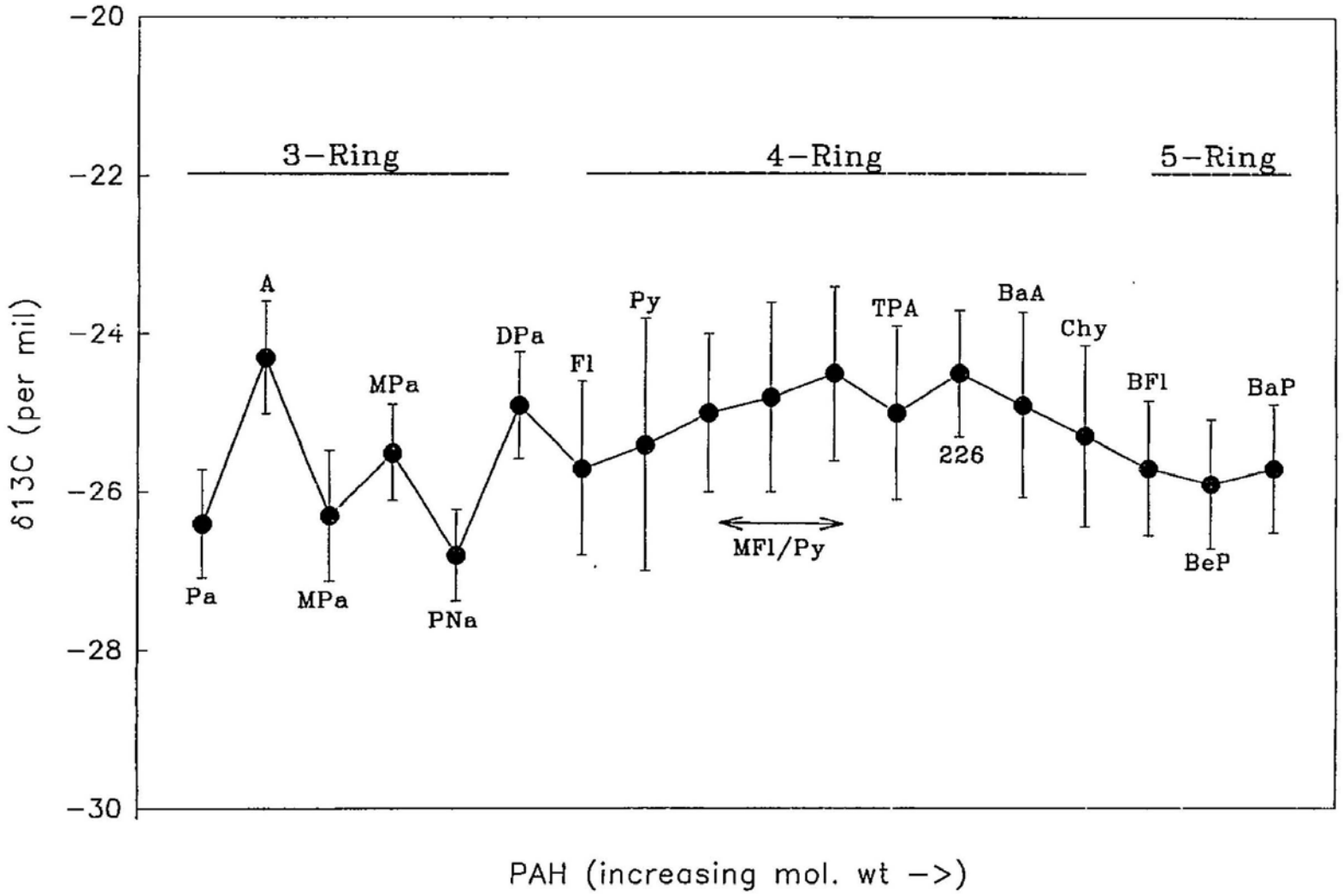
−20
−22
−24
−26
−28
−30
δ13C (per mil)
3−Ring
4−Ring
5−Ring
Pa
A
MPa
MPa
PNa
DPa
Fl
Py
MFl/Py
TPA
226
BaA
Chy
BFl
BeP
BaP
PAH (increasing mol. wt −>)

Table 10. Summary of the mean intercompound $\delta^{13}C$ range and the compounds that show the minimum and maximum sample to sample variation (2σ) observed for the primary, secondary and sediment samples.

* = range observed between the most depleted and enriched individual compounds in the mean overall $\delta^{13}C$ values

** = compounds that show the minimum and maximum sample to sample variation

Sample	Intercompound $\delta^{13}C$ Range (‰)*	Intersample Variation (‰)(2σ)**
Fireplace soot:		
Overall range	-26.8(PNa) to -24.3(A)	0.58(PNa) to 1.60(Py)
Parental PAH	-26.4(Pa) to -24.3(A)	0.69(Pa) to 1.60(Py)
Alkylated PAH	-26.8(PNa) to -24.5(DPa)	0.58(PNa) to 1.20(MFl/Py)
Car soot:		
Overall range	-26.9(MPa) to -23.6(Ace)	0.07(Ace) to 1.76(BaP)
Parental PAH	-26.3(Chy) to -23.6(Ace)	0.07(Ace) to 1.76(BaP)
Alkylated PAH	-26.9(MPa) to -25.5(MNa)	0.35(MFl/Py) to 1.00(MPa)
Other comb. sources:		
Overall range	-26.8(MFl/Py) to -25.4(Pa)	
Parental PAH	-26.5(BaA/Chy) to -25.4(Pa)	
Alkylated PAH	-26.8(MFl/Py) to -26.0(MPa)	
Crankcase oil:		
Overall range	-28.9(Pa) to -26.2(MNa)	0.21(BaA+Chy) to 1.00(BFl)
Parental PAH	-28.9(Pa) to -26.6(Na)	0.21(BaA+Chy) to 1.00(BFl)
Alkylated PAH	-27.8(MPa) to -26.2(MNa)	0.22(TNa) to 0.87(MNa)
Crude oil:		
Arabian (overall)	-30.6(DDBT) to -22.7(DNa)	
Calgary (overall)	-32.2(DDBT) to -25.0(DNa)	
Outboard motor	-28.5(Pa) to -24.5(DNa)	
#2 fuel oil (Na only)	-27.0(Na) to -25.5(DNa)	
Road sweeps:		
Open-road (parent)	-27.1(BFl) to -23.7(A)	0.34(BFl) to 1.20(BaA+Chy)
Asphalt range	-30.3(MPa) to -27.3(MNa)	
Cement range	-28.4(BFl) to -26.4(BeP+BaP)	
Sewage (parent only)	-26.4(BFl) to -24.5(A)	
Snow (parent only)	-26.9(BFl) to -24.9(Pa)	
St. John's Harbour:		
Overall range	-26.6(MPa) to -24.6(A)	0.21(Pa) to 0.96(DPa)
Parental PAH	-26.4(BFl) to -24.6(A)	0.21(Pa) to 0.60(Fl)
Alkylated PAH	-26.6(MPa) to -26.0(MPa)	0.35(MFl/Py) to 0.96(DPa)
Conception Bay:		
Overall range (parent)	-27.2(BFl) to -25.8(BaA+Chy)	0.24(Fl) to 0.62(BFl)

Figure 28. The trend observed in the single and composite fireplace soot samples. Composite sample represented by hollow squares. Pa = Phenanthrene, A = Anthracene, MPa = Methyl Phenanthrene, PNa = Phenyl Naphthalene, Fl = Fluoranthene, Py = Pyrene, MFl-Py = Methyl Fluoranthene-Pyrene, BaA = Benz(a)anthracene, Chy = Chrysene, BFl = Benzofluoranthenes, BeP = Benzo(e)pyrene and BaP = Benzo(a)pyrene.

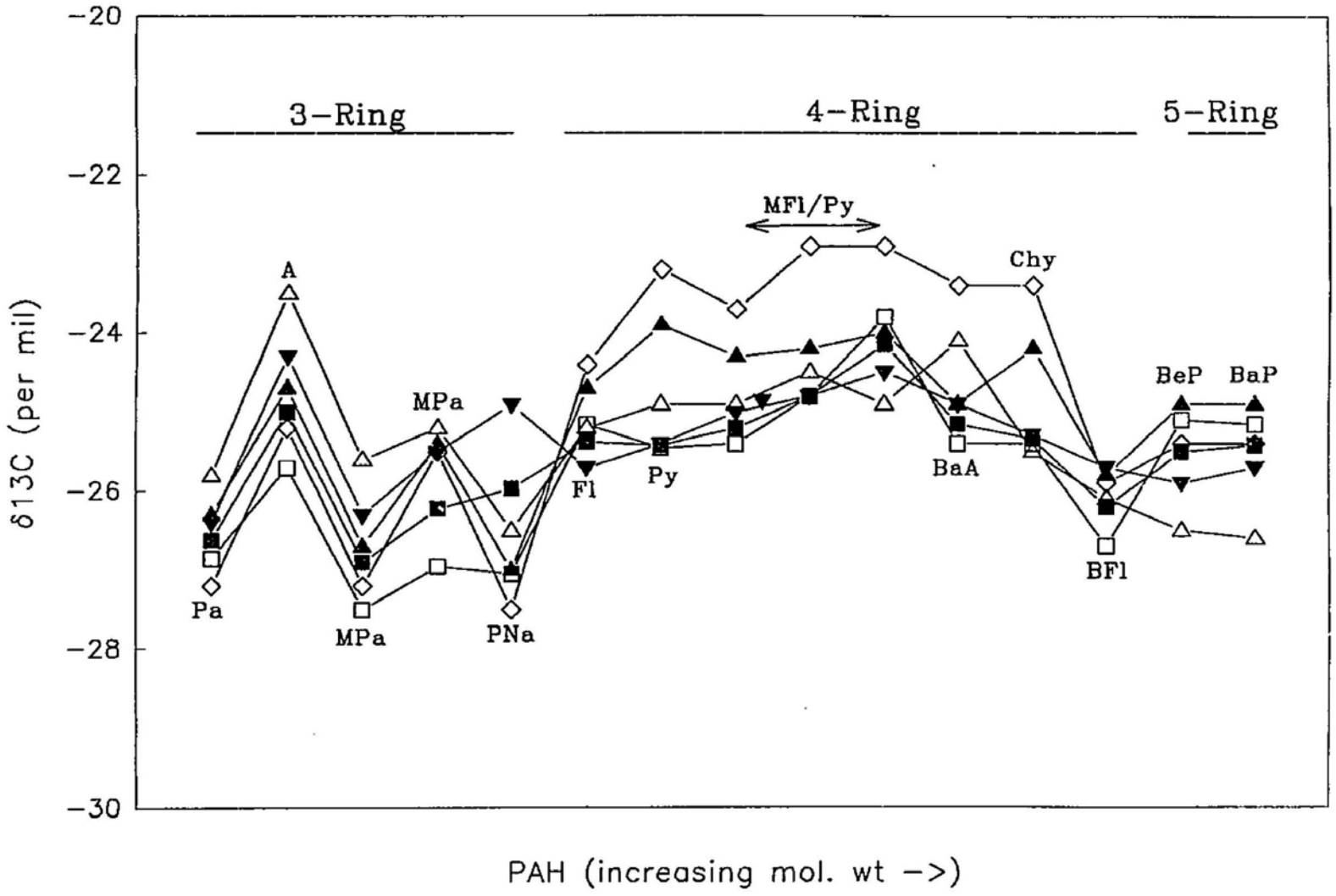
−20
−22
−24
−26
−28
−30
δ13C (per mil)
3−Ring
4−Ring
5−Ring
MFl/Py
A
Chy
MPa
BeP
BaP
Fl
Py
BaA
BFl
Pa
MPa
PNa
PAH (increasing mol. wt −>)

analyzed isotopically was noted in some samples and a mean isotopic value of -26.5‰ was obtained for this compound.

3.4.2 Car soot:

3.4.2.1 Molecular signature:

The prominent molecular ions identified in the single and composite car soot samples extended from 2-ring linear to 6-ring peri-condensed parental, methylated and substituted PAH (Table 11). From the range of samples investigated, two prominent signatures were evident, some samples had a dominance of 2, 3, 4 and 5-ring species, while the 2-ring compounds, naphthalene and methylated naphthalenes were absent in others. Methylated 2, 3 and 4-ring PAH were identified, but their parental homologues were generally present in greater concentrations. Sulphur substituted compounds, dibenzothiophene (DBT) and methylated DBT were also identified along with the m/z 218 and 226 amu species previously described. The presence of a prominent UCM extending from 32 to 66 minutes (RI 1500-2600) was also evident in most analyzed samples (Appendix F2). The concentration of the prominent parental PAH in the single and composite samples varied significantly and the normalized concentrations are shown in Figure 29. The most abundant compounds are methylated 2-ring (MNa) and 3, 4 and 5-ring parental PAH (Pa, Fl, Py and BFl). Pa is significantly more abundant than its corresponding isomer, A and its methylated derivatives, while Fl was generally more abundant than Py.

3.4.2.2 Carbon isotopes:

The mean and variance in the $\delta^{13}C$ values of the prominent PAH identified in the composite car soot samples are summarized in Figure 30. Generally, the mean values for

Table 11. The range of PAH isolated from the single (Sing) and composite (Comp) car soot samples. (++ = most abundant compounds that were isotopically measurable; + = detected but not isotopically analyzed). DBT = Dibenzothiophene, B(ghi)Fl = Benzo(ghi)fluoranthene, CP(cd)Py = Cyclopenta(cd)pyrene, Ind = Indeno(123 cd) pyrene, B(ghi)Per = Benzo(ghi)perylene, Anthant = Anthanthrene.

No	PAH	Mol Wt	Comp 1-3	Comp 4-9	Comp 9-11	Comp 1-9	Comp 1-5	Sing 1	Sing 1 Repeat	Sing 2	Sing 3	Sing 4	Sing 5
1	Na	128			++	++	++	++	++	++	+		
2	Methyl Na	142			++	++	++	++	++	++	+		+
3	Methyl Na	142		+	++	++	++	++	++	++	+		+
4	Ace	154	+	+	++	++	++	++	++	++	+		+
5	Dimethyl Na	156		+	+	+	+	+	+	+	+		+
6	Ay	152	+	+	+	+	+	+	+	+	+	+	+
7	Dibenzofuran*	168	+	+	+	+	+	+	+	+	+	+	+
8	Trimethyl Na	170	+			+		+	+		+	+	+
9	F	166	+	+	+	+	+	+	+	+	+	+	+
10	DBT	184	+		+	+		+	+		+	+	+
11	Pa	178	++	++	++	++	++	++	++	++	++	++	++
12	A	178	++	++	++	++	++	++	++	++	++	++	++
13	Methyl DBT	198		+	+	+	+			+	+	+	+
14	Methyl Pa	192	++	++	++	++	++	++	++	++	++	++	++
15	Methylene Pa/A*	190	++	++	++	++	++	++	++	++	++	++	++
16	Methyl Pa	192	++	++	++	++	++	++	++	++	++	++	++
17	Phenyl Na	204	++	++	++	++	++	++	++	++	++	++	++
18	Dimethyl Pa	206	+	+	+	+	+	+	+	+	+	+	+
19	Fl	202	++	++	++	++	++	++	++	++	++	++	++
20	Py	202	++	++	++	++	++	++	++	++	++	++	++
21	Unknown	218	+	+	+	+	+	+	+	+	+	+	+
22	Trimethyl Pa	220	+	+	+	+	+	+	+	+	+	+	+
23	Methyl Fl/Py*	216	++	++	++	++	++	++	++	++	++	++	++
24	Methyl Fl/Py*	216	+	+	+	+	+	+	+	+	+	+	+
25	B(ghi)Fl/I(cd)Py*	226	++	++	++	++	++	++	++	++	++	++	++
26	BaA	228	++	++	++	++	++	++	++	++	++	++	++
27	Chy	228	++	++	++	++	++	++	++	++	++	++	++
28	BFl	252	++	++	++	++	++	++	++	++	++	++	++
29	BeP	252	++	++	++	++	++	++	++	++	++	++	++
30	BaP	252	++	++	++	++	++	++	++	++	++	++	++
31	Perylene	252	+		+	+		+	+			+	
32	I(cd)Py/B(ghi)Per/Anth*	276	+	+	+	+	+	+	+	+			

++ = Most abundant

* = Tentatively identified by GC-MS

Figure 29. Mean normalized concentrations of the 2, 3, 4 and 5-ring PAH in the single and composite car soot samples. Na = Naphthalene, MNa = Methyl Naphthalene, DNa = Dimethyl Naphthalene, TNa = Trimethyl Naphthalene, Pa = Phenanthrene, A = Anthracene, MPa = Methyl Phenanthrene, Fl = Fluoranthene, Py = Pyrene, BaA = Benz(a)anthracene, Chy = Chrysene, BFl = Benzofluoranthenes, BeP = Benzo(e)pyrene and BaP = Benzo(a)pyrene.

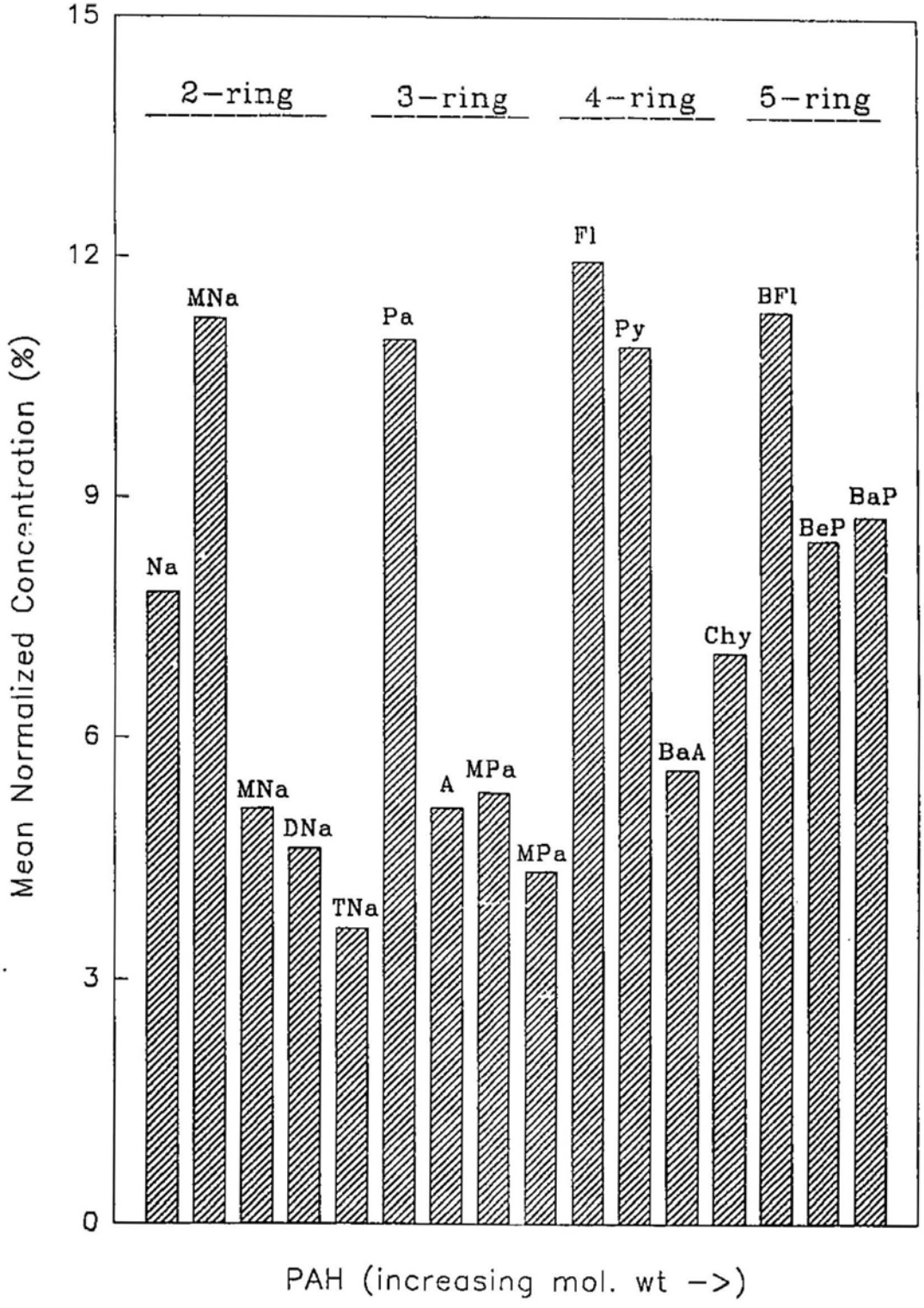
15
12
9
6
3
0
2-ring
3-ring
4-ring
5-ring
Mean Normalized Concentration (%)
Na
MNa
MNa
DNa
TNa
Pa
A
MPa
MPa
Fl
Py
BaA
Chy
BFl
BeP
BaP
PAH (increasing mol. wt ->)

Figure 30. Mean and range (standard deviation; 2σ) of the $\delta^{13}C$ of the individual 2, 3, 4 and 5-ring parental, methylated and substituted PAH isolated from the single and composite car soot samples. Na = Naphthalene, MNa = Methyl Naphthalene, Ace = Acenaphthene, F = Fluorene, Pa = Phenanthrene, A = Anthracene, MPa = Methyl Phenanthrene, PNa = Phenyl Naphthalene, Fl = Fluoranthene, Py = Pyrene, BaA = Benz(a)anthracene, Chy = Chrysene, BFl = Benzofluoranthenes, BeP = Benzo(e)pyrene and BaP = Benzo(a)pyrene

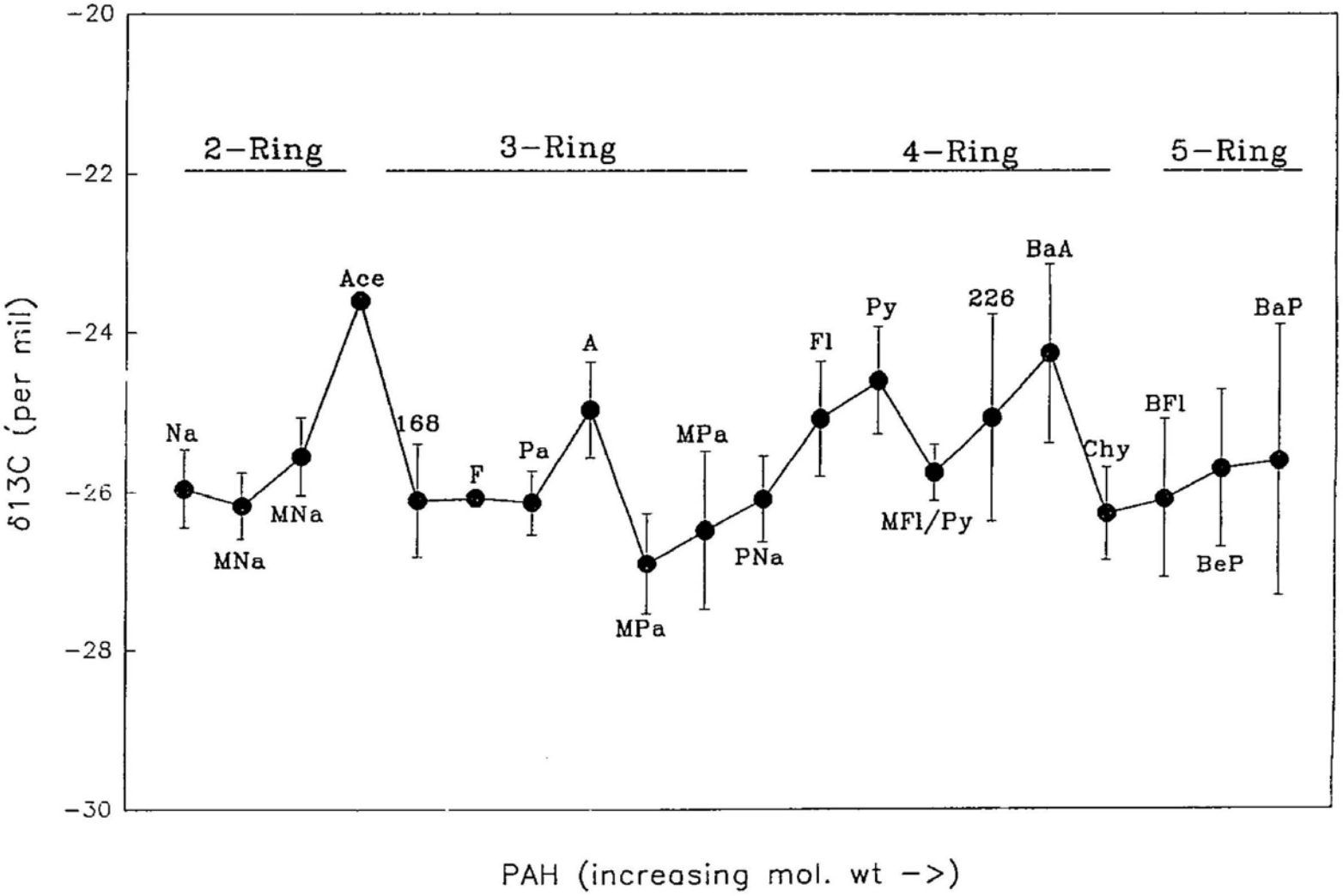
−20
−22
−24
−26
−28
−30
δ13C (per mil)
2−Ring
3−Ring
4−Ring
5−Ring
Na
MNa
MNa
Ace
168
F
Pa
A
MPa
MPa
PNa
Fl
Py
MFl/Py
226
BaA
Chy
BFl
BeP
BaP
PAH (increasing mol. wt −>)

the entire suite of compounds ranged between -26.9°/$_{oo}$ and -23.6°/$_{oo}$ and the variation (SD) ranged between 0.07 and 1.76°/$_{oo}$ (Table 10). The isotopic values of the parental compounds ranged between -26.3°/$_{oo}$ and -23.6°/$_{oo}$, while the methylated species ranged between -26.9°/$_{oo}$ and -25.5°/$_{oo}$, with variations of 0.07 to 1.76°/$_{oo}$ and 0.35 to 1.00°/$_{oo}$, respectively. Based on the overall range in isotopic values, the compounds can be clustered into two group. One consists primarily of parental PAH (Ace, A, Fl, Py, 226 and BaA) with enriched $\delta^{13}C$ values ranging between -25.1°/$_{oo}$ to -23.6°/$_{oo}$. The isotopic values of the second group (remaining compounds) are more depleted and ranged between -26.9°/$_{oo}$ and -25.5°/$_{oo}$. With the exception of Ace (-23.6°/$_{oo}$), the isotopic values of the parental and methylated 2 and 3-ring compounds ranged between -26.9°/$_{oo}$ and -25.0°/$_{oo}$. In comparison, the values for Fl, Py, methyl Fl-Py, substituted 226 and BaA were generally more enriched with mean values ranging between -25.7°/$_{oo}$ and -24.6°/$_{oo}$. Finally, the range in $\delta^{13}C$ values (-26.3°/$_{oo}$ to -25.5°/$_{oo}$) for Chy (4-ring), BFl, BeP and BaP (5-ring) (-26.3°/$_{oo}$ to -25.6°/$_{oo}$) is comparable to the range observed for the 2 and 3-ring PAH (Figure 30). Another salient feature of the overall trend, is the more enriched $\delta^{13}C$ values noted in A and BaA compared to their corresponding isomers Pa and Chy, also to a lesser extent Py compared to Fl. Inter-sample variations in the 2 and 3-ring compounds were less than the variation observed in the 4 and 5-ring species.

3.4.3 Other primary combustion sources:

3.4.3.1 Molecular signature:

The molecular signature of the composite soot samples obtained from the power generating station (PGS) and two domestic heating furnaces are shown in Table 12. The

Table 12. The concentration (ng/g) of the dominant compounds isolated from the hopper soot of the power generating station and domestic furnaces composite soots samples. DBT = Dibenzothiophene, B(ghi)Fl = Benzo(ghi)fluoranthene, CP(cd)Py = Cyclopenta(cd)pyrene

No	PAH	Mol Wt	Stack Hop	Dom. Furn. I	Dom. Furn. II
1	Na	128	+	-	-
2	Methyl Na	142	+	-	-
3	Ace	154	+	-	-
4	Dimethyl Na	156	+	-	-
5	Ay	152	+	-	-
6	Dibenzofuran*	168	+	+	+
7	F	166	+	-	+
8	Trimethyl Na	170	+	+	+
9	DBT	184	+	+	+
10	Pa	178	126!	196	118
11	A	178	+	-	-
12	Methyl DBT*	198	-	+	+
13	Methyl Pa	192	74	315	117
14	Methylene-Pa/A*	190	+	+	+
15	Methyl Pa	192	65	155	39
16	Phenyl Na	204	+	-	+
17	Dimethyl Pa/A	206	+	+	178
18	Fl	202	69	67	161
19	Py	202	87	63	62
20	Methyl Fl/Py*	216	+	-	+
21	Methyl Fl/Py*	216	+	-	+
22	Trimethyl Pa/A	220	+	+	-
23	B(ghi)Fl/CP(cd)Py*	226	+	+	+
24	BaA	228	82	79	-
25	Chy	228	182	-	36
26	Methyl BaA/Chy	242	+	-	-
27	BFl	252	85	-	-
28	BeP	252	76	-	-
29	BaP	252	60	-	-

! = Concentrations in ng/g of soot material
+ = Identified
- = Not detected
* = Tentatively identified by GC-MS

composite PGS soot consisted of 2 to 5-ring parental, methylated or substituted compounds, with parental PAH more abundant. The methylated PAH consisted mainly of mono-, di- and trimethylated Na and Pa. DBT and its methylated homologues, phenyl Na and the m/z 226 amu species were also identified. Individual concentrations were generally low, with Pa (3-ring) and Chy (4-ring) being the most abundant compounds identified in the stack hopper. The furnace soots were collectively characterized by the similar dominance of 3 and 4-ring compounds with the methylated Pa (3-ring) in equal or greater concentrations than their parental analogue. The 3-ring compounds were generally more abundant in both samples, but furnace soot II also had elevated concentrations of Fl (Fl/Py, 2.60 compared to Fl/Py, 1.06 in furnace soot I). All three samples were characterized by the absence of a significant UCM.

3.4.3.2 Carbon isotopes:

The $\delta^{13}C$ values of the PAH isolated from the PGS soot ranged between -26.5‰ and -25.6‰ (Figure 31). The parental values ranged between -25.7‰ and -25.6‰ and the methylated compounds ranged between -26.8‰ and -26.0‰ (Table 10). In general, the parental compounds were isotopically enriched compared to their methylated derivatives. PAH isotopic values isolated from furnace soot I ranged between -27.9‰ and -25.7‰. The most prominent features are the isotopically depleted MPa and BFl. The range in isotopic values of furnace soot II was between -27.3‰ and -25.4‰, which are very similar to the PGS composite soot sample.

Figure 31. $\delta^{13}C$ of the individual 3, 4 and 5-ring parental and methylated PAH isolated from the power generating station and domestic furnace composite soot samples. Pa = Phenanthrene, MPa = Methyl Phenanthrene, PNa = Phenyl Naphthalene, DPa = Dimethyl Phenanthrene, Fl = Fluoranthene, Py = Pyrene, BaA+Chy = Benz(a)anthracene and Chrysene, BFl = Benzofluoranthenes, BeP+ BaP = Benzo(e)pyrene and Benzo(a)pyrene

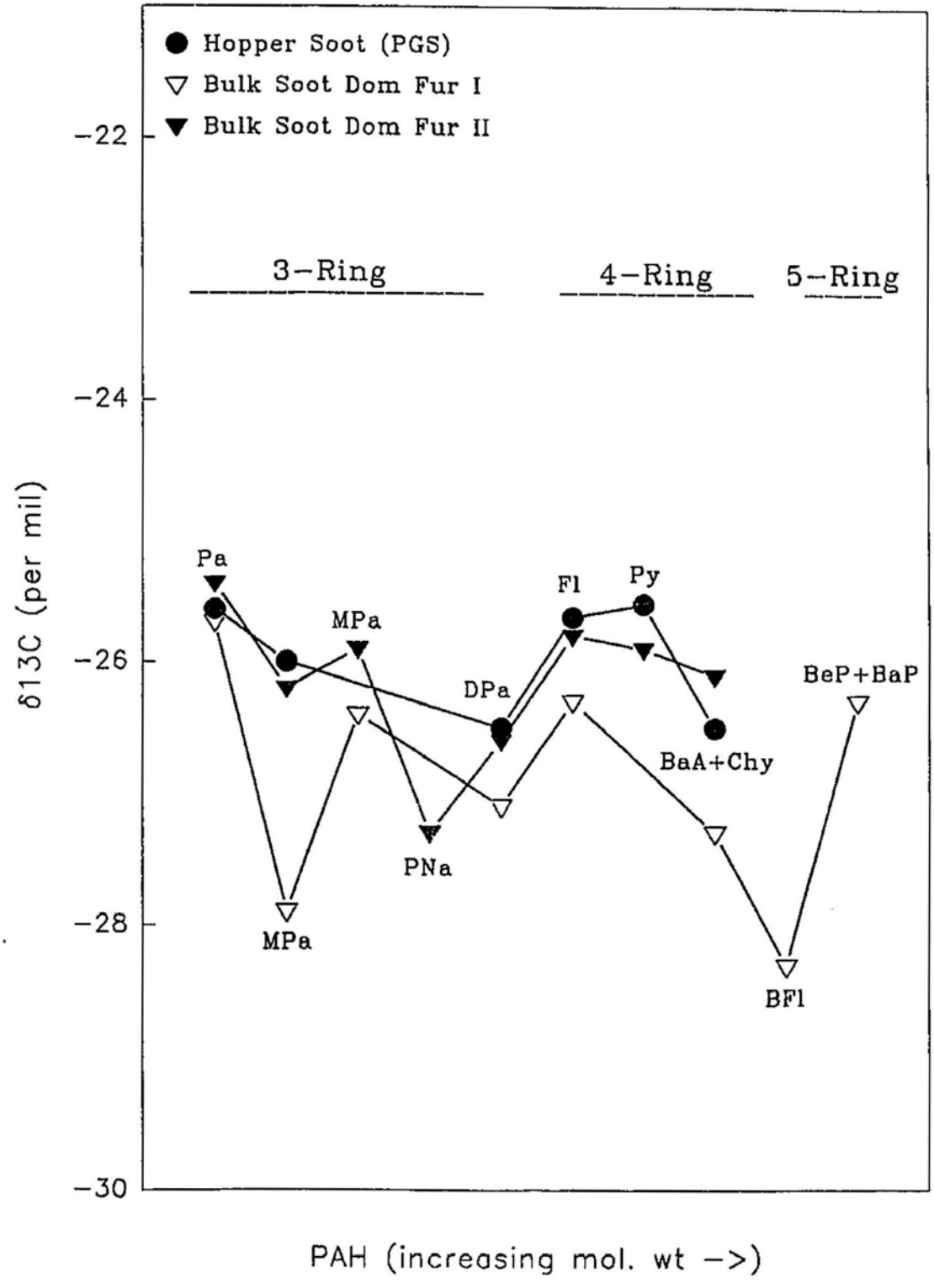
Hopper Soot (PGS)
Bulk Soot Dom Fur I
Bulk Soot Dom Fur II
3-Ring
4-Ring
5-Ring
-22
-24
-26
-28
-30
δ13C (per mil)
Pa
MPa
MPa
PNa
DPa
Fl
Py
BaA+Chy
BeP+BaP
BFl
PAH (increasing mol. wt ->)

3.4.4 Used crankcase oil:

3.4.4.1 Molecular signature:

The PAH inventory of individual and composite used crankcase oil samples was comprised of a range of parental, methylated and substituted linear 2 to 5-ring peri-condensed PAH (Table 13). The 2, 3 and 4-ring methylated PAH were the most prominent, while parental compounds were less abundant. The samples were also collectively characterized by the presence of the sulphur substituted DBT and methyl DBT species. Dibenzofuran and phenyl Na were also identified by GC-MS. A variable UCM occurring prominently between 40 and 82 minutes (RI 1750-3100) in some samples (Figure 14) and between 24 and 63 minutes (RI 1440-2500) in others was also observed in the analyzed samples. The mean normalized concentrations of the prominent compounds are characterized by the dominance of the 2 and 3-ring parental and methylated PAH (Figure 32). With the exception of Py, the concentrations of the higher molecular weight compounds (4 and 5-ring) were lower than the 2 and 3-ring species.

3.4.4.2 Carbon isotopes:

The carbon isotope values of individual and composite crankcase oil samples are summarized in Figure 33. Because of the difficulty in separating the higher molecular weight co-eluting isomers, individual mean isotopic values are reported for BaA+Chy and BeP+BaP. The mean $\delta^{13}C$ values of the individual PAH isolated from the composite crankcase oil samples ranged between -28.9‰ and -26.2‰ with maximum sample to sample variation ranging between 0.21 and 1.00‰ (Figure 33; Table 10). The $\delta^{13}C$ values of the parental compounds ranged between -28.9‰ and -26.6‰ and the

Table 13. The range of PAH isolated from the composite crankcase oil samples. (++ = most abundant compounds that were isotopically measurable; + = detected but not isotopically analyzed). DBT = Dibenzothiophene

No	PAH	Mol W	Comp 1	Comp 2	Comp 3	Comp 4	Comp 5	Comp 6
1	Na	128	+	+	+	+	+	+
2	Methyl Na	142	++	++	++	++	++	++
3	Methyl Na	142	++	++	++	++	++	++
4	Dimethyl Na	156	++	++	++	++	++	++
5	Dimethyl Na	156	++	++	++	++	++	++
6	Dimethyl Na	156	++	++	++	++	++	++
7	Dimethyl Na	156	++	++	++	++	++	++
8	Dimethyl Na	156	++	++	++	++	++	++
9	Dibenzofuran*	168		+	+	+	+	+
10	Trimethyl Na	170	+	+	+	+	+	+
11	Trimethyl Na	170	++	++	++	++	++	++
12	Trimethyl Na	170	++	++	++	++	++	++
13	Trimethyl Na	170	+	+	+	+	+	+
14	Trimethyl Na	170	+	+	+	+	+	+
15	F	166	++	++	++	++	++	++
16	Methyl F	180	+	+	+	+	+	+
17	DBT	184		+	+	+	+	+
18	Pa	178	++	++	++	++	++	++
19	A	178	+	+	+	+	+	+
20	Methyl DBT	198	+	+	+	+	+	+
21	Methyl Pa	192	++	++	++	++	++	++
22	Methylene-Pa-A*	190	+	+	+	+	+	+
23	Methyl Pa	192	++	++	++	++	++	++
24	Phenyl Na	204	++	++	++	++	++	++
25	Dimethyl Pa	206	++	++	++	++	++	++
26	Dimethyl Pa	206	++	++	++	++	++	++
27	Dimethyl Pa	206	++	++	++	++	++	++
28	Fl	202	++	++	++	++	++	++
29	Py	202	++	++	++	++	++	++
30	Trimethyl Pa/A*	220	+		+	+	+	+
31	Trimethyl Pa/A*	220	+		+		+	+
32	Methyl Fl-Py*	216	++	++	++	++	++	++
33	Methyl Fl-Py*	216	++	++	++	++	++	++
34	Methyl Fl-Py*	216	++	++	++	++	++	++
35	Dimethyl Fl-Py*	230	+	+	+	+	+	+
36	Dimethyl Fl-Py*	230	+	+	+	+	+	+
37	BaA	228	++	++	++	++	++	++
38	Chy	228	++	++	++	++	++	++
39	Methyl BaA-Chy'	242	+	+	+	+	+	+
40	BFl	252	++	++	++	++	++	++
41	BeP	252	++	++	++	++	++	++
42	BaP	252	+	+	+	+	+	+

++ = Most abundant
* = Tentatively identified by GC-MS

Figure 32. Mean normalized concentrations of the 2, 3, 4 and 5-rin : PAH in the composite crankcase oil samples. PAH concentrations in the single samples were summed and treated as an individual composite sample. Na = Naphthalene, MNa = Methyl Naphthalene, DNa = Dimethyl Naphthalene, TNa = Trimethyl Naphthalene, F = Fluorene, Pa = Phenanthrene, A = Anthracene, MPa = Methyl Phenanthrene, DPa = Dimethyl Phenanthrene, Fl = Fluoranthene, Py = Pyrene, BaA = Benz(a)anthracene, Chy = Chrysene, BFl = Benzofluoranthenes, BeP = Benzo(e)pyrene and BaP = Benzo(a)pyrene

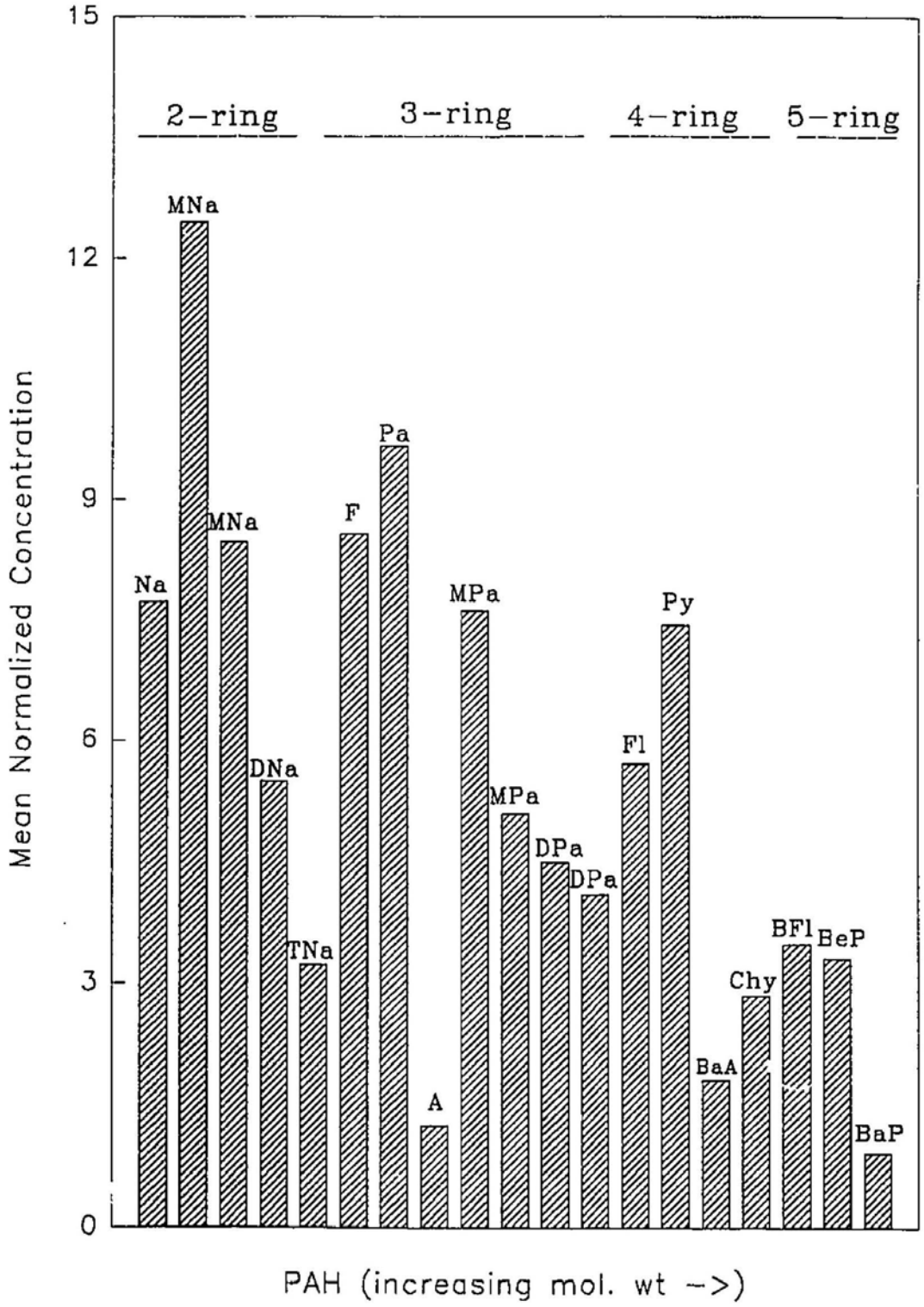
15
12
9
6
3
0
2-ring
3-ring
4-ring
5-ring
Mean Normalized Concentration
Na
MNa
MNa
DNa
TNa
F
Pa
A
MPa
MPa
DPa
DPa
Fl
Py
BaA
Chy
BFl
BeP
BaP
PAH (increasing mol. wt ->)

Figure 33. Mean and range (standard deviation; 2σ) of the $\delta^{13}C$ of the individual 2, 3, 4 and 5-ring parental and methylated PAH isolated from the composite crankcase oil samples. Isotopic values of the PAH in the single samples were summed and treated as an individual composite sample. Na = Naphthalene, MNa = Methyl Naphthalene, DNa = Dimethyl Naphthalene, TNa = Trimethyl Naphthalene, F = Fluorene, Pa = Phenanthrene, MPa = Methyl Phenanthrene, PNa = Phenyl Naphthalene, DPa = Dimethyl Phenanthrene, Fl = Fluoranthene, Py = Pyrene, MFl-Py = Methyl Fluoranthene-Pyrene, BaA+Chy = Benz(a)anthracene and Chrysene, BFl = Benzofluoranthenes, BeP+BaP = Benzo(e)pyrene and Benzo(a)pyrene

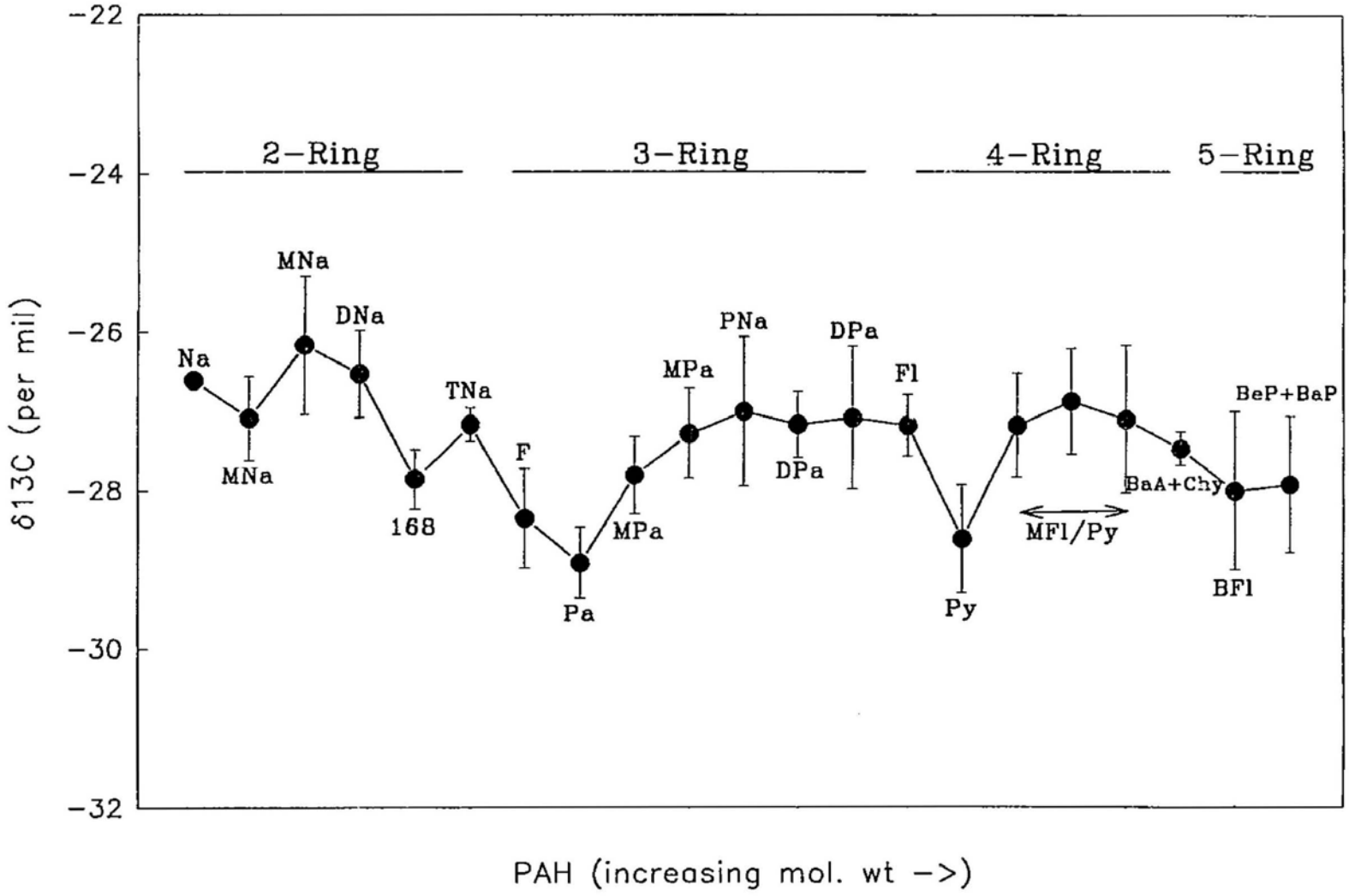
−22
−24
−26
−28
−30
−32
δ13C (per mil)
2−Ring
3−Ring
4−Ring
5−Ring
Na
MNa
MNa
DNa
168
TNa
F
Pa
MPa
MPa
PNa
DPa
DPa
Fl
Py
MFl/Py
BaA+Chy
BeP+BaP
BFl
PAH (increasing mol. wt −>)

variance was similar to that reported above. The $\delta^{13}C$ values of the methylated species ranged between -27.8°/$_{oo}$ and -26.2°/$_{oo}$, with variations between 0.22 and 0.87°/$_{oo}$. The general trend is characterized by isotopically enriched Na and MNa and significantly depleted Pa and Py. These trends were consistently reflected in all the samples investigated in the present study. The $\delta^{13}C$ values of the remaining 4-ring (Fl, Methyl Fl-Py, BaA+Chy) and 5-ring (BFl and BeP+BaP) ranged between -28.0°/$_{oo}$ and -26.9°/$_{oo}$. Pa and Py were consistently more depleted than their methylated derivatives and Fl was consistently more enriched than Py. Inter-sample variation was similar for most compounds, except for the parental PAH, phenyl Na and the BFl, with mean variations of 0.97 and 1.00 °/$_{oo}$, respectively. MNa and DPa also had high variations of 0.90°/$_{oo}$.

3.4.5 Other primary petroleum sources:

The following section briefly describes the molecular and carbon isotope signatures of crude petroleum, #2 fuel oil (fresh petroleum samples) and the bulk condensate collected from two-stroke outboard motor engines (used petroleum sample; Table 14). These samples were analyzed to further constrain the isotopic signatures of petroleum-related compounds.

3.4.5.1 Molecular signature:

The molecular signature of the crude petroleum samples comprised predominantly of 2 and 3-ring parental, mono-, di- and trimethylated naphthalene and phenanthrene as well as sulphur substituted PAH, DBT and its methylated homologues. The methylated PAH were the most prominent, while the parental compounds were less abundant. A relatively small UCM extending from 17 to 40 minutes (RI = 1210- 1750),

Table 14. The range of PAH isolated from crude petroleum and petroleum products. (++ = most abundant compounds that were isotopically measurable). Arab. Crude = Arabian Crude, Cal Crude = Calgary Crude, C.Case Oil = Crankcase Oil, O.board Motors = Two-stroke outboard motors.

No	PAH	Mol Wt.	Arab Crude	Cal Crude	C.Case Oil	O.board Motors	# 2 Fuel Oil
1	Na	128	++	++	+	++	++
2	Methyl Na	142	++	++	++	++	++
3	Methyl Na	142	++	++	++	++	++
4	DimethylNa	156	++	++	+	++	++
5	DimethylNa	156	++	++	++	++	++
6	Dimethyl Na	156	++	++	++	++	++
7	Dimethyl Na	156	++	++	++	++	++
8	Dimethyl Na	156	++	++	++	++	++
9	TrimethylNa	170	++	++	+	++	++
10	Trimethyl Na	170	++	++	+	++	++
11	Trimethyl Na	170	++	++	++	++	++
12	Trimethyl Na	170	++	++	+	++	++
13	DBT	184	++	++	++	+	++
14	Pa	178	++	++	++	++	-
15	MethylDBT	198	++	++	+	+	-
16	Methyl DBT	198	++	++	+	+	-
17	Methyl DBT	198	++	++	+	-	-
18	Methyl Pa	192	++	++	++	++	-
19	Methyl Pa	192	++	++	++	+	-
20	Dimethyl DBT*	212	++	++	+	+	-
21	Dimethyl DBT*	212	++	++	+	+	-
22	Dimethyl DBT*	212	++	++	+	-	-
23	Dimethyl Pa/A*	206	++	++	++	-	-
24	Trimethyl DBT*	226	++	++	+	-	-
25	Trimethyl DBT*	226	++	++	+	-	-
26	Fl	202	-	-	++	++	-
27	Py	202	+	-	++	++	-
28	Baa/Chy	228/228	-	-	++	+	-
29	BFl	252	-	-	++	+	-
30	BaP/BeP	252/252	-	-	++	+	-

* = Tentatively identified by GC-MS

was also notable in these samples. Despite the difference in the nature of the #2 fuel oil and the outboard motor condensate samples they both had very similar molecular signatures, except for the presence of 4 and 5-ring parental compounds in the latter sample.

3.4.5.2 Carbon isotopes:

Individual isotopic measurements were generally possible only on the more abundant methylated PAH in the crude oil samples. Na and Pa were the only adequately resolved parental compounds allowing isotopic determinations. Despite a 0.25 to 2.93°/$_{oo}$ difference in the isotopic values of the individual compounds, both crude oil samples had similar trends of isotopically enriched $\delta^{13}C$ values for Na and MNa and relatively depleted Pa and DBT (Figure 34). The PAH $\delta^{13}C$ values of the Arabian crude ranged between -30.6°/$_{oo}$ and -22.7°/$_{oo}$ and values of the Calgary crude ranged between -32.2°/$_{oo}$ and 25.0°/$_{oo}$. These values are significantly less depleted than those reported by Chung (1992). Differences were also observed in the isotopic values of alkylated isomers, e.g. dimethyl Na, values ranged between -27.0°/$_{oo}$ and -23.9°/$_{oo}$. The methylated DBT isomers exhibited the most consistent trends becoming increasingly enriched in ^{13}C with different sites of alkylation (Figure 34).

The $\delta^{13}C$ values of the parental and methylated PAH isolated from the condensate of the two-stroke outboard motor ranged between -28.5°/$_{oo}$ and -24.5°/$_{oo}$ (Figure 35), with no obvious difference between the values of the parental and methylated compounds. Similar to the crude oils, the most distinctive feature of the outboard motor condensate is the presence of isotopically enriched methylated Na's (2-ring), with more depleted 3 and 4-ring compounds. Methylated naphthalenes were the most prominent species

Figure 34. $\delta^{13}C$ of the individual 2 and 3-ring parental and methylated PAH isolated from the two crude petroleum samples. Na = Naphthalene, MNa = Methyl Naphthalene, DNa = Dimethyl Naphthalene, TNa = Trimethyl Naphthalene, DBT = Dibenzothiophene, Pa = Phenanthrene, MDBT = Methyl Dibenzothiophene, MPa = Methyl Phenanthrene, DPa = Dimethyl Phenanthrene, DDBT = Dimethyl Dibenzothiophene, Trimethyl Dibenzothiophene

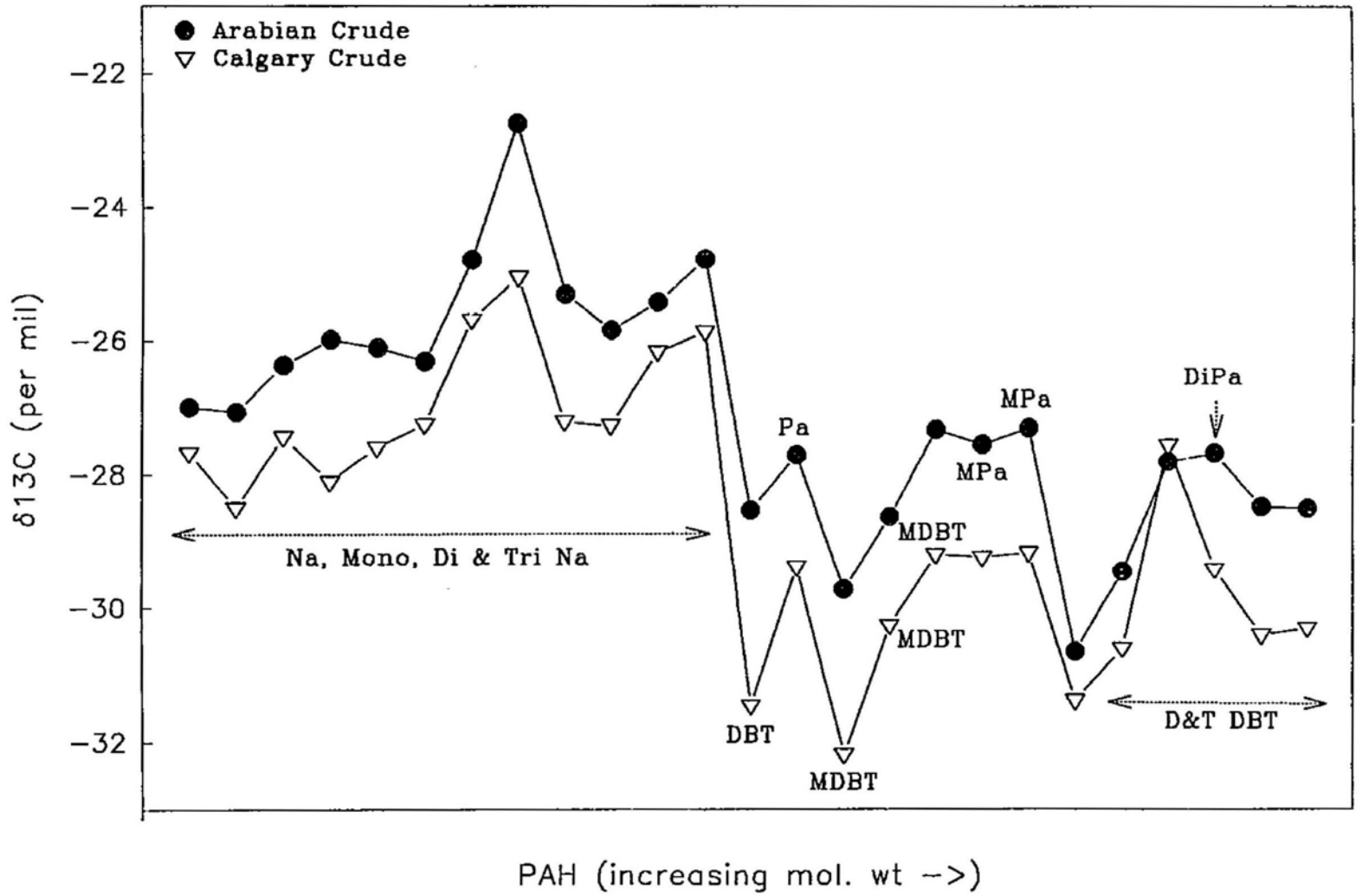
Arabian Crude
Calgary Crude
−22
−24
−26
−28
−30
−32
δ13C (per mil)
Na, Mono, Di & Tri Na
Pa
DBT
MDBT
MDBT
MDBT
MPa
MPa
DiPa
D&T DBT
PAH (increasing mol. wt −>)

Figure 35. The $\delta^{13}C$ values of individual PAH isolated from outboard motor condensates compared to the $\delta^{13}C$ of used crankcase oils. Na = Naphthalene, MNa = Methyl Naphthalene, DNa = Dimethyl Naphthalene, TNa = Trimethyl Naphthalene, Pa = Phenanthrene, MPa = Methyl Phenanthrene, Fl = Fluoranthene, Py = Pyrene

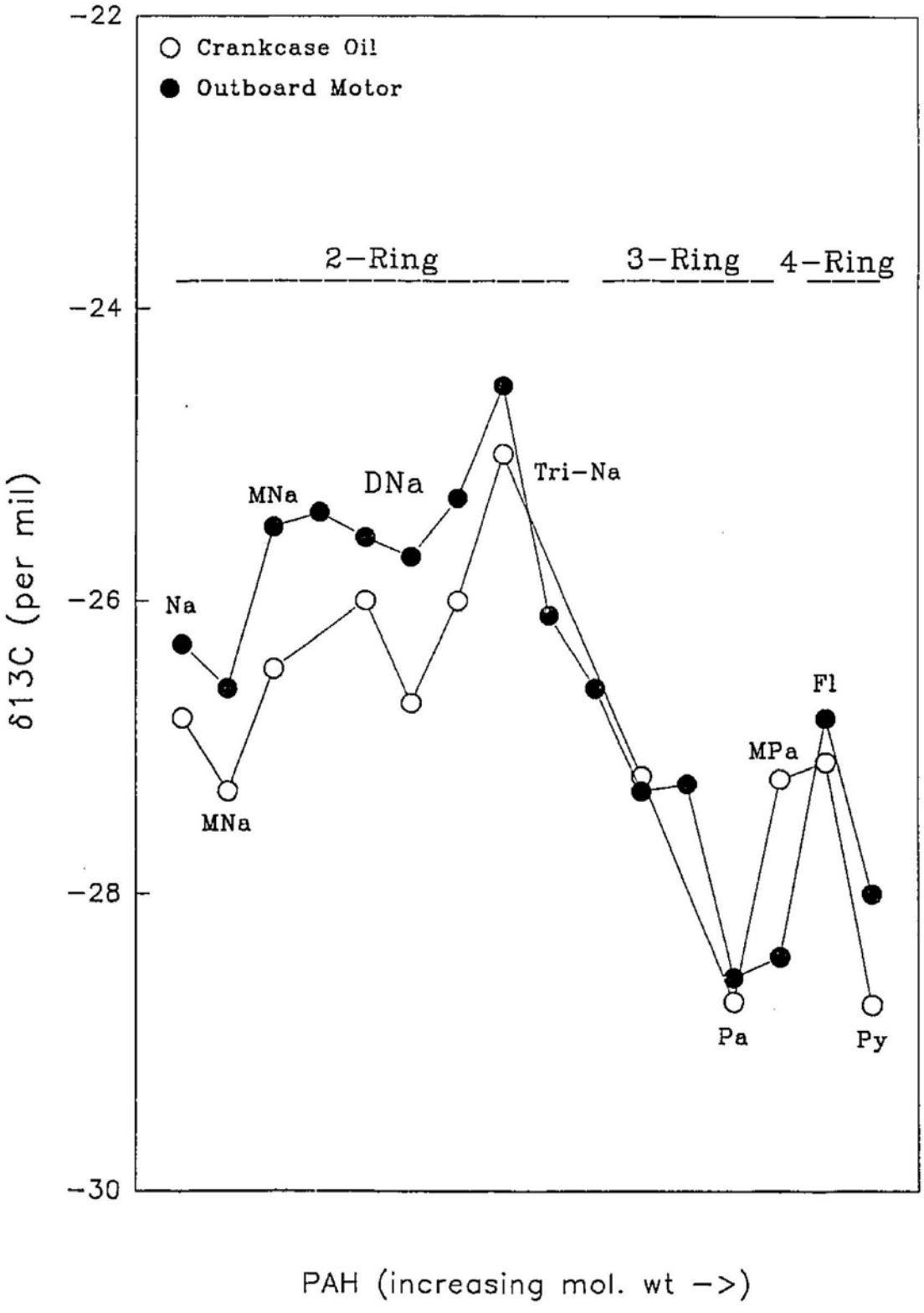
Crankcase Oil
Outboard Motor
2-Ring
3-Ring
4-Ring
Na
MNa
DNa
Tri-Na
MNa
MPa
Fl
Pa
Py
δ13C (per mil)
-22
-24
-26
-28
-30
PAH (increasing mol. wt ->)

identified in #2 fuel oil and the isotopic values ranged between -27.0°/$_{oo}$ and -25.5°/$_{oo}$ and followed very similar intermolecular trends as the other petroleum products investigated (Figure 36).

3.5 Molecular and carbon isotope signatures of the secondary sources:

3.5.1 Road surface sweeps:

3.5.1.1 Molecular signature:

The suite of road surface sweeps investigated consisted of samples from open roads and from underground car parks with either a cement or asphalt paved surface. The combined molecular signatures of these samples are shown in Table 15. Open-road samples (n = 9) were generally characterized by the dominance of a UCM extending from 40 to 65 minutes (RI 1750-2500) with well resolved 3, 4 and 5-ring parental PAH in measurable concentrations (Figure 37; Appendix F2). Although only in trace concentrations, a range of other parental, methylated and substituted compounds were also identified: Na, F, DBT and methylated Na, DBT, Pa, Fl-Py and BaA-Chy. Dibenzofuran, phenyl Na and the m/z 226 amu compound were also identified in most of the samples investigated. A plot of the mean normalized concentration shows that the 3 (Pa), 4 and 5-ring parental PAH are the most abundant compounds in the open-road sweeps (Figure 37). Fl concentrations were generally slightly higher than Py, while Pa was significantly more abundant than A. The molecular signature of the composite sweep from the cement paved car park was similar to the open-road surface signature. However, the concentration of the resolved compounds from the cement paved surface were generally lower with Fl dominating.

Figure 36. The $\delta^{13}C$ values of Naphthalene (Na), Methyl Naphthalene (MNa), Dimethyl Naphthalene (DNa) and Trimethylated Naphthalenes (TNa) isolated from crude petroleum and petroleum products.

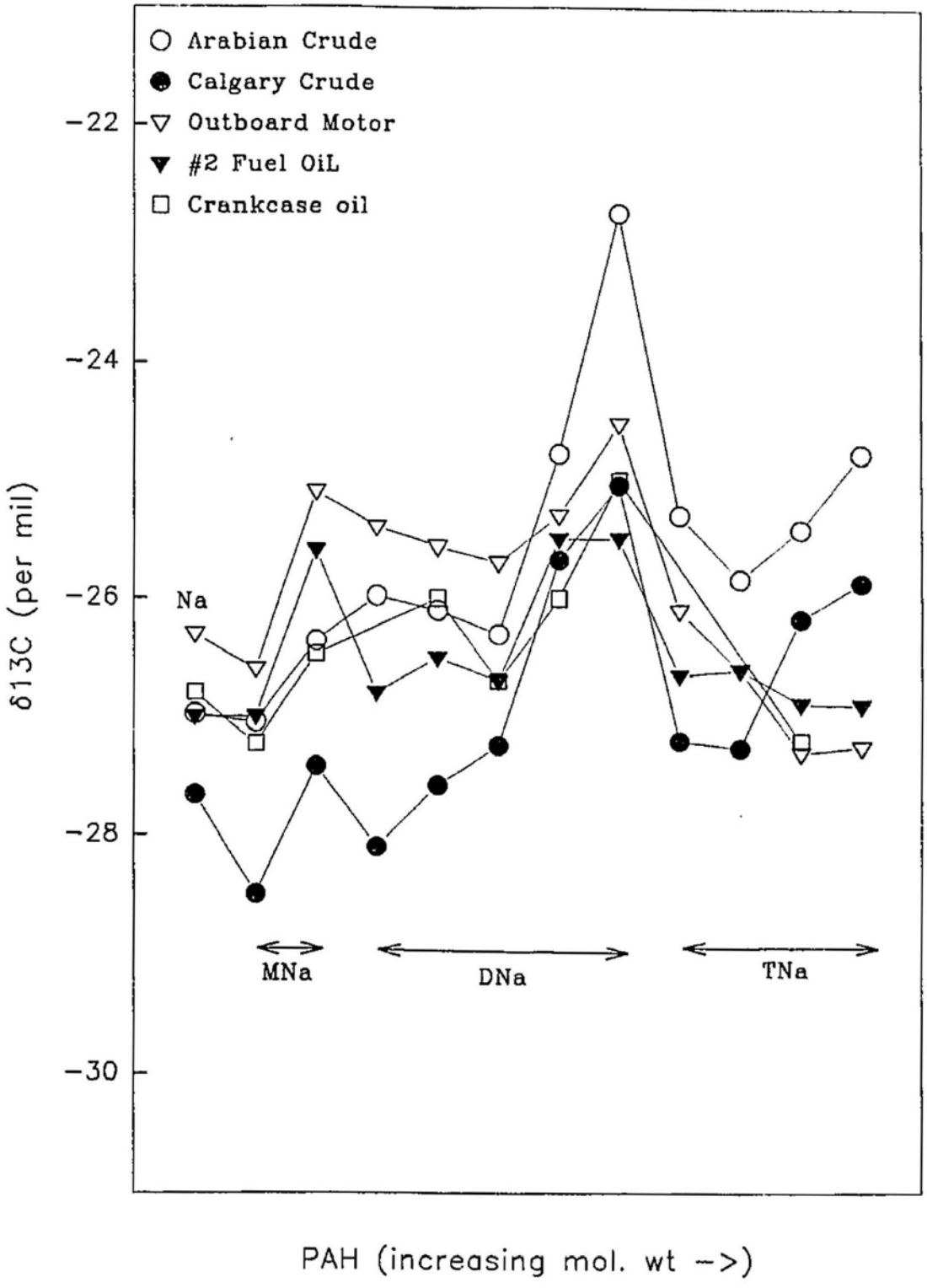
Arabian Crude
Calgary Crude
Outboard Motor
#2 Fuel OiL
Crankcase oil
−22
−24
−26
−28
−30
δ13C (per mil)
Na
MNa
DNa
TNa
PAH (increasing mol. wt −>)

Table 15. The range of PAH isolated from open-road and enclosed car park sweep samples. (++ = most abundant compounds that were isotopically measurable; + = detected but not isotopically analyzed). DBT = Dibenzothiophene, B(ghi)Fl =Benzo(ghi)fiuoranthene, CP(cd)Py = Cyclopenta(cd)pyrene, I(cd)Py= Indeno(123 cd) pyrene, B(ghi)Per = Benzo(ghi)perylene, Anthant= Anthanthrene.

No	PAH	Mol Wt	Sing 1	Sing 2	Sing 3	Sing 4	Sing 5!	Sing 6!!	Sing 7	Sing 8	Sing 9	Sing 10	Sing 11
1	Na	128		+		+		+	+		+		
2	Methyl Na	142		+		+		++	+		+		
3	Methyl Na	142		+				++			+		
4	Ace	154						+	+		+		
5	Dimethyl Na	156						++	+		+		
7	Dibenzofuran*	168			+	+	+	++	+		+		
8	Trimethyl Na	170						+			+		
9	F	166	+	+	+	+	+	++	+		+	+	+
10	DBT	184	+		+	+		+	+		+	+	+
11	Pa	178	++	++	++	++	++	++	++	++	++	++	++
12	A	178	+	+	+	++	+	+	+	+	+	+	++
13	Methyl-DBT	198				+		+			+	+	+
14	Methyl Pa	192	+	+	++	++	+	++	+	++	+	+	+
15	Methylene Pa-A*	190	+	+	+	+		+	+	+	+	+	+
16	Methyl Pa	192	+	+	+	+	+	++	+	++	+	+	+
17	Phenyl Na	204	+	+	+	+	+	+	+		+	+	+
18	Dimethyl Pa	206	+	+	+	+	+	++	+	++	+	+	+
19	Fl	202	++	++	++	++	++	++	++	++	++	++	++
20	Py	202	++	++	++	++	++	++	++	++	++	++	++
21	Trimetyl Pa-A*	220	+	+	+	+	+	+	+		+	+	+
22	Methyl Fl-Py*	216	+	+	+	+	+	+	+	+	+	+	+
23	Methyl-Fl-Py*	216	+	+	+	+		+	+	+	+	+	+
24	Methyl Fl-Py*	230	+	+	+	+						+	+
25	B(ghi)Fl/CP(cd)Py*	226	+	+	+	+	+	+	+		+		+
26	BaA	228	++	++	++	++	++	+	+	+	+	+	+
27	Chy	228	++	++	++	++	++	+	+	+	+	+	+
28	Methyl BaA-Chy*	242	+	+	+				+				
29	BFl	252	++	++	++	++	++	++	++	++	++	++	++
30	BeP	252	++	++	++	++	++	++	++	++	++	++	++
31	BaP	252	++	++	++	++	++	++	++	++	++	++	++
32	Perylene	252	+		+	+			+		+	+	+
33	I(cd)Py/B(ghi)Per/Anth*	276	+	+		+		+	+		+	+	+
34	I(cd)Py/B(ghi)Per/Anth*	276	+	+		+		+	+		+	+	+

! = Cement Paved Car Park
!! = Asphalt Paved Car Park
++ = Most abundant
* = Tentatively identified by GC-MS

Figure 37. The mean normalized concentrations of the 2, 3, 4 and 5-ring PAH isolated from the open-road sweeps and enclosed cement and asphalt paved car park samples. MNa = Methyl Naphthalene, Pa = Phenanthrene, MPa = Methyl Phenanthrene, Fl = Fluoranthene, Py = Pyrene, BaA = Benz(a)anthracene, Chy = Chrysene, BFl = Benzofluoranthenes, BeP = Benzo(e)pyrene and BaP Benzo(a)pyrene

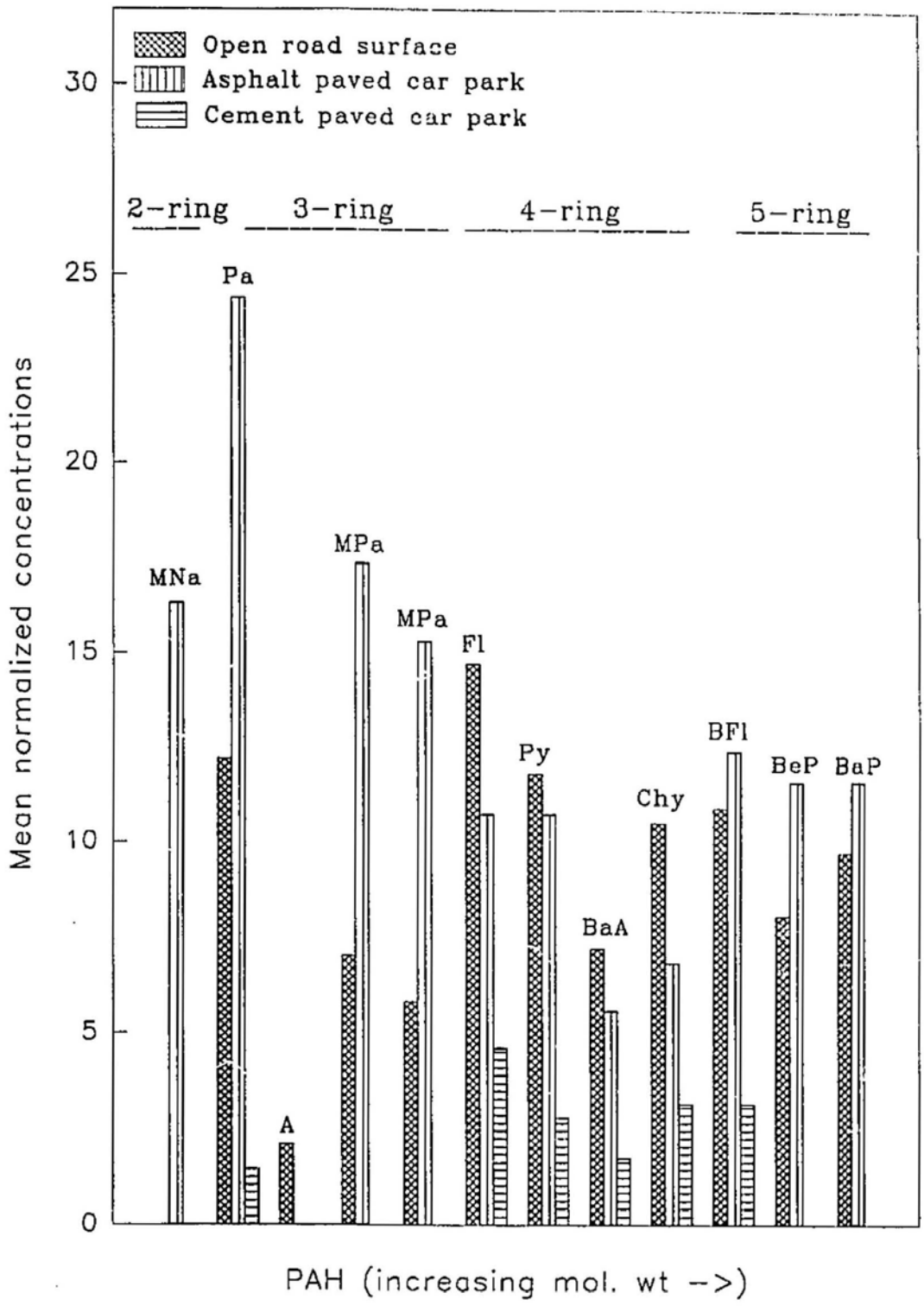
Open road surface
Asphalt paved car park
Cement paved car park
2-ring
3-ring
4-ring
5-ring
Mean normalized concentrations
0
5
10
15
20
25
30
MNa
Pa
A
MPa
MPa
Fl
Py
BaA
Chy
BFl
BeP
BaP
PAH (increasing mol. wt ->)

The signature of the asphalt paved surface sweep was bimodal (two distinct humps), consisting initially of 2 and 3-ring parental and methylated compounds, followed by 4 and 5-ring parental PAH (Figure 37). Methylated Na, Pa and its methylated derivatives were the most abundant compounds in this composite sample. The UCM was not as prominent as that identified in both the open road surface and the cement paved car park.

3.5.1.2 Carbon isotopes:

The isotopic signatures of the PAH extracted from the different road surface sweeps, along with the mean and variation of the individual PAH from the open-road samples are shown in Figure 38. Since the total PAH concentrations in the open road samples were relatively low, individual isotopic measurements of A and the methylated Pa were only performed on a limited number of samples. Individual isotopic values are again reported for BaA+Chy and BeP+BaP. The overall mean isotopic values ranged between -27.1°/$_{oo}$ and -23.7°/$_{oo}$ with variations ranging between 0.34 to 1.25°/$_{oo}$ (Table 10). The most prominent features in the overall trend are isotopically enriched A (-23.7°/$_{oo}$), depleted BaA+Chy, BFl and BeP+BaP (-26.5, -27.1°/$_{oo}$ and -26.1°/$_{oo}$) and intermediate values for Pa, methyl Pa, Fl and Py (-25.7°/$_{oo}$ to -25.1°/$_{oo}$). The general trend is for the isotopic value of the individual compounds to show increasing depletion in ^{13}C with increasing molecular weight. The isotopic values of the corresponding PAH isolated from the underground car park sweeps were significantly depleted, especially the sweep from the asphalt paved surface (Figure 38). The $\delta^{13}C$ values of the parental and methylated PAH isolated from these composite samples ranged between -30.4°/$_{oo}$ and -27.3°/$_{oo}$, for asphalt and -28.4°/$_{oo}$ to -26.4°/$_{oo}$, cement. Parental PAH were the only compounds present

Figure 38. Mean and range (standard deviation; 2σ) of the $\delta^{13}C$ of the individual 3, 4 and 5-ring parental and methylated PAH isolated from the single open-road sweep samples along with the $\delta^{13}C$ values of the PAH from the cement and asphalt paved enclosed car park. MNa = Methyl Naphthalene, DNa = Dimethyl Naphthalene, F = Fluorene, Pa = Phenanthrene, MPa = Methyl Phenanthrene, Fl = Fluoranthene, Py = Pyrene, BaA+Chy = Benz(a)anthracene and Chrysene, BFl = Benzofluoranthenes, BeP+BaP = Benzo(e)pyrene and Benzo(a)pyrene

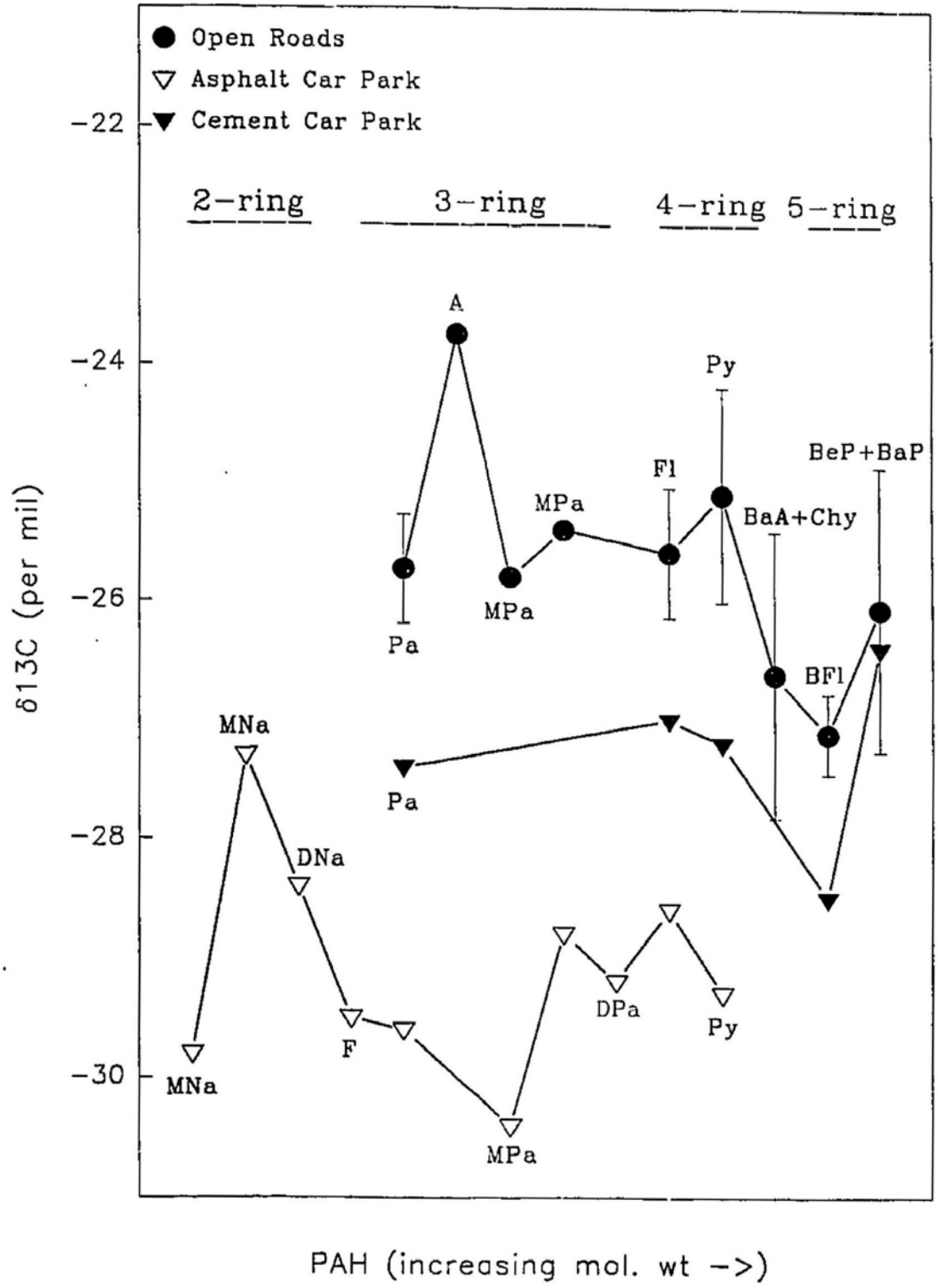
Open Roads
Asphalt Car Park
Cement Car Park
2-ring
3-ring
4-ring
5-ring
δ13C (per mil)
-22
-24
-26
-28
-30
A
Py
Fl
BeP+BaP
MPa
BaA+Chy
Pa
MPa
BFl
MNa
Pa
DNa
F
DPa
Py
MNa
MPa
PAH (increasing mol. wt ->)

sufficient quantities for isotopic determination in the cement paved extract.

3.5.2 Untreated domestic sewage:

3.5.2.1 Molecular signature:

The molecular trace for the two untreated domestic sewage samples were similar and consisted primarily of well-resolved 3, 4 and 5-ring parental PAH, along with a prominent UCM extending from 32 to 80 minutes (RI = 1500-3100) (Figure 39). The prominent compounds identified in measurable concentrations were 3, 4 and 5-ring parental PAH and 3-ring methylated compounds (Figure 40). Fl and Py were the most abundant, and Pa, Chy and BFl were in comparable concentrations. Again, relatively low concentration of A and methylated Pa were observed.

3.5.2.2 Carbon isotopes:

Only parental compounds and one isomer of methyl Pa was present in sufficient quantities for reliable isotopic determinations. Generally, the isotopic values of the 3 to 5-ring PAH ranged between -26.4‰ and -24.5‰ (Figure 41). The trend suggests that the isotopic values of the individual compounds become gradually depleted with increasing molecular weight. The most notable features in the overall isotopic signatures were the presence of enriched A, relatively depleted Py compared to Fl and depleted BFl and BeP+BaP.

3.5.3 Composite snow:

3.5.3.1 Molecular Signature:

The molecular signature of the composite snow sample was characterized by the presence of well-resolved 3, 4 and 5-ring parental PAH along with a prominent UCM

Figure 39. Total ion chromatogram (TIC) of a sewage sample comprising mainly of 3, 4 and 5-ring parental PAH. IS = Internal standard, 1 = Phenanthrene and Anthracene, 2 = Fluoranthene, 3 = Pyrene, 4 = Benz(a)anthracene and Chrysene, 5 = Benzofluoranthenes and 6 = Benzo(e)pyrene and Benzo(a)pyrene.

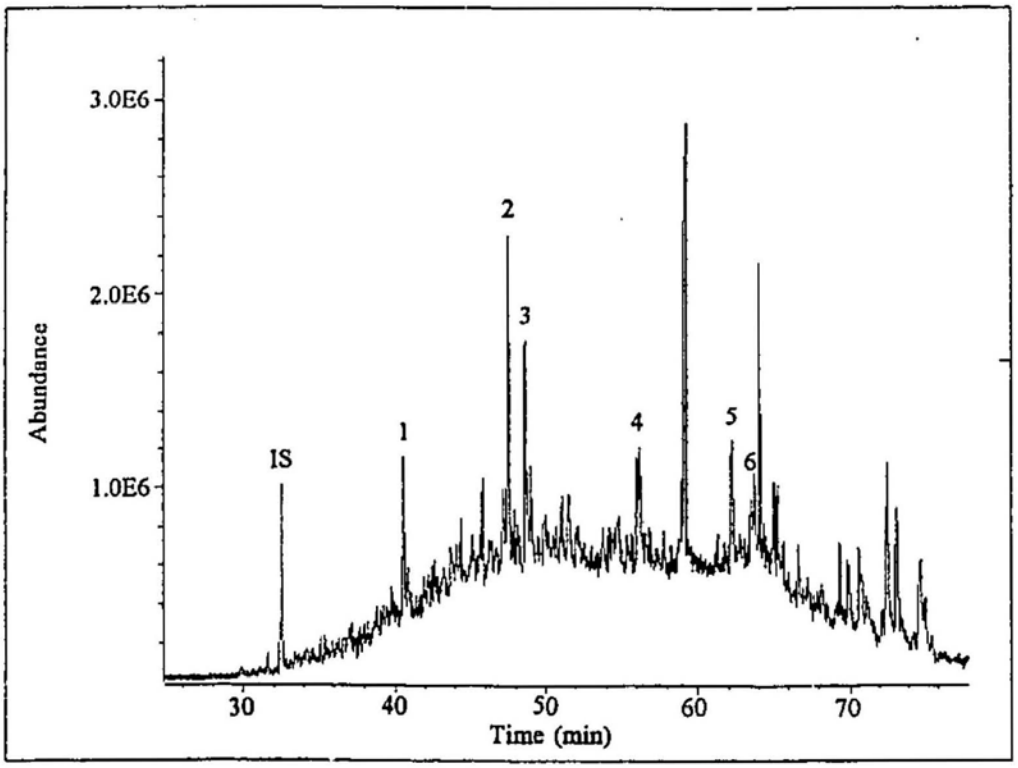
3.0E6
2.0E6
1.0E6
Abundance
IS
1
2
3
4
5
6
30
40
50
60
70
Time (min)

Figure 40. Mean normalized concentrations of the 3, 4 and 5-ring parental and methylated PAH in the sewage samples. Pa = Phenanthrene, A = Anthracene, MPa = Methyl Phenanthrene, Fl = Fluoranthene, Py = Pyrene, BaA = Benz(a)anthracene, Chy = Chrysene, BFl = Benzofluoranthenes, BeP = Benzo(e)pyrene and BaP = Benzo(a)pyrene.

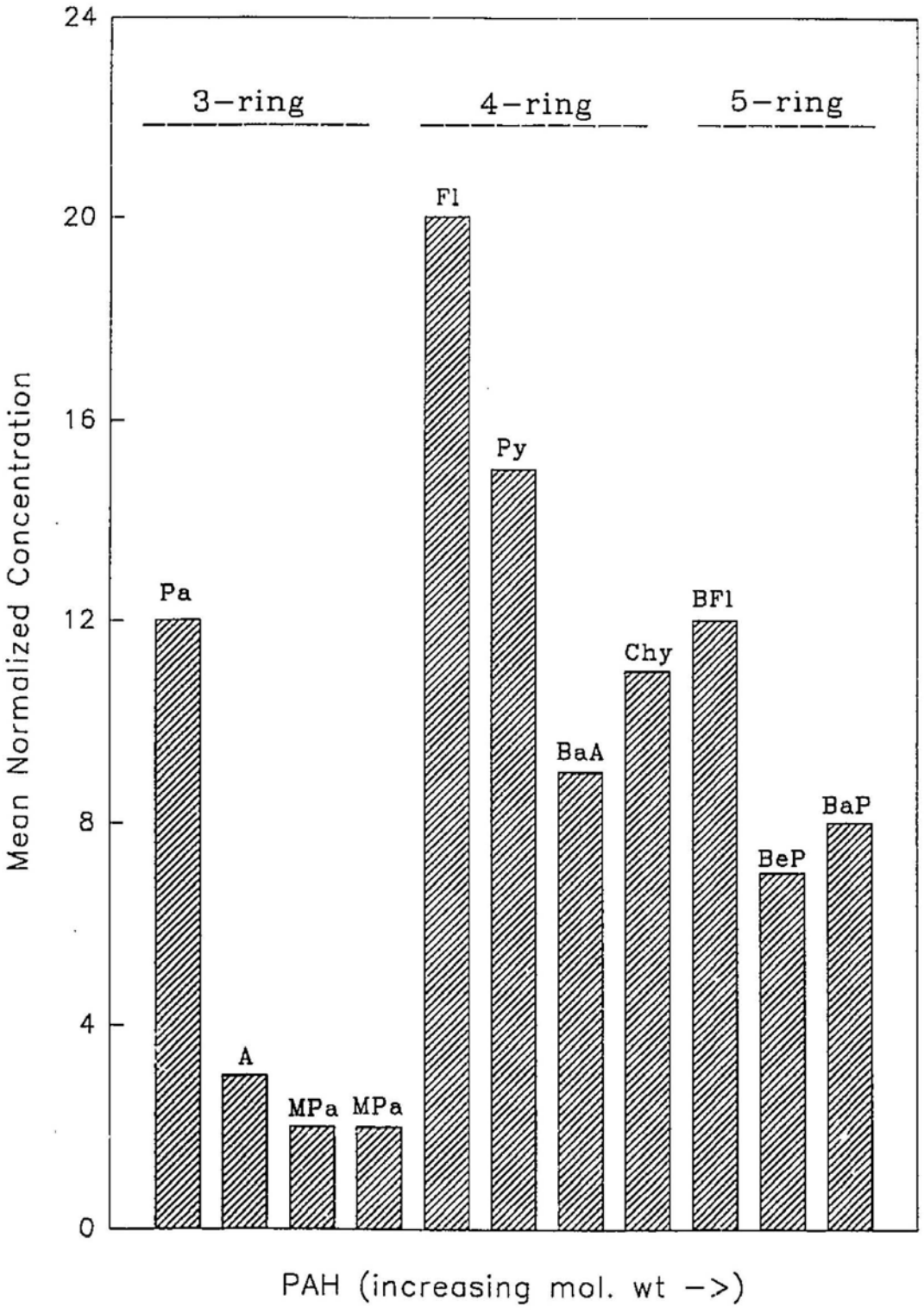
24
20
16
12
8
4
0
Mean Normalized Concentration
3-ring
4-ring
5-ring
Pa
A
MPa
MPa
Fl
Py
BaA
Chy
BFl
BeP
BaP
PAH (increasing mol. wt ->)

Figure 41. Mean $\delta^{13}C$ of the individual 3, 4 and 5-ring parental PAH isolated from the sewage samples. Pa = Phenanthrene, A = Anthracene, Fl = Fluoranthene, Py = Pyrene, BaA+Chy = Benz(a)anthracene and Chrysene, BFl = Benzofluoranthenes, BeP+BaP = Benzo(e)pyrene and Benzo(a)pyrene

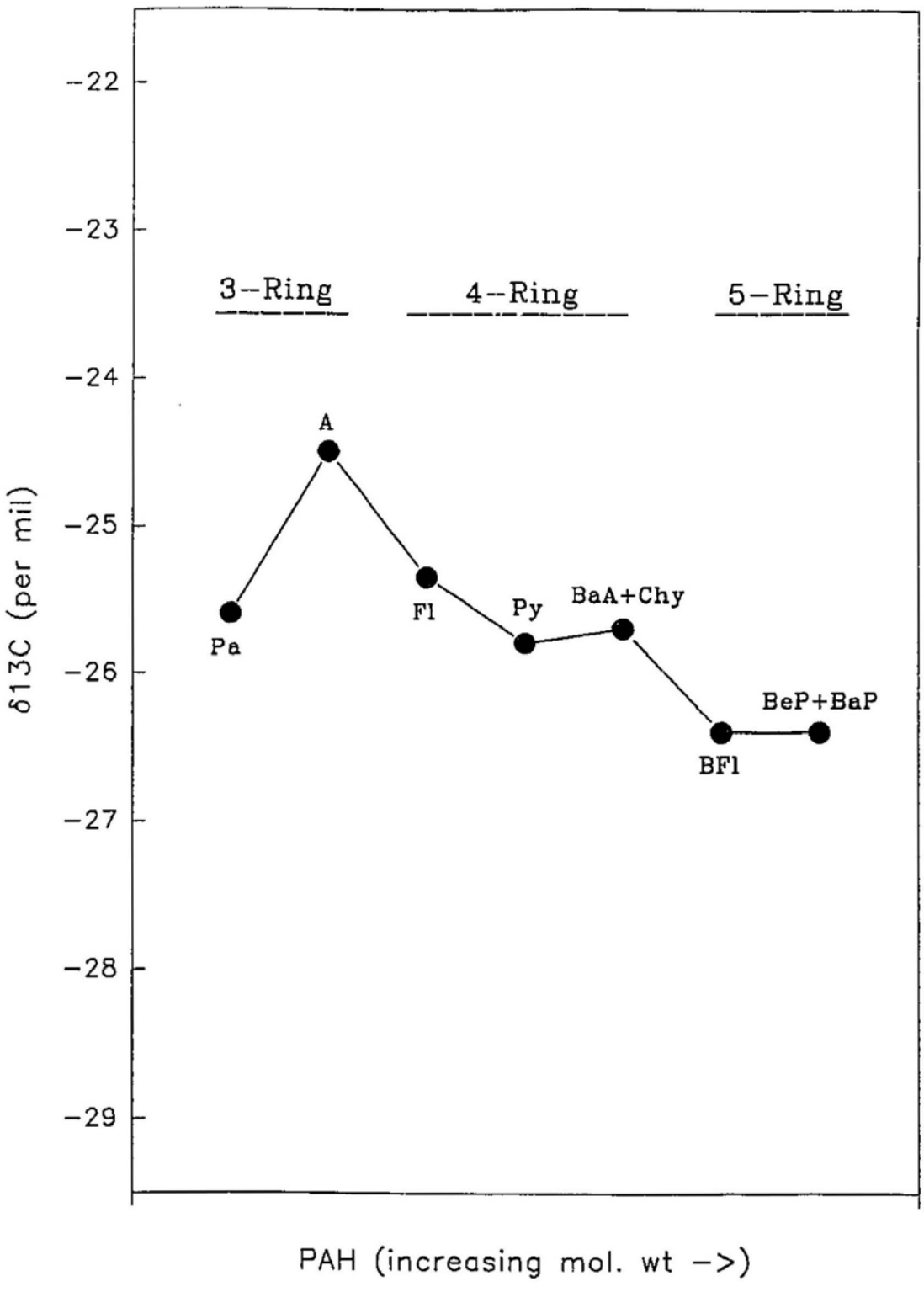
-22
-23
-24
-25
-26
-27
-28
-29
δ13C (per mil)
3--Ring
4--Ring
5--Ring
Pa
A
Fl
Py
BaA+Chy
BeP+BaP
BFl
PAH (increasing mol. wt ->)

extending from 40 to 80 minutes (RI 1750-3100) (Figure 42). The most abundant compounds present were 3, 4 and 5-ring parental PAH along with generally low concentrations of methylated species. The concentration of these compounds ranged between 0.20 µg and 2.95 µg/g with Pa, Fl and Py being the most abundant. Trace concentrations of 3 to 5-ring methylated PAH, DBT and its methylated derivatives were also identified.

3.5.3.2 Carbon isotopes:

The $\delta^{13}C$ values of the 3 to 5-ring parental compounds isolated from the composite snow sample ranged between -26.9°/$_{oo}$ and -24.9°/$_{oo}$. The overall intermolecular trend in $\delta^{13}C$ values was increasing depletions in ^{13}C with increasing molecular weight. Pa is the most enriched (-24.9°/$_{oo}$) while Py (-25.7°/$_{oo}$) is comparable to Fl (-25.4°/$_{oo}$). BaA+Chy and BFl are the most depleted, with similar $\delta^{13}C$ values (-26.9°/$_{oo}$).

3.6 Molecular and carbon isotope signatures of St. John's Harbour sediments:

3.6.1 Molecular signature:

The molecular signatures of prominent PAH isolated from St. John's Harbour sediments are summarized in Table 16. The PAH ranged from 2 to 6-ring parental, methylated and sulphur substituted derivatives with a prominent UCM extending from 30 to 60 minutes (RI = 1566-3100; Appendix F3). The dominant compounds comprised of 4-ring parental and methylated PAH and 5-ring peri-condensed systems, along with angular and linear 3-ring species (Pa and A) and their methylated derivatives. Retene, the 3-ring substituted m/z 218 amu compound and the m/z 226 amu compounds were also

Figure 42. Total ion chromatogram (TIC) of the composite roadside snow sample comprising mainly of 3 and 4 parental PAH. IS = Internal standard, 1 = Phenanthrene and Anthracene, 2 = Fluoranthene, 3 = Pyrene, 4 = Benz(a)anthracene and Chrysene, 5 = Benzofluoranthenes and 6 = Benzo(e)pyrene and Benzo(a)pyrene.

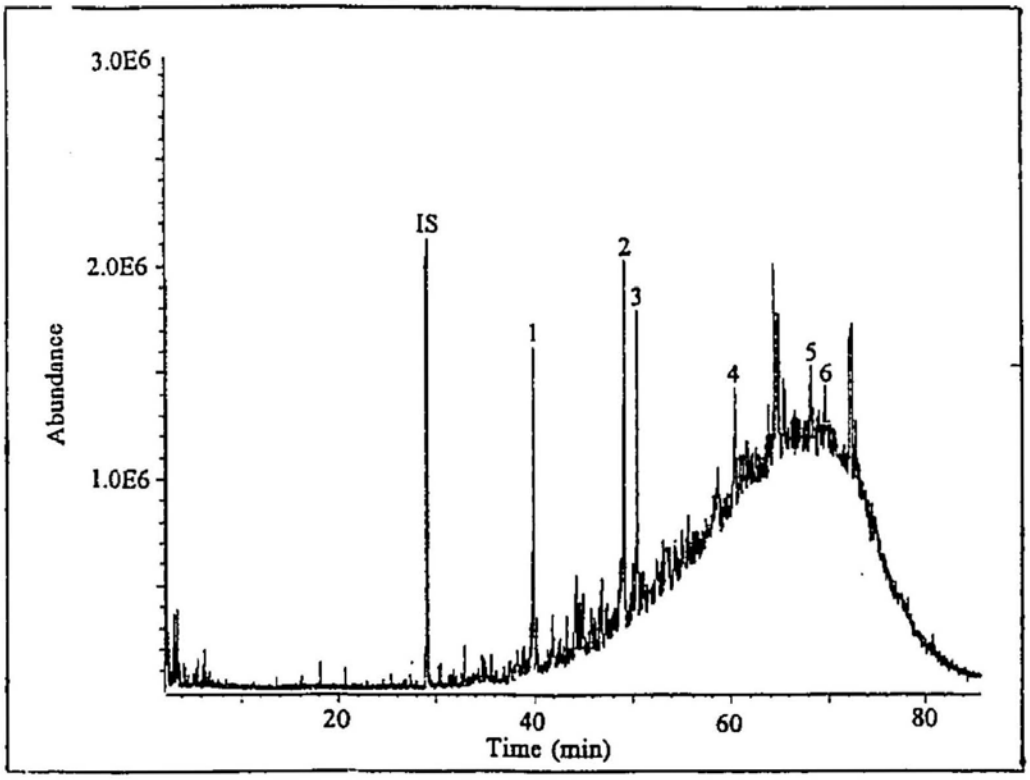
3.0E6
2.0E6
1.0E6
Abundance
IS
1
2
3
4
5
6
20
40
60
80
Time (min)

Table 16. The range of PAH isolated from the surface and deeper sediment samples of St. John's harbour. (++ = most abundant compounds that were isotopically measurable; + = detected but not isotopically analyzed). DBT = Dibenzothiophene, B(ghi)Fl = Benzo(ghi)fluoranthene, CP(cd)Py = Cyclopenta(cd)pyrene, Ind = Indeno(123 cd) pyrene, B(ghi)Per = Benzo(ghi)perylene, Anth = Anthanthrene

No	PAH	Mol Wt.	Sam A	Sam B	Sam C	Sam D	Sam E	Sam F	Sam G	Sam H	Sam I
1	Na	128	+	+	+	+	+	+	+	+	+
2	Methyl Na	142	+	+	+	+	+	+	+	+	+
3	Methyl Na	142	+	+	+	+	+	+	+	+	+
4	Ace	154	+	+	+	+	+	+	+	+	+
5	Dimethyl Na	156	+	+	+	+	+	+	+	+	+
6	Ay	152	+	+	+	+	+	+	+	+	+
7	Dibenzofuran*	168	+	+	+	+	+	+	+	+	+
8	Trimethyl Na	170	+	+	+	+	+	+	+	+	+
9	F	166	+	+	+	+	+	+	+	+	+
10	DBT	184	+	+	+	+	+	+	+	+	+
11	Pa	178	++	++	++	++	++	++	++	++	++
12	A	178	++	++	++	++	++	++	++	++	++
13	Methyl DBT	198	+	+	+	+	+	+	+	+	+
14	Methyl Pa	192	++	++	++	++	++	++	++	++	++
15	Methylene Pa-A	190	++	++	++	++	++	++	++	++	++
16	Methyl Pa	192	++	++	++	++	++	++	++	++	++
17	Phenyl Na	204	++	++	++	++	++	++	++	++	++
18	Dimethyl Pa	206	++	++	++	++	++	++	++	++	++
19	Fl	202	++	++	++	++	++	++	++	++	++
20	Py	202	++	++	++	++	++	++	++	++	++
21	Unknown	218	++	++	++	++	++	++	++	++	++
22	Trimethyl Pa*	220	+	+	+	+	+	+	+	+	+
23	Methyl Fl-Py*	216	++	++	++	++	++	++	++	++	++
24	Methyl Fl-Py*	216	++	++	++	++	++	++	++	++	++
25	Retene*	234	+	+	+	+	+	+	+	+	+
26	Dimethyl Fl-Py*	230	+	+	+	+	+	+	+	+	+
27	B(ghi)Fl/CP(cd)Py*	226	++	++	++	++	++	++	++	++	++
28	BaA	228	++	++	++	++	++	++	++	++	++
29	Chy	228	++	++	++	++	++	++	++	++	++
30	Methyl BaA-Chy*	242	+	+	+	+	+	+	+	+	+
31	BFl	252	++	++	++	++	++	++	++	++	++
32	BeP	252	++	++	++	++	++	++	++	++	++
33	BaP	252	++	++	++	++	++	++	++	++	++
34	Perylene	252	++	++	++	++	++	++	++	++	++
35	Ind/B(ghi)per/Anth*	276	+	+	+	+	+	+	+	+	+
36	Ind/B(ghi)per/Anth*	276	+	+	+	+	+	+	+	+	+

Sam D = 10 cm Deep

Sam E = 20 cm Deep

++ = Most abundant

* = Tentatively identified by GC-MS

prominent. The 2-ring Na, methylated Na and sulphur substituted compounds, DBT and methyl DBT were generally present in trace concentrations. The concentration of individual PAH in surface sediments varied significantly. A plot of mean concentrations showed that 3, 4 and 5-ring parental PAH were most prominent in surface sediments, with Fl and Py being the most abundant (Figure 43). In general, concentrations of Fl were greater than Py, while Pa, BaA, Chy, BFl had similar concentrations. The mean concentration of A and methylated Pa were generally low, while perylene, a presumed diagenetic compound was also present in measurable concentrations. Generally, the concentrations of the prominent PAH decreased with depth but a slight increase in concentrations was observed at 20 cm (Figure 44). The concentration of individual anthropogenic PAH (excluding perylene) at 30 cm, varied between 0.04 and 0.11 μg/g, while the range for the corresponding compounds outside the Harbour was between 0.05 and 0.09μg/g. Concentration of perylene in the top 30 cm of core 18 decreased, going from 1.57 μg/g at the surface to 0.47 μg/g at a depth of 30 cm (dry wt.). Retene concentrations are not reported, because authentic standard were not available although they appear to remain relatively constant with depth.

3.6.2 Carbon isotopes:

The mean carbon isotope signatures of the 3, 4 and 5-ring parental, substituted and methylated PAH in surface (n=10) and the deeper sediments of core 18, ranged between -26.6°/$_{oo}$ and -24.8°/$_{oo}$ (Figure 45), with a variation ranging between 0.21 and 0.96°/$_{oo}$. The parental compounds ranged between -26.4°/$_{oo}$ and -24.6°/$_{oo}$, with a variation of 0.20 to 0.60°/$_{oo}$ and their methylated homologues between -26.5°/$_{oo}$ and -26.0°/$_{oo}$, with variations

Figure 43. Mean surface concentrations (ng/g) of the 3-ring parental and methylated compounds and 4 and 5-ring parental PAH normalized to % total organic carbon (TOC) in St. John's Harbour and Conception Bay. Pa = Phenanthrene, A = Anthracene, MPa = Methyl Phenanthrene, Fl = Fluoranthene, Py = Pyrene, BaA = Benz(a)anthracene, Chy = Chrysene, BFl = Benzofluoranthenes, BeP = Benzo(e)pyrene, BaP = Benzo(a)pyrene and Pery = Perylene.

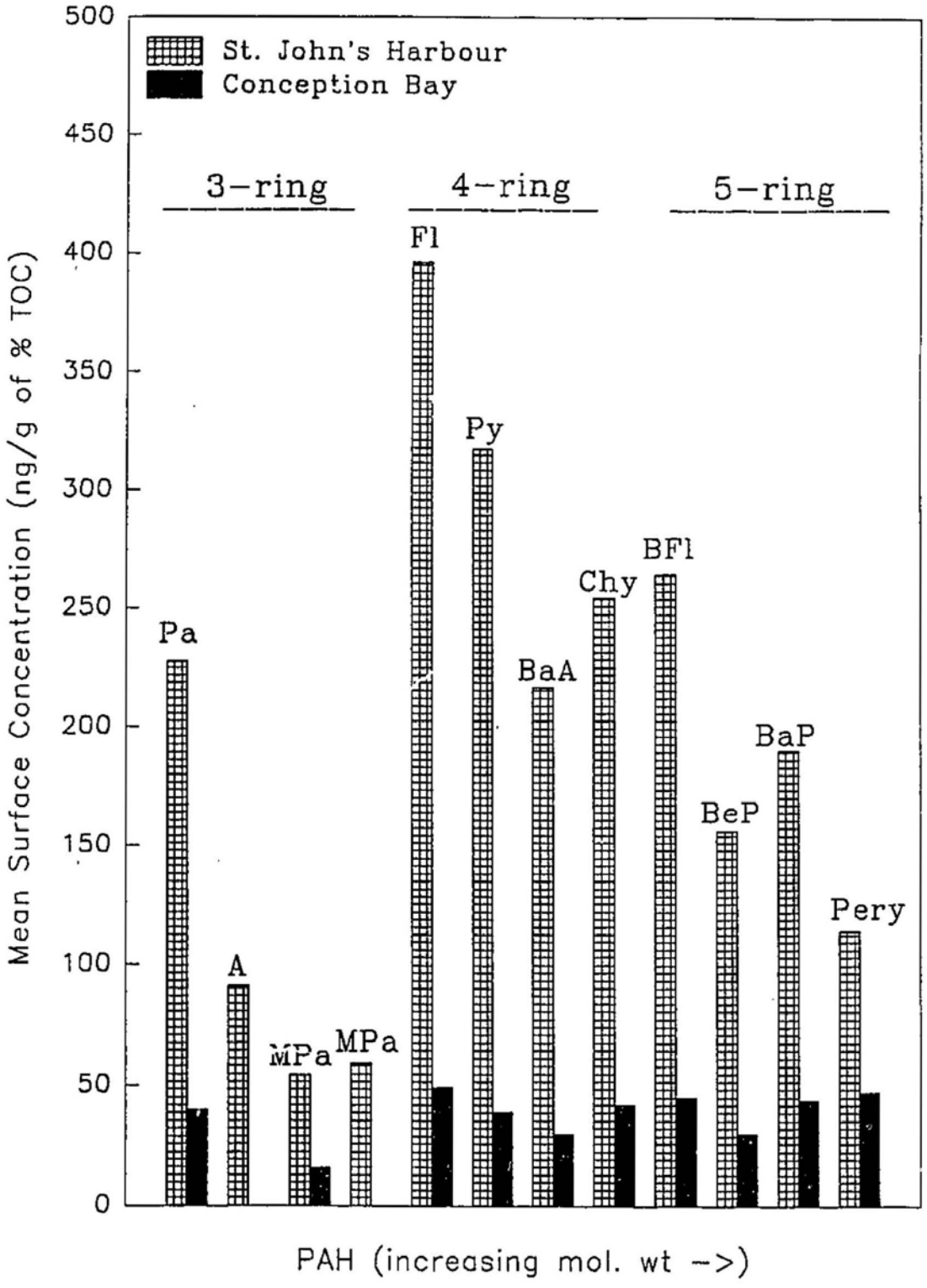
St. John's Harbour
Conception Bay
3-ring
4-ring
5-ring
Mean Surface Concentration (ng/g of % TOC)
PAH (increasing mol. wt ->)
0
50
100
150
200
250
300
350
400
450
500
Pa
A
MPa
MPa
Fl
Py
BaA
Chy
BFl
BeP
BaP
Pery

Figure 44. Change in individual PAH concentrations (μg/g of dry sediment) with increasing depth.

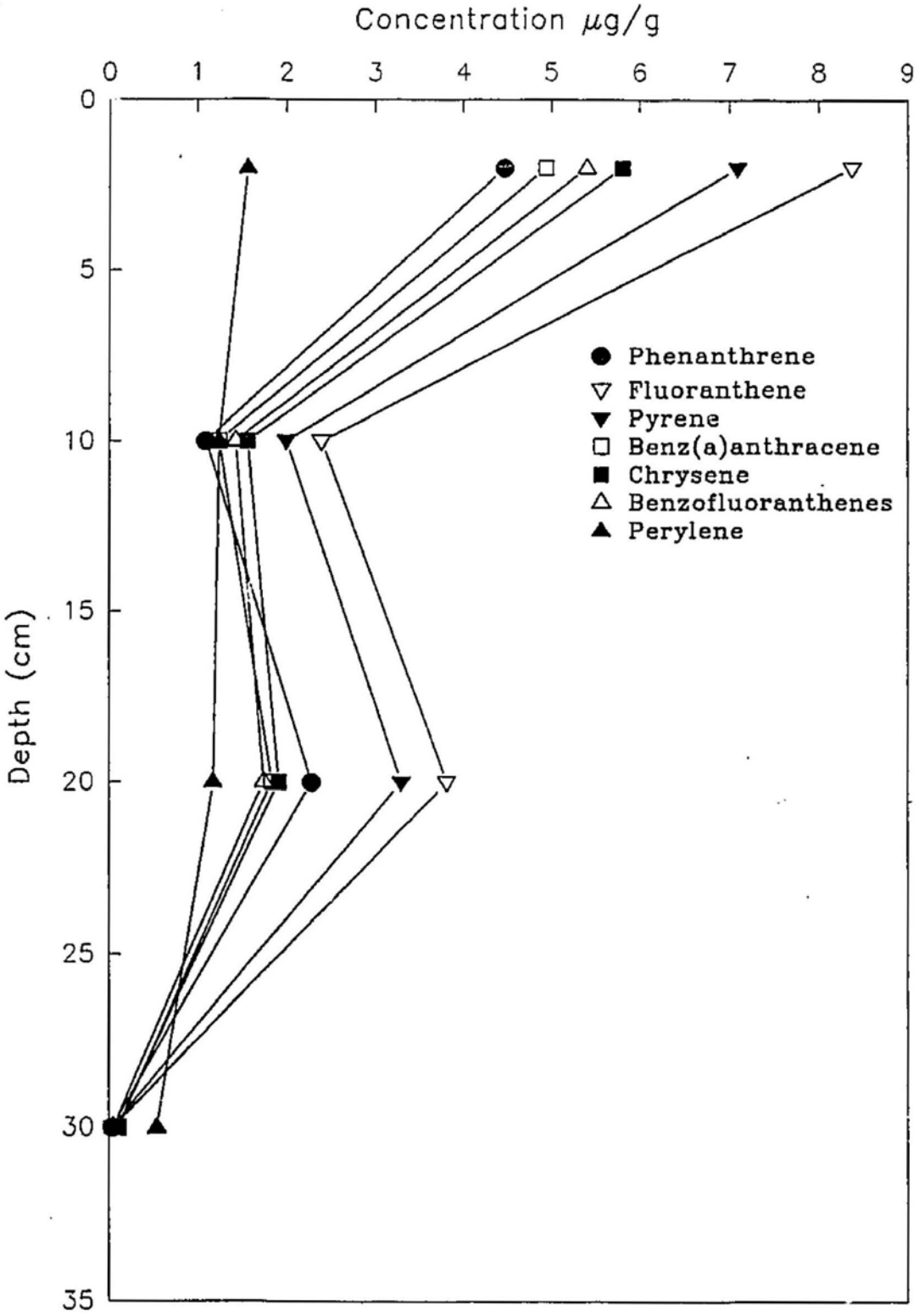
Concentration μg/g
0
1
2
3
4
5
6
7
8
9
Depth (cm)
0
5
10
15
20
25
30
35
Phenanthrene
Fluoranthene
Pyrene
Benz(a)anthracene
Chrysene
Benzofluoranthenes
Perylene

Figure 45. Mean and range (standard deviation; 2σ) of the $\delta^{13}C$ of the individual 3, 4 and 5-ring parental and methylated PAH isolated from the surface sediments in St. John's Harbour Pa = Phenanthrene, A = Anthracene, MPa = Methyl Phenanthrene, PNa = Phenyl Naphthalene, Dimethyl Phenanthrene, Fl = Fluoranthene, Py = Pyrene, MFl-Py = Methyl Fluoranthene-Pyrene, BaA = Benz(a)anthracene, Chy = Chrysene, BFl = Benzofluoranthenes, BeP = Benzo(e)pyrene and BaP = Benzo(a)pyrene

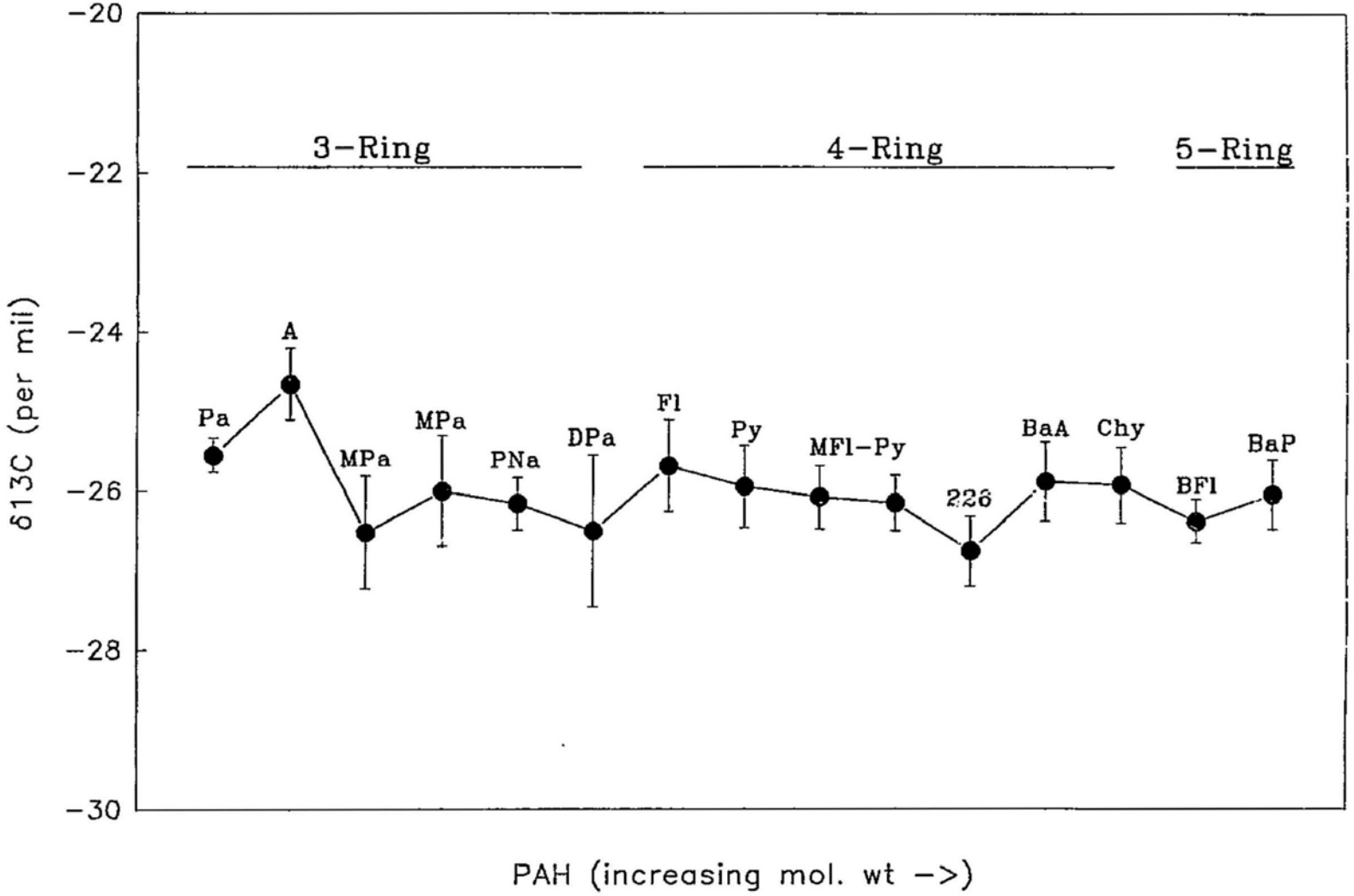
−20
−22
−24
−26
−28
−30
δ13C (per mil)
3−Ring
4−Ring
5−Ring
Pa
A
MPa
MPa
PNa
DPa
Fl
Py
MFl−Py
226
BaA
Chy
BFl
BaP
PAH (increasing mol. wt −>)

of 0.35 to 0.96‰ (Table 10). The substituted compounds, retene and the 226 species had mean values of -26.3‰ and -26.7‰, respectively. Consistent isotopic values were not obtained for perylene because of poor chromatographic resolution. Generally, the isotopic values of the parental compounds became progressively depleted with increasing molecular weight and there was no obvious trend in the methylated PAH (values as above). The most distinctive features in the overall trend can be summarized as significantly enriched A, Pa more enriched than MPa, and Py marginally more depleted than its corresponding isomer Fl. The latter observation is quite interesting in that only crankcase oil exhibited this pattern among the investigated primary sources. BaA and Chy have similar isotopic values and BFl are marginally more depleted than BaP. The variation in the individual isotopic measurements was similar for all compounds and lower than that observed in the primary and secondary source samples. No dramatic changes in $\delta^{13}C$ values of individual compounds were observed with increasing depth (Figure 46). Notable exceptions are Fl and Py that appear clearly enriched at 30 cm. The variation in the $\delta^{13}C$ values of the other compounds are within the variations observed within the same depth levels.

3.7 Molecular and Carbon isotope signatures of Conception Bay sediments:

3.7.1 Molecular signature:

The series of compounds isolated from the surface and deeper sediments from Conception Bay ranged from 2 to 5-ring parental and methylated PAH along with some sulphur heterocyclics (Table 17). In distinct contrast with St. John's Harbour sediments

Figure 46. Change in the $\delta^{13}C$ values of the individual PAH isolated from Core 18 (sampled inside St. John's Harbour) with increasing depth. Error bars (standard deviation; 2σ) represents the mean variation recorded for the corresponding compounds in the surface sediments. Pa = Phenanthrene, A = Anthracene, MPa = Methyl Phenanthrene, PNa = Phenyl Naphthalene, Dimethyl Phenanthrene, Fl = Fluoranthene, Py = Pyrene, MFl-Py = Methyl Fluoranthene-Pyrene, BaA = Benz(a)anthracene, Chy = Chrysene, BFl = Benzofluoranthenes, BeP = Benzo(e)pyrene and BaP = Benzo(a)pyrene.

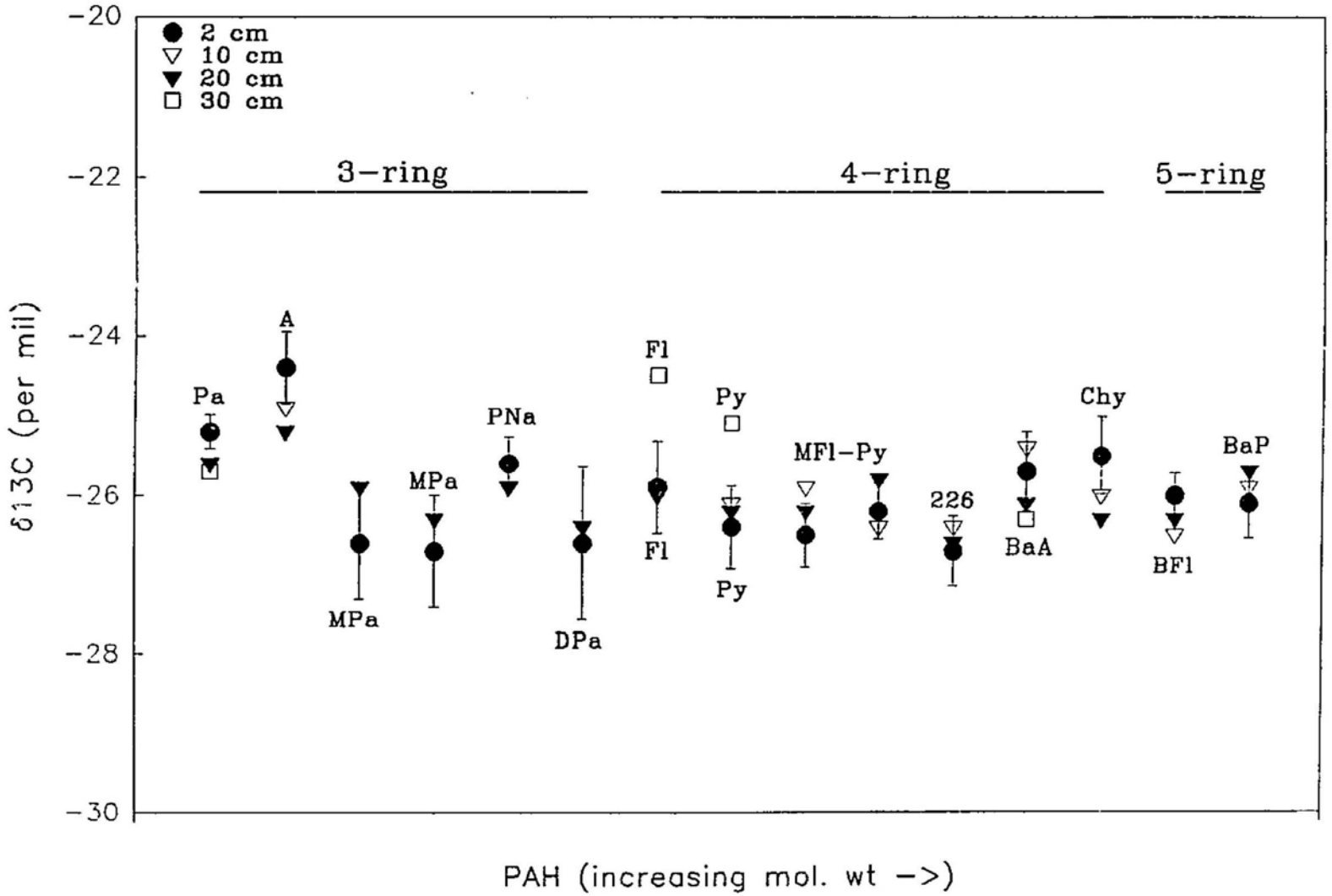
2 cm
10 cm
20 cm
30 cm
3-ring
4-ring
5-ring
-20
-22
-24
-26
-28
-30
δ13C (per mil)
Pa
A
MPa
MPa
PNa
DPa
Fl
Fl
Py
Py
MFl-Py
226
BaA
Chy
BFl
BaP
PAH (increasing mol. wt ->)

Table 17. The range of PAH isolated from the surface and deeper sediment samples of Conception Bay. (++ = most abundant compounds that were isotopically measurable; + = detected but not isotopically analyzed).

No	PAH	Mol Ion	CC6 2 cm	CW4 2 cm	BRLP5 2 cm	BRLP5 6 cm	BRLP5 14 cm	CTR23 2 cm	CC1 2 cm	US3.5 2 cm
1	Na	128	+	+		+	+	+	+	+
2	Ace	154	+	+		+		+	+	+
3	Methyl Na	156	+	+	+	+	+	+	+	+
4	Dibenzofuran*	168	+	+	+	+	+	+	+	+
5	F	166	+	+	+	+	+	+	+	+
6	Pa	178	++	++	++	++	++	++	++	++
7	A	178	+	+	+	+	+	+	+	+
8	Methyl DBT	198	+	+	+	+	+	+	+	+
9	Methyl Pa	192	+	+	+	+	+	+	+	+
10	Methylene Pa-A*	190	+	+	+	+	+	+	+	+
11	Methyl Pa	192	+	+	+	+	+	+	+	+
12	Dimethyl Pa	206	+	+	+	+	+	+	+	+
13	Fl	202	++	++	++	++	++	++	++	++
14	Py	202	++	++	++	++	++	++	++	++
15	Methyl Fl-Py*	216	+	+	+	+	+	+	+	+
16	Methyl Fl-Py*	216	+	+	+	+	+	+	+	+
17	Retene*	234	++	++	++	++	++	++	++	++
18	BaA	228	++	++	++	++	++	++	++	++
19	Chy	228	++	++	++	++	++	++	++	++
20	BFl	252	++	++	++	++	++	++	++	++
21	BeP	252	++	++	++	++	++	++	++	++
22	BaP	252	++	++	++	++	++	++	++	++
23	Perylene	252	++	++	++	++	++	++	++	++

++ = Most abundant

* = Tentatively identified by GC-MS

the molecular signature of these sediments was characterized by the absence of a significant UCM (Appendix F3). The low molecular weight compounds, including Na and its substituted homologues, Ace, F were not present in sufficient quantities to be isotopically measured (detected using specific ion monitoring). The compounds present in measurable concentrations were 3, 4 and 5-ring parental and 3-ring methylated PAH. While the PAH molecular distribution were similar to the Harbour sediments, the concentrations of the individual compounds in the Conception Bay sediments were significantly lower (Figure 43). In general, the concentration of the parental PAH in surface sediments did not vary significantly, and mean concentrations ranged between 23.9 ng/g and 38.6 ng/g (dry weight). The concentration of individual PAH fluctuated with depth, but some (e.g., Chy and BFl) clearly decreased with increasing depth. Perylene is an exception showing higher concentrations in the deeper samples (Figure 47). Again, retene is present but was not quantified, although it seemed to remain fairly constant with depth.

3.7.2 Carbon isotopes:

Because of the relatively low individual PAH concentrations, only mean isotopic values for isomers of BaA+Chy and BeP+BaP are reported. The $\delta^{13}C$ values of the 3, 4 and 5-ring parental PAH ranged between -27.2‰ and -25.8‰ (Table 10). The mean isotopic signatures of Pa, Fl, Py, BaA+Chy and BeP+BaP were very similar with values ranging between -26.5‰ and -25.8‰ and a variation between 0.24‰ and 0.47‰ (Figure 48). However, the mean isotopic value of the BFl was slightly more depleted, with a mean value of -27.2‰ and a standard deviation of 0.62‰. Generally, the 5-ring compounds were isotopically lighter than the 3 and 4-ring species. Similar to what was

Figure 47. Change in individual PAH concentrations (ng/g of dry sediment) with increasing depth in Conception Bay sediments.

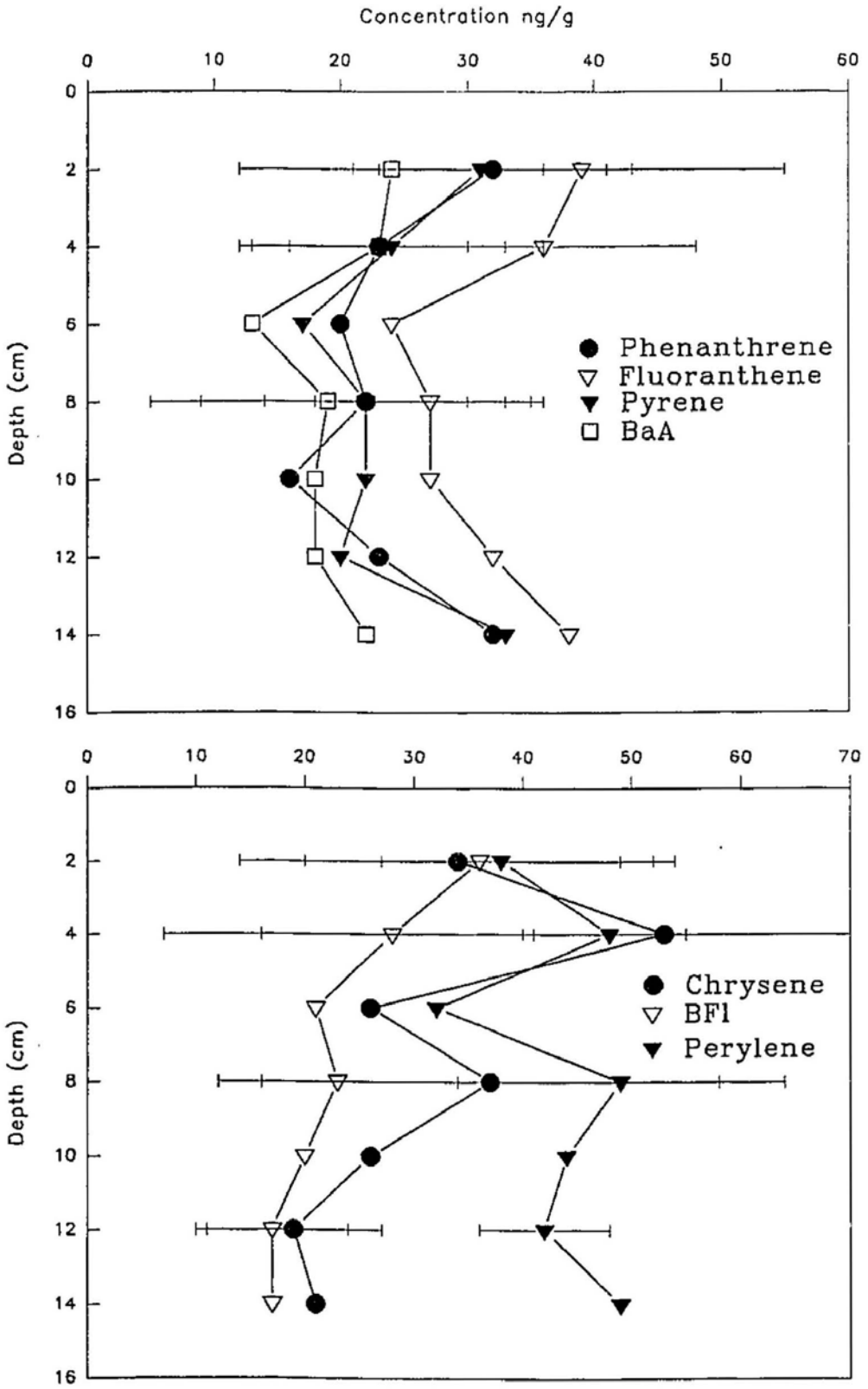
Concentration ng/g
0
10
20
30
40
50
60
Depth (cm)
0
2
4
6
8
10
12
14
16
Phenanthrene
Fluoranthene
Pyrene
BaA
0
10
20
30
40
50
60
70
Depth (cm)
0
2
4
6
8
10
12
14
16
Chrysene
BFl
Perylene

Figure 48. Mean and standard deviation (2σ) of the $\delta^{13}C$ of the individual 3, 4 and 5-ring parental PAH isolated from the surface sediment samples in Conception Bay. Pa = Phenanthrene, A = Anthracene, Fl = Fluoranthene, Py = Pyrene, BaA+Chy = Benz(a)anthracene and Chrysene, BFl = Benzofluoranthenes, BeP+BaP = Benzo(e)pyrene and Benzo(a)pyrene.

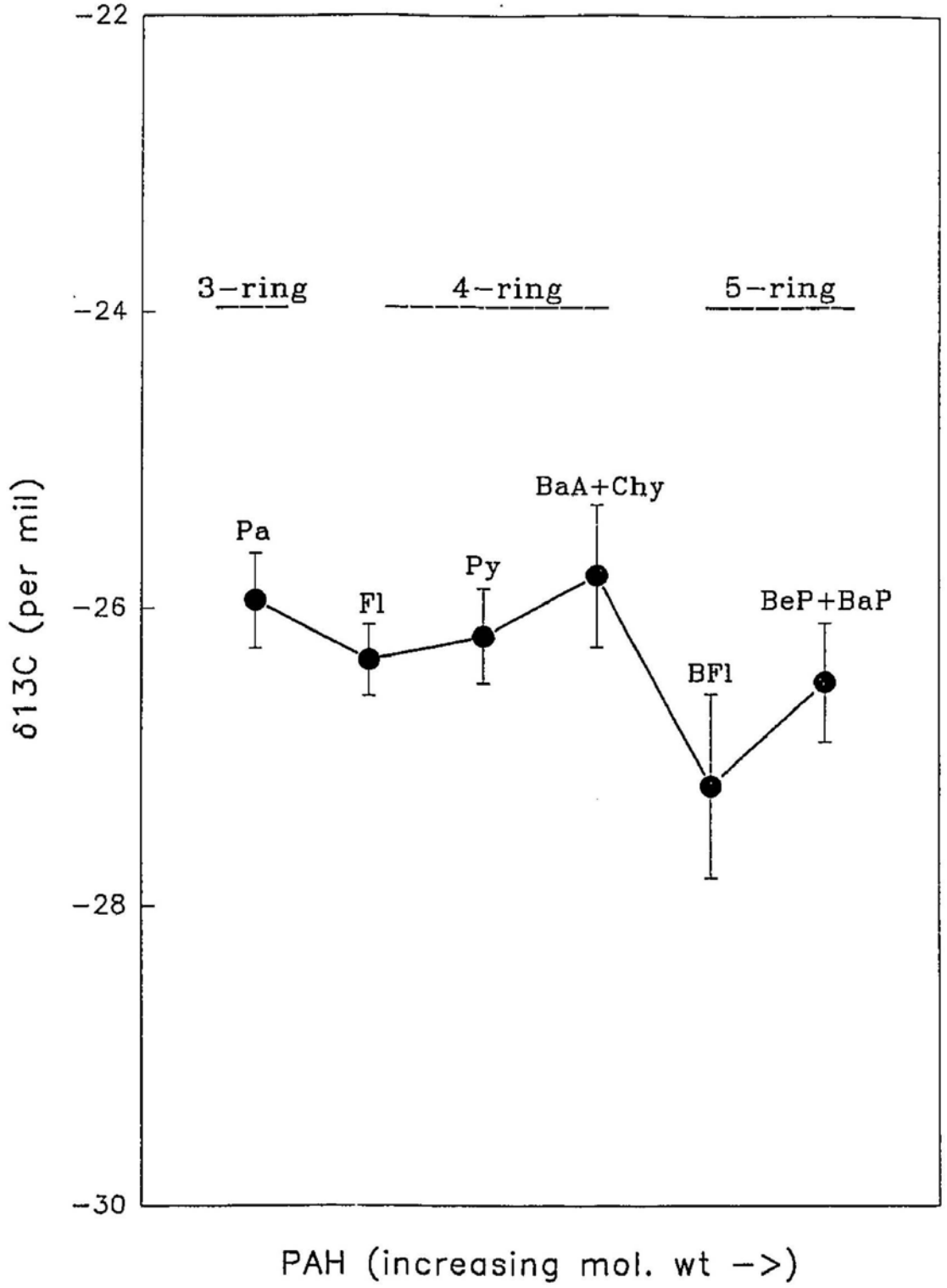
-22
-24
-26
-28
-30
3-ring
4-ring
5-ring
Pa
Fl
Py
BaA+Chy
BFl
BeP+BaP
δ13C (per mil)
PAH (increasing mol. wt ->)

observed in the Harbour, there was no significant deviation in the isotopic signatures of the PAH with increasing depth and any variations in the individual measurements were within variations observed with a given depth and the analytical precision (Figure 49). Finally, the isotopic values of retene ranged between -28.1°/$_{oo}$ and -24.5°/$_{oo}$, with a mean variation of 0.77°/$_{oo}$, while perylene ranged between -25.2°/$_{oo}$ and -22.4°/$_{oo}$, with a variation of 0.82°/$_{oo}$.

Figure 49. Mean and standard deviation of the $\delta^{13}C$ values of the individual parental PAH with increasing depth. BaA+Chy = Benz(a)anthracene and Chrysene, BFl = Benzofluoranthenes

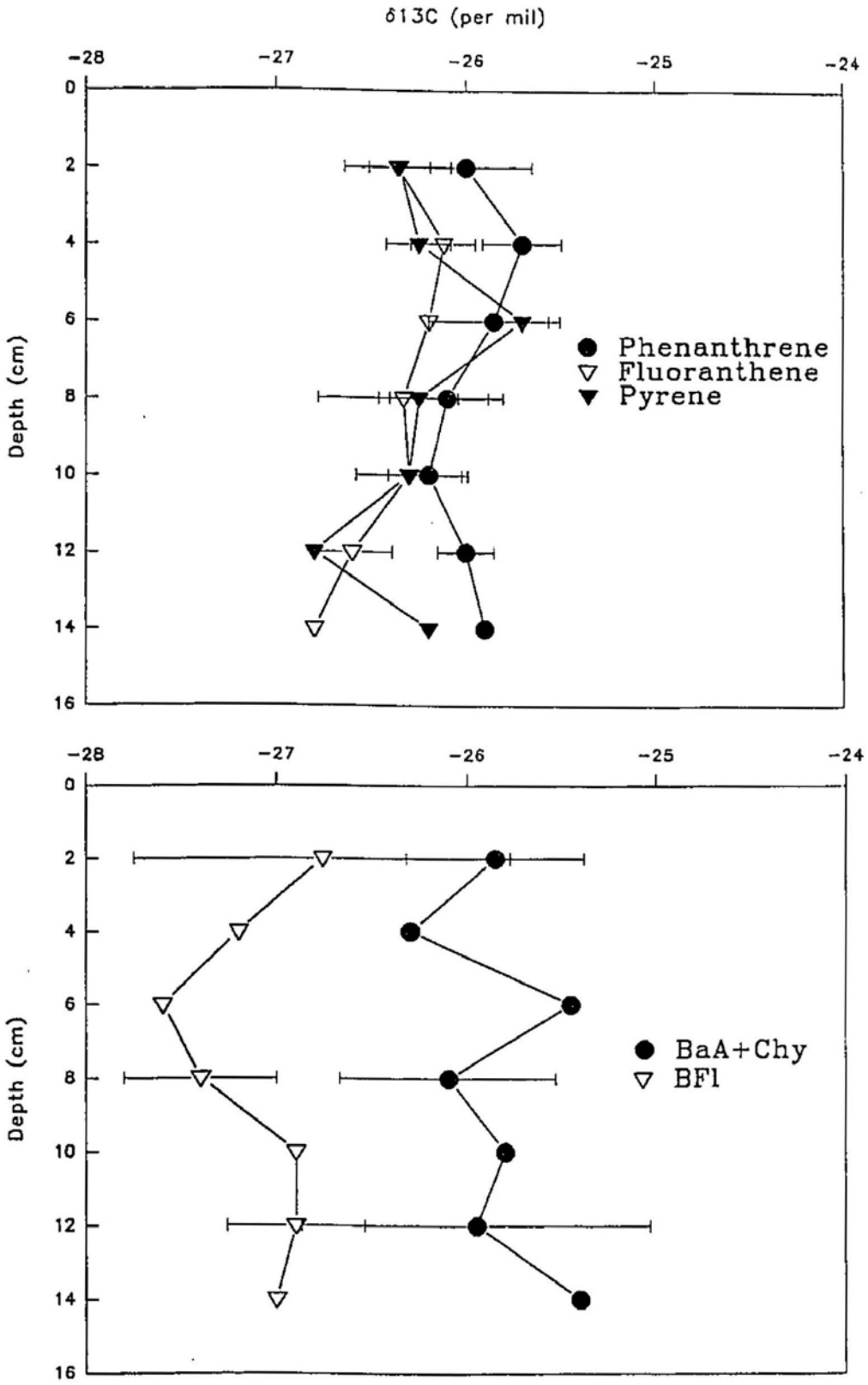
δ13C (per mil)
-28
-27
-26
-25
-24
0
2
4
6
8
10
12
14
16
Depth (cm)
Phenanthrene
Fluoranthene
Pyrene
BaA+Chy
BFl

4.0 DISCUSSION

4.1 Accuracy and precision of CSIA determinations using standard and field samples:

With the exception of Na and F, there are no significant differences among isotopic values obtained for Ace, Pa, A, Fl, Py, BaA, B(b)Fl and BaP using conventional IRMS and GC/C/IRMS methods of analysis (rank sum two-sample Mann-Whitney test). Taking the $\delta^{13}C$ of the conventional measurements to be the "true" isotopic values of the standard PAH, the accuracy of the GC/C/IRMS measurements of these compounds were within 0.41‰ of the conventional IRMS values. The apparent systematic shift towards lighter isotopic values, though interesting, is not statistically significant and mean values for most compounds are within precision limits of the instrument. There is no obvious explanation for the anomalous difference in the $\delta^{13}C$ values of Na and F using the two measurements techniques, since the precision of the repeated measurements was well within the limits of precision of both instruments. The precision in the GC/C/IRMS measurements was similar for the 2, 3 and 4-ring compounds, but a slight increase in variation was observed for the higher molecular weight 5-ring PAH. This loss of precision in $\delta^{13}C$ is likely related to the loss of chromatographic resolution resulting in peak broadening and loss of precision (e.g., Goodman and Brenna, 1992) for late eluting peaks.

The field samples selected to assess the reproducibility of GC/C/IRMS determinations had variable backgrounds levels (UCM). The magnitude of the background changed in the general sequence: sediment >fire soot >car soot. These

samples were both manually (guided by the internal standards) and automatically background corrected. The use of internal standards with known isotopic values aided the careful selection of background points so that the $\delta^{13}C$ values of the individual PAH sitting on a significant UCM could be reliably determined. For well separated compounds, reproducibility of the $\delta^{13}C$ values was within the precision range recorded for the individual PAH of the standard solution. This is true regardless of background levels. However in some samples, the precision of the replicate isotopic measurements was greater for the higher molecular weight isomeric compounds. This was particularly evident in the 4 and 5-ring (BaA+Chy and BeP+BaP) species (Figure 18), even though the maximum variation was recorded for anthracene in the fireplace soot sample (Figure 17). The anomalous variation in the anthracene isotopic values may be related to poor separation due to the dissimilarity in the concentration of Pa and A (isomers) in the extract.

In the case of well separated compounds, there was no relationship between the magnitude of the UCM and the reproducibility of the individual isotopic measurements. The precision of the internal standards (Ace, C_{21} and C_{25}) did not vary significantly in the three field samples despite the difference in the intensity of their UCM's. The anomalous variation in the precision in the C_{21} standard of the fireplace soot extract was due mainly to the difficulty in resolving this peak from a coeluting peak. Similar to the standard PAH solution, the precision of the internal standards degraded somewhat with increasing molecular weight. Despite the low background in the car soot, variation in the measurement of the individual $\delta^{13}C$ PAH values was greater than that observed for the

sediment and fire soot samples. This variation, particularly in the 4 and 5-ring isomeric compounds, may be due primarily to peak broadening effects (overlapping) and the differential concentrations of these compounds in the sample extract. The variation in the precision of these higher molecular weight compounds was significantly improved by using faster temperature ramp rates during the initial stages of the chromatography. This resulted in sharper and better resolved peaks. Reproducibility of measurements on the field samples was also assessed by comparing the $\delta^{13}C$ of the recovered internal standards to their respective conventional IRMS values. $\delta^{13}C$ values of the internal standards in the sediment and fire soot samples ranged between 0.07 and 0.23‰ of their respective conventional $\delta^{13}C$ values using manual background subtraction. The $\delta^{13}C$ values of the internal standards in the car soot sample were recovered to within 0.30 and 0.80‰ of the IRMS values.

There were no detectable differences in the $\delta^{13}C$ of the standard PAH isolated from the sterile sediments using the adopted extraction and purification methods (even with recoveries as low as 45% as observed for F; Figure 19). The mean isotopic values of all the recovered PAH were within 0.43‰ of their original $\delta^{13}C$ values. Greater variation in the precision was again observed for the higher molecular weight species. The concentration of PAH recovered as a result of Soxhlet extraction and purification is primarily influenced by evaporation (volatilization) and adsorption losses. Photodegradation losses were reported by Low (1987), but since the present Soxhlet extractions were performed in the absence of light, PAH losses due to photodegradation should be negligible. With the exception of F, recoveries of the 3, 4 and 5-ring

compounds were generally better than 70%. This study indicates that no significant isotopic fractionation (associated with evaporation and adsorption losses) occurs during extraction and purification of PAH using the methods adopted in the present study.

4.2 Isotopic effects due to photolysis:

The calculated degradation rates (k) and half-lives of the studied PAH indicate that F, Pa, Fl, Py and B(b)Fl are relatively photostable, while A and Ace are quite susceptible to photo-degradation (Table 8, Figures 20, 21 and 23). The susceptibility of the individual compounds to photolysis are similar to those previously reported (Korfmacher et al., 1980; Low et al., 1987; Behymer and Hites, 1988; Paalme et al., 1990; Sanders et al., 1993). The rate constants and half-lives are different as may be expected from differences in experimental conditions utilized. For example, PAH were exposed to natural sunlight in the present study, while previous experiments were conducted under controlled laboratory conditions, with constant light intensity (Krofmacher et al., 1980; Kamens et al., 1988; Sanders et al., 1993). Kamens et al. (1988) reported rates of photo-degradation that were proportional to light intensity. Similar to Low et al. (1987), higher degradation rates and shorter half-lives were found in this study for Fl and Py when dissolved in the more polar solvent dichloromethane (Table 8). The reason for the apparent stability of Pa and Fl and B(b)Fl is related to the chemical structure of the individual compounds (Paalme et al., 1990). For example, the low photo-reactivity of phenanthrene has been attributed to its angular configuration (Krofmacher et al., 1980; Sanders et al., 1993), whereas Clar, (1964) suggested that this is primarily due to the

presence of two benzenoid rings. In contrast, anthracene may be less stable since it has only one benzenoid ring (Clar, 1964). The stability of Fl has been attributed to its "nonalternant" structure (consisting of five and six-membered rings) which is highly stable in an excited state and has a low affinity for capturing low energy electrons (Zander, 1983).

No pronounced effects of photolytic degradation were observed on the $\delta^{13}C$ of standard PAH experimentally exposed to natural sunlight. The $\delta^{13}C$ of F, Pa, Fl, Py and BbF during the various exposure periods were particularly stable despite up to a 40% reduction in the initial concentration of pyrene (Figure 20). However, it should be noted that the mean isotopic values of A and Ace appeared to have become enriched during similar experiments. Although similar degrees of degradation were recorded in repeated anthracene experiments using different solvent substrates under comparable conditions, the $\delta^{13}C$ enrichments noted during the initial studies were not observed in these repeated experiments. This fact is demonstrated by the stability of the $\delta^{13}C$ value of anthracene recovered from these experiments (Figure 20). The mean $\delta^{13}C$ of anthracene recovered from cyclohexane and in the absence of a solvent substrate ranged between 0.01 and 0.53‰ of its conventional IRMS value.

The results of the repeated photolytic, volatilization and evaporation studies indicate that the $\delta^{13}C$ values of the PAH studied, particularly the higher molecular weight compounds, are stable during these reactions. The absence of significant kinetic isotope effects in the systems studied here may be related to the relatively high molecular weights of the compounds and low reduced mass differences involved.

The photolysis experiments in the present study were conducted to optimise photodegradation rates. In natural systems, PAH (especially high molecular weight compounds) are sorbed onto particulate surfaces significantly reducing their susceptibility to photodegradation (Valerio and Lazzarotto, 1985; Yokely et al., 1986; Behymer and Hites, 1988; Coutant et al., 1988). PAH photodegradation rates are dependent on the nature of the binding substrates and on variables such as length of day, sunshine intensity, extent of cloud cover and temperature. These can all contribute to the persistence or removal of PAH from the environment (Masclet et al., 1986; Hwang et al., 1987; Bunce and Dryfhout, 1992; Sanders et al., 1993). The effects of all these parameters cannot be assessed independently in the natural environment. However, parameters such as particulate association, low temperatures, sunshine intensity and extent of cloud cover provide strong evidence to support the suggestion that PAH photodegradation rates will be relatively low during transportation in the selected study areas (Suess, 1976; McVeety and Hites, 1988; Baek et al., 1991a). The elevated levels of suspended solids in the water of St. John's Harbour could also significantly reduce the degree of PAH degradation in the photic zone of the water column by limiting light penetration (Newfoundland Design Associates Ltd., 1987-1988). Finally, colder waters inhibit specific steps leading to photolytic degradation of certain compounds (Hwang et al., 1987).

4.3 Isotopic effects due to microbial degradation:

Microbial degradation experiments performed in the present study showed negligible shifts in the $\delta^{13}C$ values of the two PAH investigated (Na and Fl; Figures 24 and 25). Bacteria degrade PAH by enzymatic attack which can be influenced by a

number of environmental factors (Cerniglia, 1991) (also see, section 1.5.2). The catabolic pathway by which compounds are degraded is dependant primarily on the bacterial strain (Table 5) and the type of enzymes used for metabolism (Zylstra et al., 1992). Alteration of the original isotopic values of Na and Fl may be expected, since most PAH degradation pathways involve ring cleavage (loss of carbon) (Mueller et al, 1990; Cerniglia, 1991). For bacterial degradation to occur, the PAH is normally incorporated into the bacterial cells where enzymes are produced. The pathway by which PAH enter bacterial cells may dictate whether isotopic alterations will occur as a result of microbial degradation. This pathway is not well understood, but it is postulated that bacteria either ingest PAH that are associated with organic matter, or because of their lipophilic properties, PAH may be diffused in solution across the cell wall membrane. Hayes et al. (1989) suggested that organisms do not isotopically discriminate between heavy and light carbon when ingesting organic material from homogenous mixtures. In this case, the isotopic ratio of the unconsumed residue will not be different from the starting material. Even if cell wall diffusion was the predominant pathway, isotopic fractionation will again be limited by the small relative mass difference between a ^{12}C and ^{13}C containing PAH. It is for this reason that most isotopic fractionations in biological systems can be traced back to the initial carbon (i.e., CO_2, CH_4) fixation steps. Since no enrichments were observed in the isotopic signature of the microbially reduced concentrations of naphthalene and fluoranthene, no mass discrimination must have occurred either during direct ingestion or cell wall diffusion. If the controlling step for the incorporation of all PAH are similar, isotopic alterations resulting from microbial degradation would be expected to be insignificant.

In natural environments such as St.John's Harbour and Conception Bay, it is unlikely that micro-organisms are exposed to single compounds, and mixtures of PAH are much more likely to occur. It is widely recognized that certain mixtures are more susceptible to degradation than when the compounds are present singularly (MaCarty et al., 1984; Smith et al., 1991). Also, some compounds in a mixture can exacerbate or suppress degradation rates (Bauer and Capone; 1988; Smith, 1990). However, these studies are based on work with non-growth supporting secondary substrates, in which the biomass being created by one or more easily degraded primary substrates. Presently, little is known about substrate interactions among biodegradable aromatic hydrocarbons present in growth supporting medium. Microbial degradation of PAH in St. John's Harbour is expected to be negligible, due to the presence of more accessible organic carbon forms that bacteria tend to degrade preferentially (Shiaris, 1989). Indeed, experiments conducted by Stahl (1980) and Wehner et al. (1985) showed that the $\delta^{13}C$ of the aromatic fraction is not significantly altered during the biodegradation of crude oil in spite of significant $\delta^{13}C$ alterations of other fractions. Isotopic shifts in the altered fractions appear to have been related to the preferential consumption of specific compounds (with different isotopic compositions) rather than the preferential consumption of ^{12}C or ^{13}C bearing compounds. Since the year round temperatures and PAH concentrations in Conception Bay are generally low, bacterial activity is often suppressed (Pomeroy et al., 1991) and they may not have developed the ability to degrade PAH in this system. Microbial adaptations to degrade PAH are largely developed from the chronic exposure to elevated concentrations of these compounds (Cerniglia and Heitkamp, 1989).

Isotopic effects associated with phase separation or PAH solubility in aqueous environments are possibly also manifested in these studies. Bacterial utilization is predominantly associated with water soluble PAH (Weissenfels et al., 1990; Boldrin et al., 1993) and any preferential separation of the light and heavy carbon in the aqueous phase would have been reflected by an isotopically enriched residue. As noted above, evidence of preferential solubilization between the light and heavy carbon was not observed, implying that no isotopic discrimination occurs during PAH dissolution.

4.4 Molecular signatures of the prominent primary sources:

The PAH isolated from the prominent primary sources varied in composition, with fireplace soots and crankcase oils exhibiting the most repetitive signatures. The mean and standard deviation (2σ) of the compositional ratios of these primary sources are summarized and compared to literature values in Figure 50 (Rudling et al. 1982; Stenburg, 1983; Grimmer et al. 1983a; Alsberg et al., 1985; Masclet et al., 1986; Westerholm et al., 1988; Broman et al. 1988; Freeman and Cattell, 1990; Takada et al., 1990).

4.4.1 Fireplace soots:

Individual fireplace soot samples, from hard and softwood burning open fireplaces were consistently dominated by 3, 4 and 5-ring parental PAH with generally lower concentrations of methylated compounds (Figure 51). These observation are in accordance with previous findings on the molecular signature of wood combustion (e.g., DeAngelis et al., 1981; Rudling et al. 1982; Grimmer et al. 1983a; Freeman and Cattell, 1990). Also, the molecular signature of soot produced from the combustion of

Figure 50. Mean and range (standard deviation; 2σ) of the compositional ratios of prominent PAH in fire and car soots and crankcase oil compared to literature data.

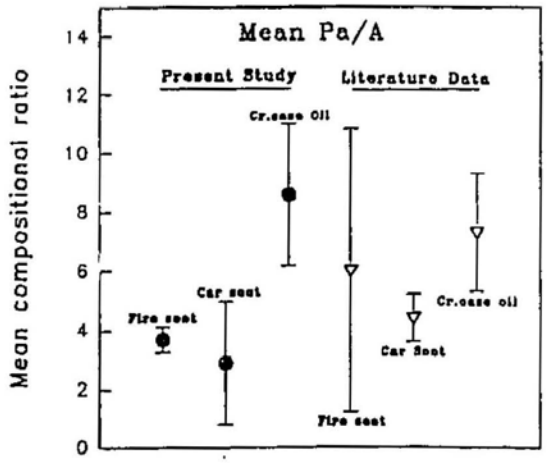
Mean Pa/A
Present Study
Literature Data
Mean compositional ratio
14
12
10
8
6
4
2
0
Fire soot
Car soot
Cr.case Oil
Fire soot
Car Soot
Cr.case oil

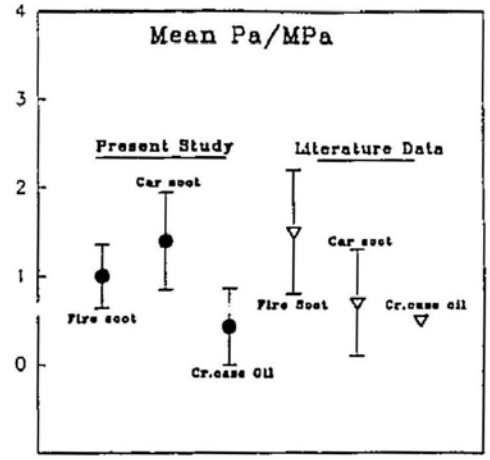
Mean Pa/MPa
Present Study
Literature Data
4
3
2
1
0
Car soot
Fire soot
Cr.case Oil
Fire Soot
Car soot
Cr.case oil

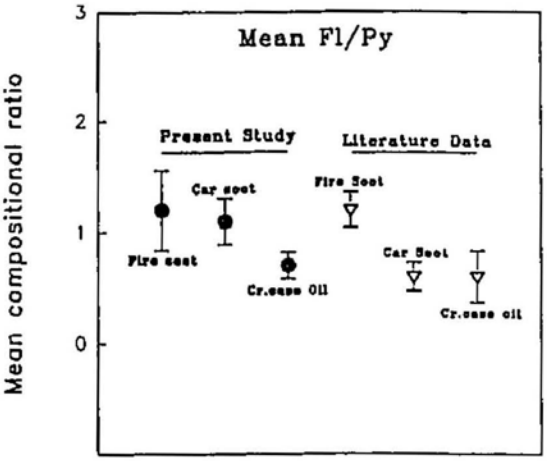
Mean Fl/Py
Present Study
Literature Data
Mean compositional ratio
3
2
1
0
Fire soot
Car soot
Cr.case Oil
Fire Soot
Car Soot
Cr.case oil

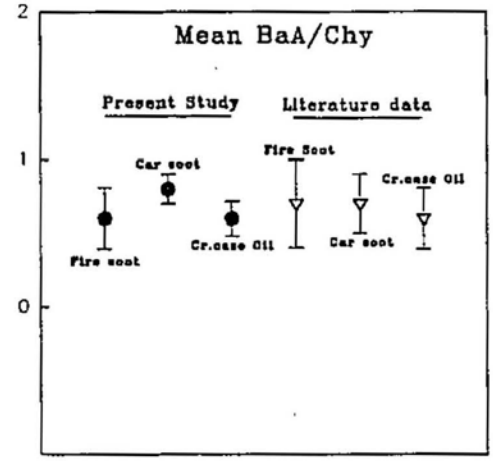
Mean BaA/Chy
Present Study
Literature data
2
1
0
Fire soot
Car soot
Cr.case Oil
Fire Soot
Car soot
Cr.case Oil

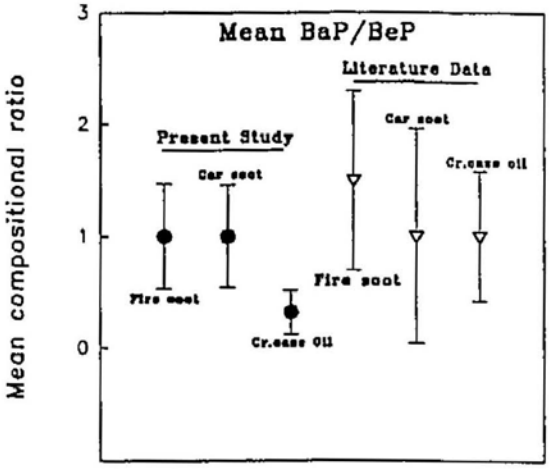
Mean BaP/BeP
Literature Data
Present Study
Mean compositional ratio
3
2
1
0
Car soot
Cr.case oil
Fire soot
Car soot
Fire soot
Cr.case Oil

Figure 51. Summary of the mean normalized concentrations of the PAH isolated from the primary sources.

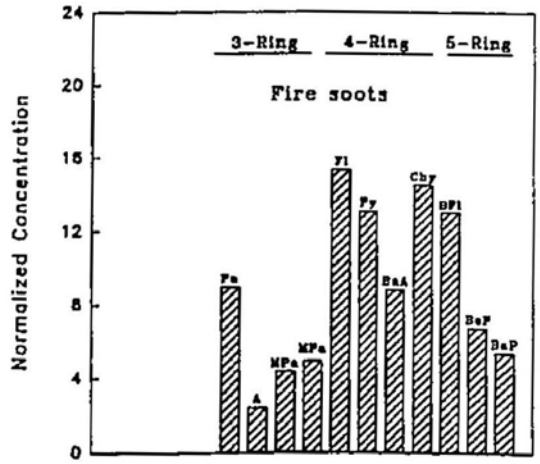
3-Ring
4-Ring
5-Ring
Fire soots
Normalized Concentration
PAH (increasing mol. wt ->)

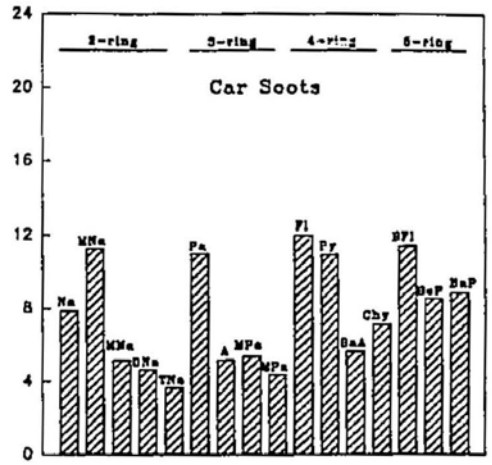
Car Soots
PAH (increasing mol. wt ->)

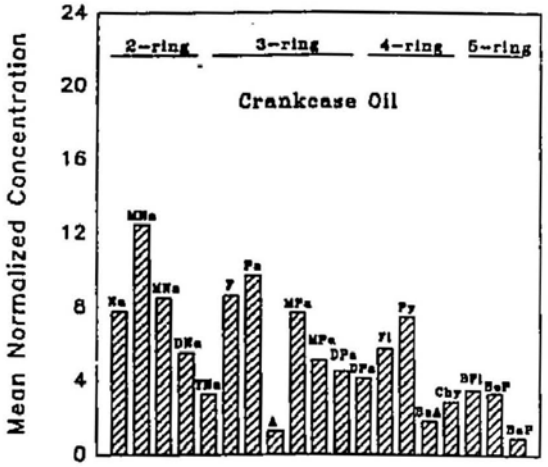
2-ring
3-ring
4-ring
5-ring
Crankcase Oil
Mean Normalized Concentration

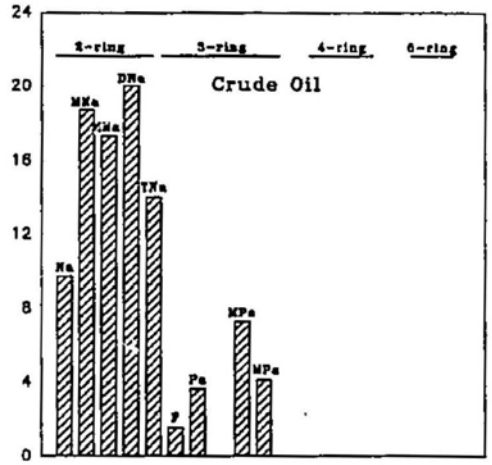
Crude Oil

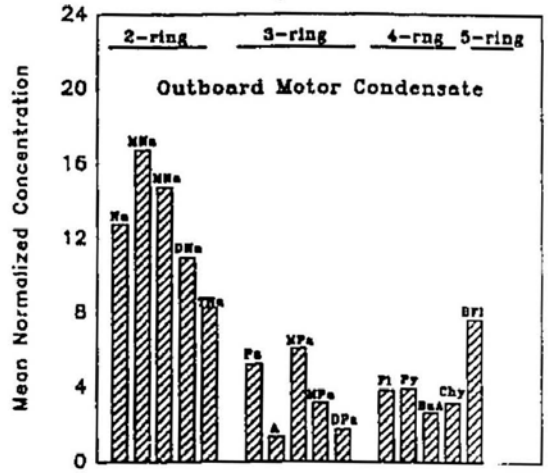
2-ring
3-ring
4-rng
5-ring
Outboard Motor Condensate
Mean Normalized Concentration

artificial fuel was comparable to the wood derived signatures (Figure 52). On average, the concentration of the 4 and 5-ring compounds represented 79% of the total PAH in the fireplace soot samples.

It is difficult to compare the yield of PAH in the open fireplaces investigated in the present study because most previous studies have concentrated on PAH emissions from wood stoves (McCrillis et al., 1992). The yields of PAH produced during open flame combustion are difficult to assess due to the uncontrolled combustion conditions (Ramdahl, 1983b). In general, open fireplaces have lower PAH yields than wood stoves. This is attributed to higher temperatures and richer air supply in open fireplaces. Temperatures of 200 to 800°C have been recorded in open flames, and these are thought to be conducive to the formation of both substituted and unsubstituted PAH (Neff, 1979). The presence of substituted and unsubstituted PAH is reflected consistently in the open fireplace soot samples analyzed in the present study. The total PAH concentration in individual samples varied, but the mean normalized concentrations showed a predominance of the 4 and 5-ring compounds, normally associated with high temperature open fireplace combustion systems (Figure 51; DeAngelis et al., 1981; Rudling et al., 1982; MacVetty and Hites, 1988; Freeman and Cattell, 1990). Retene (1-methyl-7-isopropylphenanthrene; Figure 4), a tricyclic hydrocarbon reported to be formed by the thermal degradation of resinous abietic acids in coniferous woods (softwood) was prominent in a few of the individual fireplace soot samples, and in the individual wood stove and composite samples (Ramdahl, 1983a). The yield of retene during combustion has been reported to be highly dependent on temperature and air supply with starved air

Figure 52. Molecular signature of open fireplace artificial fuel combustion compared to open fireplace wood burning. IS = internal standard, 1 = Phenanthrene/Anthracene, 2 = Fluoranthene, 3 = Pyrene, 4 = Benz(a)anthracene/Chrysene, 5 = Benzofluoranthenes and 6 = Benzo(e)pyrene/Benzo(a)pyrene

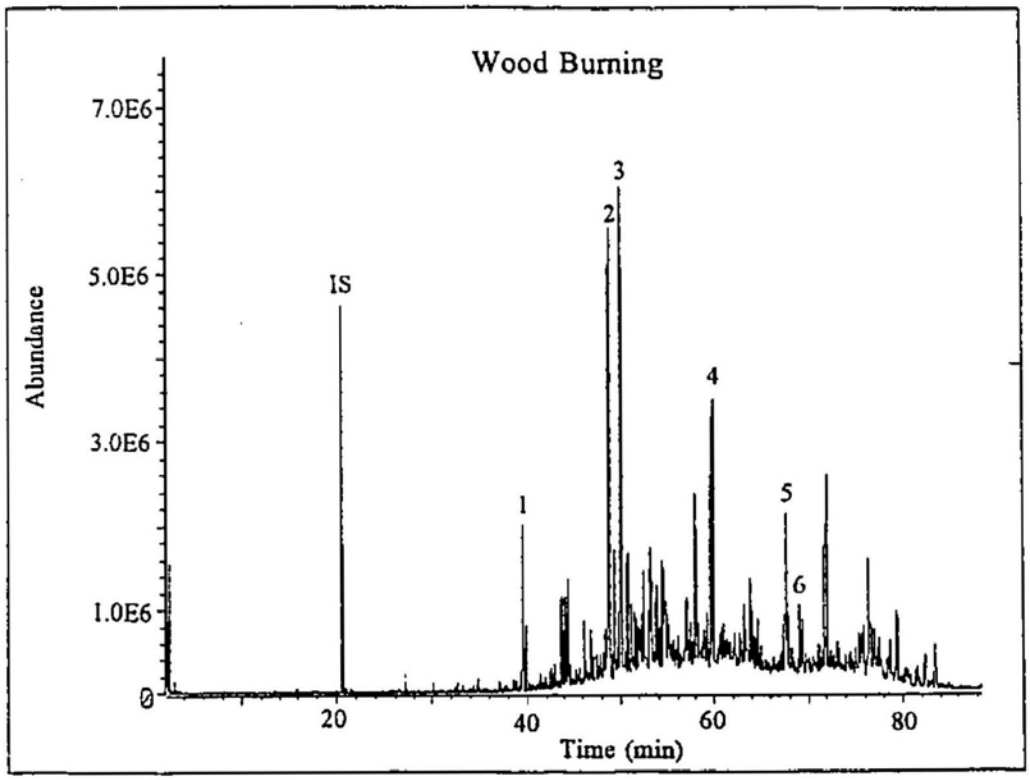
Wood Burning
7.0E6
5.0E6
3.0E6
1.0E6
0
Abundance
IS
1
2
3
4
5
6
20
40
60
80
Time (min)

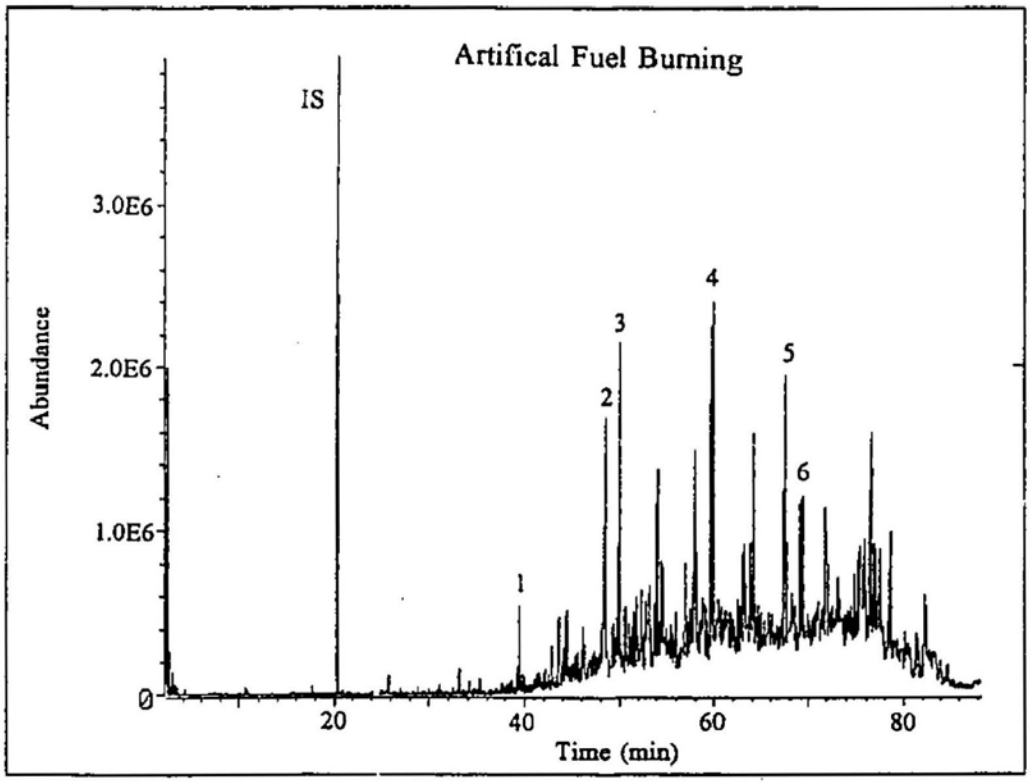
Artifical Fuel Burning
3.0E6
2.0E6
1.0E6
0
Abundance
IS
1
2
3
4
5
6
20
40
60
80
Time (min)

conditions and low temperatures tending to favour high retene yields. Since retene is formed by thermal alteration and not by pyrosynthesis, the lower yields at higher temperatures may be due to its destruction as a result of secondary reactions or the thermal cracking of its precursor compounds (Standley and Simoneit, 1987). The high abundance of retene in the composite sample may be due to the predominance of wood stove soots which were found in the present study to have elevated levels of retene (Figure 53) compared to the relatively low concentrations found in the open fireplace soots samples. This is also consistent with the observation that wood stoves tend to burn in oxygen-deficient conditions compared to open fireplaces (DeAngelis et al., 1981; McCrillis et al., 1992; Mitra and Wilson, 1992). Also, hardwoods are poorer precursors of retene than softwoods (Alsberg and Stenberg, 1979; Ramdahl, 1983a). Since softwood combustion also took place in the open fireplaces we investigated, the general absence of retene in these samples is more likely associated with high temperature oxygen-enriched degradation reactions.

4.4.2 Car soots:

The composite and single car soot samples were mainly characterized by the presence of combustion-derived 3, 4 and 5-ring parental PAH (produced as a result of pyrolysis and pyrosynthesis) which is consistent with previous findings for car soot emissions (Wakeham et al., 1980a; Stenburg, 1983; Alsberg et al., 1985; Masclet et al., 1986; DiLorenzo and Polletta, 1987; Westerholm et al., 1988; Broman et al. 1988; Takada et al., 1990). In addition to the 3, 4 and 5-ring PAH, some of the samples investigated were also characterized by the presence of lower molecular weight 2-ring parental and methylated naphthalenes (Figure 51). Therefore, the mean trend observed consisted of

Figure 53. Molecular signature of a woodstove soot sample showing elevated retene (R) compared to Phenanthrene/Anthracene (1), Fluoranthene (2), Pyrene (3), Benz(a)anthracene/Chrysene (4), Benzofluoranthenes (5) and Benzo(e)pyrene/Benzo(a)pyrene (6).

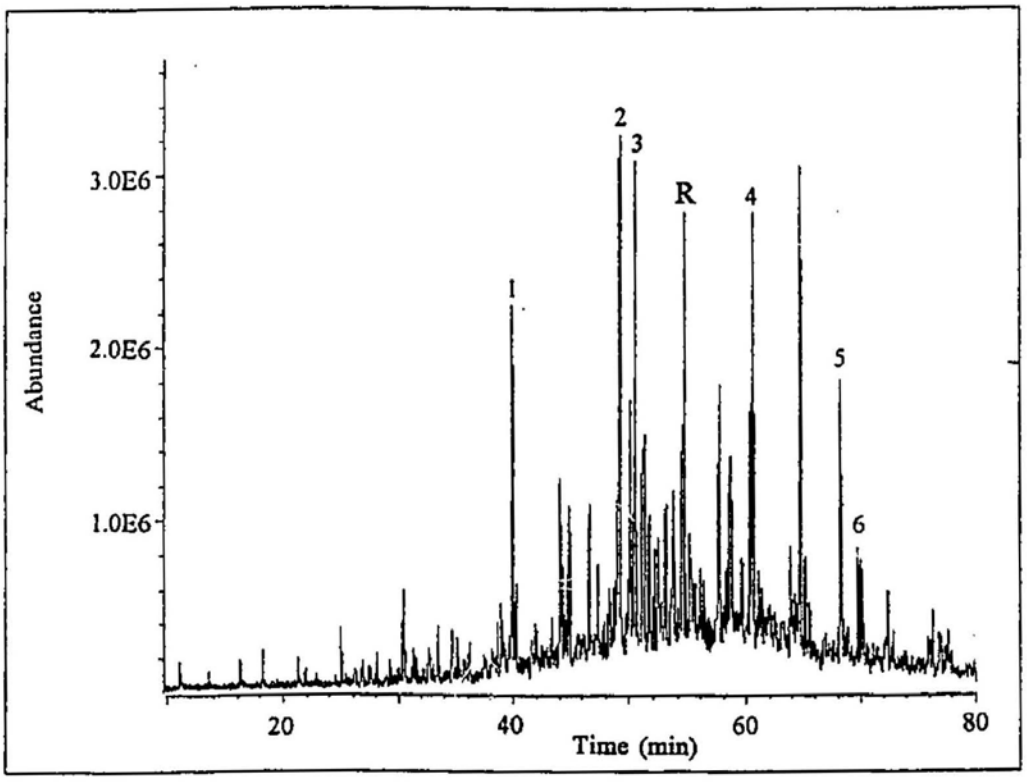
Abundance
3.0E6
2.0E6
1.0E6
1
2
3
R
4
5
6
20
40
60
80
Time (min)

similar concentrations of 2-ring parental and methylated Na and 3, 4 and 5-ring parental and methylated PAH, with the 4 and 5-ring species representing 66% of the total measurable PAH. The concentration of total measurable PAH in the individual samples varied significantly, ranging between 3.4 µg/g and 92.6 µg/g of soot material with mean normalized concentrations indicating a dominance of 2-ring as well as 3, 4 and 5-ring PAH (Figure 51).

The range and concentration of PAH that accumulates in car mufflers are dependent on car age, engine operating conditions, catalytic converter efficiency and general driving conditions (Pedersen et al., 1980; Stenberg, 1983; Rogge et al, 1993). Begeman and Burgan (1970) and Jensen and Hites (1983) reported significant increases in BaP production when the air:fuel ratio was changed from 14:1 to 10:1. Furthermore, BaP emissions were found to increase with increased engine use and higher emissions are also produced during cold-starts and slow driving conditions. Rogge et al. (1993) also reported greater PAH emissions occurred from non-catalytic automobiles compared to vehicles with catalytic systems. Since the majority of mufflers sampled in the present study were generally from older cars, the presence of naphthalene and methylated naphthalenes, indicative of petroleum-related sources (i.e., PAH produced as a result of thermal alteration reactions of natural or biogenic compounds), may be due to unburned fuel or oil components in some of the car soot samples (Guerin, 1978; Simoneit, 1985; Rogge et al., 1993). This normally occurs as a car engine deteriorates. The fuel composition and combustion characteristics are altered as a result of lubricating oil being drawn into and burned in the combustion chamber eventually leading to some

uncombusted oil components being deposited in the muffler (Guerin, 1978). The possibility of uncombusted oil components making it to the muffler system is also supported by the work of Pedersen et al. (1980) who demonstrated that between 2-25% of the particulates in vehicle exhaust emissions originated from the lubricating oil. However, it should also be noted that since these oil components must first pass through the combustion chamber, the possibility of Na and MNa being generated due to combustion reactions cannot be overlooked.

Perylene, a pentacyclic hydrocarbon, reported to be predominantly of diagenic origin (LaFlamme and Hites, 1978; Prahl and Carpenter, 1979; Wakeham et al., 1980b; Colombo et al., 1989) was also identified in some of the investigated car soots samples, although in very low concentrations. Blumer et al. (1977) were the first to report an anthropogenic origin for perylene when it was isolated from car emissions. Lipiatou and Saliot (1992) recently reported that perylene may also be derived from coal pyrolysis.

4.4.3 Other combustion sources:

The range and distribution of PAH isolated from the composite soots sampled from the hopper of the power generating station consisted of 2 to 5-ring PAH (Table 12). The dominance of parental compounds suggests they are mainly combustion-derived, however the presence of petroleum associated compounds such as Na and DBT also indicates a petroleum related input. The presence of petroleum PAH in the accumulated soot of the hopper may be due to uncombusted fuel making it through the burner system (Williams et al., 1993). Total PAH concentrations were generally low, with Pa (3-ring) and Chy (4-ring) being the most abundant. Past studies on PAH emissions from power

plants have mainly concentrated on coal-fired systems (Warman, 1983). Similar to the present study, the concentration of PAH reported in soot samples (particulate phase) from the hopper of coal-fired systems were generally low while significantly higher concentrations were observed in the corresponding vapour phase (Bonfanti et al., 1988). The elevated concentrations of PAH in the vapour phase of the hopper system may be related to the high temperature of the flue gas at this stage of emission. Van Vaeck and Van Cauwenberghe (1985) demonstrated that PAH are normally concentrated in the vapour phase at elevated temperatures, and only condense to the particulate phase when the emission cools. Condensation of PAH to the particulate phase as the emission cools suggests that PAH soot concentrations increase with increasing distance from the burner system (Howard and Longwell, 1983). Also, the low concentration of PAH identified in the soot sample of this particular power generating plant may be due to the high efficiency (85%) of its burner system (Ricketts, pers comm). These factors may also explain the relatively low PAH concentrations observed in soots from the domestic heating furnaces which were sampled close to the exit of the burner unit. The distribution of PAH in furnace soot II is similar to the power generating station indicating that they are primarily derived from combustion reactions. However, the elevated concentrations of MPa in furnace soot I, generating a low Pa/MPa ratio (0.6), suggests that the range of PAH in this composite sample is not only derived from combustion reactions but also from uncombusted petroleum components.

4.4.4 Crankcase oil:

The molecular signatures of single and composite crankcase oils were quite distinct and consisted of 2 and 3-ring parental and methylated compounds with lower concentrations of higher molecular weight parental PAH (4 and 5-ring; Figure 51). This is consistent with the results of previous studies (Alsberg et al., 1985; Pruell and Quinn, 1988; Vazquez-Duhalt 1989; Latimer et al., 1990). Of the total measurable PAH in these samples, 25.5% comprised of 4 and 5-ring parental compounds. PAH concentrations in the investigated crankcase oils were comparable to levels reported by Pruell and Quinn (1988). Also, like previous studies, virgin crankcase oil samples were found to contain no resolvable PAH (Pruell and Quinn, 1988; Latimer et al., 1989). Since virgin crankcase oils are devoid of measurable PAH, the most probable source of PAH in used crankcase oil is speculated to be due to thermal alteration reactions of oil components in the car engine (Pruell and Quinn, 1988; Latimer et al., 1990). Therefore, similar to the muffler soots, the distribution of PAH in crankcase oils would depend on several factors including temperature of reaction, engine design and general operating conditions. Since the engine operating temperatures are relatively high, the likely products resulting from these reactions include 3, 4 and 5-ring unsubstituted compounds such as Pa, Fl, Py, BaA, Chy, BeP and BaP. Pruell and Quinn (1988) also suggested that lower molecular compounds (1 and 2-ring) may be accumulated in crankcase oils from gasoline which are reported to contain elevated concentrations of these compounds (Korte and Boedefeld, 1978). Since the concentration of both the low and high molecular weight PAH in crankcase oil increase with increasing car use, the inter-sample variations in the total PAH

concentration observed in the present study are probably related to a combination of gasoline contamination, engine temperature and use of the oil (Pruell and Quinn, 1988).

4.4.5 Outboard motor:

The molecular signature of the composite condensate from two-stroke outboard motors was similar to crankcase oils consisting primarily of a mixture of 2 to 5-ring methylated and parental PAH (Figure 51). The lower molecular weight compounds are possibly derived from uncombusted petroleum components since 20 to 40% of the condensate released from two-stroke outboard motors during operation consists of uncombusted fuel (Wachs et al., 1992). The higher molecular weight PAH (particularly 4 and 5-ring) may again be attributed to combustion reactions that occur during engine operation. Since recreational boating activity is widely practised in Conception Bay, condensates from two-stroke outboard motors may be an important source contributor of PAH to the sediments.

4.4.6 Crude oil:

In accordance with previous findings, the range of PAH isolated from the crude petroleum samples consisted mainly of 2 and 3-ring compounds (Figure 51) Anderson et al., 1974; Pancirov and Brown, 1975; Grimmer et al., 1983b). Higher molecular weight compounds were also identified in the samples of the present study, although in very low concentrations. Methylated PAH concentrations were significantly higher than the parent compounds. Crude oils are also rich in heterocyclic species particularly thiophenes (e.g., dibenzothiophenes). Significant molecular variations and PAH concentrations have been reported for individual crude oil samples, and this is mainly attributed to their origin and

maturity (Neff, 1979; Grimmer et al., 1983b).

4.4.7 Other primary sources:

Other potential primary sources of PAH not investigated in the present study that may contribute to the PAH inventory of the studied sediments are asphalt road surfaces and tire wear particulates. Similar to petroleum sources, asphalt is reported to consist primarily of a complex mixture of alkyl-substituted PAH and benzothiophenes along with reduced concentrations of higher molecular weight parental compounds (Wallcave et al., 1971; Ostman and Colmsjo, 1988; Takada et al., 1990). However, Wakeham et al. (1980a) also reported weathered asphalt to consist of well resolved 3, 4 and 5-ring parental PAH which is similar to the signatures derived from the combustion of organic material. The variations in molecular signatures of asphalt largely results from the formulations used to prepare the asphalts. For example, in North America, used crankcase oil is used in variable amounts in these formulations (GESAMP, 1993). The distribution of PAH in tire-wear particulates on the other hand consists predominantly of heterocyclics, particularly sulphur and nitrogen containing compounds. Inputs of tire-wear particulates to sediments have also been identified using a compound known as 2-methylthiobenzothiazole, a degradation product of a common antioxidant used in tire manufacturing (Spies et al., 1987; Killops and Howell, 1988).

4.4.8 Comparison of primary source molecular signatures:

The calculated mean and standard deviation (2σ) of the compositional ratios of the dominant PAH in the three prominent primary sources (fireplace soot, car soot and crankcase oil) are summarized and compared to literature data in Figure 50.

Compositional ratios have been used extensively as a source tracing tool of PAH in the natural environment. Generally, the dominance of low molecular weight parental and alkyl-substituted PAH are believed to signify a prominent petroleum influence, whereas the persistence of higher molecular weight parental PAH (4 and 5-ring) is indicative of high temperature combustion reactions.

The mean Pa/A ratios (3-ring angular/linear PAH) for the fireplace (3.7) and car soots (3.0) were comparable and similar to previously reported values (Figure 50, DeAngelis et al., 1981; Rudling et al., 1982; Alsberg et al., 1985; Masclet et al., 1986; MacVetty and Hites, 1988; Broman et al. 1988; Freeman and Cattell, 1990; Takada et al., 1990). In contrast, the mean Pa/A ratio for used crankcase oils was much higher (8.6) and compared favourably to those reported elsewhere for the same source (Lake et al., 1979; Pruell and Quinn, 1988; Latimer et al., 1990). The low mean Pa/A ratio for the furnace soot samples is also consistent with a combustion origin for these compounds, whereas the high Pa/A ratio of 7.0 for the outboard motor condensate is similar to crankcase oils (Figure 54). Lower Pa/A ratios are normally associated with combustion processes since combustion reactions tend to produce elevated concentrations of A. Anthracene concentration in crude petroleum and petroleum products are generally low and Pa/A values greater than 50 have been reported for crude petroleum (Colombo et al., 1989; Brooks et al., 1990). Anthracene was not measurable in the crude petroleum samples investigated in the present study, therefore the Pa/A ratio is also expected to be high.

The mean Pa/MPa ratio for the fireplace (1.0), car (1.4) and furnace soots (1.6)

Figure 54. Summary of the mean and range (standard deviation; 2σ) of the compositional ratios calculated for primary, secondary source and sediment samples investigated.

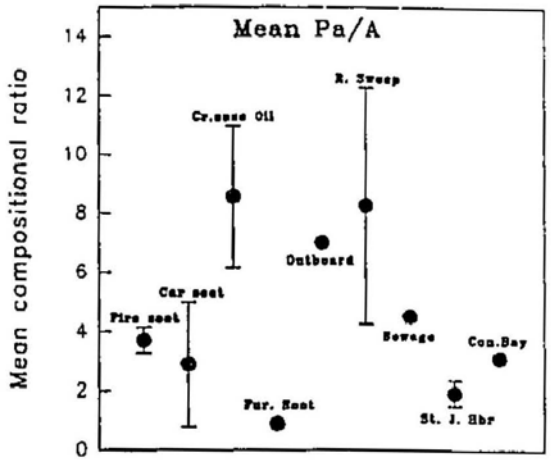
Mean Pa/A
Mean compositional ratio
14
12
10
8
6
4
2
0
Fire soot
Car soot
Cr.case Oil
Fur. Soot
Outboard
R. Sweep
Sewage
Con.Bay
St. J. Hbr

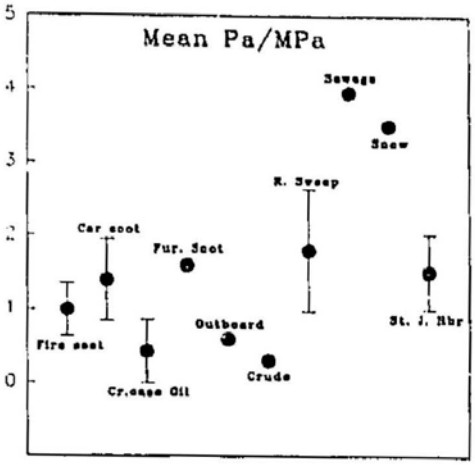
Mean Pa/MPa
5
4
3
2
1
0
Sewage
Snow
R. Sweep
Car soot
Fur. Soot
Outboard
St. J. Hbr
Fire soot
Cr.case Oil
Crude

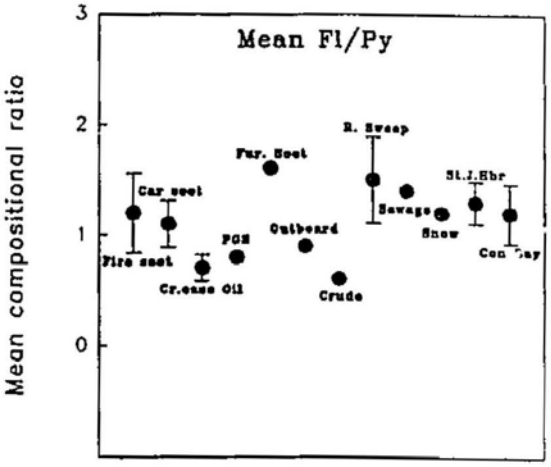
Mean Fl/Py
Mean compositional ratio
3
2
1
0
R. Sweep
Fur. Soot
St.J.Hbr
Car soot
Sewage
Snow
Con Bay
Fire soot
PGS
Outboard
Cr.case Oil
Crude

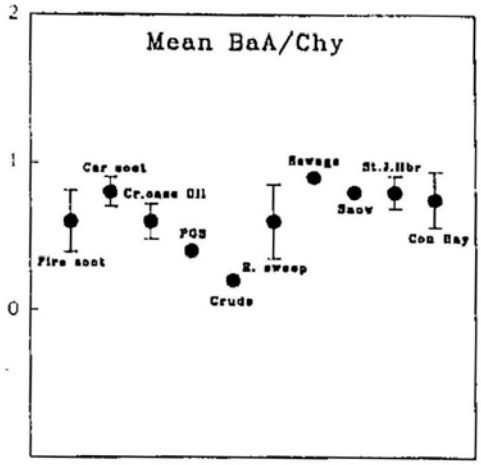
Mean BaA/Chy
2
1
0
Car soot
Sewage
St.J.Hbr
Cr.case Oil
Snow
Fire soot
PGS
Con Bay
R. sweep
Crude

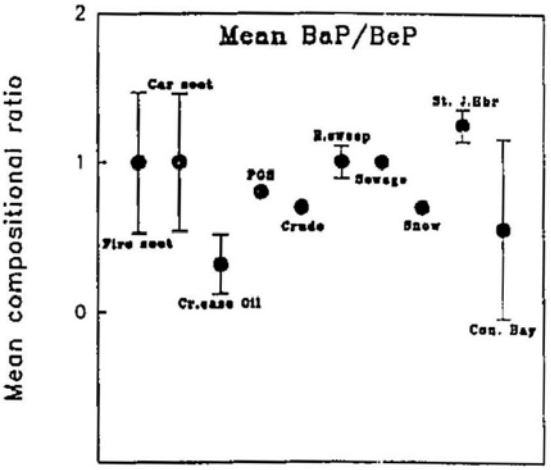
Mean BaP/BeP
Mean compositional ratio
2
1
0
Car soot
St. J.Hbr
R.sweep
PGS
Sewage
Crude
Snow
Fire soot
Cr.case Oil
Con. Bay

samples were greater than the mean values for crankcase oil (0.4), crude petroleum (0.3) and outboard motor condensate (0.6). The significantly lower Pa/MPa ratio in petroleum and petroleum products is due to the elevated levels of alkyl-substituted PAH that are generated during the low temperature formation of crude oils (Youngblood and Blumer, 1975). A mean Fl/Py ratio (nonalternant/alternant PAH) of one or greater, for the fireplace, car and furnace soot samples normally signifies compounds of combustion origin because elevated concentrations of nonalternant compounds, particularly Fl, normally occurs during the combustion of organic matter. However, the Fl/Py ratio (0.8) of the soot from the hopper of the power generating station is less than one (Figure 54). The Fl/Py ratio of the fire soots is in accordance with previous findings (DeAngelis et al., 1980; Rudling et al., 1982; McVeety and Hites 1988), while the mean and range of values for the car soots reported in the literature were generally lower (Giger and Schaffner, 1978; Neff, 1979; Wakeham et al., 1980a; Stenburg, 1983; Alsberg et al., 1985; Masclet et al., 1986; DiLorenzo and Polletta, 1987; Broman et al. 1988). The lower Fl/Py ratio in the car soots may be related to the fact that most of the literature values were determined prior to the widespread introduction of catalytic converters. This suggests that catalytic converters may be preferentially altering the concentrations of PAH prior to emission. Tan et al. (1992) speculated that since parental PAH are planar in shape compared to their alkylated analogues, they may be more readily ruptured or destroyed on the metallic surfaces of catalytic converters. The notable decrease in Py concentrations suggest that it may be more susceptible to destruction than the other parental compounds. There is no plausible explanation based on the molecular structures of these compounds

to support this observation. The low Fl/Py ratio (0.7) (elevated Py) for crankcase oils is comparable to previous findings (Pruell and Quinn, 1988; Latimer et al., 1990). Crude oils are reported to have varying concentrations of Fl and Py, but it is generally accepted that Py is more prominent (Grimmer et al., 1983b). The Fl/Py ratio of the outboard motor condensate is again similar to the crankcase oil value. The mean BaA/Chy ratio was less than unity for all samples with fireplace soots, crankcase oil and power generating station having values between (0.5 and 0.6), while values for the car soots were generally higher (0.8) (Figure 54). This may be due to either different combustion conditions or the initial aromaticity of the fuel (Pedersen et al., 1980). With the exception of coal tars, which generally have elevated concentrations of BaA, the BaA/Chy ratios reported in the literature are also generally less than one making it difficult to distinguish between individual sources using this particular ratio (Canton and Grimalt, 1992). Mean BaP/BeP ratios observed for fireplace and car soot samples were similar to the power generating station and crude oil but the ratio for crankcase oils was generally lower. High values tend to be associated with combustion reactions, but since BaP is quite unstable in the environment, this particular ratio also has limited applicability (Daisey et al., 1986).

In summary, some compositional ratios of PAH in primary sources discriminate between compounds derived from combustion (fire, car and furnace soots samples) and petroleum related sources (crude, crankcase oils and outboard motor condensate). The possibility that crankcase oil (lubricating oil) is an important contributor of parental PAH to muffler soots is not supported by the mean compositional ratios of Pa/A, Pa/MPa, and Fl/Py which tend to indicate PAH of combustion origin. However, it does not exclude

crankcase oil as a possible contributor of hydrocarbons that are subsequently combusted or pyrolyzed to PAH in the muffler. It should also be noted, that even though the mean compositional ratios of the furnace soots indicated that they are mainly combustion-derived, the PAH in furnace soot II seem to consist of both combustion and petroleum related PAH. A petroleum origin is also implicated for the higher molecular weight PAH in the soot of the power generating station. Finally, since fresh asphalt is reported to consist primarily of alkyl-substituted PAH, the compositional ratios are expected to resemble petroleum sources while ratios of weathered asphalt and tire-wear particulates may be similar to combustion PAH (Wakeham et al., 1980a).

4.5 Isotopic signatures of the prominent primary sources:

The following discussion mainly concentrates on the $\delta^{13}C$ trends (compound to compound variation) observed for the parental PAH isolated from the prominent primary sources. However, the $\delta^{13}C$ of the alkyl-substituted compounds will be occasionally addressed for comparative purposes. Due to variations observed in the $\delta^{13}C$ of high molecular weight co-eluting isomers in a number of crankcase oil and car soot samples, individual mean values are reported for combined BaA+Chy, BFl (benzofluoranthenes) and BeP+BaP.

4.5.1 Fireplace soots overall signatures:

Irrespective of the range observed in the $\delta^{13}C$ of the fire soot PAH, the overall trend in the mean $\delta^{13}C$ values indicate that with the exception of anthracene, the lower molecular weight compounds (3-ring) are isotopically more depleted than 4-ring PAH, whereas 5-ring compounds have $\delta^{13}C$ values similar to the 3-ring species (Figure 55).

Figure 55. Summary of the mean $\delta^{13}C$ of the parental PAH isolated from the three prominent primary sources. Error bars represent the range (2σ) observed in the single and composite samples of these sources.

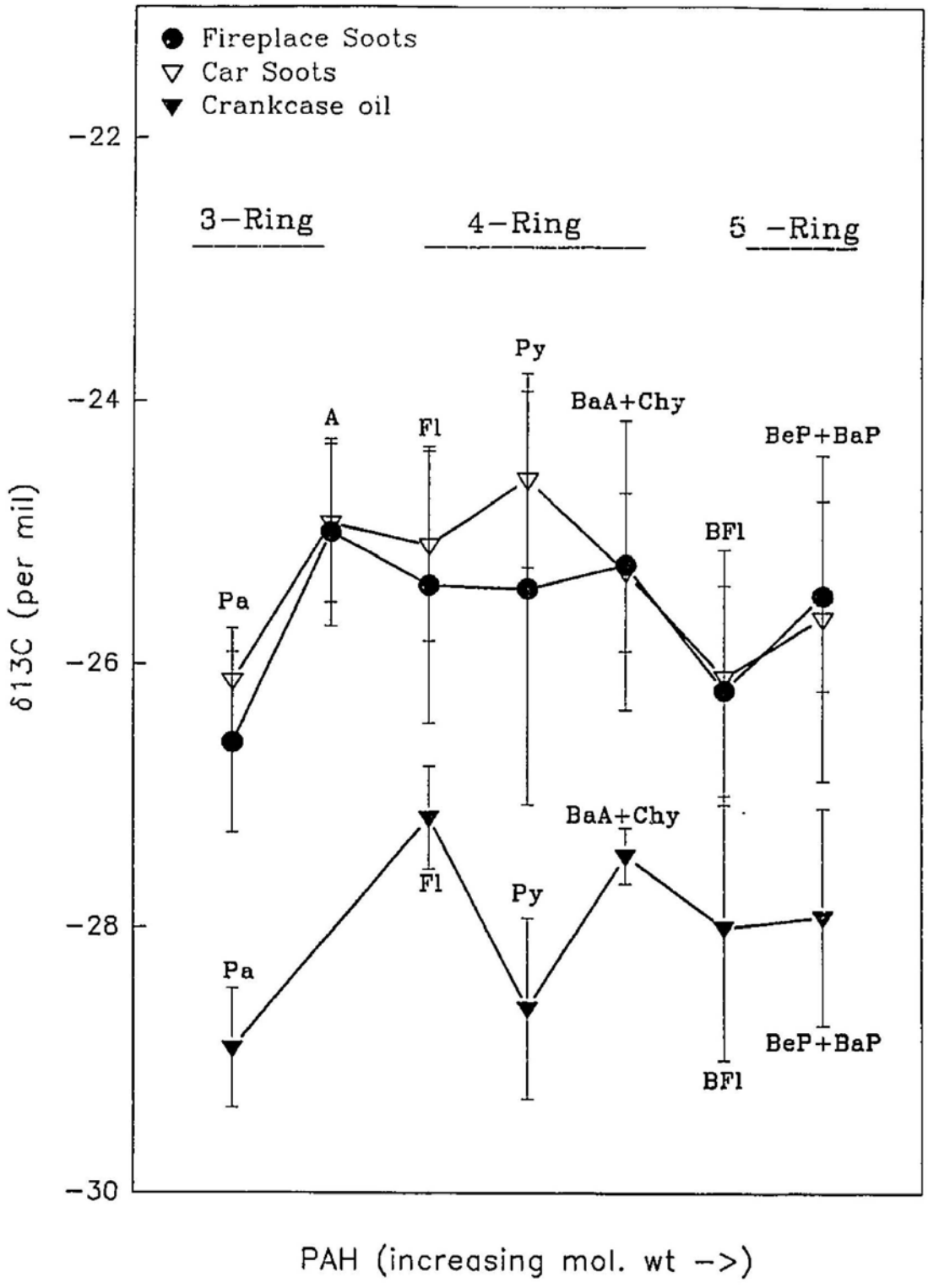
Fireplace Soots
Car Soots
Crankcase oil
3−Ring
4−Ring
5 −Ring
−22
−24
−26
−28
−30
δ13C (per mil)
Pa
A
Fl
Py
BaA+Chy
BeP+BaP
BFl
Pa
Fl
Py
BaA+Chy
BeP+BaP
BFl
PAH (increasing mol. wt −>)

This trend was consistently observed in the single source samples investigated and particularly in the composite sample which consisted of twenty six individual samples of different origin (Figure 28). The increasing isotopic enrichment between the 3 and 4-ring compounds was found to be significant (95% CI) using Pages L-test which is a procedure for testing a monotonic hypothesis concerning experimental means (Page, 1963). Differences were also observed between some of the 3 and 4-ring compounds using rank sum two-sample Mann-Whitney tests. Since PAH are the products of incomplete combustion, the range in isotopic values generated during combustion is related to the isotopic signature of their initial precursors and the fractionations that are associated with primary and secondary reactions that occur during their formation (Fuex, 1977; Sackett, 1978; Arneth and Matzigkeit, 1986a). The trend observed in the $\delta^{13}C$ of the 3, 4 and 5-ring PAH in this combustion process indicate the following possibilities:

(a) the individual compounds were derived from isotopically distinct precursors in the original combustion source that underwent pyrolysis and pyrosynthesis possibly at different temperature ranges,

(b) the overall isotopic variation was primarily dictated by the formation and carbon branching pathways that occurred during pyrosynthesis, or

(c) some combination of (a) and (b).

Since the investigated fire soots were obtained from open fireplaces and wood stoves combusting both hard and softwoods, it is necessary to outline briefly the mechanism of combustion in these two sources. Wood in low-energy open fires (<270°C) in the presence of excess oxygen, undergoes intermolecular dehydration where the

volatiles are initially combusted or expelled, followed by oxygen attack of the carbonaceous residue to yield glowing combustion (Kanury, 1978, Ramdahl, 1983b). Wood in high-energy fires (>340°C) undergoes depolymerization, resulting in a phenomenon called flaming combustion, where carbon monoxide and hydrogen along with other gases are produced. Similar to low energy fires, wood stoves also tend to burn at low temperatures, but wood stove environments are usually more oxygen deficient. Wood primarily consists of hemi-cellulose, cellulose, lignin and a range of solvent extractables (e.g., waxes) (Ramdahl, 1983b; Benner et al., 1987; Goldstein, 1991). Cellulose, hemi-cellulose and lignin constitute up to 90-95% of dried wood, with softwoods containing 28-34% lignin and hardwoods generally less (between 18 and 27%; Goldstein, 1991). The exact precursors of PAH during wood combustion are not clearly identified. However, PAH have been produced during the combustion and pyrolysis of specific groups of compounds such as cellulose and lignin (Liverovskii et al., 1972; Schmeltz and Hoffmann, 1976; Maja 1986). Benner et al. (1987) analyzed the $\delta^{13}C$ of various wood components and reported that cellulose, hemi-cellulose and an uncharacterized fraction (solvent extractable) were respectively 1.3, 0.3 and 1.0‰ more enriched in ^{13}C than the total wood tissue, whereas lignins were 2.6‰ more depleted than the whole-plant (cf., Deines, 1980). A mean $\delta^{13}C$ range for these individual components in hardwoods and softwoods in the northern hemisphere is summarized (Figure 56) (Lowden and Dyck, 1974; Deines, 1980; Freyer and Belacy, 1983; Leavitt and Long, 1986; Benner et al., 1987; Leavitt 1993). Wood combustion in open fireplaces could resemble a stepped combustion process where hemicellulose normally degrades first, followed by cellulose

Figure 56. The range in $\delta^{13}C$ values for various wood components, bulk gasoline, virgin crankcase oil and venezuelan crude (aromatic fraction) along with the range of $\delta^{13}C$ values of the PAH from the primary sources.

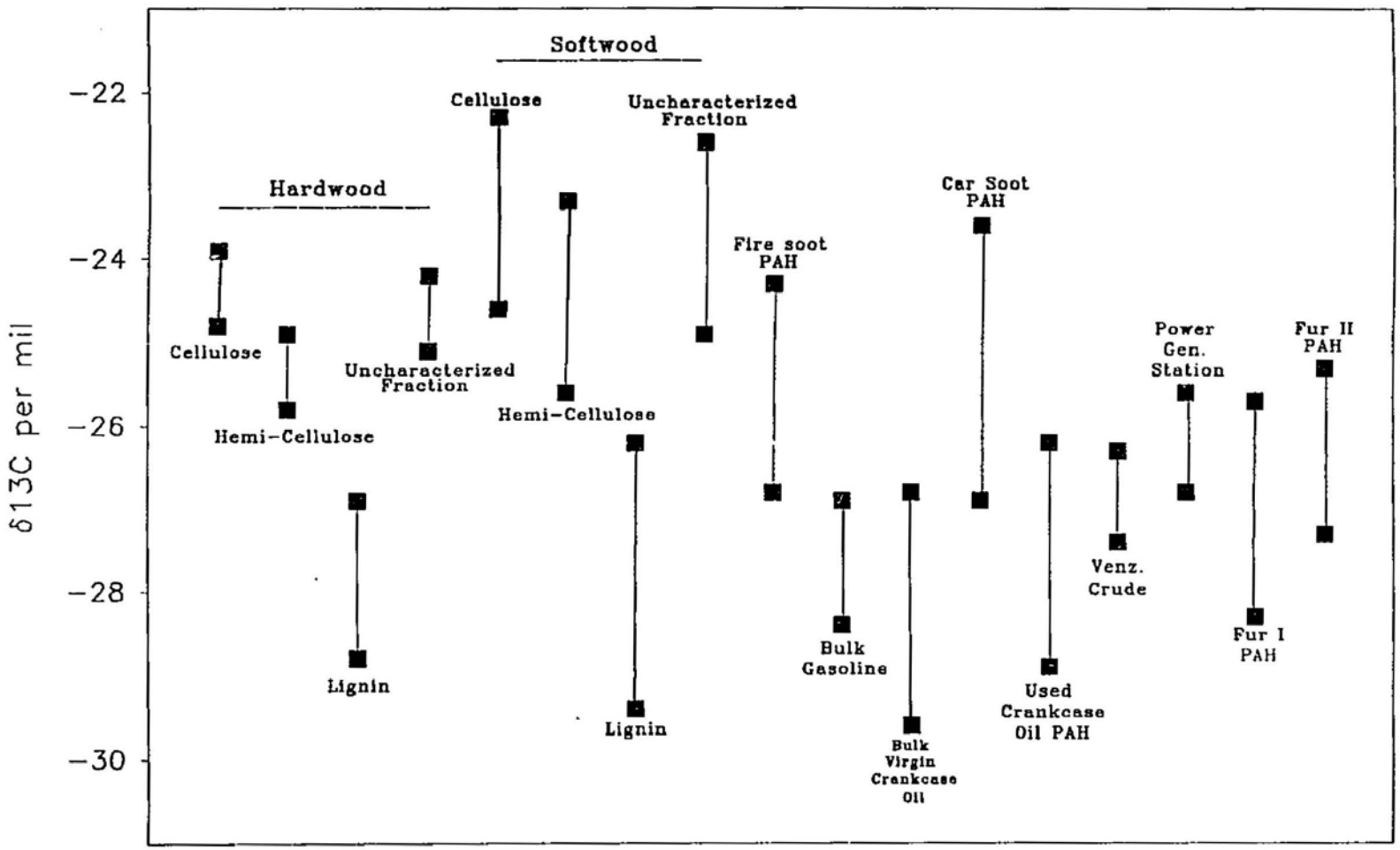
δ13C per mil
−22
−24
−26
−28
−30
Softwood
Hardwood
Cellulose
Hemi-Cellulose
Lignin
Uncharacterized Fraction
Cellulose
Hemi-Cellulose
Lignin
Uncharacterized Fraction
Fire soot PAH
Bulk Gasoline
Bulk Virgin Crankcase Oil
Car Soot PAH
Used Crankcase Oil PAH
Venz. Crude
Power Gen. Station
Fur I PAH
Fur II PAH

and then the lignins (Ramdhal, 1983b). If the carbon isotopic compositions of hemicellulose, cellulose and lignin are sole factors in determining the overall isotopic signature of the fire soots, then the $\delta^{13}C$ depleted PAH may be primarily derived from lignin, while the more enriched compounds may originate from the heavier cellulose or uncharacterized fractions. The uncharacterized fraction of wood also contains certain compounds that are good PAH precursors. Examples of such precursors are terpenes (turpentines, resin acids and sterols), fatty acids and other aromatic compounds including acids, aldehydes and alcohols. The most common triterpenoid (β-sitosterol) has been shown to be an excellent precursor of BaP and other PAH (Schmeltz and Hoffmann, 1976). However, triterpenoids are only common in softwoods and usually occur in relatively low concentrations (Zavarin and Cool, 1991). It is difficult to isolate the most likely specific precursors of individual PAH during wood combustion, since any compound with a carbon and hydrogen skeleton has the potential to generate PAH. However, some compounds are more efficient than others, for example, cyclic or ringed compounds are recognized to be much more efficient at producing PAH than branched or straight chain species (Halaby and Fagerson, 1971; Neff, 1979). Since lignins are the most predominant aromatic compounds and the more isotopically depleted fraction in the wood source, they are good candidates as direct precursors to the isotopically depleted PAH in the wood soots. In contrast, the generally more enriched 4-ring PAH may be formed, at least in part, from more enriched precursors.

As an alternative, the trend in the isotopic signature of fire soot PAH may be controlled by the formation and carbon branching pathways followed by individual

compounds during pyrosynthesis. For example Lang et al. (1963), Halaby and Fagerson (1971) showed that low molecular weight PAH undergo secondary condensation and cyclodehydrogenation reactions during pyrolysis to produce more condensed high molecular weight compounds. Therefore, during the combustion process, low molecular weight compounds, generally formed at lower temperatures may be actual precursors to the higher molecular weight species which are formed subsequently. Gleason and Kyser (1984) and Holt and Abrajano (1991) concluded from kerogen burning studies that these materials burn by a kinetic process whereby the light carbon is preferentially oxidized relative to the heavy carbon leaving an enriched residue. Therefore, since this is a temperature dependent effect (Arneth and Matzigkeit, 1986), the PAH forming radicals produced at lower temperatures are expected to be depleted in ^{13}C compared to radicals formed at higher temperatures. Temperature plays an important role in PAH generation such that different temperature optima exist for the pyrosynthesis of individual PAH compounds (Colket and Hall, 1992). Schmeltz and Hoffmann (1976) exposed malic acid to a range of temperatures between 500 and 900°C and observed that more complex compounds were formed as the temperature increased. If the higher molecular weight compounds are generated at higher temperatures (from ^{13}C enriched radicals), the $\delta^{13}C$ should increase with increasing molecular weight. While this may be the case for the 3 to 4-ring compounds, temperature dependent kinetic isotope effects would not account for the generally ^{13}C depleted 5-ring PAH. Since there is no corresponding increase in the $\delta^{13}C$ with increasing molecular weight, this suggests that the temperature effect previously discussed cannot be solely responsible for the trend observed in the $\delta^{13}C$ of the 3, 4 and

5-ring compounds. Before this model can be used to explain the overall trend observed in the fire soot PAH, a separate radical recombination pathway must be invoked to account for the lower $\delta^{13}C$ values of the 5-ring compounds. Although the most widely documented formation pathway for PAH during combustion is the stepwise recombination (pyrosynthesis) of free radicals (e.g., Figure 6; Badger et al., 1960; Crittenden and Long, 1976; Bittner et al., 1981; Howard and Longwell, 1983; Colket and Hall, 1992), Schmeltz and Hoffmann (1976) concluded from extensive pyrolysis studies that it was difficult to propose any one general pathway for production of PAH since it involved a multiplicity of pathways and various reaction intermediates. Following Schmeltz and Hoffmann (1976) the $\delta^{13}C$ trend observed in the wood burning source can arise from the utilization of a separate pathway or pathways for the formation of 5-ring compounds. One possibility, is the direct condensation of binaphthyls to perylene or benzofluoranthenes during the pyrolysis of naphthalene (Figure 7; Lang et al., 1963).

The compound-specific $\delta^{13}C$ trend may also be explained by invoking secondary reactions of the 3, 4 and 5-ring primary PAH after their initial formation. Using this alternative, an initial monotonic $\delta^{13}C$ trend in the primary combustion/pyrolysis product is altered by subsequent formation or destruction reactions of the primary PAH. Examples of such secondary reactions are condensation of low molecular weight PAH to produce higher molecular weight compounds or their oxidation to CO or CO_2.

If it is accepted that the different PAH are related by one or more condensation reactions, the "precursor" hypothesis cannot be singularly responsible for the overall trend observed in the 3, 4 and 5-ring compounds. In fact, it is reasonable to assume that

"precursor" effects will probably be more evident when comparing sample to sample variations of the corresponding PAH. Since the magnitude of sample to sample variations are lower than the compound to compound isotopic variations, the use of secondary reactions are necessary to explain the $\delta^{13}C$ trend observed in this source. Therefore a combination of both the isotopic variations of the "precursors" and secondary reactions may be responsible for the trend observed in the $\delta^{13}C$ of the 3, 4 and 5-ring compounds in the wood burning soots. Although it is virtually impossible at present to isolate the individual secondary reactions that could dictate the overall intermolecular patterns, some of the likely reactions that may be involved were outlined above (also see section 4.5.3).

4.5.2 Car soots overall signatures:

Despite the difference in the combustion processes, materials and conditions, the $\delta^{13}C$ of the parental PAH isolated from car soots follow a similar trend to the fire soot PAH (Figures 55 and 57). Unlike open fire combustion, the combustion process in the gasoline engine may be described as spontaneous or shock combustion (Barrere, 1981; Hucknall, 1985) whereby gasoline is initially vapourized and mixed with air prior to combustion in the combustion chamber. The PAH produced during this process are reported to be primarily dependent on the fuel:air ratio and the initial aromaticity of the fuel (Begeman and Burgan, 1970; Jensen and Hites, 1983). Gasoline consists of n-alkanes ranging from C_1 - C_{15}, and 20-30% aromatic hydrocarbons (benzene and alkyl-benzenes) which are added to increase its octane rating (Korte and Boedefeld, 1978; Neff, 1979).

Figure 57. Summary of the mean $\delta^{13}C$ values for both the parental and alkyl-substituted PAH isolated from the three prominent primary sources.

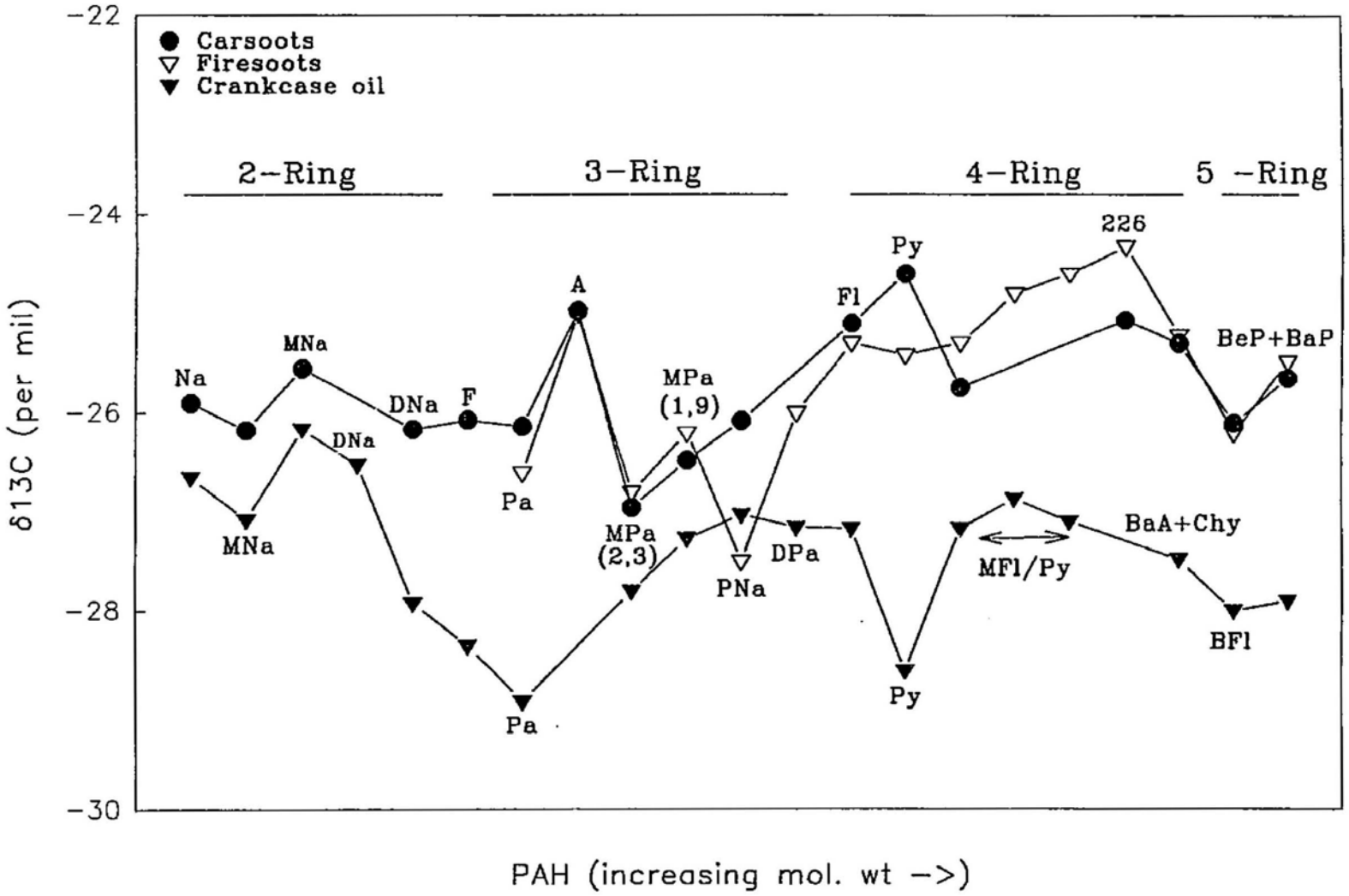
Carsoots
Firesoots
Crankcase oil
2-Ring
3-Ring
4-Ring
5 -Ring
-22
-24
-26
-28
-30
δ13C (per mil)
Na
MNa
MNa
DNa
DNa
F
Pa
A
MPa (2,3)
MPa (1,9)
PNa
DPa
Pa
Fl
Py
Py
226
BeP+BaP
BaA+Chy
MFl/Py
BFl
PAH (increasing mol. wt ->)

While alkanes are poor PAH precursors, gasoline itself has been shown to be a good precursor of PAH (Neff, 1979; Hiereth, 1988). This suggests that benzene and alkylated benzenes may be the primary precursors of PAH during gasoline combustion. Benzene was demonstrated to be a good precursor of naphthalene, (Schmeltz and Hoffmann, 1976) and Colket and Hall (1992) obtained a complex range of PAH from the combustion of 1% toluene (alkyl benzene) at various temperatures. Combustion of crankcase oil in the combustion chamber was also suggested to be a potential contributor of PAH to muffler soots as it can make its way to the combustion chamber via the piston, piston rings, positive crankcase ventilation system and intake valve guides (Pedersen et al. 1980). Repeated isotopic measurements of a variety of bulk gasolines and virgin crankcase oils showed values ranging between -28.4°/$_{oo}$ and -26.9°/$_{oo}$ for the former and -29.6°/$_{oo}$ and -26.8°/$_{oo}$ for the latter (Santrock, pers. comm.; Figure 56). These values are comparatively more depleted in ^{13}C than the isotopic values of car soot PAH. The overall trend in the $\delta^{13}C$ values of the car soot PAH, suggests that the mechanisms involved in controlling the isotopic signature of car soot PAH are similar to those that occur during fire soot PAH formation. Since the $\delta^{13}C$ of the parental PAH in these two sources are broadly similar, it is unlikely that the specific combustion conditions or "precursor" compounds are the dominant factors in controlling the compound to compound $\delta^{13}C$ patterns.

4.5.3 $\delta^{13}C$ patterns in the individual PAH of the fire and car soot samples:

A number of differences in the detailed PAH $\delta^{13}C$ patterns of the fire and car soots are notable. Pyrene is consistently more enriched in the car soots compared to the fire soot samples (Figure 57). The difference in the isotopic value of Py in the two

sources was initially suspected to be related to the post-synthesis pathway followed by car soots before being deposited in the muffler. Prior to deposition, PAH pass through a catalytic converter whose metallic surface has been shown to rupture parental PAH because of their planar structures (Tan et al., 1992). Based on the molecular abundance on cars with and without catalytic converters, Py seems to be preferentially destroyed compared to fluoranthene. However, since all compounds are destroyed by the action of catalytic converters and there were no isotopic alterations associated with any of weathering experiments, it is improbable that the enriched pyrene in the car soots can be attributed to kinetic isotope effects due to preferential loss. Therefore, the notable enrichment observed in the car soot Py compared to the fire soot Py is quite likely related to differences in the pyrosynthetic pathways leading to Py formation in the two combustion sources.

The MPa groups (peaks that represent methylations at sites 2 & 3 and at sites 1 & 9) in both combustion sources have similar trends with the mean isotopic value of the 1,9 group more enriched that the mean value of the 2,3 group (Figure 57). The difference in the isotopic values of these methyl phenanthrene groups suggest either that (a) differential isotopic fractionations may be associated with methylation reactions or successive demethylation at different sites on a benzenoid ring or (b) the 2,3 and 1,9 groups have different precursors compounds. The 1,9 positions on the phenanthrene molecule are the weaker α-sites which have been shown to be more susceptible to substitution reactions than the 2,3 β-sites (Figure 3; Clar, 1964; Radke, 1987). However, since substitution reactions do not destroy the aromaticity of the benzenoid and there are no isotope effects associated with such reactions (Melander and Saunders, 1980), the

difference observed in the isotopic values of these methylated compounds are probably related to the origin of their precursor compounds. The mean isotopic value of parental phenanthrene in the fire place soots was comparatively more enriched than the 2,3 methyl group and more depleted than the 1,9 group while car soot Pa was generally more enriched than both its methylated homologues (Figure 57). Since this trend was consistent in the single and composite samples investigated, it may provide a means of discriminating between wood and gasoline combustion in depositional environments.

In conclusion, the trend observed in the $\delta^{13}C$ of the 3, 4 and 5-ring parental PAH in the two primary combustion sources seems to have resulted from a combination of both the isotopic variations of the "precursors" and a series of secondary reactions that occur duing pyrosynthesis. Regardless of the origin of the $\delta^{13}C$ signature, the isotopically enriched Py and the trend observed in the Pa and MPa and PNa $\delta^{13}C$ values may potentially be used to discriminate between wood burning and gasoline combustion sources in depositional environments.

4.5.4 Other combustion sources:

The $\delta^{13}C$ of the PAH isolated from the composite hopper soot of the power generating station and furnace soots are compared to the fire and car soots in Figure 58. The $\delta^{13}C$ values of the PAH in the power generating station and furnace II soots closely resemble the values observed for the previously described combustion PAH, while the PAH in furnace I seem to be influenced by petroleum related sources. These observations are mainly in accordance with conclusions derived from the compositional ratios of the molecular signatures. The power generating plant combusts bunker C residual oil

Figure 58. $\delta^{13}C$ comparison of the prominent PAH isolated from the combustion sources.

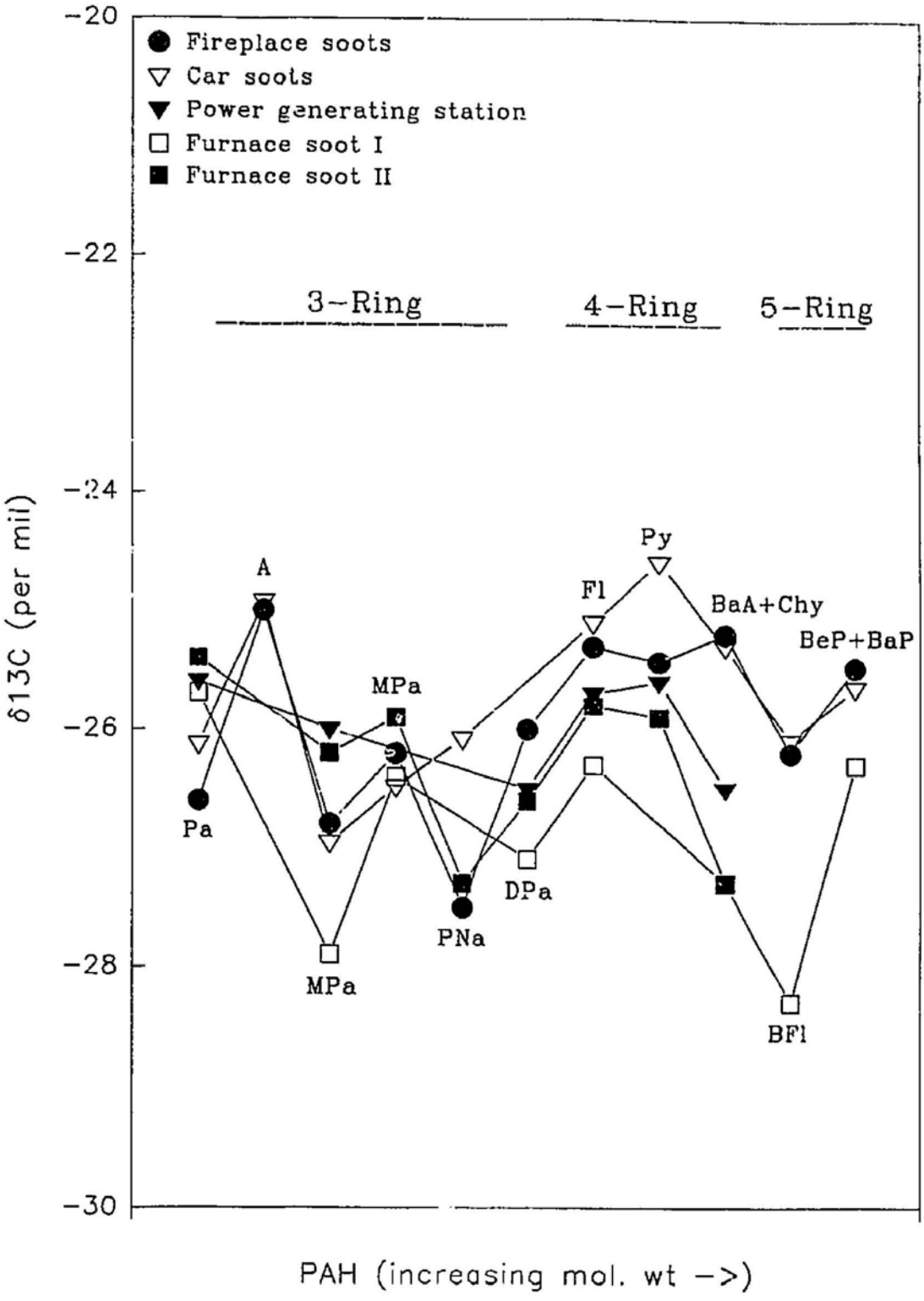
Fireplace soots
Car soots
Power generating station
Furnace soot I
Furnace soot II
3-Ring
4-Ring
5-Ring
-20
-22
-24
-26
-28
-30
δ13C (per mil)
PAH (increasing mol. wt ->)
Pa
A
MPa
MPa
PNa
DPa
Fl
Py
BaA+Chy
BeP+BaP
BFl

(#6 Fuel oil) derived from Venezuelan crude. Sofer (1984) reported a range of -27.4°/$_{oo}$ to -26.3°/$_{oo}$ for the bulk aromatic fraction of Venezuelan crude which is marginally more depleted than the range of $\delta^{13}C$ values reported for PAH isolated from the composite soot sample (Figure 56). The similarity of the $\delta^{13}C$ values of the Power Plant PAH and the aromatic fraction of Venezuelan crude suggests that the mechanisms involved in controlling the isotopic signature during PAH formation are similar to those occurring during fire and car soot PAH formation and are not reflective of "unburned" contributions from the "raw" materials. The #2 fuel oil, used in domestic heating furnaces was analyzed in this study and found to contain mainly 1, 2 and 3-ring aromatic compounds. The $\delta^{13}C$ of naphthalene compounds in fuel oil ranged between -27°/$_{oo}$ and -25.5°/$_{oo}$ (Figure 36). With the exception of the more depleted values in furnace I, the isotopic values of the PAH in these two combustion sources have similar trends. There is no obvious explanation for the isotopically depleted compounds in furnace soot I, unless it can be attributed to petroleum contamination or it may be related the natural variability expected for such samples. Further samples analysis is therefore necessary in order to clarify these observations.

4.5.5 Crankcase oil:

In contrast to the fireplace and car soot signatures, the $\delta^{13}C$ of the PAH isolated from used crankcase oils were significantly more depleted (Figure 55). Also, the range of $\delta^{13}C$ values measured was only marginally enriched compared to the range of bulk isotopic values (-29.6°/$_{oo}$ and -26.8°/$_{oo}$) reported for virgin crankcase oil (Santrock, pers. comm.; Figure 56). Freeman (1991) demonstrated the $\delta^{13}C$ relationship between

diagenetically altered hydrocarbons and their precursors in natural systems. An analogy may be drawn between the diagenetic system that was investigated by Freeman and the artificial "diagenetic" system in car engines. Unlike combustion, where a significant portion of the precursor source materials is initially fragmented into smaller radicals prior to PAH formation, the PAH in used crankcase oil may be largely derived from a series of thermally-induced aromatization reactions of natural precursors that exist in the oil. Freeman (1991) reported that there was very little isotopic alteration associated with the aromatization of a range of triterpenoid-derived polycyclic aromatic hydrocarbons, although it should be stressed that the aromatization reactions investigated were microbially-mediated as opposed to the thermally-induced aromatization being examined. Crankcase oils derived from petroleum consists primarily of naphthenes (hump) with a minor n-alkane content ($< C_{25}$) and traces of steranes and triterpanes (Simoneit, 1985). In addition to these compounds, they also consists of 14% by volume of various natural and synthetic additives used to enhance their physical properties. The additives include alcohol and solvent-based compounds with trace amounts of n-fatty acid detergents (Weinstein, 1974; Simoneit, 1985; GESAMP, 1993). Santrock (pers. comm.) also reported that virgin crankcase oil (bulk $\delta^{13}C$ values) tends to become marginally enriched with increased use and time in the engine. Therefore, the variation observed in the $\delta^{13}C$ of the PAH in the individual samples may be attributed to the age and use of the oil. Increased time and temperature within the car engine may result in increased aromaticity and polymerization of PAH precursors materials which eventually produce isotopically enriched PAH.

Of the parental compounds isolated from the crankcase oils, Pa and Py were generally more depleted than Fl, BaA/Chy, BFl and BeP/BaP (Figure 57). The difference in the isotopic values of these two groups of parental compounds suggests that they may be derived from different precursors in the oil. The similarity in the isotopic values of Pa and Py, indicate that they may be derived from precursor materials which have a common origin or a common synthesis pathway that is distinct from those followed by other high molecular weight PAH (e.g., Grimmer and Bohnke, 1978). The assignment of aromatic structures to their biological precursors in crude oils has proved difficult (Radke, 1987). However, it is now well established that the saturated or partially unsaturated six-membered rings in steroids and polycyclic terpenoids undergo a process of stepwise aromatization (Ludwig et al., 1981; Mackenzie, 1984). Mair and Martinez-Pico (1962) observed that Pa, Py and their methyl derivatives had structures that were similar to a range of compounds produced in crude petroleum at temperatures of between 305 and 405°C mainly as a result of the dehydrogenation of steroids and alkaloid (Py) (thebenol) related compounds. The elevated concentrations of Pa in used crankcase oil suggests that it is possibly derived from aromatized steranes (Figure 5; Mackenzie, 1984), whereas Py (VIII) may be derived form some other natural products such as alkaloids (Mair et al., 1962) or it may be formed from Pa (VI) following the pathway proposed by Grimmer and Bohnke (1978; Figure 59). The 4-ring BaA and Chy may be formed by the sequential aromatization of pentacyclic triterpenoids (e.g., α- or β-amyrins) which have been postulated as possible precursors of hydrochrysene and methylated chrysene (Figure

Figure 59. Structural relationships between various PAH observed by Grimmer and Bohnke (1978) in crude oils. Broken arrows represent pathways of minor importance (modified from Radke, 1987).

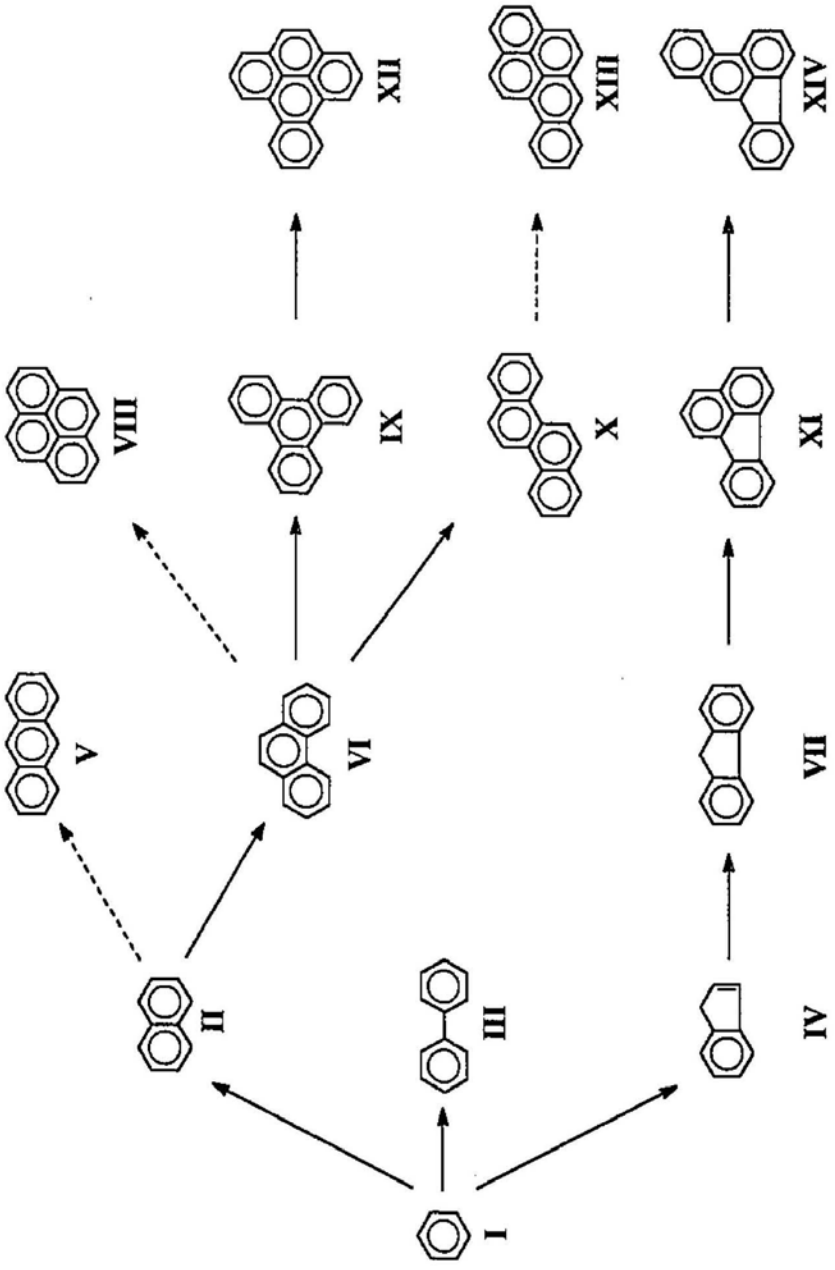
I
II
III
IV
V
VI
VII
VIII
IX
X
XI
XII
XIII
XIV

Figure 60. Scheme illustrating the possible diagenetic pathways leading to alkylchrysenes from α- and β-amyrin (modified from Wakeham et al., 1980b and Tan and Heit 1981).

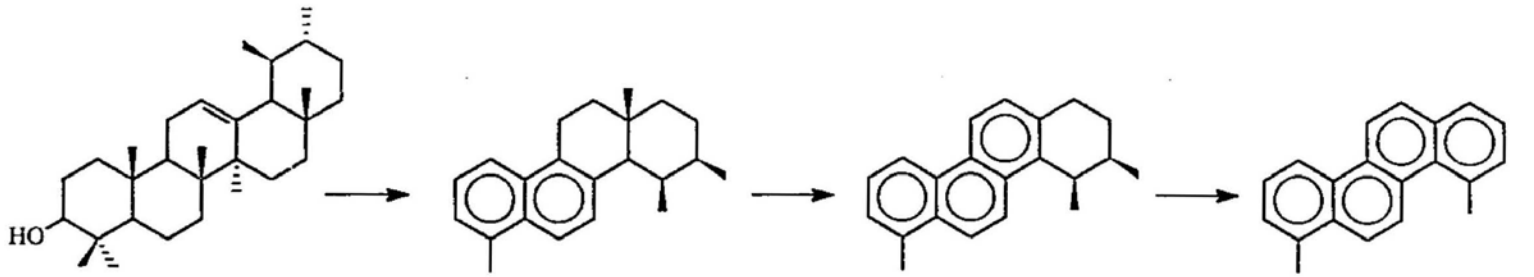

α-Amyrin

3,4,7,12a-Tetramethyl-1,2,3,4,4a, 11,12,12a-octahydro-chrysene

3,4,7-Trimethyl-1,2,3,4-tetrahydro-chrysene

Alkylated-chrysene

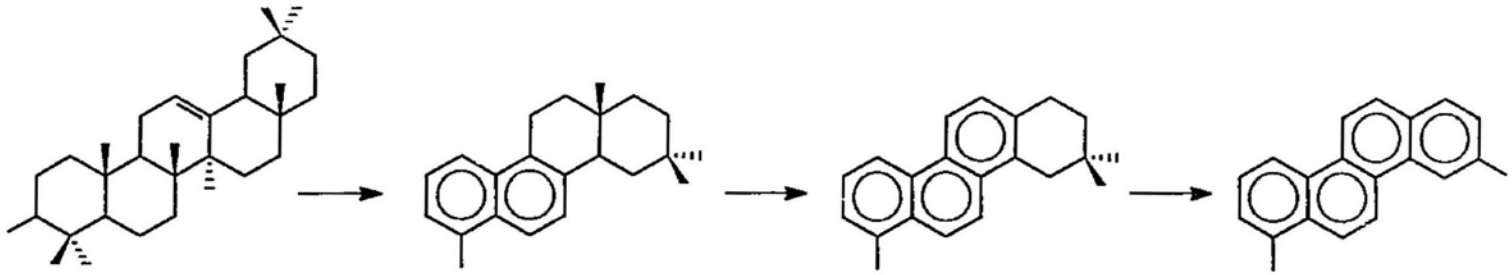

β-Amyrin

3,3,7,12a-Tetramethyl-1,2,3,4a, 11,12,12a-octahydro-chrysene

3,3,7-trimethyl-1,2,3,4-tetrahydro-chrysene

Alkylated-chrysene

60; Wakeham et al., 1980b; Tan and Heit, 1981; Freeman, 1991). Carotenes are also common precursors of higher molecular weight hydrocarbons in crude petroleum (Speers and Whitehead, 1969), but there is no evidence in the literature to suggest they may be related to specific PAH formation. There are no reported biological precursors for the more ^{13}C enriched Fl(XI), BFl(XIV) and BeP+BaP (XII and XIII) hence they are likely derived from angular fusion of intermediate aromatic compounds (Figure 59; Grimmer and Bohnke, 1978).

The Na and MNa are the most ^{13}C enriched compounds isolated from the crankcase oil samples (Figure 57). Alkylated benzenes in crankcase oils may be a product of thermal alteration of terpenoids in virgin oil (Mair, 1964) or they can also occur as a direct input from gasoline (Pruell and Quinn, 1988). Regardless of their origin, it is quite possible, that they are the intermediate compounds (precursors) to the formation of Na. This is also supported by preliminary isotopic measurements performed on a series of alkylated benzenes isolated from the outboard condensate which ranged between -27.5‰ and -25.5‰. The trend (compound to compound variation) in the $\delta^{13}C$ values of the 1,9 and 2,3 methylated phenanthrene is comparable to the trend obtained for these compounds in the combustion sources. However, unlike the combustion sources, both groups in the crankcase oil samples were significantly more enriched in ^{13}C than parental Pa. This trend may again serve as a useful indicator of crankcase oil inputs to depositional environments.

4.5.6 Other petroleum sources:

The PAH isolated from the bulk outboard motor condensate were isotopically very similar to the mean isotopic values of the PAH in used crankcase oil, except the outboard motor condensates were generally more enriched in ^{13}C (Figure 35). This similarity to crankcase oils was also observed using the compositional ratio of the prominent compounds from the molecular signatures of these two sources. The apparent enrichment in ^{13}C of naphthalene and its methylated derivatives in the outboard motor sample may be due to the partial combustion of gasoline that is characteristic of two-stroke outboard motor engines.

The $\delta^{13}C$ of the PAH isolated from the crude petroleum samples have similar trends (compound to compound variatios), except that the Calgary crude PAH were generally lighter (-32.2‰ to 25.1‰) than the Arabian sample (-30.0‰ to -22.7‰; Figure 34). This variation in isotopic values is possibly related to the origin or maturity of these samples (Clayton, 1991; Chung et al., 1992). Differences in the $\delta^{13}C$ values of the isomeric compounds suggests that these compounds may originate from different precursor products or by different formation pathways. In contrast to Chung (1992) who reported 8 to 7‰ differences between parental and methylated PAH in a crude oil, the $\delta^{13}C$ of the parental and alkyl-substituted PAH in these samples were similar and are in accordance with the finding of Clayton (1992). Naphthalene and methylated naphthalenes in #2 fuel oil had isotopic values within the range observed for the crude oils and other petroleum products investigated (Figure 36).

4.5.7 Comparison of primary source signatures:

The mean isotopic values of PAH isolated from the three prominent primary sources (fire and car soots and crankcase oil; Figure 57) indicate two distinct signatures, mainly combustion and "diagenetic" (i.e, crankcase oil). Parental PAH produced as a result of combustion reactions were generally enriched compared to the corresponding compounds isolated from the crankcase oils.

In spite of the differences in the combustion processes and the nature of the primary precursor materials, the trend in the isotopic values of the combustion-derived PAH (fire and car soots) was comparable (Figure 57). Compound-specific isotopic variations of PAH in both sources are postulated to be jointly dictated by the precursor compounds in the original source material and by secondary reactions during pyrosynthesis. Although, the overall isotopic signatures were comparable, differences such as the ^{13}C enriched Py in car soots, the trend between the Pa and MPa and dissimilar PNa $\delta^{13}C$ values may be potentially useful in discriminating between inputs from these two sources in depositional environments. The isotopically depleted PAH isolated from the crankcase oils (petroleum) were attributed to thermally-induced aromatization reactions of natural compounds that exist in oil, a process analogous to diagenetic (catagenic) reactions in natural systems. The very similar isotopic values for the corresponding PAH isolated from crude oils support the suggestion that the processes occurring in the car engine may be similar to diagenetic alteration. Together with their generally ^{13}C depleted values, crankcase oils were also characterized by the presence of significantly depleted Pa and Py. Unlike the combustion sources, parental phenanthrene was isotopically more

depleted in ^{13}C than its methylated derivatives and Py was significantly more depleted in ^{13}C than fluoranthene. These two distinct characteristics have the potential to be used as petroleum source tracing tools.

The patterns in the $\delta^{13}C$ values of the PAH from the two combustion sources and crankcase oil provide the potential for quantitative apportionment studies to be undertaken on PAH from these sources in depositional environments. Apportionment of individual input sources requires that they are isotopically distinct and that their natural variability does not overwhelm the isotopic differences. Despite the overlap in the fire and car soots signatures, the isotopically enriched Py and the trend in the Pa and MPa may be potentially useful in elucidating PAH contributions from these two important sources.

4.6 Molecular signatures of the secondary source samples:

Secondary source PAH from the study sites consist of mixtures of PAH from the primary sources discussed previously. The mean compositional ratios of the prominent compounds in the road sweep, sewage and snow samples are summarized and compared to the primary sources in Figure 54. The concentration of individual PAH showed the general pattern road sweep < snow < sewage samples.

4.6.1 Road sweeps:

Resolution of individual PAH from the open-road sweep samples was generally hindered by their relatively low concentrations and the presence of a prominent UCM. However, despite the poor resolution, a range of parental compounds with mean concentrations ranging between 0.04 and 2.60 μg/g of sweep material (dry weight) were

resolved from these UCM's. The dominance of 3, 4 and 5-ring PAH suggests that these compounds are mainly of combustion origin and the most probable sources are likely to be domestic fires and vehicle exhaust emissions (Figure 61).

Various analytical methods have been used to quantify individual concentrations of PAH in road sweeps materials, therefore it is difficult to compare the results of the present study with previous studies (e.g., Wakeham et al., 1980a; Herrmann, 1980; Takada et al., 1990). The concentration of individual PAH in open road sweeps investigated in the present study were generally low, but some samples had Fl and Py concentrations similar to previously reported values (Herrmann, 1981; Takada et al., 1990). However, Fl values were significantly less than the 10 μg/g reported by Giger and Schaffner (1978). Latimer et al. (1990) and Takada et al. (1990) postulated that particle size fractionation (dilution of fine PAH particulates with larger grain size material, i.e., sand) may be one of the principal reasons for low PAH concentration in surface road sweep samples. Different particle size fractions of road sweep material were analyzed in this study and no significant difference in the total PAH concentration of the various size fractions was observed. Moreover, greater difficulties were encountered in resolving parental compounds from the lower particulate size fractions. Reduced PAH concentrations may also be due to the continual washing of fine particulate materials from road surfaces by heavy rainfall (Hoffman et al., 1984) which is frequently experienced in the study areas. Road sweep UCM's were reported to consist of a variety of degraded highly complex mixture of materials derived from automobile exhausts, asphalt, used crankcase oil, tire and brake particles and atmosphere fallout (e.g., Novotny et al., 1985). Frequent road repairs are carried out in the St. John's city area, because road surfaces are

Figure 61. Summary of the mean normalized concentrations of the PAH isolated from the secondary source and sediment samples..

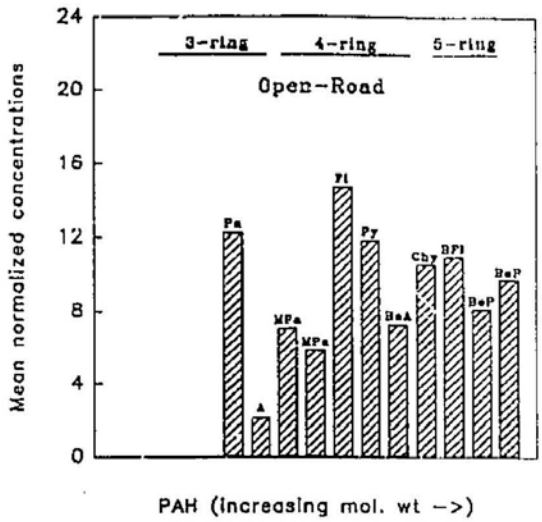
3-ring
4-ring
5-ring
Open-Road
Mean normalized concentrations
PAH (increasing mol. wt ->)

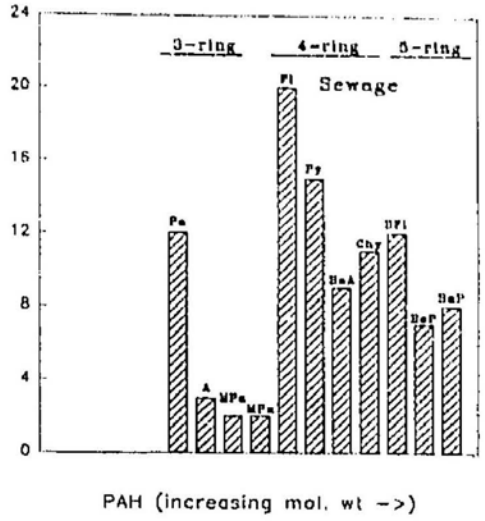
3-ring
4-ring
5-ring
Sewage
PAH (increasing mol. wt ->)

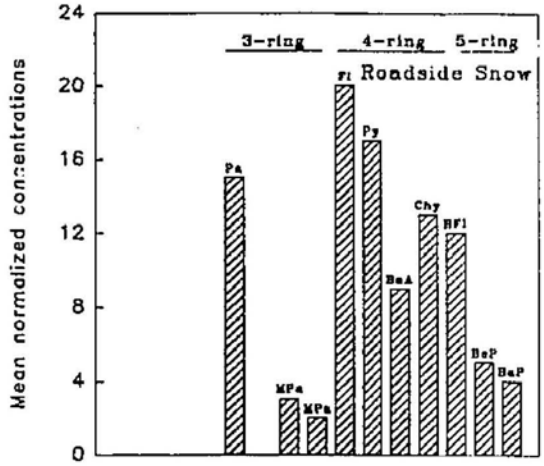
3-ring
4-ring
5-ring
Roadside Snow
Mean normalized concentrations

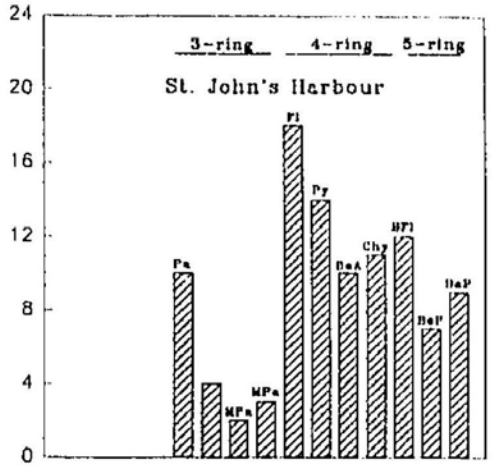
3-ring
4-ring
5-ring
St. John's Harbour

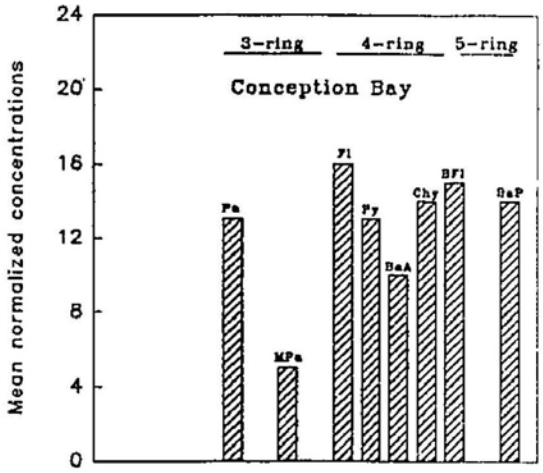
3-ring
4-ring
5-ring
Conception Bay
Mean normalized concentrations

extensively weathered during the winter months as a result of a series of melt-freeze cycles and from the abrasive action of steel-studded car tires. These activities may result in PAH contributions from both fresh and weathered asphalt to the road sweep samples. With the exception of chrysene, fresh asphalt mainly consists of a complex mixture of alkyl-substituted PAH and a prominent UCM (Ostman and Colmsjo, 1988; Takada et al., 1990), while highly weathered asphalt has a signature similar to combustion sources (Wakeham et al., 1980a). Using the observed molecular signatures, weathered asphalt cannot be discounted as a potential contributor of PAH to the road sweep samples. However, recent PAH inputs from fresh asphalt were probably insignificant because of the notable absence of alkyl-substituted PAH in these samples. Tire-wear particles were also not likely to be important contributors of PAH to the road sweep samples due to the conspicuous absence of heterocyclic PAH (Wakeham et al., 1980a; Spies et al., 1987; Killops and Howell, 1988) in the samples investigated. The prominent UCM and the generally low concentration of parental PAH in the cement paved underground car park sample may also be related to weathered asphalt transported on car tires, crankcase oil and car emissions. PAH contributions from domestic fires are considered to be negligible in this particular sample since the car park is enclosed. The molecular signature of the asphalt paved car park sweep was comparable to crankcase oil, and the dominance of crankcase oil in such samples suggests that open-road runoff may consist of significant quantities of crankcase oil hydrocarbons (cf.; Wakeham et al., 1980a; Eganhouse and Kaplan, 1982; Latimer et al., 1990).

Despite the dominance of 3, 4 and 5-ring PAH, the mean compositional ratios of

the prominent compounds in the open-road sweep reflect combined contributions from combustion and crankcase oil sources (Figure 54). When compared to the compositional ratios of the primary sources, the Pa/A ratio (8.3) suggests crankcase oil inputs and this observation is also supported by the low concentrations or absence of anthracene in most of the samples investigated. Both the Pa/MPa (1.9) and the Fl/Py (1.5) ratios support contributions from fire and car soots emissions with the Pa/MPa ratio possibly favouring a greater contribution from car soots (cf., Takada et al., 1990). The BaA/Chy ratio could correspond to any of the three prominent sources, while the BaP/BeP ratio indicates combustion-derived PAH resulting from both fireplace and car soot emissions and possibly weathered asphalt. In summary, using the mean compositional ratios of the prominent PAH alone in open-road sweep samples, individual primary source contributions cannot be clearly elucidated. The compositional ratios suggests that all three sources contribute to the PAH inventory of the open-road sweep samples along with possible inputs from weathered asphalt.

4.6.2 Sewage:

The molecular signatures of untreated sewage, obtained from the main sewage outfall in St. John's Harbour were quite similar to the signatures of the open-road sweep samples (Figure 61). Consistent with our observation, PAH concentrations in untreated sewage have been reported to vary considerably (Wild et al., 1990; Wild and Jones, 1993). The dominance of 3, 4 and 5-ring PAH suggests that these compounds are of combustion origin with 82.5% of the total PAH comprising of 4 and 5-ring compounds (Figure 61). This is also supported by the presence of elevated concentrations of five-

membered ring PAH (non-alternant; Fl and BFl) which are commonly associated with combustion processes (Simoneit, 1985). Mean compositional ratios also indicate that the prominent inputs of PAH to the untreated sewage samples are of combustion origin. However, again it is not possible using the compositional ratios alone to discriminate clearly between inputs from the different combustion sources because of the overlap in these source signatures. The slightly elevated BaA/Chy ratio suggests that car soot emissions may be significant in these samples, but crankcase oil inputs are also implicated from this ratio. More importantly, weathering effects can alter the molecular signatures such that low molecular weight PAH, particularly the alkyl-substituted compounds tend to be degraded at a faster rate than the high molecular weight compounds.

The similarity between the molecular signature of the road sweeps and the sewage samples is not surprising because of the combined nature of the sewer system. In the older section of St. John's city, road surface runoff combines with the sewer system before being discharged to the Harbour. Therefore, since there are no important sources of industrial effluents in this area, the PAH inputted to the Harbour in domestic sewage effluents consist primarily of aerially deposited combusted products, vehicle emissions, crankcase oil and weathered asphalt particulates from road surfaces. In a sense, the sewage system can be viewed as a combination of "secondary" sources.

4.6.3 Snow:

The mean concentrations of individual PAH in the residual particulates of the evaporated composite snow sample were higher (per g of snow particulates vs. per g of road sweep particulates, dry weight) than the open-road sweep samples. Snow was

collected from a number of busy road sides and this would account for the resemblance between the molecular signatures of the snow and open-road sweep samples (Figure 61). The dominant PAH identified are mainly derived from combustion sources with 81% of the total measurable PAH consisting of 4 and 5-ring compounds (Figure 61). Snow has been shown to have the ability to concentrate and retain PAH despite going through a number of melt-freeze cycles (Herrmann, 1981; Schoandorf and Harrmann, 1987; Leuenberger et al., 1988; Boom and Marsalek 1988). The most prominent PAH sources likely to accumulate in road side snow are aerially deposited combustion products which will also be scrubbed from the atmosphere during snowfall, direct vehicle emissions and weathered road surface asphalt (Brorstroem-Lunden and Loevblad, 1991). The mean compositional ratios of Pa/MPa (3.5) and Fl/Py (1.2) BaP/BeP (0.7) reflect fire and car soot emissions whereas the BaA/Chy ratio (0.8) suggest contributions from all three sources. The absence of measurable concentrations of anthracene (high Pa/A ratio) indicates inputs from crude petroleum.

In conclusion, using the compositional ratios of the prominent PAH in the three outlined secondary sources, it is difficult to discriminate clearly between individual inputs from the prominent primary sources. This is mainly due to the similarities in the molecular signatures of the various combustion and petroleum sources and to the uncertain effects of weathering on the molecular signature. Additionally, quantification of the various sources is difficult even if a select set of molecular parameters are utilized.

4.7 Isotopic signatures of the secondary sources:

Since one of the primary objectives of this study is to determine whether CSIA can provide quantitative complementary information to molecular signatures in elucidating inputs of primary source PAH to depositional environments, the $\delta^{13}C$ of the secondary source parental PAH are compared to their respective molecular signatures. The $\delta^{13}C$ values of secondary source parental PAH were similar in all samples and were generally more depleted in ^{13}C with increasing molecular weight (Figure 62). As expected, the overall isotopic signature of the secondary sources, reflects inputs of both combustion and petroleum-derived components.

4.7.1 Road Sweeps:

The isotopic signature of road sweep PAH shows some dependence on sampling location with depleted compounds being derived from enclosed areas while more enriched PAH were associated with open-road samples (Figure 63; and section 4.6). The isotopically enriched A and Py and the trend between Pa and MPa values in the open-road samples, indicate that they are mainly of combustion origin, with enriched Py manifesting a definite car soot input. Anthracene and the MPa's could only be isotopically analyzed in three of the investigated samples, but it is interesting to note that in conjunction with Pa, these compounds are more enriched in the open-road samples than in the two primary combustion sources (Figure 63). The apparent $\delta^{13}C$ enrichment of these 3-ring compounds in the open-road sweep compared to the combustion sources may be due to a photodegradation effect arising from prolonged exposure on the open-road surface, an explanation which may also account for the inconsistent Pa/A ratio observed for the

Figure 62. Comparison of the mean $\delta^{13}C$ of the 3, 4 and 5-ring parental PAH isolated from the prominent primary and secondary source samples. Pa = Phenanthrene, A = Anthracene, Fl = Fluoranthene, Py = Pyrene, BaA+Chy = Benz(a)anthracene and Chrysene, BFl = Benzofluoranthenes, BeP+BaP = Benzo(e)pyrene and Benzo(a)pyrene.

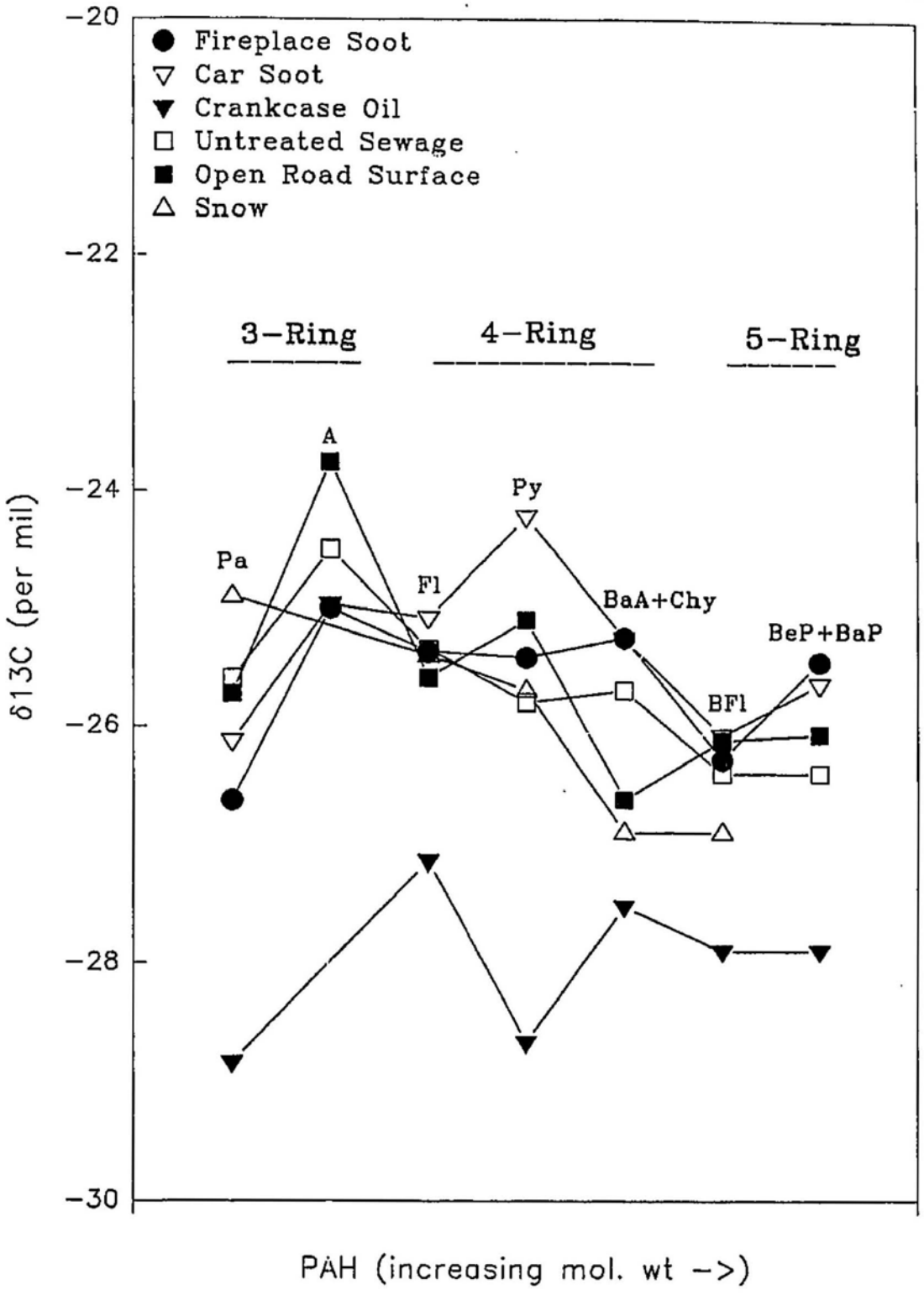
Fireplace Soot
Car Soot
Crankcase Oil
Untreated Sewage
Open Road Surface
Snow
3–Ring
4–Ring
5–Ring
A
Py
Pa
Fl
BaA+Chy
BeP+BaP
BFl
−20
−22
−24
−26
−28
−30
δ13C (per mil)
PAH (increasing mol. wt −>)

Figure 63. Comparison of the $\delta^{13}C$ in the open-road and enclosed car park sweeps with the prominent primary sources. MNa = Methyl Naphthalene, DNa = Dimethyl Naphthalene, F = Fluorene, Pa = Phenanthrene, A = Anthracene, MPa = Methyl Phenanthrene, DPa = Dimethyl Phenanthrene, Fl = Fluoranthene, Py = Pyrene, BaA+Chy = Benz(a)anthracene and Chrysene, BFl = Benzofluoranthenes, BeP+BaP = Benzo(e)pyrene and Benzo(a)pyrene.

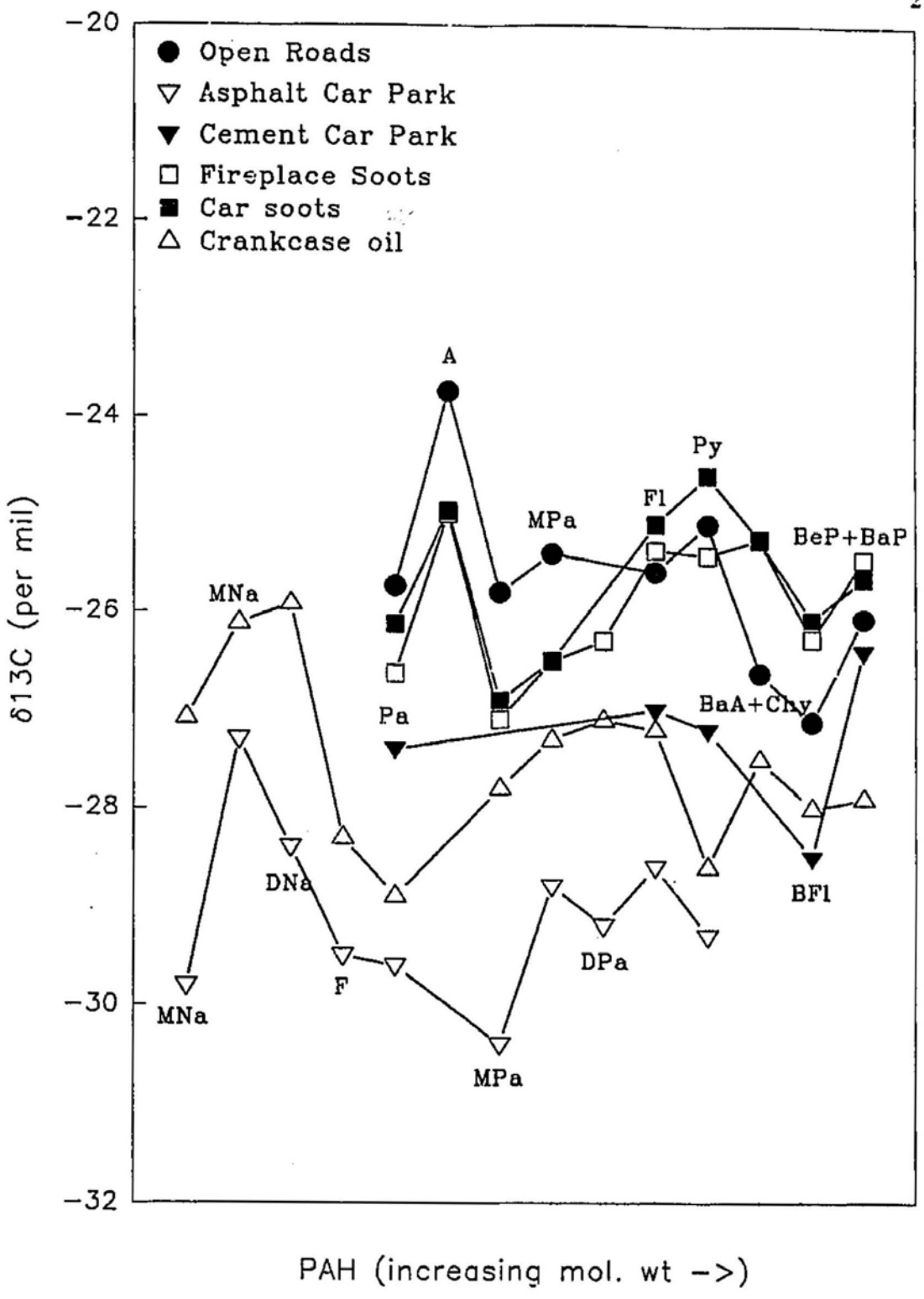
Open Roads
Asphalt Car Park
Cement Car Park
Fireplace Soots
Car soots
Crankcase oil
−20
−22
−24
−26
−28
−30
−32
δ13C (per mil)
A
MPa
Fl
Py
BeP+BaP
MNa
Pa
BaA+Chy
DNa
F
MNa
MPa
DPa
BFl
PAH (increasing mol. wt −>)

molecular signatures (Figure 54). Sampling of these surfaces was conducted after dry and sunny periods, therefore potentially biasing the sampling in favour of extensively photodegraded samples. In the present study, however, Pa was demonstrated to be isotopically stable during photodegradation over short exposure periods. However, photodegradation may be occurring during relatively extended exposure periods on the open-road surfaces. If photodegradation can enrich the $\delta^{13}C$ values of 3-ring compounds, then A and MPa should be more enriched than Pa (as observed) because of the greater susceptibility of A and MPa to photodegradation than Pa (Radding et al., 1976; Ehrhardt et al., 1992; Sanders et al., 1993). As an alternative, the enriched $\delta^{13}C$ values of MPa and A could also be explained by the existence of an uncharacterized source for these 3-ring compounds. One such source, for example, may be weathered road surface asphalt which was also assumed to be a possible PAH contributor to the open-road sweeps based on their molecular signature. Asphalt is recognised to be rich in PAH since PAH produced during the thermal cracking of crude petroleum are normally concentrated in the asphalt fraction (Guerin, 1978; Neff, 1979). Microscopic examination of the road sweep material shows a number of darkened particulates that appeared to be asphalt. Asphalt, was also postulated to account for the dark bitumen like residue (non-hexane soluble, asphaltenes) obtained during extraction of these samples with dichloromethane. This suggests that weathered asphalt may be a possible contributor of PAH to the open-road sweeps.

The $\delta^{13}C$ of Fl and Py are similar to combustion-derived PAH with an apparent Py enrichment which is characteristic of car soot emissions. There is no definitive indicator in the $\delta^{13}C$ values of the PAH in the open-road sweeps to suggest that wood

burning was an important contributor. The absence of retene (wood combustion-derived marker) in the molecular signatures of these open-road sweep samples, suggests that wood burning may not be an important component. Since parental PAH concentrations were generally low in these samples, retene may not have been in sufficient concentrations to be detected. Contributions of minute amounts of wood burning PAH to the open-road sweeps cannot be discounted, since it is widely practised in the city area. The depleted isotopic values of the combined BaA+Chy, BFl and BeP+BaP suggests that the $\delta^{13}C$ of these compounds are also influenced by crankcase oil inputs. Based on the molecular signature of the enclosed asphalt paved car park, crankcase oil contamination is postulated to be the most probable petroleum source likely to influence the $\delta^{13}C$ of open-road sweep PAH. In summary, the overall isotopic signatures of the individual compounds in the open-road sweeps suggests predominant PAH inputs from combustion in 4-ring compounds and a mixture of petroleum and combustion inputs in the 4 and 5-ring compounds. The 3-ring compounds cannot be simply assigned to combustion and petroleum sources (Figure 63).

Since the higher molecular weight compounds (4 and 5-ring) in the open-road sweeps seem to mainly consist of a mixture of the three prominent primary sources, quantitative apportionment of these sources in the open-road PAH can be attempted using mass balance calculations of the form:

$$\delta^{13}C_A = \sum_{k=1}^{n} \delta^{13}C_A^{\,k}\, f_A^{\,k} \qquad \text{(Eq.2)}$$

$$\text{where } \sum_{k=1}^{n} f^{\,k} = 1$$

A = Compound of interest

k = Sources of interest

f = fractional contribution of A from k

With no further constraints, this equation can only be solved uniquely if only two major components are contributing to the mix. For example, we can combine all the combustion sources into a "combustion source " and the petroleum-related sources into a "petroleum source" and uniquely solve the contributions of the two sources in the secondary reservoirs. Take for example, Fl with a mean $\delta^{13}C = -25.6^{o}/_{oo}$ in the open road sweep, the contributions from combustion (80%) and petroleum (20%) was determined using the above equation as follows:

$$\delta^{13}C_{(Fl\ road\ sweep)} = \delta^{13}C_{(Fl\ comb)}(f) + \delta^{13}C_{(Fl\ pet)}(1 - f)$$

$$-25.6 = (-25.25)(f) + (-27.20)(1 - f)$$

$$25.25f\ \ -27.20f = -27.20 + 25.6$$

$$-1.95f = -1.60$$

$$\therefore\ f = 1.60/1.95 = 0.82$$

Note that what we are constraining in each case is the contribution of the particular compound within an individual source and not the overall PAH contribution from that source. Source contributions of PAH can be more accurately assessed if, in addition to the isotopic abundance, the molecular abundance of each compound from each primary source or end-member is included in a two component mixing equation (e.g., Langmuir et al., 1978) The mixing equation of Langmuir et al. (1978) is hyperbolic and has the form:

$$Ax + Bxy + Cy + D = 0 \qquad \text{(Eq. 3)}$$

where x and y are the general variables along the abscissa and ordinate, respectively, and A,B,C and D are the coefficients of the general variables x and y. For ratio-ratio plots, the coefficients of the general equation are described as follows:

$$A = a_2b_1y_2 - a_1b_2y_1$$

$$B = a_2b_1 - a_1b_2$$

$$C = a_2b_1x_1 - a_1b_2x_2$$

$$D = a_1b_2y_1 - a_2b_1y_2$$

For example, if we are mixing Fl and Py in the car soot and crankcase oil end-members then:

$x_1 = \delta^{13}C$ of Fl in car soot

$x_2 = \delta^{13}C$ of Fl in crankcase oil

$y_1 = \delta^{13}C$ of Py in car soot

$y_2 = \delta^{13}C$ of Py in crankcase oil

a_1 = concentration of Fl in car soot

a_2 = concentration of Fl in crankcase oil

b_1 = concentration of Py in car soot

b_2 = concentration of Py in crankcase oil

Using this mixing equation it is assumed that the compounds inputted to a depositional environment from each source is strictly according to the relative abundance of those compounds in the source (i.e., no significant preferential loss or gain prior to deposition). Because of this assumption, calculations will only be performed on the 4 and 5-ring PAH as they have been shown to be more stable in environmental systems. The concentrations of the individual 4 and 5-ring compounds were initially normalized to the total 4 and 5-ring PAH content of their respective source or end-member. Using the

mixing equation, mixing curves were generated for various permutations of the 4 and 5-ring compounds isolated from the three prominent primary sources investigated. Separate mixing curves were defined for the fire soot/crankcase oil and car soot/crankcase oil end-members pairs. For the open-road sweep used in the example above (Fl = -25.6‰; Py = -25.2‰), approximately 20% of the total PAH input can be attributed to crankcase oil inputs.

The results using the "first approach" (Eq. 2) for the open-road sweep samples are summarized in Figure 64 in which the PAH $\delta^{13}C$ values are quantitatively compared to the combined primary "combustion sources" and "petroleum sources". Assuming the primary sources identified are the main contributors of PAH to the open-road sweeps, then from the isotopic signature alone, Fl, Py and BeP+BaP consists of over 80% combustion-derived PAH. BaA+Chy and BFl seem to be strongly influenced by petroleum contributions (up to 60%) even though petroleum sources have been shown in the present study to be relatively depleted in high molecular weight compounds. Petroleum inputs to these samples were indicated from the Pa/A ratio, but its dominance in the higher molecular weight compounds was not apparent from the molecular signature data.

PAH from petroleum-derived sources seem to have a greater influence on the signature of the enclosed cement paved car park (Figure 63). Pa consist of an equal mix of both combustion and petroleum-derived sources, whereas the $\delta^{13}C$ of Fl, Py and BFl appear to be predominantly of petroleum origin. The $\delta^{13}C$ of BeP+BaP is similar to its counterpart isolated from the open-road samples showing a greater influence of combustion-derived sources. Since this is an enclosed car park, it is very likely that car

Figure 64. Apportionment of the contribution of "combustion" and "petroleum "-derived PAH in the individual 4 and 5-ring PAH in the open-road sweep using only the mean isotopic values of the combined combustion and petroleum sources in two component mass balance calculations. Pa = Phenanthrene, A = Anthracene, Fl = Fluoranthene, Py = Pyrene, BaA+Chy = Benz(a)anthracene and Chrysene, BFl = Benzofluoranthenes, BeP+BaP = Benzo(e)pyrene and Benzo(a)pyrene.

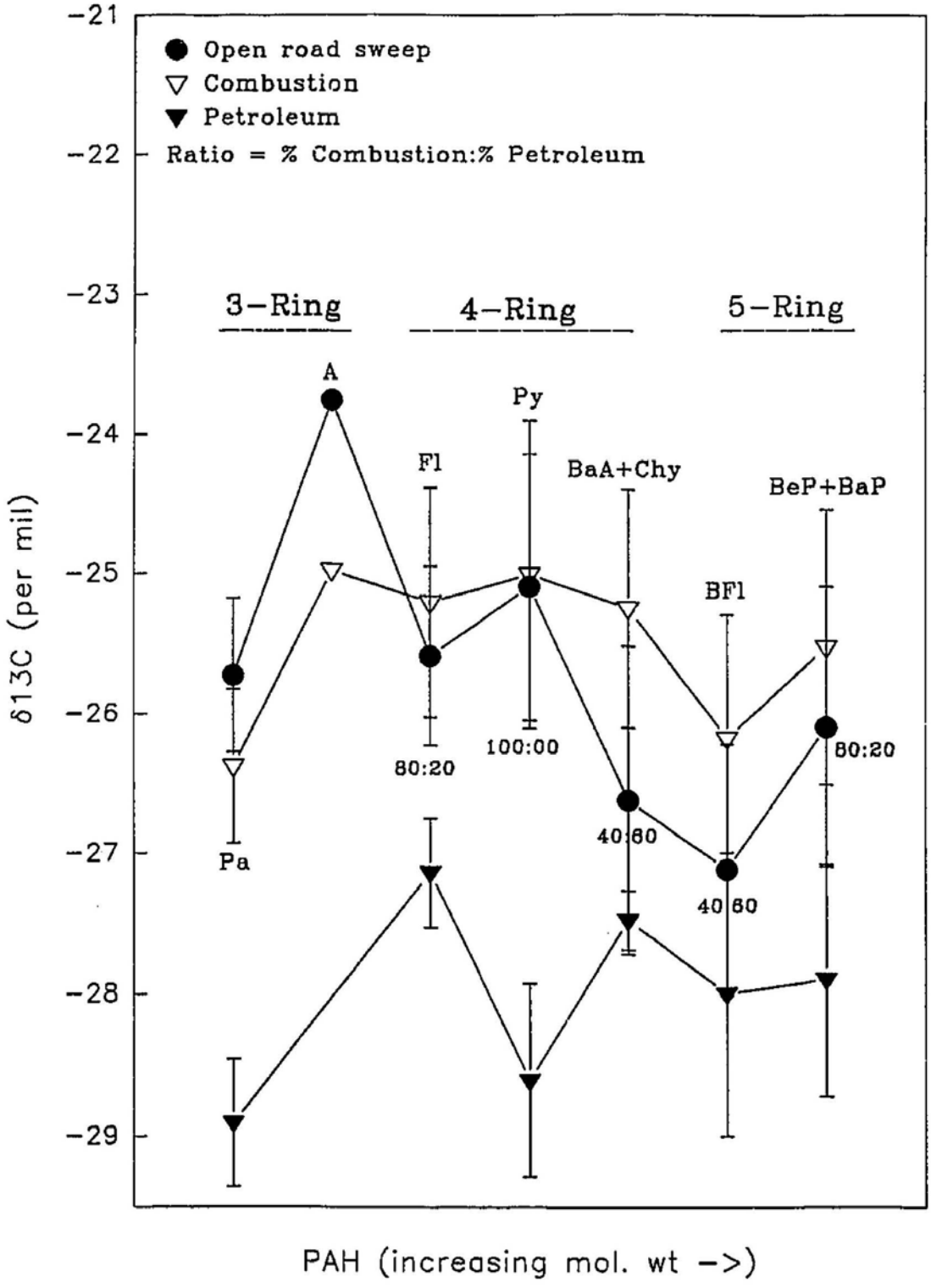
Open road sweep
Combustion
Petroleum
Ratio = % Combustion:% Petroleum
3-Ring
4-Ring
5-Ring
A
Py
Fl
BaA+Chy
BeP+BaP
BFl
Pa
80:20
100:00
40:60
40:60
80:20
δ13C (per mil)
-21
-22
-23
-24
-25
-26
-27
-28
-29
PAH (increasing mol. wt ->)

emissions are the exclusive contributor of BeP+BaP. The significantly depleted $\delta^{13}C$ values of the PAH isolated from the enclosed asphalt paved car park can be fully reconciled with petroleum-derived contributions (Figure 63). The $\delta^{13}C$ values are significantly lighter than the mean values of crankcase oils but are within the range observed for single source samples.

The results of the "second approach" (Eq. 3) are broadly consistent with those obtained using (Eq. 2) with an overall mean input of crankcase oil to the open-road sweep samples of approximately 30% from the various mixing permutations of the 4 and 5-ring compounds. Since open-roads are frequently washed due to rainfall, they are considered to be a temporary repository for PAH deposits and this affect may account for the variability observed in the molecular and isotope signatures. The combustion PAH seem to be mainly derived from car emissions based on the mean values of the 4 and 5-ring compounds plotting either on or close to the car soot/crankcase oil mixing curve.

4.7.2 Sewage:

Similar to the molecular signature data, the overall $\delta^{13}C$ of the PAH in untreated sewage samples were similar to the open-road sweeps (Figure 62). A distinct predominance of combustion products is indicated by Pa and A being more enriched than their counterparts in the primary combustion sources (Figure 62). Based on the mass balance calculation (Eq. 2), Fl and Py consisted of over 90%, BaA+Chy and BFl over 80% and BeP+BaP 65% combustion-derived. However, unlike the open-road sweeps, Py in the sewage samples was more depleted than Fl indicating a possible petroleum influence. The input of petroleum was confirmed using Eq. 3 where the overall input of

crankcase oil to the sewage was determined to be approximately 20%, whereas the combustion PAH seemed to be derived from both fire and car emissions. The dominance of combustion PAH in the sewage suggests that these compounds are continually being flushed to the storm sewers from the open-road surfaces due to rainfall where they combine with domestic sewage prior to discharge (Hoffman et al., 1984; Broman et al., 1988; Wild and Jones, 1993). Interestingly, the sewage itself does not appear to contribute PAH that could have significantly altered the road sweep signature. Road sweep inputs to the sewers are also apparent from the magnitude of the UCM which was similar for both the open-road sweep and sewage samples.

4.7.3 Snow:

Similar to open road sweeps and sewage samples, the $\delta^{13}C$ values of high molecular weight PAH in bulk snow were isotopically depleted compared to lower molecular weight compounds (Figure 62). Pa in snow was enriched more enriched in ^{13}C than Pa in the prominent primary sources and the $\delta^{13}C$ values of Fl, Py, BaA+Chy and BFl are potentially related to a combination of these sources. Using Eq. 2, over 90% of Fl and Py are of combustion origin, while BaA+Chy and BFl comprise of 25 and 55% combustion-derived sources, respectively. As was also observed for the open-road sweep samples, the influence of petroleum on these high molecular weight compounds was not reflected in the BaA/Chy and BaP/BeP compositional ratios (molecular signatures).

Similar estimates of PAH origin can be drawn from the use of Eq. 3 where the mean input of crankcase oil was estimated to be approximately 30%. The mean values of the high molecular weight compounds plot closer to the crankcase oil end-member,

indicating the dominance of crankcase oil in these compounds and similar to the sewage the combustion contributions seem to comprise of a combination of both fire and car soot emissions.

4.7.4 Summary of secondary isotopic signatures:

CSIA of the individual PAH in secondary sources allows for the determination of relative contributions of "combustion" and "petroleum"-derived PAH to be quantitatively estimated using simple two component mass balance calculations. These calculations indicate that Fl and Py in all three sources (open-road, sewage and snow) and BaA+Chy, BFl and BeP+BaP in sewage seem to be predominantly of "combustion origin". In contrast, BaA+Chy, BFl and BeP+BaP in open-road sweeps and composite snow samples are influenced primarily by "petroleum" inputs. The relative proportion of combustion and petroleum derived-PAH in the secondary sources indicate that the individual compounds from the primary sources have specific pathways and modes of degradation that are preferentially undergone prior to deposition. Their physical and chemical characteristics dictate the pathway they follow and their susceptibility to degradation reactions. In contrast to Eq. 2, the overall contribution of PAH to the secondary sources from the three prominent primary sources investigated can be further elucidated using a combination of the carbon isotope and molecular abundance data in two component Langmuir mixing calculations (Eq. 3). Using both equations, greater crankcase oil contributions were identified in the PAH of the open-road sweeps and roadside snow samples compared to the sewage samples. The combustion PAH in the open-road sweeps seem to be mainly derived from car emissions whereas, inputs from both fire and car

emissions are implicated for the roadside snow and sewage samples

Although, only a limited number of sewage and snow samples were analyzed, the overall isotopic signatures of the three secondary sources were comparable. The similarity in the $\delta^{13}C$ values was also reflected in their respective molecular signatures where all sources were characterized by the presence of 3, 4 and 5-ring parental PAH and a prominent UCM. However, the prominent petroleum influence in the high molecular weight compounds of the open-road sweeps and composite snow sample was not evident in the compositional ratios of their respective molecular signatures. The dominance of combustion-derived PAH in the untreated sewage samples, suggests the continual flushing of these compounds from road surfaces to the sewer system and sewage itself does not seem to influence the $\delta^{13}C$ of road runoff PAH. The $\delta^{13}C$ of Pa, MPa and A seem to be influenced by weathering or by contributions of these 3-ring compounds from an uncharacterized source. The use of the molecular signature and carbon isotope data was found to be highly complementary in elucidating specific primary PAH sources in secondary reservoirs. The advantages of carbon isotope analysis is highlighted in where the contribution of "combustion" and "petroleum"-derived sources can be quantitatively estimated for the individual compounds in the various secondary source samples. Also, the overall PAH contribution from the prominent primary sources can be more accurately quantified using a combination of the carbon isotope and molecular abundance data in two component mass-balance calculations.

4.8 Source apportionment of PAH in St. John's Harbour

4.8.1 Molecular signatures:

The molecular signature of the surface and deeper sediments in St. John's Harbour is characterized by varying concentrations of 3, 4 and 5-ring parental PAH (Figure 61). irrespective of the range in PAH concentrations, the relative distribution of these compounds is indicative of high temperature combustion (Laflamme and Hites, 1978; Lake et al., 1979; Wakeham et al., 1980a; Gschwend and Hites, 1981; Prahl and Carpenter, 1983; Boehm and Requejo, 1986; Killops and Howell, 1988; Brown and Maher, 1992). Also, the molecular signatures were characterized by the presence of methylated-PAH and a UCM indicating possible petroleum inputs (Dastillung and Albrecht, 1976; Boehm and Farrington, 1984, Socha and Carpenter, 1987; Kennicutt II et al., 1991; Kennicutt II et al., 1992; Volkman et al., 1992). Finally, the presence of retene and perylene which may be either anthropogenic or diagenetic (early) in nature was also identified (Wakeham et al., 1980b; Tissier and Saliot, 1983; Venkatesan, 1988; Colombo et al., 1989; Lipiatou and Saliot, 1992). In summary, the molecular signature of the St. John's Harbour sediments suggests PAH contributions from at least three potential sources: combustion, petroleum and possibly diagenesis.

In order to compare the PAH concentrations inside and outside the Harbour, the concentrations of the individual compounds were normalized to the mean total organic carbon content (TOC) recorded for samples inside (TOC: 11%) and outside (TOC: 0.5%) the Harbour. After normalization to TOC, higher PAH concentrations inside the Harbour were recorded in samples close to the sewage outfalls, and thus seem to be related to their

proximity to the various input sources. PAH concentrations outside the Harbour were lower, indicating that PAH rich sediments are trapped inside the Harbour or that the sediments outside the Harbour are diluted with PAH-poor particulates. The concentration of the individual parental PAH were generally greater than the methylated compounds and based on the results from Core 18 (sampled inside the Harbour), concentrations generally decreased with depth with the exception of a slight increase occurring at approximately at 20 cm (Figure 44).

Compositional ratios of the prominent PAH in the surface and deeper samples are summarized in Figure 65. Mean surface sample ratios are compared to the values of the primary and secondary sources investigated in the present study in Figure 54. The relatively low Pa/A ratio (1.9) in the surface sediment, which is indicative of significant combustion contributions, is similar to those calculated in previous studies (Table 18; Larsen et al., 1983; Killops and Howell, 1988; Brown and Maher, 1992). Low Pa/A ratios in sediments have been previously attributed to solubility and reactivity differences where Pa is approximately 20 times more soluble than anthracene in natural aqueous environments (Lake et al., 1979; Readman et al., 1982; Sporstol et al., 1983). Despite this difference in solubility, these compounds are still extremely hydrophobic and the relatively low Pa/A ratios (i.e., lower than the mean combustion ratios) is probably related to mixing of different combustion sources since Pa/A ratios as low as 1.4 have been recorded in a number of the car soot samples in the present study. The Fl/Py ratio (1.2), again a prominent indicator of combustion, is comparable to the Fl/Py ratios reported for sediments from other similar systems (e.g., Penobscot Bay, Boston Hbr., Severn Estuary,

Figure 65. Mean and range (standard deviation; 2σ) of compositional ratios of the prominent PAH in the surface and deeper samples of St. John's Harbour and Conception Bay.

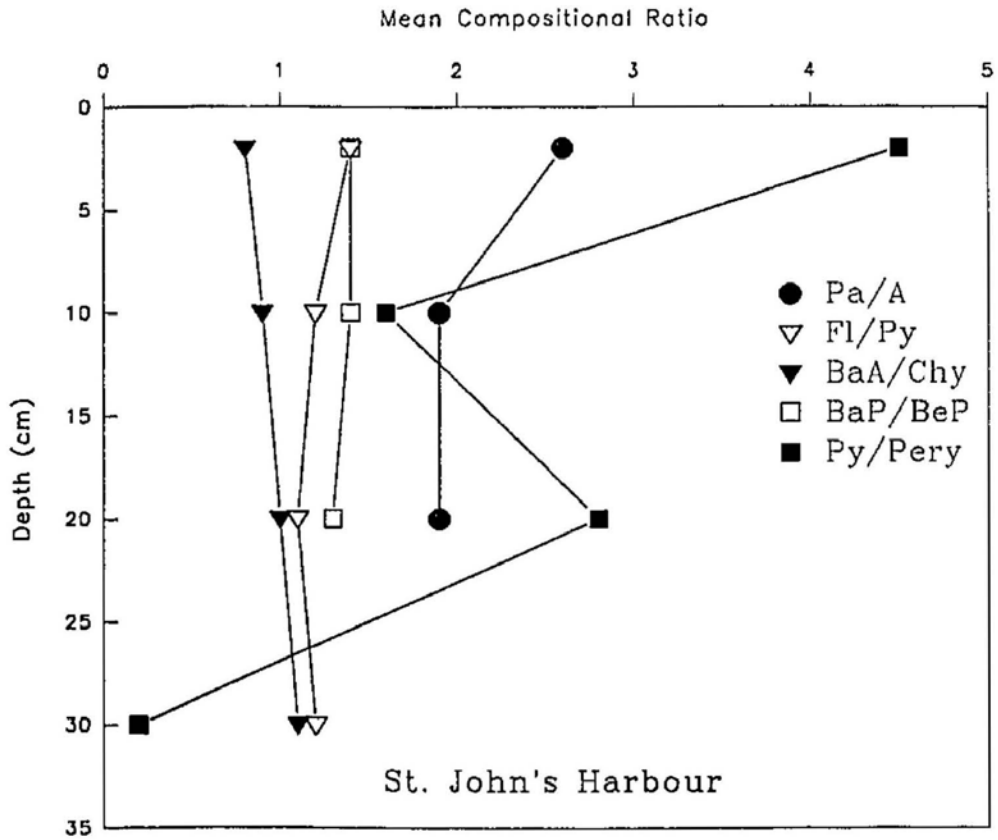
Mean Compositional Ratio
0
1
2
3
4
5
Depth (cm)
0
5
10
15
20
25
30
35
Pa/A
Fl/Py
BaA/Chy
BaP/BeP
Py/Pery
St. John's Harbour

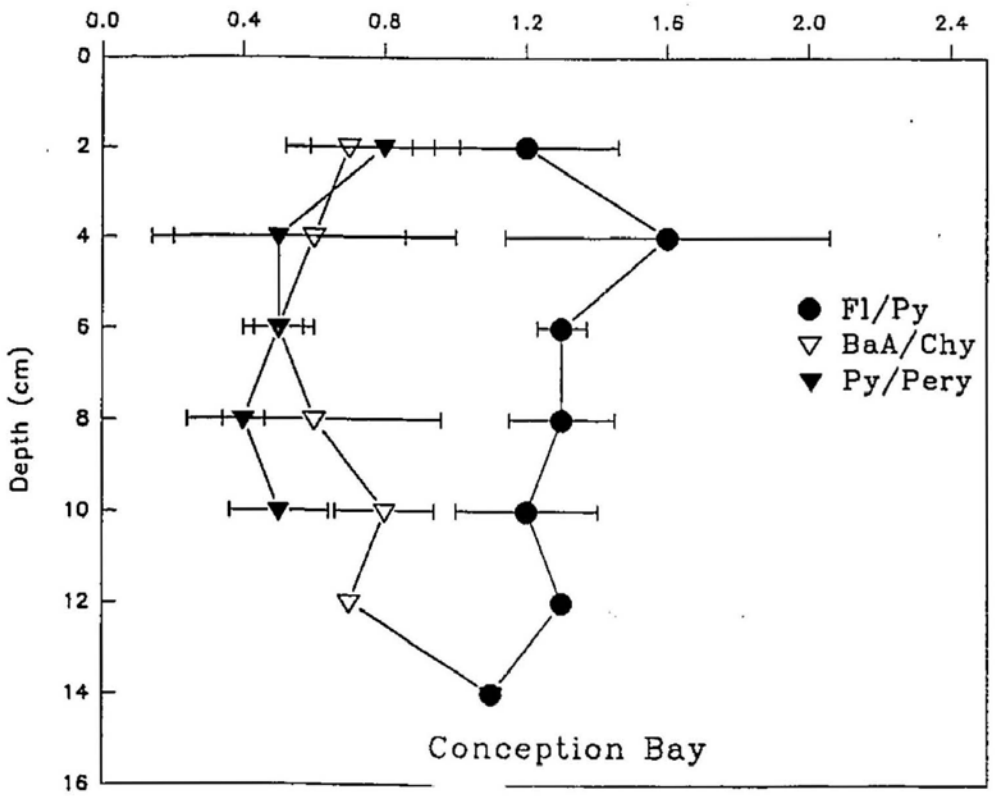
0.0
0.4
0.8
1.2
1.6
2.0
2.4
Depth (cm)
0
2
4
6
8
10
12
14
16
Fl/Py
BaA/Chy
Py/Pery
Conception Bay

Table 18. A comparison of the reported compositional ratios for a range of PAH isolated from surface sediments with the mean values obtained for St.John's Harbour and Conception Bay.

Study Site	Pa/A	Fl/Py	BaA/Chy	Reference
Severn Estuary	2.9	1.2	0.7	*Killops & Howell (1988)*
Severn Estuary	3.8	1.6	1.1	
Severn Estuary	-	1.2	-	
Tamer Estuary	3.9	0.9	0.8	*Readman et al. (1986)*
Wash. State	3.8	1.0	-	*Prahl & Carpenter (1983)*
Puget Sound	4.0	0.9	0.6	*Bates et al. (1984)*
Puget Sound	4.5	0.9	0.6	
Penobscot Bay	0.8	1.3	1.1	*Johnson et al. (1985)*
Puget sound	-	1.0	-	*Socha & Carpenter (1987)*
Med. (West)	5.9-10.6	1.6	0.4	*Lipiatou & Saliot (1991)*
Casco Bay	2.6	0.8	0.9	*Larsen et al. (1983)*
Penobscot Bay	5.1	6.9-9.7	0.9	*Johnson et al. (1985)*
Elizabeth	-	1.5	0.6	*Bieri et al. (1986)*
Boston Harbour	125.6	1.3	-	*Shiaris et al. (1986)*
Chesapeake Bay	-		0.8	*Foster & Wright (1988)*
Chesapeake Bay	-	0.8-3.5	0.6	*Huggett et al. (1988)*
Bedford Harbour	3.6-6.1	1.1	1.1	*Pruell et al. (1990)*
Halifax Harbour	4.1	1.2	0.9	*Gearing et al. (1991)*
Australia	2.5-3.6	0.9-0.3	-	*Maher & Aislabie (1992)*
Georges River	1.7	0.9	1.3	*Brown and Mahar (1992)*
Gulf of Mexico	3.5	1.0	0.7	*Brooks (1990)*
St. John's Harbour	1.9	1.2	0.8	*Present Study*
Conception Bay	-	1.2	0.7	*Present Study*

Bedford Hbr. and Halifax Hbr. (Table 18; Johnson et al., 1985; Shiaris and Jambard-Sweet, 1986; Killops and Howell, 1988; Pruell et al, 1990; Gearing et al., 1991). However, the Fl/Py ratios of the St. John's Harbour sediments cannot be conclusively related to either of the two primary combustion sources. The mean ratios of the fire and car soot samples suggest possible contributions from both of these prominent combustion sources. Similarly, the BaA/Chy ratio (0.80) also indicates that BaA and Chy are of combustion origin. However, unlike Fl and Py, the generally higher BaA/Chy ratio suggests that the primary source of these particular compounds may be related to car emissions. The BaP/BeP and the Pa/MPa ratios of the sediment cannot be clearly reconciled with any of the primary source signatures. This could indicate that these ratios have limited value for source apportionment because of the reactivity of BaP and methylated Pa in the environment (Kamens et al., 1988; Canton and Grimalt, 1992; Ehrhardt et al., 1992). In summary, the compositional ratios of the prominent compounds suggest that the PAH in St. John's harbour sediments are predominantly of combustion origin, with possible evidence from the Pa/A and BaA/Chy ratios to specifically support car soot inputs. The reactivity of MPa and BaP seems to have resulted in the alteration of their source compositional ratios during transportation and therefore may not be a reliable source indicator.

In addition to the compositional attributes of the parental PAH, the presence of methylated compounds and a UCM in the surface sediments indicates possible petroleum inputs of PAH to the Harbour. The UCM is generally indicative of petroleum and petroleum products, and is a widely used indicator of petroleum contamination in

sediments (Simoneit and Kaplan, 1980; Barrick et al., 1980; Prahl and Carpenter, 1983; Volkman et al., 1992). It is commonly assumed that a UCM consists primarily of an accumulation of multi-branched structures that are formed as a result of biodegradation reactions (Killops and Juboori, 1990; Volkman et al., 1992). Since no clear indication of petroleum-derived inputs can be discerned from the compositional ratios of the prominent PAH in the sediments, it is concluded that the compositional ratios of prominent petroleum PAH are masked by combustion-derived components. Also, the absence of a clear petroleum signature in the Harbour sediments may be due to preferential degradation because of the reported weak association of petroleum compounds with particulates (Prahl and Carpenter, 1984; Maher and Aislabie, 1992).

Retene and perylene, which can have either a diagenetic or anthropogenic origin were also identified in the surface sediments. Retene is usually derived from the transformation of diterpenoids with an abietane skeleton, such as dehydro-abietic acid (Figure 4). This transformation can occur either by early diagenesis in the sediment (Wakeham, et al., 1980b, Tan and Heit, 1981) or through the thermal degradation of wood resins during combustion (Ramdahl 1983a). The presence of retene in varying quantities in all surface sediments, and its conspicuous absence in the prominent secondary sources (road sweep and sewage samples) suggests that it was primarily derived by *in-situ* early diagenesis. Perylene, a pentacyclic unsubstituted PAH, was also found in most of the surface samples. The origin of perylene is controversial with both natural and anthropogenic sources proposed (Prahl and Carpenter, 1979; Colombo et al., 1989; Tissier and Saliot, 1983; Saliot et al., 1988; Venkatesan, 1988; Lipiatou and Saliot, 1992).

Tissier and Saliot (1983) reported that a perylene contribution of more than 10% to the total unsubstituted PAH in sediments is indicative of a diagenetic origin. Since perylene only accounts for 2 to 3% of the total unsubstituted PAH, it may be derived from anthropogenic inputs. The origin of perylene has also been traced using the Py/Pery ratio where values greater than one are indicative of anthropogenic origin and values less than one are associated with diagenetic production (Lipiatou and Saliot, 1992). The mean Py/Pery ratio for the St John's Harbour surface sediments is significantly greater than unity, therefore supporting anthropogenic contributions of perylene. However as was also observed by Wakeham et al. (1980b), in the deeper samples of Core 18, the Py/Pery ratio decreased indicating that perylene is also diagenetically produced (Figure 65). Since only one core was analyzed in this study, further analysis of other cores would confirm this observation.

With the exception of Py/Pery (discussed previously), the compositional ratio of the prominent PAH did not vary significantly in the top 30 cm of Core 18 (Figure 65). This suggests either the PAH input sources have not drastically changed or the concentrations are not being altered due to weathering reactions. Samples greater than 30 cm deep were not investigated since the concentration of the individual compounds of interest were generally low and our initial sediment sample sizes were not adequate to allow isotopic measurements to be performed.

Secondary sources were investigated to elucidate pathways by which PAH are deposited in the Harbour sediments. The compositional ratios (Pa/MPa, Fl/Py and BaA/Chy) and the relative contributions of 4 and 5-ring PAH in the Harbour are similar to the road sweep, sewage and snow samples (Figure 54). This suggests that surface

runoff and runoff via the sewer system and snow inputs are the predominant pathways for PAH deposition in the sediments. The lower PAH concentrations outside the Harbour also support this observation. Several studies have identified surface runoff, due to elevated precipitation, as an important mechanism for PAH deposition in coastal environments (Hoffman et al., 1984; Broman et al., 1988; Latimer et al., 1990; Evans et al., 1990; Naf et al., 1992). Snow, with the ability to concentrate both combustion and petroleum PAH, is also an important pathway for PAH deposition both through direct dumping in the winter and snow melting in the spring (Boom and Marsalek 1988; Pham et al., 1993). Preliminary investigations of PAH concentrations in atmospheric particulates from the St. John's area indicate that concentrations are generally very low, and are therefore unlikely to be a major pathway for direct PAH deposition in the Harbour. However, dry and wet deposition of atmospheric particulates into the watershed emptying into the Harbour can be indirectly important, as indicated by the wood burning signature detected in the sewage and snow samples.

4.8.2 Carbon Isotope Signature:

There is no characteristic trend in the $\delta^{13}C$ between the low and high molecular weight PAH in the surface and deeper sediments of St. John's Harbour. However, the isotopically enriched A and the trend between Pa and MPa suggests combustion-derived PAH whereas the marginally depleted Py compared to Fl suggest inputs of petroleum sources. As observed for the secondary source signature, the mean isotopic values of Pa, MPa and A are more enriched than their counterparts in the primary source samples. This was attributed to either a contribution from an uncharacterized source or isotopic shifts

due to extensive photolytic degradation of these compounds. However, the isotopic signatures of these 3-ring compounds in the sediment, appear to have been simply inherited from the secondary sources. Interestingly, variations between the individual isotopic values of the PAH in the sediments were significantly less than observed for the corresponding compounds in the primary sources. As observed for the molecular signatures, there was no systematic change in the $\delta^{13}C$ with increasing depth (Figure 46). Also, there was no apparent seasonal difference in the $\delta^{13}C$ values of the PAH isolated from the samples collected during fall '92 and summer '93. This suggests that the sediments are isotopically well mixed or there is very little temporal variability in the isotopic value of the combined primary source inputs.

The isotopic signature of the PAH from all the surface samples are broadly similar and can be quantitatively related to the prominent primary sources investigated in the present study (Figure 66). Significant enrichments of Pa, MPa and A relative to the 4 and 5-ring compounds were consistently observed in all the individually analyzed samples. This may be attributed to the input of road sweep material, via the sewer system which was demonstrated in the present study to be an important source of these isotopically enriched 3-ring compounds. Road sweep inputs to the Harbour were also recognised as an important pathway for PAH deposition, based on the compositional ratios of the secondary sources. The consistency in the $\delta^{13}C$ of Pa (-25.9‰ to -25.2‰) in the surface sediments suggests that it is possibly derived from an isotopically enriched source rather than from some alteration reaction. In this study, Pa has been shown to be photostable and if degradation was occurring in the water column and sediments, it is unlikely that

Figure 66. Comparison of the 3-ring parental and methylated PAH and the 4 and 5-ring parental compounds in the surface sediments of St. John's harbour with the three prominent primary sources. Also included is the relative contribution of "combustion" and "petroleum"-derived PAH. Pa = Phenanthrene, A = Anthracene, MPa = Methyl Phenanthrene, Fl = Fluoranthene, Py = Pyrene, BaA+Chy = Benz(a)anthracene and Chrysene, BFl = Benzofluoranthenes, BeP+BaP = Benzo(e)pyrene and Benzo(a)pyrene.

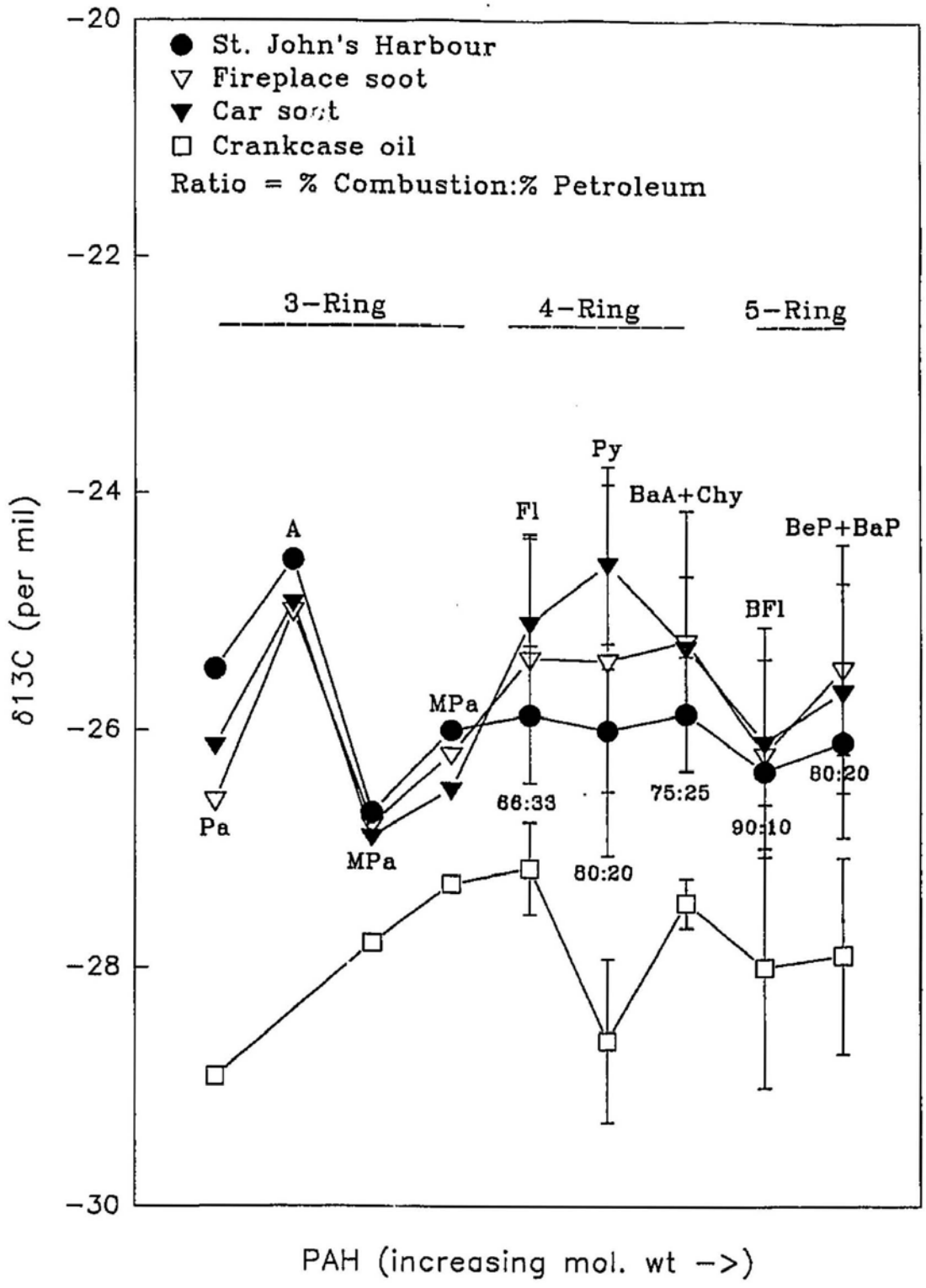
St. John's Harbour
Fireplace soot
Car soot
Crankcase oil
Ratio = % Combustion:% Petroleum
3-Ring
4-Ring
5-Ring
−20
−22
−24
−26
−28
−30
δ13C (per mil)
Pa
A
MPa
MPa
Fl
66:33
Py
80:20
BaA+Chy
75:25
BFl
90:10
BeP+BaP
80:20
PAH (increasing mol. wt ->)

it would be altered to the same degree in all samples, because of the varying water and sediment characteristics in the Harbour. Isotopic fractionations due to Pa solubility are also unlikely as shown by the microbial experiments in an aqueous media. In summary, in spite of the enriched $\delta^{13}C$ of Pa, MPa and A in the surface sediment, the absolute $\delta^{13}C$ values of these 3-ring compounds suggest a dominant combustion origin. Evidence of petroleum contamination is indicated by the relatively depleted pyrene, a trend which was consistently observed in most of the samples investigated.

As previously described in section 4.7.1, quantitative apportionment of the higher molecular weight parental compounds (4 and 5-ring) can be undertaken using two-component mass balance calculations. The mass balance calculation using Eq. 2 constrains fractions contributed by the "combustion" and "petroleum" components to the individual compounds, rather than the total PAH contribution of the source. The results using this approach suggest that contributions from petroleum sources are greater than what was originally suggested by the molecular signatures (Figure 66). The $\delta^{13}C$ of Fl, Py, BaA+Chy and BeP+BaP requires over 20% petroleum-derived PAH while the $\delta^{13}C$ of BFl is dominated by combustion inputs (90%).

A more effective approach to apportioning the primary source inputs to the total PAH inventory of the Harbour sediments was described earlier (Eq. 3). The results of the various mixing permutations performed using the 4 and 5-ring parental PAH in the prominent primary sources are summarized in Figures 67-71, along with the mean and individual $\delta^{13}C$ of the PAH isolated from the surface and deeper sediment samples. The error bars represent the natural range of isotopic values (1σ) observed for that particular

Figure 67. Fluoranthene (Fl) and pyrene (Py) $\delta^{13}C$ values of the individual sediment samples from St. John's Harbour plotted on the mixing curves generated by mixing the $\delta^{13}C$ and the normalized concentrations of these compounds in the prominent primary sources. Error bars represent the range (1σ) observed in the single and composite samples of these sources. Letters represents the sample sites sampled in St. John's Harbour (see Figure 10)

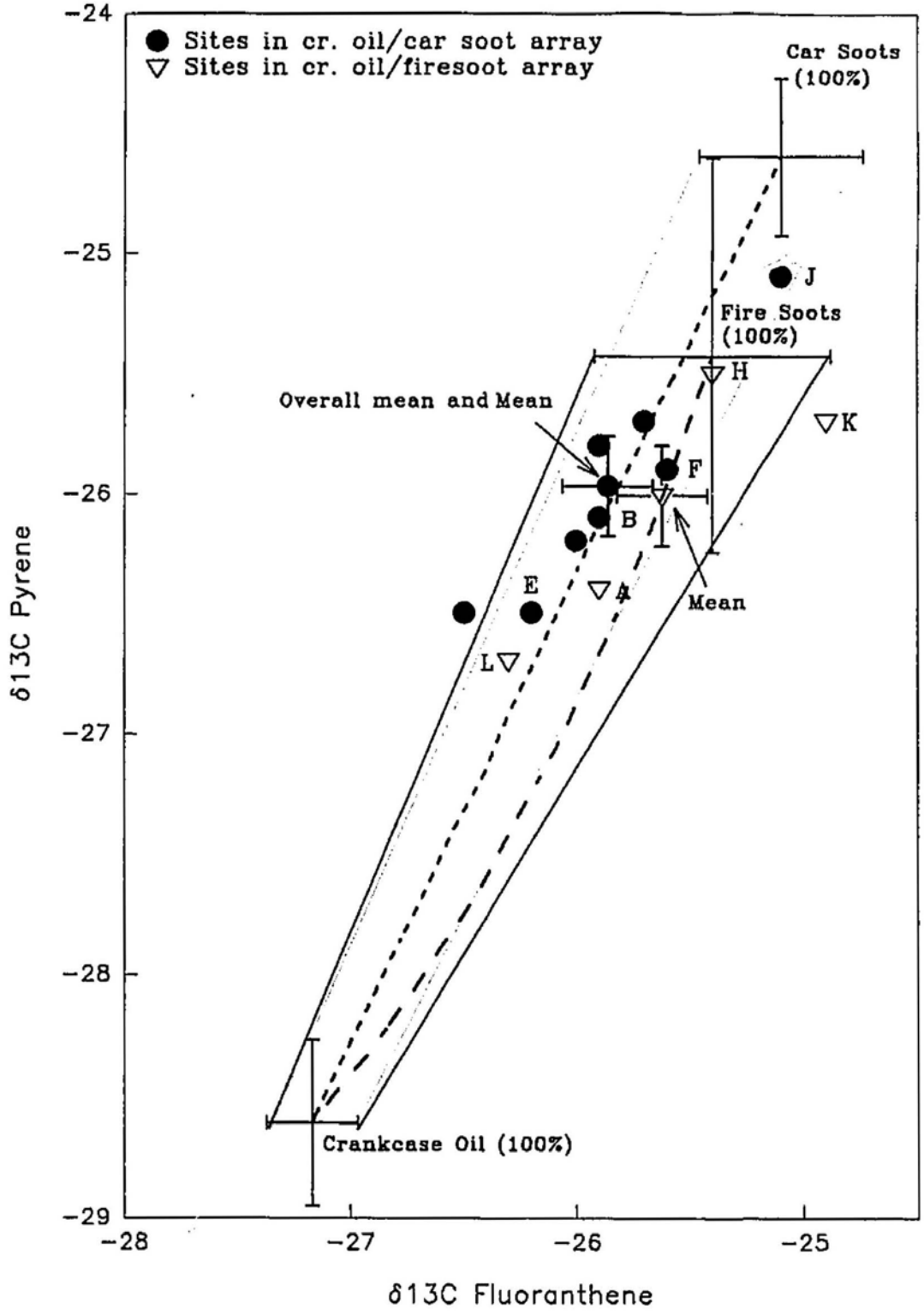
Sites in cr. oil/car soot array
Sites in cr. oil/firesoot array
Car Soots (100%)
Fire Soots (100%)
Crankcase Oil (100%)
Overall mean and Mean
Mean
J
H
K
F
B
E
A
L
−24
−25
−26
−27
−28
−29
−28
−27
−26
−25
δ13C Pyrene
δ13C Fluoranthene

Figure 68. Pyrene (Py) and combined benz(a)anthracene+chrysene (BaA+Chy) $\delta^{13}C$ values of the individual sediment samples from St. John's Harbour plotted on the mixing curves generated by mixing the $\delta^{13}C$ and the normalized concentrations of these compounds in the prominent primary sources. Error bars represent the range (1σ) observed in the single and composite samples of these sources. Letters represents the sample sites sampled in St. John's Harbour (see Figure 10)

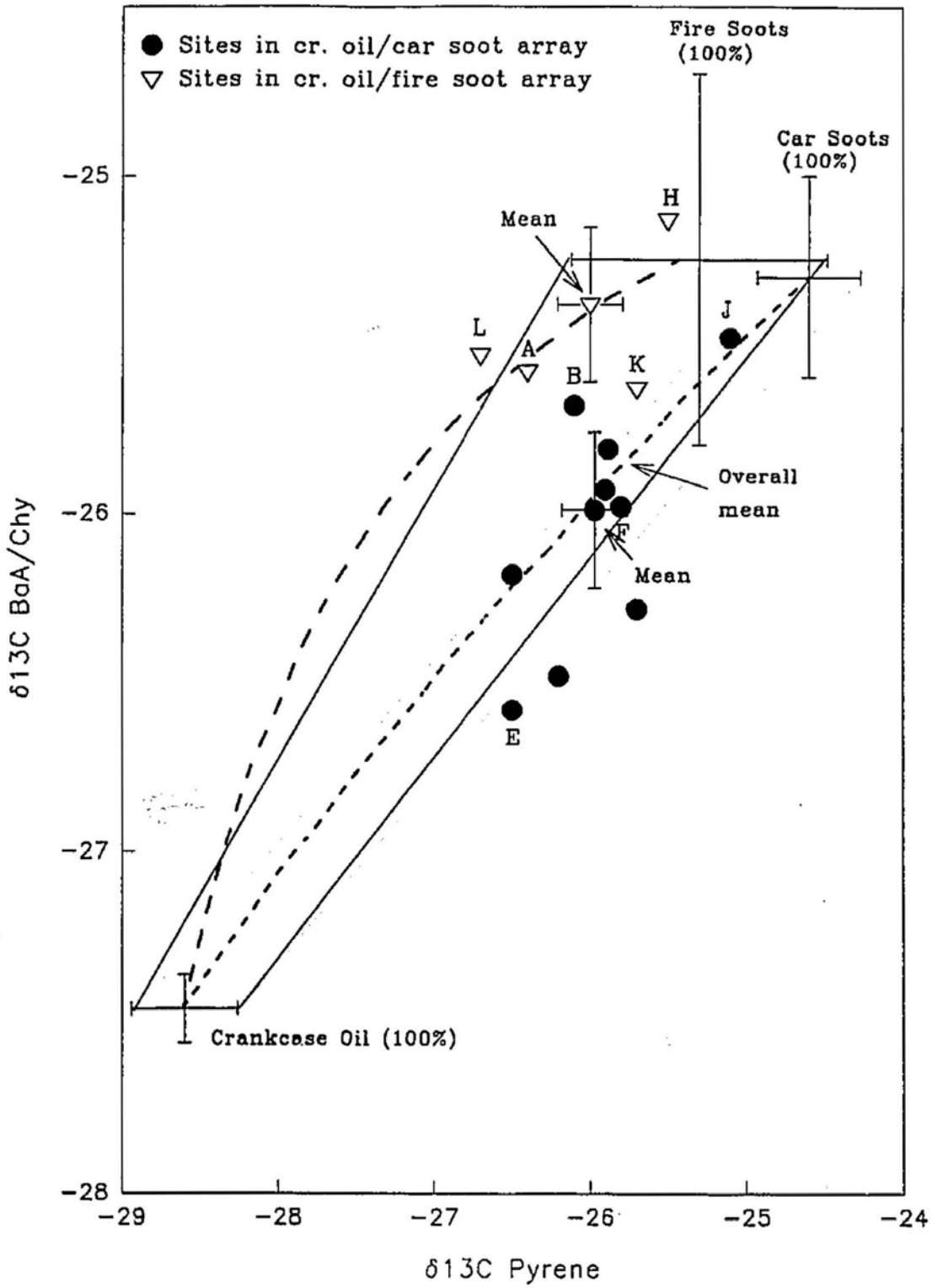
Sites in cr. oil/car soot array
Sites in cr. oil/fire soot array
Fire Soots (100%)
Car Soots (100%)
Mean
H
L
A
B
K
J
Overall mean
F
Mean
E
Crankcase Oil (100%)
δ13C BaA/Chy
δ13C Pyrene
−25
−26
−27
−28
−29
−28
−27
−26
−25
−24

Figure 69. Pyrene (Py) and combined benzo(e)pyrene+benzo(a)pyrene (BeP+BaP) $\delta^{13}C$ values of the individual sediment samples from St. John's Harbour plotted on the mixing curves generated by mixing the $\delta^{13}C$ and the normalized concentrations of these compounds in the prominent primary sources. Error bars represent the range (1σ) observed in the single and composite samples of these sources. Letters represents the sample sites sampled in St. John's Harbour (see Figure 10)

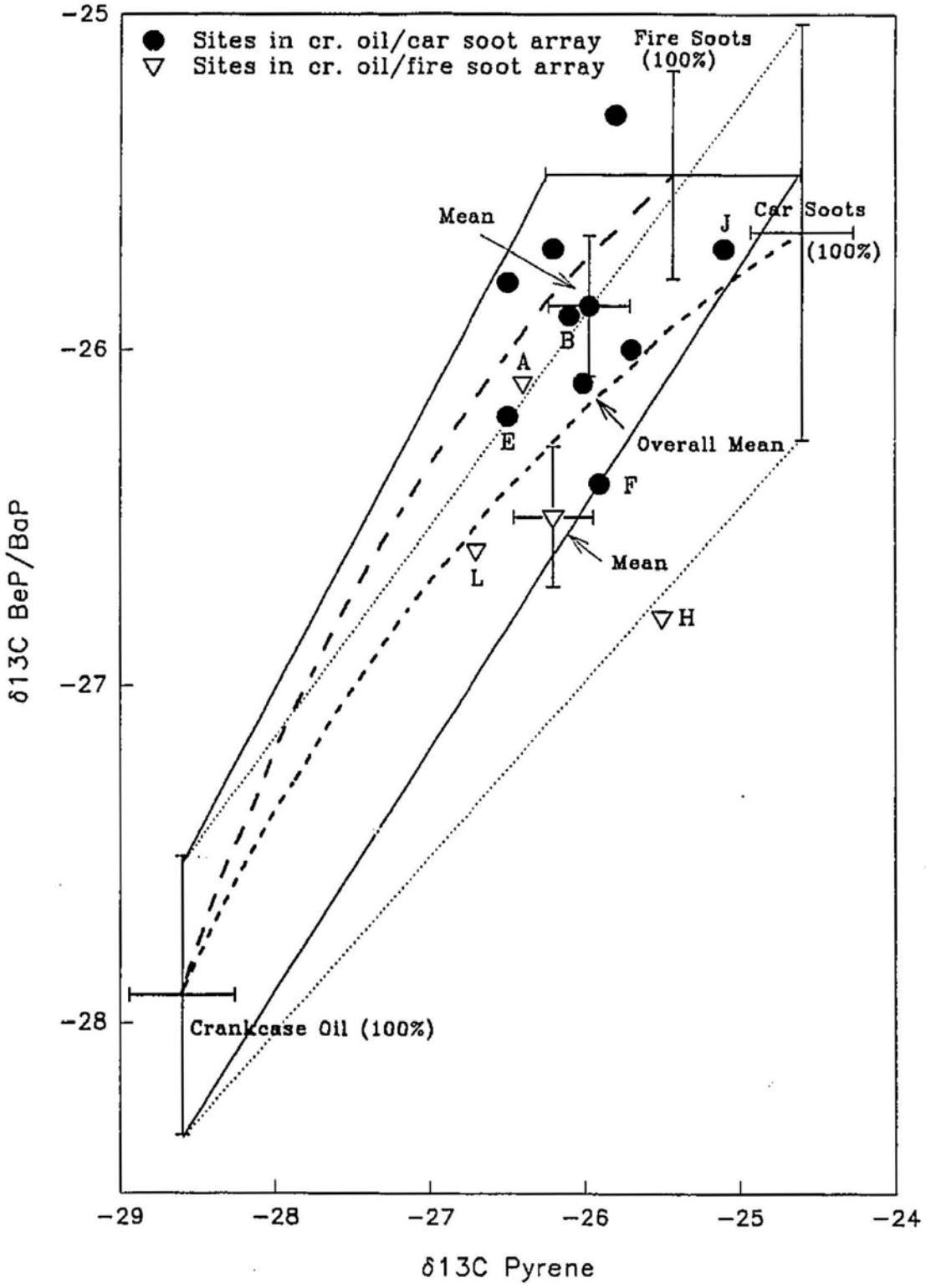
Sites in cr. oil/car soot array
Sites in cr. oil/fire soot array
Fire Soots (100%)
Car Soots (100%)
Mean
Overall Mean
Mean
Crankcase Oil (100%)
A
B
E
F
H
J
L
−25
−26
−27
−28
−29
−28
−27
−26
−25
−24
δ13C BeP/BaP
δ13C Pyrene

Figure 70. Combined benz(a)anthracene+chrysene (BaA+Chy) and benzo(e)pyrene+benzo(a)pyrene (BeP+BaP) $\delta^{13}C$ values of the individual sediment samples from St. John's Harbour plotted on the mixing curves generated by mixing the $\delta^{13}C$ and the normalized concentrations of these compounds in the prominent primary sources. Error bars represent the range (1σ) observed in the single and composite samples of these sources. Letters represents the sample sites sampled in St. John's Harbour (see Figure 10)

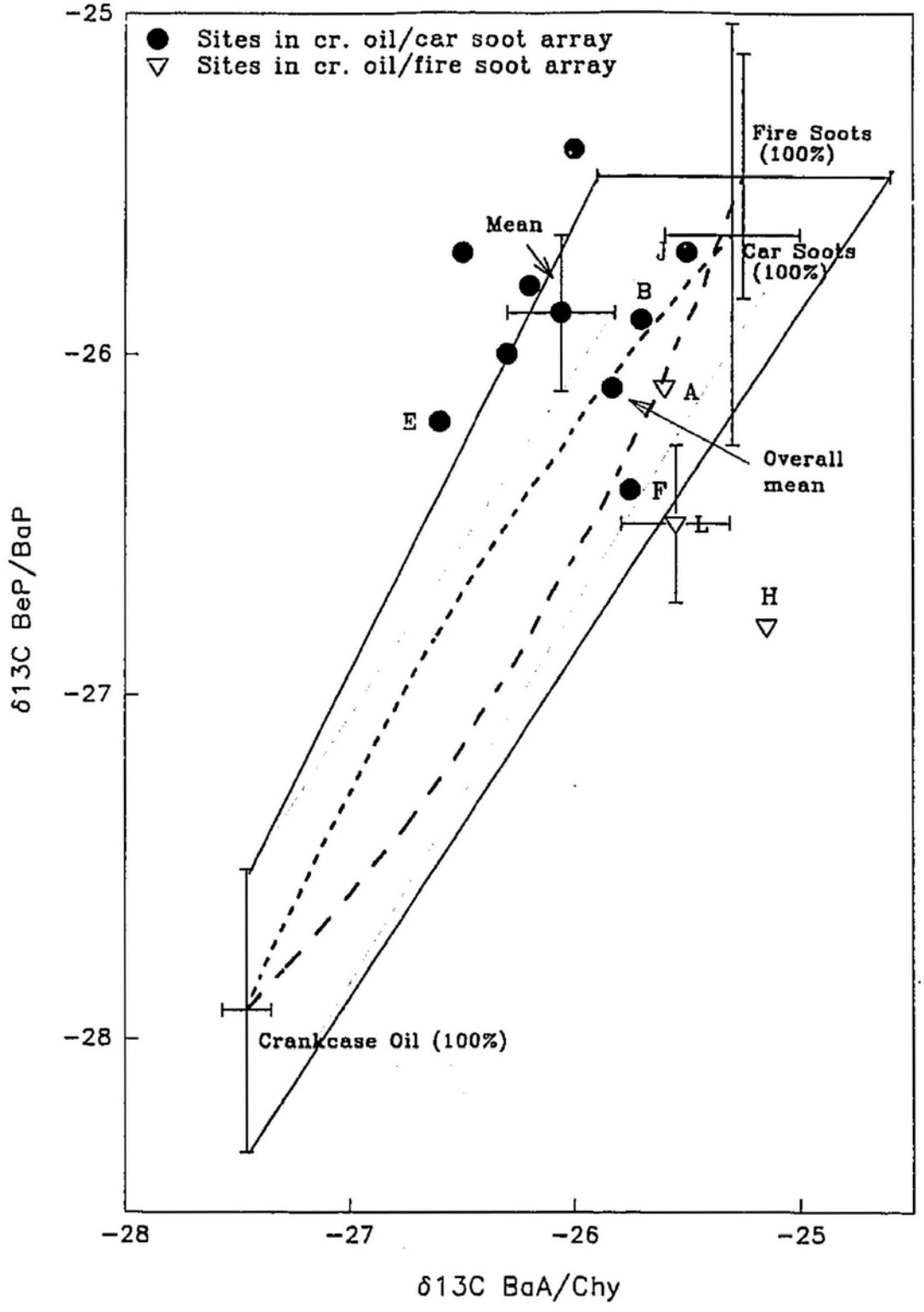
Sites in cr. oil/car soot array
Sites in cr. oil/fire soot array
Fire Soots (100%)
Car Soots (100%)
Mean
Overall mean
Crankcase Oil (100%)
A
B
E
F
H
J
L
−25
−26
−27
−28
−28
−27
−26
−25
δ13C BeP/BaP
δ13C BaA/Chy

Figure 71. Pyrene (Py) and the benzo(b)fluoranthene (BFl) $\delta^{13}C$ values of the individual sediment samples from St. John's Harbour plotted on the mixing curves generated by mixing the $\delta^{13}C$ and the normalized concentrations of these compounds in the prominent primary sources. Error bars represent the range (1σ) observed in the single and composite samples of these sources. Letters represents the sample sites sampled in St. John's Harbour (see Figure 10)

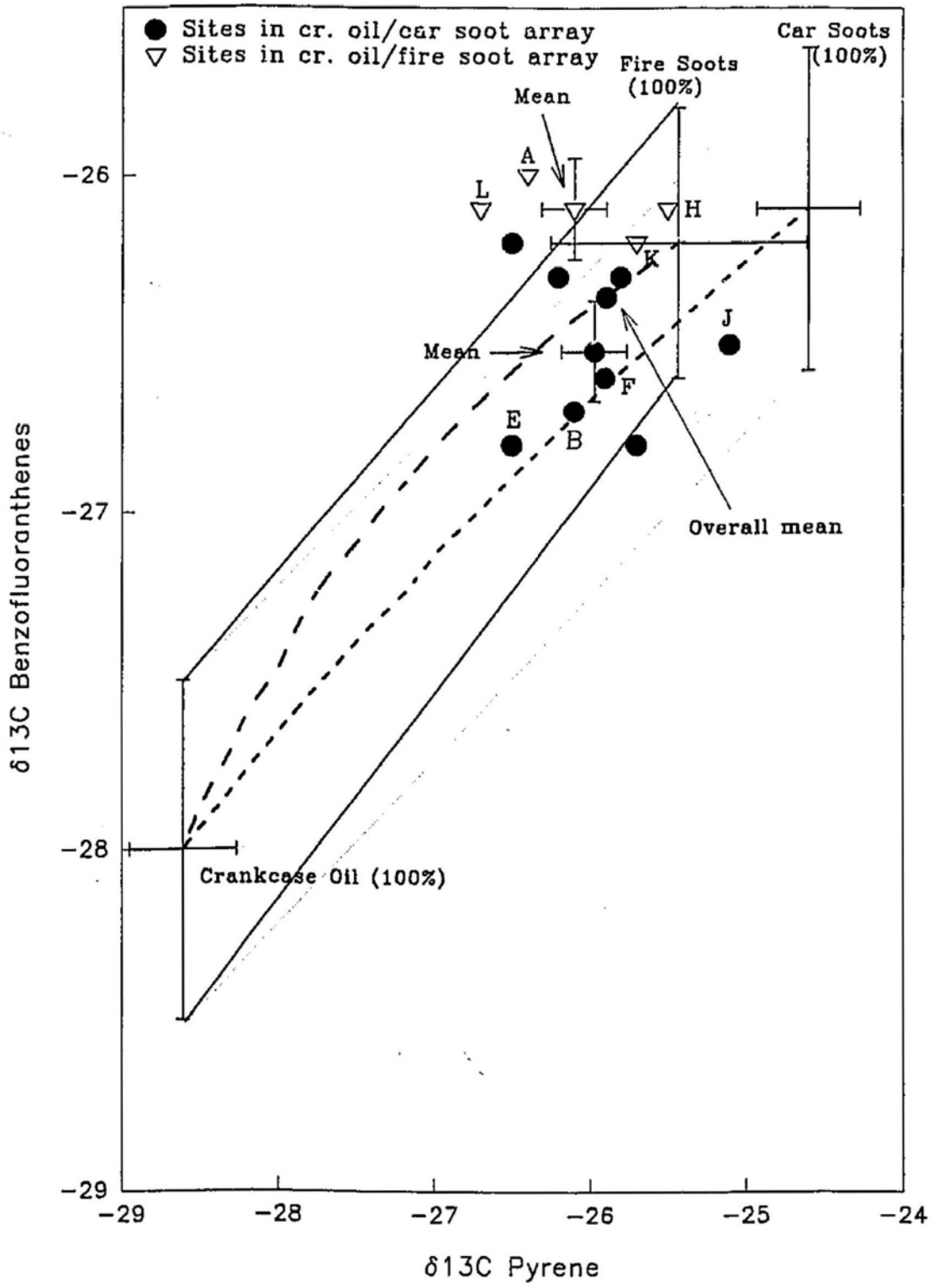
Sites in cr. oil/car soot array
Sites in cr. oil/fire soot array
Car Soots (100%)
Fire Soots (100%)
Mean
A
L
H
K
J
Mean
F
E
B
Overall mean
Crankcase Oil (100%)
−26
−27
−28
−29
−29
−28
−27
−26
−25
−24
δ13C Benzofluoranthenes
δ13C Pyrene

compound during the analysis of the various single and composite source samples. From the various mixing permutations considered, the $\delta^{13}C$ of the 4 and 5-ring PAH isolated from the various sediments generally form positive mixing arrays between the fire and car soot and crankcase oil end-members, quantitatively substantiating earlier assertions that a mixtures of these prominent primary sources could explain the range of $\delta^{13}C$ values observed in these particular sediments. The validity of these mixing arrays is further validated by unchanging relative positions of the individual sites (e.g., B, J and F; Figure 10) in the mixing array (within experimental error) regardless of the projection used. In general, as indicated by the dominance of the 3, 4 and 5-ring parental PAH in the molecular signatures, PAH of combustion origin seem to be dominant contributors to the Harbour sediments. This is shown by the bulk of the data points which are concentrated close to the two combustion end-members (Figures 67, 69, 70 and 71). From the position of the mean values on the mixing curves, the average combustion input is estimated to be approximately 70% while the remaining 30% of the PAH seem to be derived from crankcase oil contributions. Sites H and J are particularly enriched in combustion-derived PAH, while the maximum input of crankcase oil (≈50%) consistently occurred at site E indicating the heterogenous nature of these sediments which was not evident from the molecular signatures. The percentage input of crankcase oil is similar to the range (20 to 33%) calculated for the individual 4 and 5-ring compounds using the simpler mass balance approach (Eq. 1). The relative importance of the two primary combustion sources (fire soot vs. car soot) as PAH contributors to the sediments is also insinuated by these mixing curves. With the exception of sites A, H, K and L which plot closer to the fire

soot/crankcase oil mixing array, all the remaining sites tend to be concentrated close to the car soot/crankcase oil mixing curve (Figures 67, 68 and 70). This indicates that a significant portion of the combustion-derived PAH in the Harbour is of car emission origin. This characterization is particularly evident in Figures 68 and 71 where the arrays tend to be well separated. Despite the lack of distinct evidence in the molecular signature data to suggest the importance of car soot emissions in the combustion signatures, inputs of car soot PAH to the sediments were insinuated from the low Pa/A and elevated BaA/Chy compositional ratios (Figure 54). The dominance of car soot PAH compared to fire soots suggests that a significant portion of wood burning emissions are being transported away from the sampling area due to wind dispersion, and that car soot inputs mainly occur as a result of road runoff. The presence of retene, identified in most of the surface sediments samples is mainly related to early diagenesis rather than from wood burning sources (see pages 294-295), despite having a similar $\delta^{13}C$ value to these sources. This is supported by the apparent absence of retene in the open-road and sewage sample molecular signatures, which are identified to be the predominant pathways for PAH input to the Harbour. There was also a notable absence of retene in the atmospheric air samples investigated in the present study. The input of petroleum or petroleum products to the sediments is not surprising since most of the individual samples were characterized by the presence of a prominent UCM.

The prominence of car soot and crankcase oil PAH in sediments supports the suggestion that road runoff and runoff via the sewer system, and not aeolian deposition is the main pathway for PAH input to the Harbour sediments. This is also reflected by

the similarity in the isotopic values of the PAH in the sewage and sediment samples (Figure 72). Input of road sweep materials to the sediments was also supported by the presence of asphalt like particulates similar to those observed in the open-road sweeps. Due to the absence of major industries in the St. John's area, sewage is dominated by domestic sources. Sewage PAH content is therefore predominantly derived from aerially deposited combustion products, car emissions, crankcase oil by direct spillage and engine loss (GESAMP, 1993), and road sweep products such as weathered asphalt, tire and brake wear. The occurrence of early diagenesis in these sediments is supported by the presence of perylene in the deeper samples which was concluded to be derived from diagenetic alteration reactions based on the Py/Pery ratio. Reliable isotopic measurements could not be performed on perylene due to coelution with unidentified high molecular weight biological compounds.

In conclusion, using both the molecular signatures and the $\delta^{13}C$ of the PAH isolated from St. John's Harbour, sources of combustion and petroleum-derived PAH along with diagenetic sources were positively identified. From a combination of the molecular abundance data and the $\delta^{13}C$ of the individual PAH, car emissions were identified as important contributors of combustion-derived compounds whereas an average of 30% was derived from crankcase oil contributions. Direct road runoff, runoff via the storm sewers and snow dumping were identified to be the most likely pathways for PAH input to the Harbour using both the molecular signature and carbon isotope data. In this particular site, the combined use of molecular signature data and CSIA elucidated the prominent sources of PAH in the sediments. However, CSIA has the added advantage

Figure 72. Comparison of the $\delta^{13}C$ of the parental PAH in the surface sediment of St. John's Harbour and Conception Bay and the secondary source samples. Pa = Phenanthrene, A = Anthracene, Fl = Fluoranthene, Py = Pyrene, BaA+Chy = Benz(a)anthracene and Chrysene, BFl = Benzofluoranthenes, BeP+BaP = Benzo(e)pyrene and Benzo(a)pyrene.

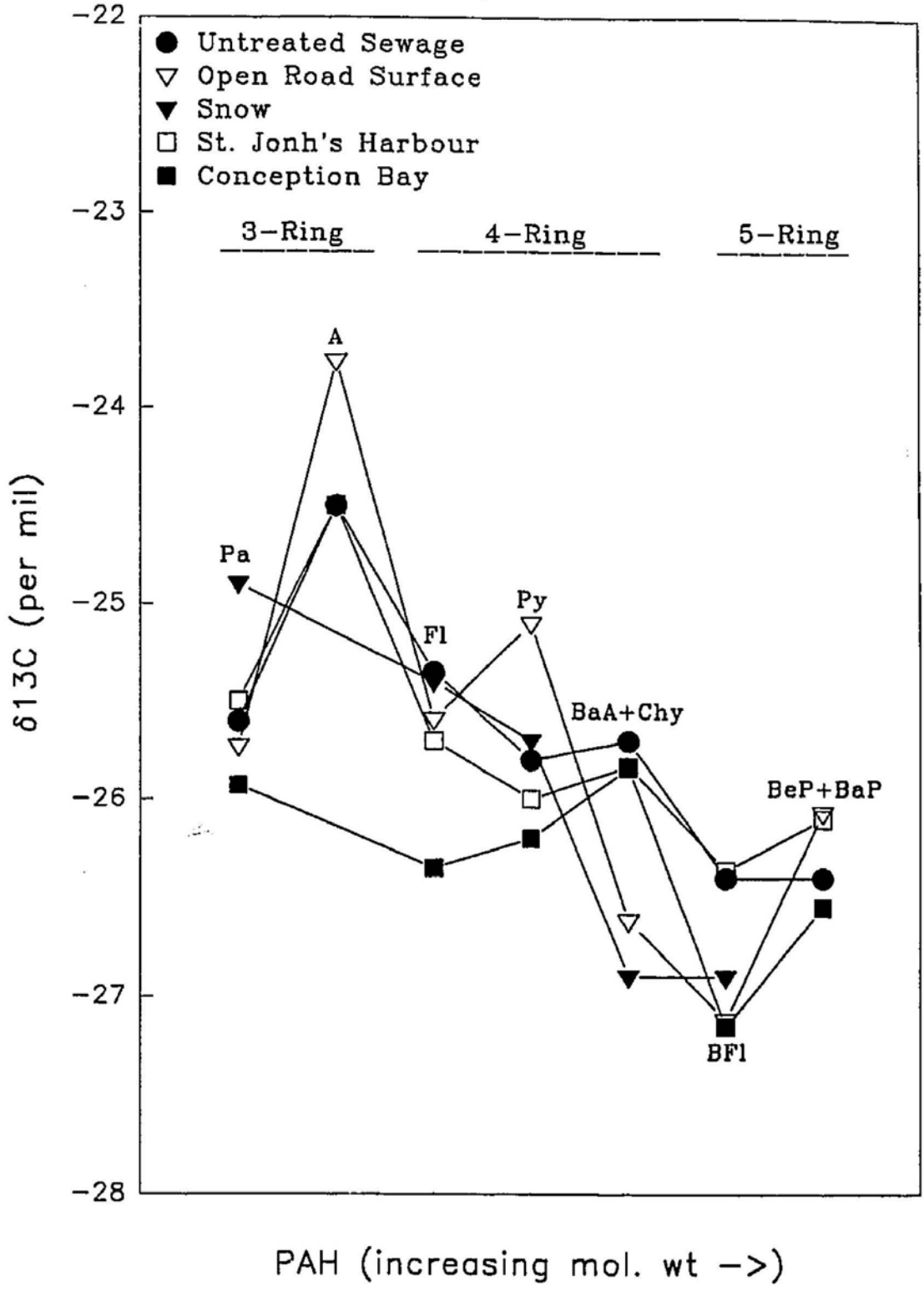
Untreated Sewage
Open Road Surface
Snow
St. Jonh's Harbour
Conception Bay
3-Ring
4-Ring
5-Ring
A
Pa
Fl
Py
BaA+Chy
BeP+BaP
BFl
−22
−23
−24
−25
−26
−27
−28
δ13C (per mil)
PAH (increasing mol. wt ->)

that a more quantitative approach to apportionment can be undertaken using the individual $\delta^{13}C$ alone or in combination with the molecular abundance data and mass-balance models. It should be noted that these mixing equations used only the more stable higher molecular weight 4 and 5-ring compounds to avoid uncertainties related to possible weathering fractionations involving lower molecular weight compounds.

4.9 Source apportionment of PAH in Conception Bay:

4.9.1 Molecular signature:

Surface and deeper sediments in Conception Bay are characterized by 3, 4 and 5-ring parental PAH, suggesting the predominance of combustion-derived inputs (Figure 61). The molecular signature is also characterized by the notable presence of retene and perylene. Concentrations (normalized to TOC, 0.8-1.0 %) of the individual compounds were considerably less than that of PAH in the Harbour site and generally below the threshold of 55 ng/g of dry sediment, considered as a baseline for uncontaminated sediments (La Flamme and Hites, 1978; Martel et al., 1986).

The mean and standard deviation of the compositional ratios of the prominent PAH are shown in Figure 54 and mean values are summarized according to depth in Figure 65. There were no distinct trends in the compositional ratios of the prominent compounds in the surface sediments with increasing distance from the shore. The variations observed in these ratios are within the analytical error normally associated with measurments at relatively low PAH concentrations. Anthracene concentrations in the sediments were generally below the level of 10 ng/g to allow reliable Pa/A ratio

determinations. However, the generally low concentration indicates that the Pa/A ratio is high and greater than the ratio observed for combustion sources. A mean Fl/Py ratio (1.2) for surface sediments is comparable to the value determined for St. John's Harbour and to values reported previously (Johnson et al., 1985; Shiaris and Jambard-Sweet, 1986; Killops and Howell, 1988; Pruell et al, 1990; Table 18). Despite the dominance of fluoranthene and pyrene in the sediments, their prominent input source cannot be elucidated from the compositional ratios of the sediments and the primary combustion sources. Also, the BaA/Chy ratio (0.7) was comparable to values reported in a number of previous studies (Table 18; Readman et al., 1986; Foster and Wright, 1988; Brooks et al., 1990). Possible PAH contributions from both fire and car soots is indicated, but again, it is not possible to discriminate between inputs from these two combustion sources. There is no association between the mean compositional ratios of surface sediments and the composite soot sample from the power generating station (Figure 54). This indicates that the PAH contributions from the power generating station to Conception Bay are not significant. In summary, the mean compositional ratios of the prominent compounds in the surface sediments of Conception Bay are primarily indicative of combustion, with little evidence of petroleum contamination. The absence of a UCM also confirms that petroleum inputs to these sediments are insignificant. In spite of the absence of an obvious petroleum signature, intermittent petroleum inputs can only account for the trace levels of sulphur heterocyclics and alkyl-substituted naphthalenes identified.

With the exception of the relatively elevated Chy concentrations in the top 4 cm at site CTR 23, inter-site variations in the concentrations of individual compounds were

generally small (Figure 43). Elevated Chy concentrations and a relatively low Fl/Py ratio (0.9) at site CTR 23 may indicate petroleum contributions at this particular site. The absence of alkylated PAH may therefore be due to the preferential weathering of these compounds in the sediments (Smith et al., 1991; Ehrhardt et al., 1992). The total PAH concentrations in the surface sediments ranged between 210 and 450 ng/g and there was no apparent relationship between total concentration and location of sampling.

There was no change in the mean Fl/Py and BaA/Chy ratios and percentage of 4 and 5-ring PAH with increasing depth (Figure 65). Samples representing depths of up to 20 cm were analyzed corresponding to approximately 40 years of sediment deposition based on a deposition rate of 0.5 cm/year (Ostrom, 1992). Concentrations of individual compounds in the top 14 cm were comparable, while levels at 20 cm were below the level of detection of 10 ng/g. This homogeneity with depth was also evident from metal concentrations and particle size analysis data (Appendix C and D). Since Conception Bay is a low energy environment, sediment mixing is chiefly related to bioturbation. The top 10 cm of sediment contains a rich population of bioturbators which include deposit feeding polychaetes (*Maldane sarsi and Prionospio steenstrupi*), mud stars (*Ctenodiscus crispatus*), bivalves (*Macoma calcarea*) and a range of sipunculida and echinodermata species (Scheibe, 1991). The mechanisms and the degree of mixing in the sediments is expected to differ with location throughout the Bay.

In contrast to the parental PAH, retene and perylene are quite prominent in the surface and deeper samples. The greater abundance of retene compared to the parental compounds suggests that it is primarily of diagenic origin. Evidence in support of a

diagenetic origin for retene was also apparent in the preliminary air samples which were characterized by the notable absence of retene. The percentage of perylene to total PAH ranged between 11.4% and 18.8% in the surface samples and between 15.8% and 29.8% in the deeper sediments. The dominance of perylene particularly in the deeper sediments and the low Py/Pery ratio (0.4 to 0.9; Figure 65) imply that it is mainly derived from the diagenetic alteration of terrestrial or marine precursors rather than from anthropogenic sources. Inputs of both marine and terrestrial sources were identified in the sediments using the enriched $\delta^{13}C$ of the bulk sediments (-21.9 to -21.5‰) and the n-alkane distribution (odd predominance) (Figure 73; Barrick et al., 1980; Saliot et al., 1988; Rowland and Robson, 1990; Morel et al., 1991; Steinhauer and Boehm, 1992; Lipiatou and Saliot, 1992).

The absence of a concentration gradient in the surface sediments with increasing distance from the shore suggests either efficient and extensive mixing in the water column or the dominance of aeolian pathways for particulate deposition. Aeolian deposition is recognised to be the most important PAH depositional pathway in similar sites that are remote from extensive urban development (Laflamme and Hites, 1978; Lake et al., 1979; Tissier and Saliot, 1983). Despite the lack of a concentration gradient, compositional ratios such as Fl/Py and BaA/Chy are comparable to those of secondary source samples such as roadsweeps. Hence, direct PAH contributions from road runoff (e.g., during spring snow melt) cannot be precluded.

4.9.2 Carbon isotope signature:

The $\delta^{13}C$ of individual parental PAH isolated from surface and deeper samples were comparable. Despite relatively low PAH concentrations identified in these

Figure 73. Total ion chromatogram of the n-alkane fraction of a surface sediment sample from Conception Bay showing a dominance of the odd numbered n-alkanes. IS = internal standard

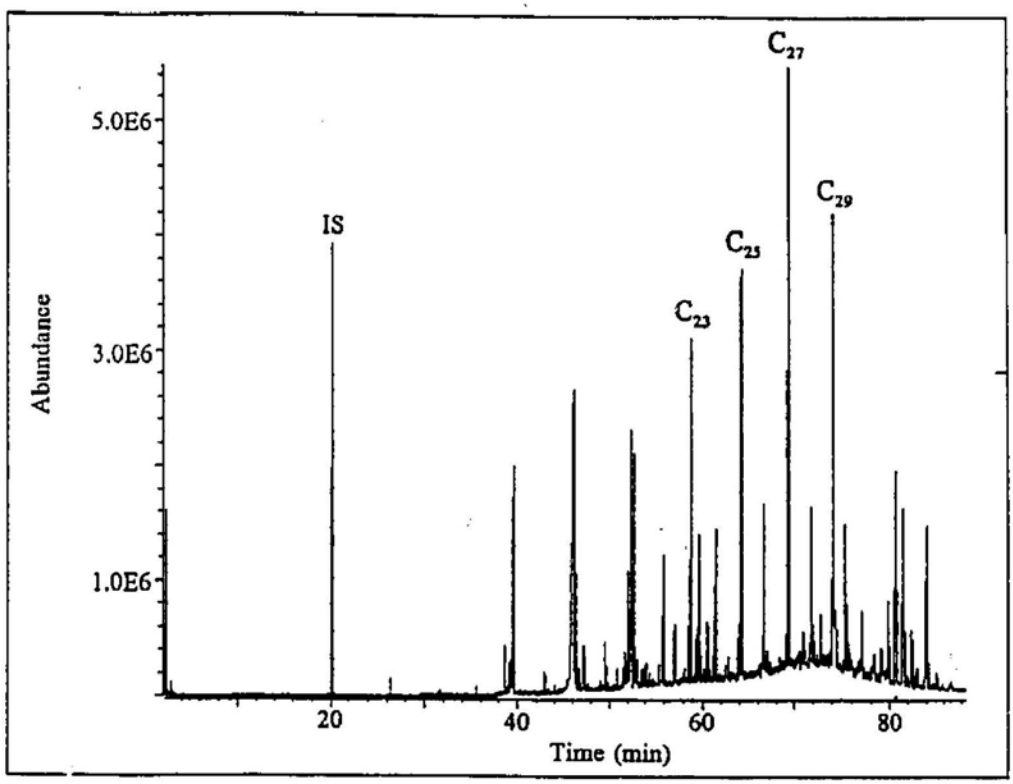
C27
5.0E6
IS
C29
C25
C23
3.0E6
Abundance
1.0E6
20
40
60
80
Time (min)

sediments, precision in the isotopic measurements was comparable to that recorded for St. John's Harbour (Figure 74). The $\delta^{13}C$ of Pa, Fl, and Py were similar while BaA+Chy was more enriched and the $\delta^{13}C$ of BFl and BeP+BaP were generally more depleted. The $\delta^{13}C$ of retene ranged between -28.1‰ and -24.5‰ and the values for perylene ranged between -25.2‰ and -22.4‰.

In contrast to the primary sources, Pa in the surface sediment is more enriched (cf., St. John's Harbour) while the higher molecular weight 4 and 5-ring PAH $\delta^{13}C$ are intermediate between combustion and petroleum sources (Figure 75). With the exception of BaA+Chy, $\delta^{13}C$ values of parental PAH in Conception Bay are comparatively more depleted than their counterparts in St. John's Harbour (Figure 74). Surprisingly, the overall isotopic signature, appears to indicate that petroleum inputs may have a greater influence on the $\delta^{13}C$ of PAH in Conception Bay than in the Harbour sediments.

On the basis of Eq.2 the mean $\delta^{13}C$ of Fl, BFl and BeP/BaP indicates inputs of between of between 40 and 55% petroleum, while pyrene and BaA/Chy comprised approximately of 25% petroleum-derived PAH (Figure 75). The $\delta^{13}C$ of the PAH from surface and deeper samples were also plotted on the same ratio-ratio mixing curves that were generated from the $\delta^{13}C$ and molecular abundances of the 4 and 5-ring PAH in the prominent primary sources (Eq. 3). These plots shown in Figures 76 to 80 are broadly consistent with two-component mixing with surface samples A, B and D consistently plotting closer to the combustion end-members and H, C and D8 are shifted in the direction of a second component. The trend in the relative positions of some of the sample sites cannot be compared because of the absence of the data points for some of

Figure 74. The mean and range (standard deviation; 2σ) of the $\delta^{13}C$ of the 3, 4 and 5-ring parental PAH in the surface sediments samples of Conception Bay and St. John's Harbour.

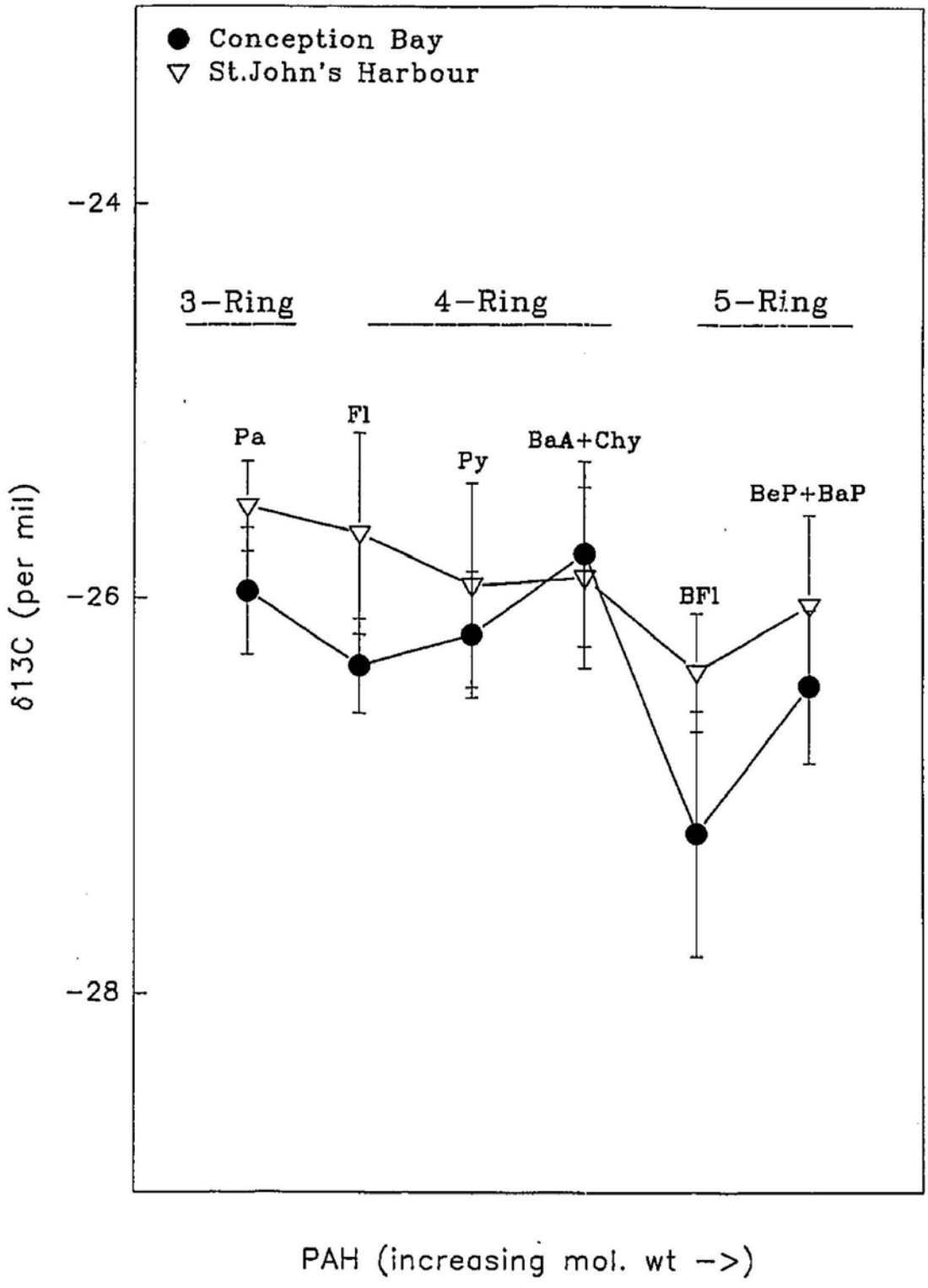
Conception Bay
St.John's Harbour
-24
-26
-28
δ13C (per mil)
3-Ring
4-Ring
5-Ring
Pa
Fl
Py
BaA+Chy
BFl
BeP+BaP
PAH (increasing mol. wt ->)

Figure 75. Comparison of the 3, 4 and 5-ring parental compounds in the surface sediments of Conception Bay with the three prominent primary sources. Also included is the relative contribution of "combustion" and "petroleum"-derived PAH. Pa = Phenanthrene, A = Anthracene, Fl = Fluoranthene, Py = Pyrene, BaA+Chy = Benz(a)anthracene and Chrysene, BFl = Benzofluoranthenes, BeP+BaP = Benzo(e)pyrene and Benzo(a)pyrene.

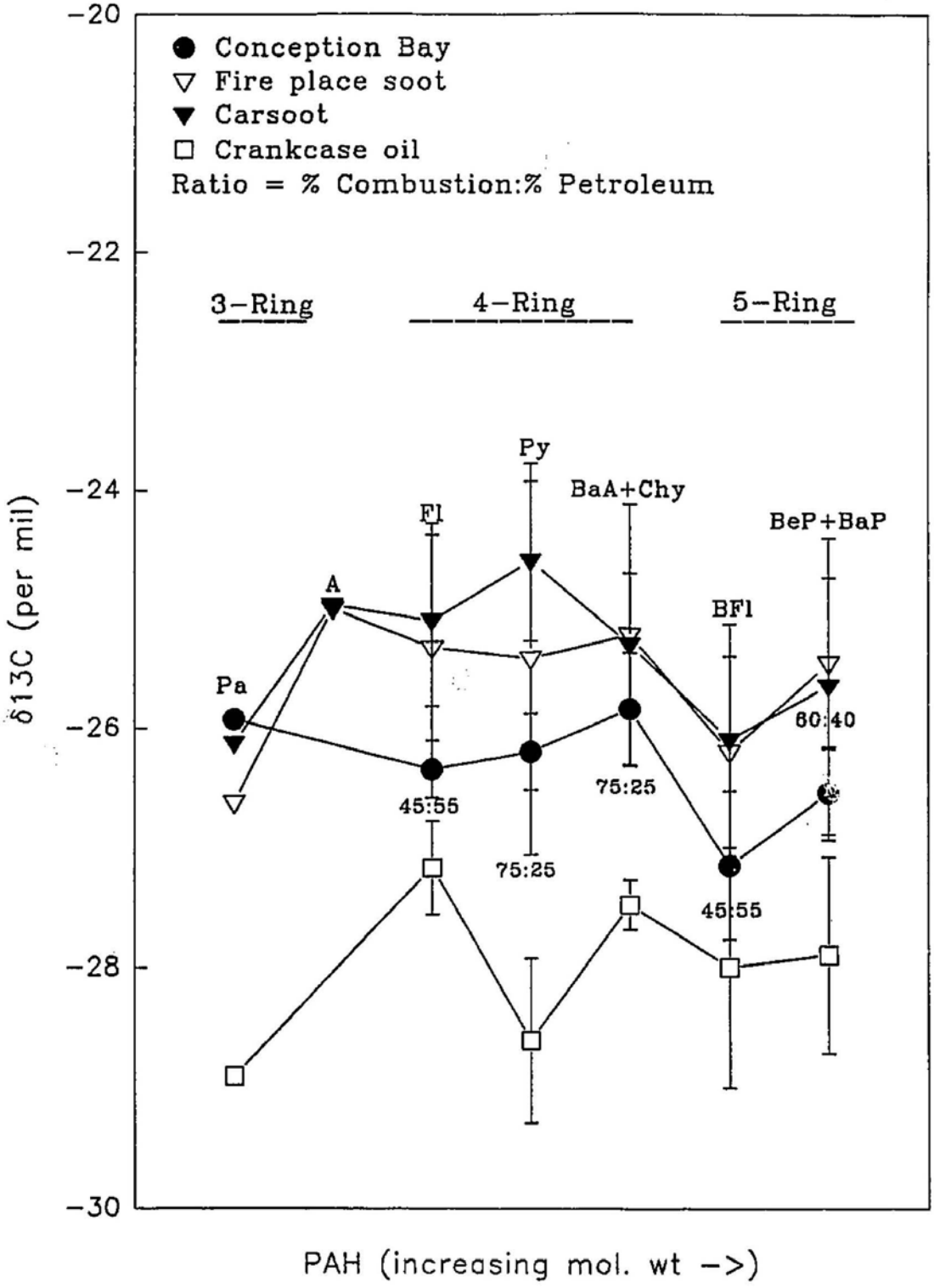
Conception Bay
Fire place soot
Carsoot
Crankcase oil
Ratio = % Combustion:% Petroleum
3–Ring
4–Ring
5–Ring
−20
−22
−24
−26
−28
−30
δ13C (per mil)
Pa
A
Fl
Py
BaA+Chy
BFl
BeP+BaP
45:55
75:25
75:25
45:55
60:40
PAH (increasing mol. wt –>)

Figure 76. Fluoranthene (Fl) and pyrene (Py) $\delta^{13}C$ values of the individual surface and deeper sediment samples from Conception Bay plotted on the mixing curves generated by mixing the $\delta^{13}C$ and the normalized concentrations of these compounds in the prominent primary sources. Error bars represent the range (1σ) observed in the single and composite samples of these sources. Arrows represents direction and possible shifts from the end-members of the mixing array.

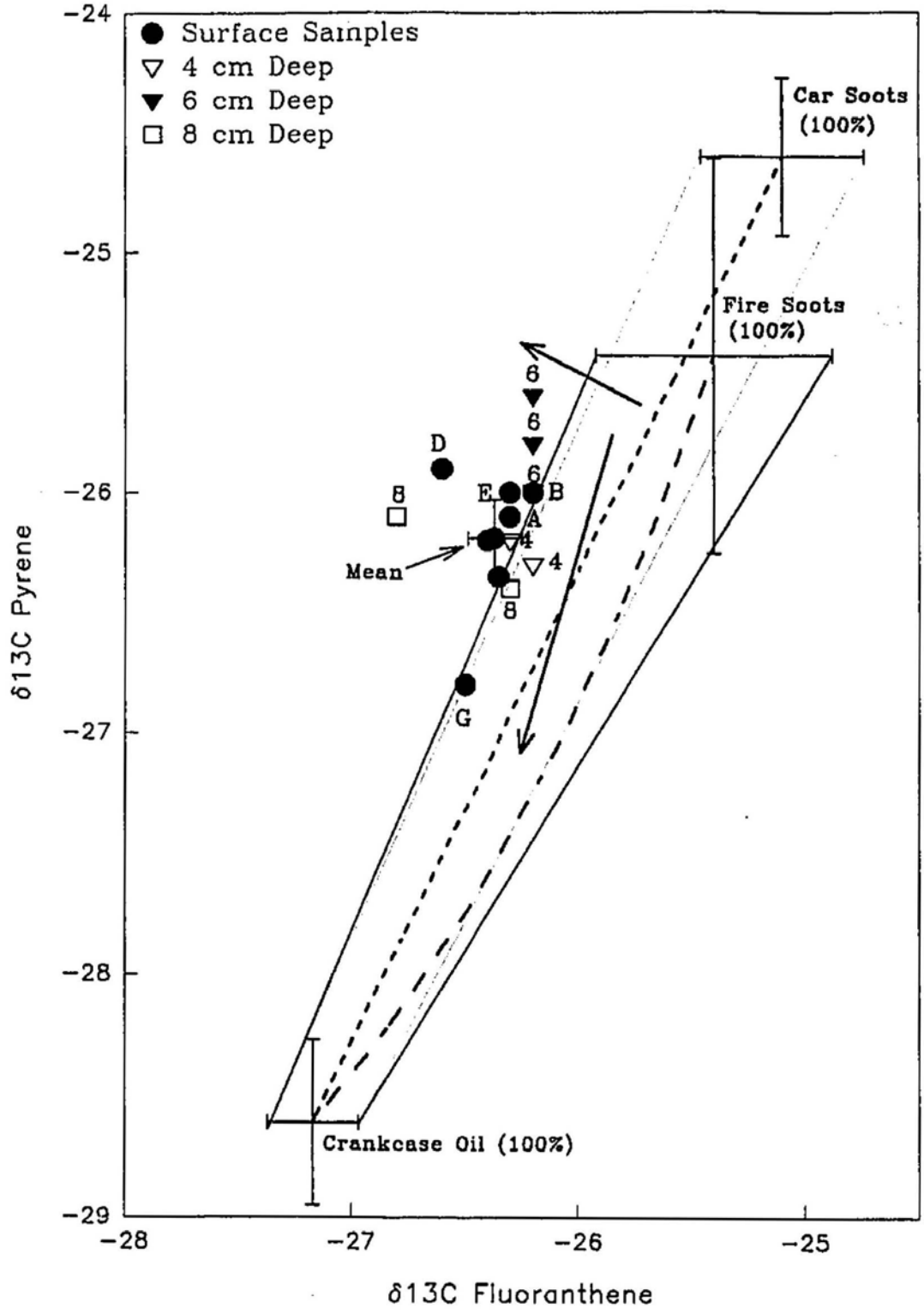
Surface Samples
4 cm Deep
6 cm Deep
8 cm Deep
Car Soots (100%)
Fire Soots (100%)
Crankcase Oil (100%)
Mean
A
B
D
E
G
δ13C Pyrene
δ13C Fluoranthene
−24
−25
−26
−27
−28
−29
−28
−27
−26
−25

Figure 77. Pyrene (Py) and the combined benz(a)anthracene+Chrysene (BaA+Chy) $\delta^{13}C$ values of the individual surface and deeper sediment samples from Conception Bay plotted on the mixing curves generated by mixing the $\delta^{13}C$ and the normalized concentrations of these compounds in the prominent primary sources. Error bars represent the range (1σ) observed in the single and composite samples of these sources. Arrows represents direction and possible shifts from the end-members of the mixing array.

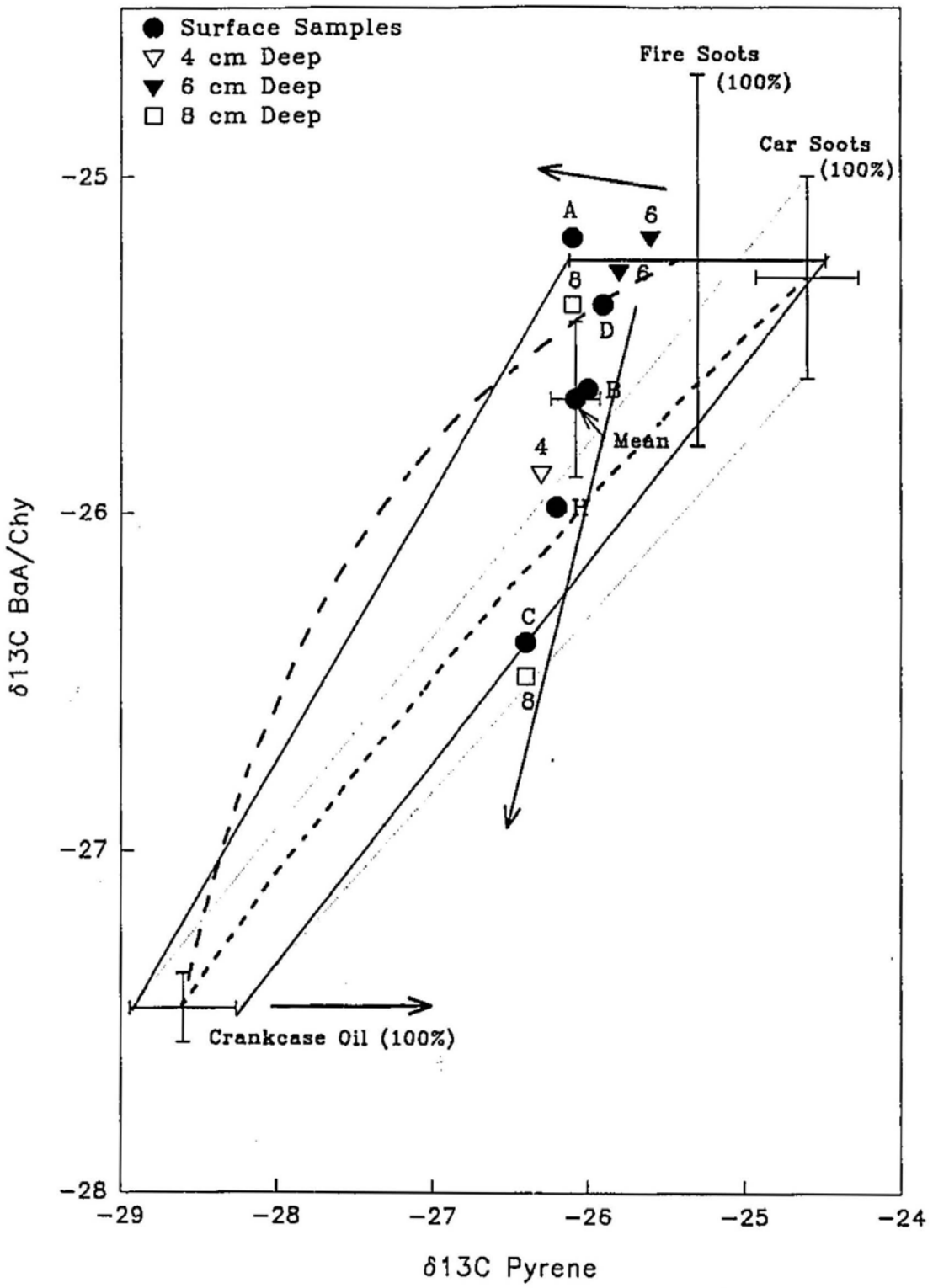
Surface Samples
4 cm Deep
6 cm Deep
8 cm Deep
Fire Soots
(100%)
Car Soots
(100%)
A
6
8
D
B
Mean
4
H
C
8
Crankcase Oil (100%)
−25
−26
−27
−28
−29
−28
−27
−26
−25
−24
δ13C BaA/Chy
δ13C Pyrene

Figure 78. Pyrene (Py) and the combined benzo(e)pyrene+benzo(a)pyrene (BeP+BaP) $\delta^{13}C$ values of the individual surface and deeper sediment samples from Conception Bay plotted on the mixing curves generated by mixing the $\delta^{13}C$ and the normalized concentrations of these compounds in the prominent primary sources. Error bars represent the range (1σ) observed in the single and composite samples of these sources. Arrows represents direction and possible shifts from the end-members of the mixing array.

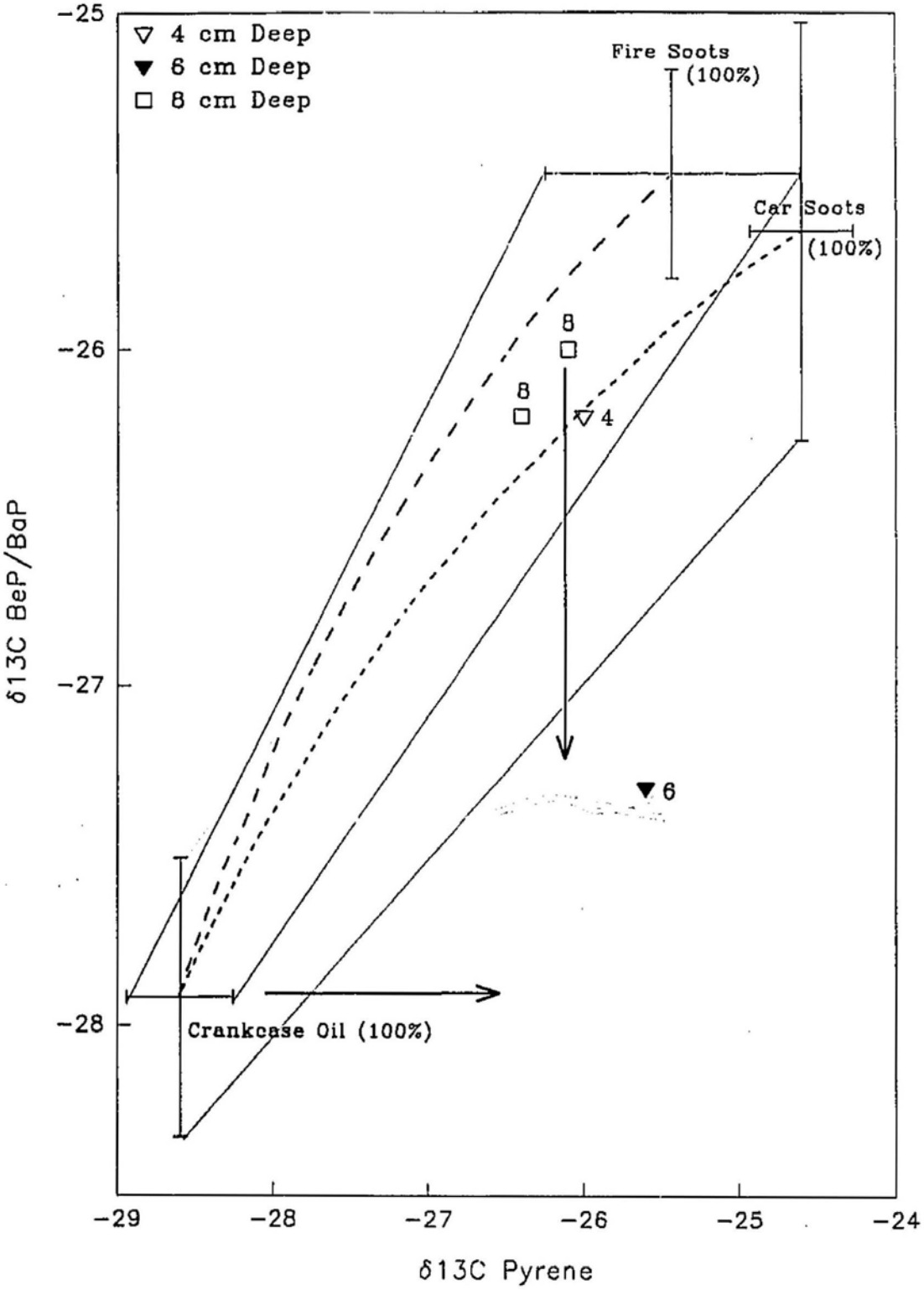
4 cm Deep
6 cm Deep
8 cm Deep
Fire Soots
(100%)
Car Soots
(100%)
Crankcase Oil (100%)
8
8
4
6
−25
−26
−27
−28
−29
−28
−27
−26
−25
−24
δ13C BeP/BaP
δ13C Pyrene

Figure 79. Pyrene (Py) and the combined benzofluoranthene (BFl) $\delta^{13}C$ values of the individual surface and deeper sediment samples from Conception Bay plotted on the mixing curves generated by mixing the $\delta^{13}C$ and the normalized concentrations of these compounds in the prominent primary sources. Error bars represent the range (1σ) observed in the single and composite samples of these sources. Arrows represents direction and possible shifts from the end-members of the mixing array.

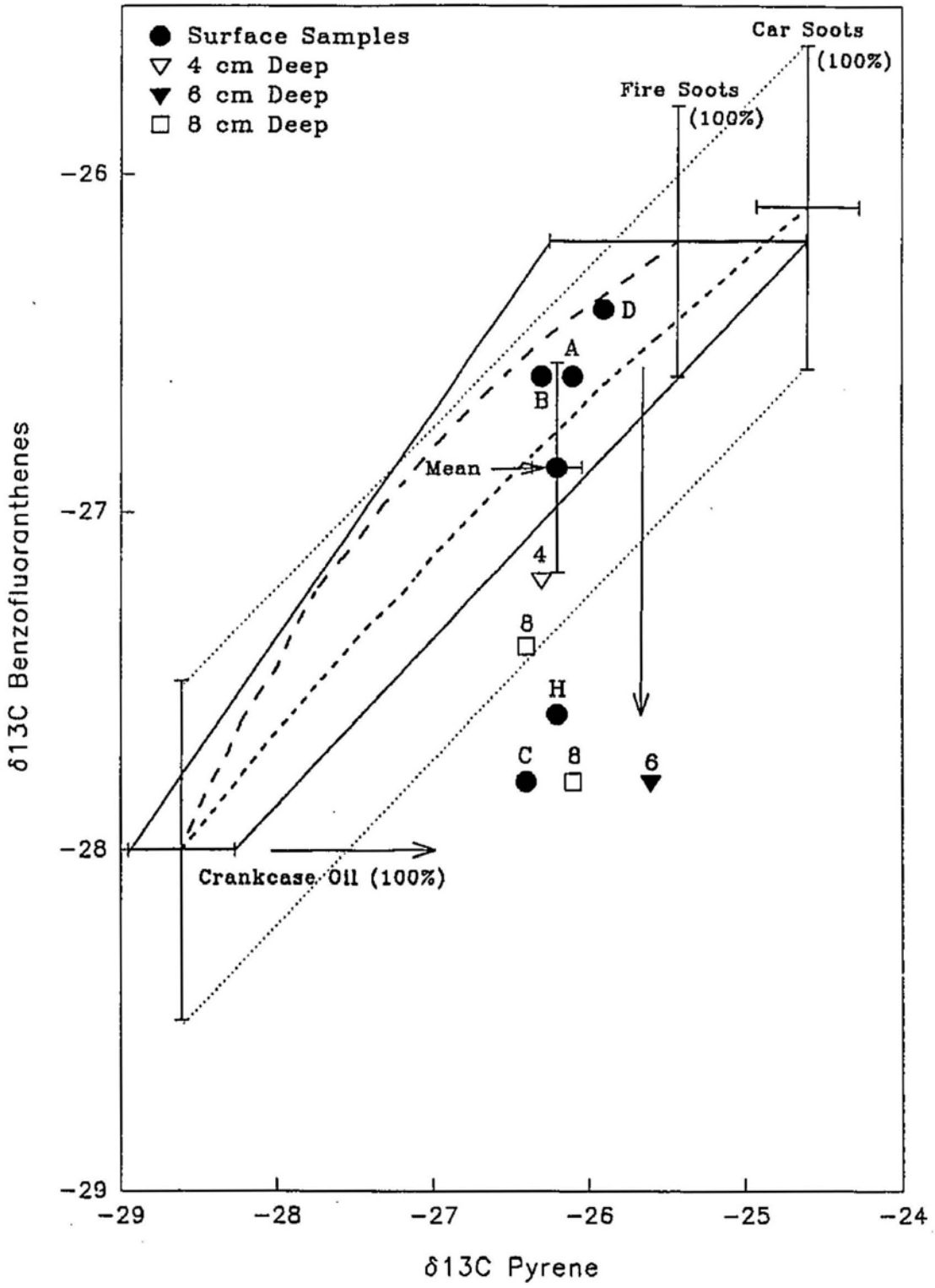
Surface Samples
4 cm Deep
6 cm Deep
8 cm Deep
Car Soots
(100%)
Fire Soots
(100%)
Mean
Crankcase Oil (100%)
A
B
C
D
H
4
6
8
8
−26
−27
−28
−29
−29
−28
−27
−26
−25
−24
δ13C Benzofluoranthenes
δ13C Pyrene

Figure 80. Combined benz(a)anthracene+Chrysene (BaA+Chy) and benzofluoranthene (BFl) $\delta^{13}C$ values of the individual surface and deeper sediment samples from Conception Bay plotted on the mixing curves generated by mixing the $\delta^{13}C$ and the normalized concentrations of these compounds in the prominent primary sources. Error bars represent the range (1σ) observed in the single and composite samples of these sources. Arrows represents direction and possible shifts from the end-members of the mixing array.

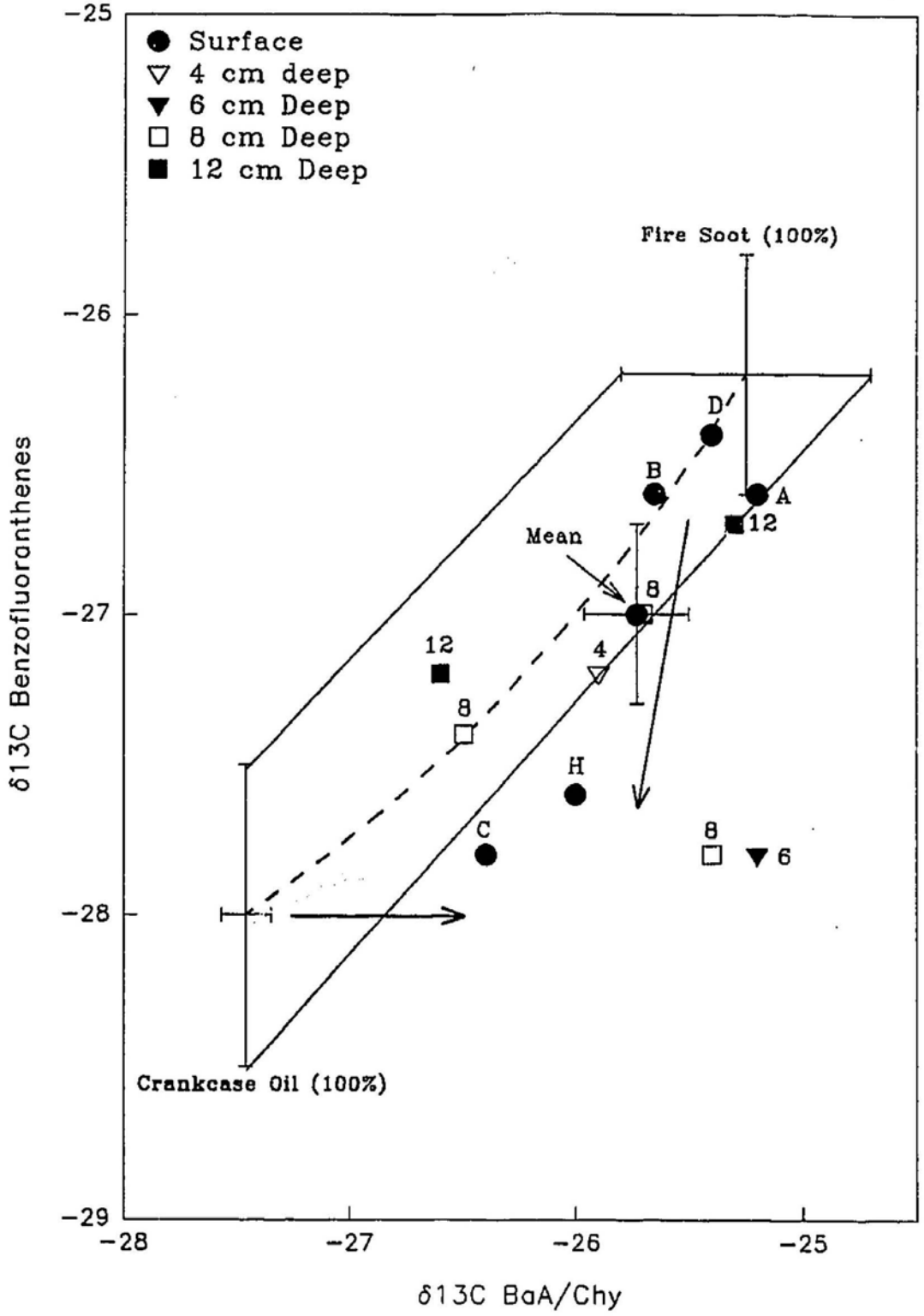
Surface
4 cm deep
6 cm Deep
8 cm Deep
12 cm Deep
Fire Soot (100%)
Crankcase Oil (100%)
Mean
A
B
C
D
H
δ13C Benzofluoranthenes
δ13C BaA/Chy
−25
−26
−27
−28
−29
−28
−27
−26
−25

the high molecular weight compounds. However, unlike St. John's Harbour, where a mixture of the three characterized primary sources accounts for the isotopic signature of the identified PAH, the trajectory of the mixing array for Conception Bay points to an alternative source or mixture of sources contributing to the total PAH inventory of these sediments. This is shown by the direction of the arrows in Figures 77, 79 and 80 where there is a tendency for the sample sites to be shifted away from the crankcase oil component toward a source with more enriched Py. Moreover, sample sites close to the combustion end-members, despite their resemblance to the fire soots, also seem to be somewhat shifted in favour of a more isotopically depleted combustion source. However, because of the variability observed in the combustion sources, combustion cannot be ruled out as an explanation for the latter observation. However despite the variability, a definite combustion input appears to be reflected in these sediments (cf., molecular signatures). Fire soots seem to be more important contributors of combustion-derived PAH than car soots, an interpretation strongly supported by the $\delta^{13}C$ value for Py. The shift away from crankcase oil tends to suggest some other source besides crankcase oil is contributing to the relatively depleted PAH in the sediment. Outboard motor condensates, which has been shown in the present study to be a potential source of both combustion and petroleum-derived PAH is one potential source of these compounds, since these are extensively used for recreational activity at this site. Despite, having a similar overall isotopic signature to crankcase oil, the $\delta^{13}C$ of the individual compounds, were generally more enriched in outboard motors, and unlike crankcase oil, Py concentrations in these condensates were generally lower and similar to Fl levels imparting a Fl/Py ratio

indicative of a combustion input source. Although, 5-ring compounds were identified in the molecular signature of outboard motor samples, reliable $\delta^{13}C$ determinations were hindered because of their relatively low concentrations and the presence of a prominent UCM. However, it is likely that these compounds will also be more enriched than their counterparts in crankcase oil since the petroleum undergoes partial combustion in the two-stroke engine prior to discharge.

There are a number of difficulties associated with using outboard motor condensates as an alternative PAH input source to the sediments, (1) only Py seems to exhibit the $\delta^{13}C$ enrichment speculated to take place in two-stroke engines (2) the molecular abundance of Py in the outboard motor condensate is too high to be overwhelmed by the "combustion" component and (3) the notable absence of a significant UCM (biodegraded oil) in the chromatograms. An attractive proposition is yet another "diagenetic" component in place of outboard motor oil. This "diagenetic" PAH component can be produced from terrestrial vegetation such as those described in section (1.4.2) and which include a wide range of polyterpenoids. Although we were unable to molecularly and isotopically characterize this diagenetic PAH component, the fact that they are mainly derived from polyterpenoids suggest that they are very likely to be depleted in $\delta^{13}C$. This suggestion is partly supported by the isotopic measurements on retene (-28.1 to -24.5$^{o}/_{oo}$). It is interesting to further speculate that the diagenetic process does not produce substantial Py (i.e., there are no known low temperature diagenetic precursors of Py) or if such formation is possible, the Py produced is isotopically enriched. The latter suggestion, although entirely speculative, is consistent with the

observation that perylene, a peri-condensed compound, is isotopically heavier (-25.2 to -22.4‰) than non-peri-condensed structures like retene. Nevertheless, there are potential problems associated with the proposed diagenetic component. One problem is that perylene concentrations are not significantly higher than what is normally expected from anthropogenic sources. Another is the abundance of nonalternant compounds, which are normally associated with combustion processess. However, the formation of combustion and diagenetic PAH are not well enough understood (e.g., Grimmer and Bohnke, 1978) to substantially rule out the proposed diagenetic component.

In contrast to the Harbour within which combustion PAH were the predominant input source, more substantial contributions from the second component are required to explain the PAH $\delta^{13}C$ values for the Conception Bay sediments. The majority of the sample sites concentrating close to the fire soot end-member suggests that Fl and Py seem to be mainly of combustion origin (Figure 76). However, greater inputs of a $\delta^{13}C$ depleted component are implicated for the higher molecular weight PAH. This is again similar to the range of values estimated for the individual compounds using Eq. 2 (Figure 75). The relative importance of the second component compared to combustion may account for the relatively depleted $\delta^{13}C$ values of the PAH in Conception Bay compared to the Harbour sediments. The influence of a second component was not evident from the compositional ratios of the prominent compounds in the molecular signature, which mainly reflected PAH of combustion origin. However, elevated Chy levels, low Fl/Py ratio at site CTR 23 and the high Pa/A ratio were all noted earlier. With the exception of alkyl chrysene, the general absence of diagenetic indicators in these sediments can be

attributed to the preferential weathering of low molecular weight and alkylated compounds in Conception Bay. For example, preferential weathering can eventually enrich a petroleum signature in parental PAH which can be mistaken to originate from incomplete combustion (Ehrhardt et al., 1992). Biodegradation, particularly by bacteria and fungi and photochemical degradation are recognised as the most important pathways for degrading low molecular weight and alkylated PAH (Leahy and Colwell, 1990; Ehrhardt et al., 1992). Saturates have the highest biodegradation rates, followed by light and alkylated aromatics, with high molecular weight parental PAH (4 and 5-ring) exhibiting low rates of degradation (Fusey and Oudot, 1984; Ehrhardt et al., 1992). Therefore, structure-dependent selectivity in the microbial and photolytic degradation of PAH sources may thus result in the loss of characteristic markers that are indicative of diagenetic inputs.

The lack of definite trends in the $\delta^{13}C$ values of the individual anthropogenic compounds in the deeper cores particularly the 3 and 4-ring PAH is consistent with the molecular data that indicates that the upper sediment layers at these sites are either homogeneously mixed or the PAH contributions and deposition are time invariant. The absence of a temporal trend also supports the suggestion that a second component is diagenetic rather than anthropogenic in nature.

The mean isotopic signature of Conception Bay surface sediments and secondary source samples are compared in Figure 72. On the basis of the compositional ratios of the molecular signatures, and the $\delta^{13}C$ of the PAH in these sources and sediments it is not possible to assess a pathway for PAH deposition in this particular site. Since this is a relatively remote site, aeolian deposition can be postulated as a prominent pathway.

To conclude, parental PAH in the Conception Bay sediments are not simple mixtures of the primary sources that was proposed for St John's Harbour. In spite of this, a combustion component was positively identified using a combination of the molecular signature and carbon isotope data. For example, the dominance of 3, 4 and 5-ring PAH in the molecular signature was indicative of combustion. However, the mixing calculations and diagrams appear to show the dominance of fire soot emissions over car emissions. The sediments were also characterized by the presence of an isotopically depleted component and two possible $\delta^{13}C$-depleted sources were described including outboard motor condensates and natural diagenetic products. Although the present work cannot definitively identify the ^{13}C-depleted component, the evidence discussed tends to favour natural diagenesis as the ^{13}C-depleted source.

On the basis of the molecular signatures alone, it is noteworthy that there was no clear evidence for the proposed second component. Also the apparent absence of other diagenetic markers in the molecular signatures is enigmatic, but it may be related to the preferential loss of low molecular weight and alkyl-substituted PAH during early diagenesis. Despite the low PAH concentration in Conception Bay, primary inputs can still be elucidated using the molecular signature and carbon isotope data collectively.

It should be noted that statistical variations around each of the selected mixing sources were not considered in the two mixing approaches (Eq. 2 and 3). Provisions for such statistical variation in the sources is expected to produce more realistic mixing calculations. If this was undertaken based solely on the assumed normal distribution around the mean isotopic compositions of the sources, only a select number of samples

or sampling sites can be assumed to require "mixed sources" (e.g., sites E for St. John's Harbour, Figures 68 and 71; site C in Conception Bay, Figures 77 and 79). It is evident, however, that the aforementioned samples are part of two-dimensional arrays of samples (i.e., with other samples within two standard deviation of the sources) in the mixing diagrams that indeed closely followed the calculated mixing curves. There are other reasons why the use of Eq. 2 and 3 is a valid representation of source mixing in the sediments. First, if the distribution of the compound-specific $\delta^{13}C$ values in the sediments simply represents statistical variations around one or both combustion sources, why are the observed values almost all depleted in ^{13}C compared to the combustion mean $\delta^{13}C$ values?. Furthermore, these values are also shown to be trending towards the ^{13}C depleted source and not randomly distributed in the mixing diagrams. Clearly, the real statistical variations around each combustion source must be substantially smaller than indicated by the assumed normal distribution based on the analyses of individual fire and car soot sources. For example, the use of Mann Whitney rank sum test (non-parametric distribution analysis) indicates that a number of sediment samples are statistically distinguishable from either of the two combustion sources (e.g., Fl and Figure 66 and 75). What is important point is the sediments generally plot in two-component mixing arrays and that the relative importance of the mixing components is unchanged even if different variables are selected (i.e., regardless of the choice of PAH) are themselves substantial evidence in support of the mixing model. It would therefore appear that the statistical limitations implied by the $\delta^{13}C$ variations in the individual sources is less severe than it appears. It is postulated that the reason for this is related to the manner by which

mixing in the sediments takes place in real systems. In systems, such as St. John's Harbour, for example, it is unlikely that individual fire or car soot samples can ever be represented in the sediments. Individual car soots are mixed with other car soots, and the same is true for fire soots. This "averaging" effect is likely to result in the deposition of composited samples whose isotopic signatures are more tightly defined than indicated by the statistical analyses we have performed on the individual samples. This is indeed what was observed in some samples composited in this present study

5.0 CONCLUSIONS

The primary aim of this study was to determine whether CSIA can provide complementary information to molecular signatures in tracing significant primary and secondary source inputs of PAH to depositional environments. The approach was to initially characterize the molecular and isotopic signatures of prominent primary and secondary PAH sources, and then to quantitatively compare these signatures to the corresponding signatures isolated from St. John's Harbour and Conception Bay sediments which were used as "model study sites". Prior to achieving this overall aim and because of the complex nature of environmental samples (UCM, coelution and varying individual PAH concentrations), suitable extraction and purification methods had to be adopted to allow CSIA measurements to be undertaken on individual compounds. Also, the stability of the $\delta^{13}C$ of standard PAH taken through the adopted work-up procedures and during a series of weathering reactions (volatilization, photolytic and microbial degradation) was assessed.

Multiple compound-specific isotope measurements on a standard mixture of PAH were performed with a precision of between 0.25 and 0.39‰ and an accuracy that ranged between 0.01‰ and 0.57‰. Reproducibility of GC/C/IRMS measurements on a range of field samples with varying UCM's and individual PAH concentrations were performed within a precision of 0.30‰ for well separated 3, 4 and 5-ring compounds while variations in precision of up 0.85‰ were recorded for some high molecular weight coeluting isomers. The precision of these measurements was unaffected by the magnitude

of the background matrix (UCM), with precisions of better than 0.24‰ recorded for the recovered internal standards from samples with prominent UCM's.

The adopted extraction and purification methods (adsorption and evaporation) did not significantly alter the isotopic integrity of the investigated PAH standards, even with recoveries as low as 45% for some low molecular weight compounds. Recoveries for the higher molecular weight PAH were generally better than 70%.

Isotopic alterations associated with the photolytic degradation of PAH standards exposed to natural sunlight in a range of organic solvents were not observed for the higher molecular weight 4 and 5-ring compounds. Microbial degradation and utilization of Na and Fl as sole carbon sources in laboratory experiments on aqueous media resulted in no significant alteration in their original $\delta^{13}C$ values. The $\delta^{13}C$ of the residual Na, with up to a 95% reduction in concentration was within 0.50‰, and Fl with up to 63% reduction was within 0.30‰, of their initial $\delta^{13}C$ values.

The molecular signatures of primary sources, based on the compositional ratios of the prominent compounds, were consistent with previous studies. Despite the presence of Na and MNa in some of the car soot samples, fireplace and car soots were characterized mainly by the dominance of 3, 4 and 5-ring parental PAH and were identified as the prominent primary combustion sources. Other primary combustion sources investigated (e.g., power generating station, domestic oil fired furnaces) had generally lower PAH levels, although they had very similar molecular signatures to the fire and car soot samples.

Crankcase oil was found to be the prominent primary petroleum source, and

consisted mainly of 2 and 3-ring parental and methylated PAH with generally lower concentrations of higher molecular weight (4 and 5-ring) parental compounds. With the exception of generally lower Py concentrations, the molecular signature of outboard motor condensates was similar to crankcase oil. The molecular signatures of crude oil and #2 fuel oil were comparable to previously reported signatures for these sources.

Some compositional ratios, particularly Pa/A, Pa/MPa and Fl/Py of the primary combustion and petroleum sources were distinct, and were used to qualitatively constrain inputs from these sources in depositional environments.

With the exception of enriched Py, $\delta^{13}C$ trends (compound to compound variations) observed in the two prominent primary combustion sources were similar and consisted of relatively depleted 3 and 5-ring PAH as well as enriched 4-ring compounds. This trend was postulated to be jointly dictated by the precursor compounds in the original source material and by a series of secondary reactions that occur during pyrolysis and pyrosynthesis. Lignins and terpenoids were proposed as important PAH precursors for the isotopically depleted PAH in fireplace soots while benzene, alkylated benzenes and crankcase oil components (e.g., terpenoids) are the most likely precursors of car soot PAH. Other primary combustion sources investigated were shown to have $\delta^{13}C$ trends that were comparable to the prominent combustion source signatures. Despite the similarity in the overall combustion $\delta^{13}C$ trends, certain distinct features in the $\delta^{13}C$ of individual compounds such as the trend between Pa and MPa and relatively enriched Py compared to Fl can potentially be used as source tracing tools if the contributions of individual combustion sources need to be elucidated.

$\delta^{13}C$ values of PAH isolated from crankcase oils and other petroleum sources were significantly more depleted than combustion-derived PAH. The isotopically depleted signatures of the PAH isolated from crankcase oils were attributed to thermally-induced aromatization reactions of natural compounds that exist in the oil, a process analogous to diagenetic (catagenic) reactions in natural systems. This analogy was supported by the comparable $\delta^{13}C$ values of corresponding PAH isolated from crude oils. It is suggested that the enhanced production of PAH in crankcase oil was due to the significant presence of cyclic precursors (e.g., naphthenes, terpenoids) in virgin crankcase oil. In contrast to combustion-derived signatures, crankcase oil Pa was significantly more depleted than its two alkyl-substituted homologues and Py was more $\delta^{13}C$-depleted than its isomeric partner Fl. The trend in the $\delta^{13}C$ of the PAH in the outboard motor condensates was similar to the trend observed in crankcase oil. However, the $\delta^{13}C$ of PAH in the outboard motor condensate were generally more enriched.

Secondary source (open-road, untreated sewage and roadside snow) molecular signatures were comparable, consisting mainly of combustion-derived 3, 4 and 5-ring parental PAH and a prominent UCM, indicative of petroleum and petroleum products. Due to similarities in these signatures and the uncertain effects of weathering, it was difficult to discriminate clearly between inputs from the primary sources investigated using only the molecular distributions of the prominent PAH. Nevertheless, the signature of the enclosed asphalt paved car park sweep was indicative of petroleum and seemed to be influenced primarily by a predominance of crankcase oil.

The trend observed in the $\delta^{13}C$ of PAH in these secondary sources was found to

be highly complementary to the molecular signature data. The overall input of crankcase oil to the open-road sweeps and roadside snow samples was estimated using Eq. 2 to be approximately 30%, while inputs to the sewage samples were generally lower (20%). Combustion inputs to the open-sweeps consisted mainly of PAH from car emission origin whereas a combination of wood burning and car emissions are implicated for the sewage and roadside snow samples.

The molecular signature of the St. John's Harbour sediments indicated the presence of PAH from combustion, petroleum and diagenetic sources. The input of combustion sources was identified using the compositional ratios of the prominent compounds whereas petroleum inputs were implied by the presence of alkyl-substituted PAH and a prominent UCM. Retene and perylene were identified to be the main compounds of diagenetic origin. Similar conclusions were obtained from the $\delta^{13}C$ values, which were found to be highly complementary to the molecular signatures in identifying primary source PAH inputs. Additionally, the prominent primary source inputs to these sediments were quantified using a combination of the $\delta^{13}C$ and the normalized molecular abundance of the individual 4 and 5-ring PAH in two component mixing calculations. The results of these mixing calculations indicated that:

(a) the PAH in St. John's Harbour comprised mainly of a mixture of the three prominent primary sources (fire and car soots, and crankcase oil), with an average 70% derived from the combined combustion inputs while the remaining 30% was attributed to crankcase oil contributions,

(b) in contrast to the inability of molecular distributions to resolve the relative

importance of the two prominent combustion sources, the results of the isotopic mass balance calculations strongly suggest that car emissions are more important than wood burning as a combustion input source to the Harbour sediments.

(c) the heterogenous nature of the sediments was also highlighted, with site E consisting of up to 50% crankcase oil while others (H and J) were predominantly of combustion origin, and

(d) in accordance with the molecular signature data, road runoff and runoff via storm sewers were identified as the most important pathways by which PAH are deposited in the Harbour.

The molecular signatures of Conception Bay sediments were primarily indicative of combustion along with PAH of diagenetic origin. The conspicuous absence of alkyl-substituted PAH and a UCM imply that petroleum inputs to these sediments are less significant compared to the Harbour sediments. The absence of a concentration gradient with distance from the shore implies that either PAH deposition to these sediments is mainly by aeolian deposition or lateral mixing in Conception Bay is extremely efficient. Although, individual PAH concentrations in these sediments were significantly lower than the Harbour, variations in the $\delta^{13}C$ measurements of PAH from both sites were comparable. Applying the same mass balance calculations (Eq. 3) to the PAH in these sediments suggested that:

(a) unlike the Harbour sediments, $\delta^{13}C$ of the parental PAH in Conception Bay cannot be explained by mixing the three prominent primary sources (wood burning, car emissions and Crankcase oil) investigated in the present study,

(b) the projection of the mixing arrays imply that wood burning emissions are possibly more important than car emissions as a combustion source, and

(c) the presence of an unidentified isotopically depleted source was also apparent, with recent diagenetic or unidentified petroleum-related sources as suitable candidates for these $\delta^{13}C$-depleted compounds.

The adoption of extraction and purification methods reduced the difficulties associated with performing reliable CSIA measurements on individual PAH from a range of environmental samples. The stability observed in the $\delta^{13}C$ of the 4 and 5-ring standard PAH suggests that the isotopic signature of these compounds isolated from depositional environments have not been significantly altered by similar weathering reactions during transport and deposition. The distinct $\delta^{13}C$ values of the PAH isolated from the two combustion sources and crankcase oil indicate unique formation pathways for PAH in these primary sources. CSIA and molecular characterization are highly complementary tools for elucidating significant primary and secondary source contributions of PAH to depositional environments. Additionally, CSIA in combination with mass-balance calculations allows for a more quantitative approach to apportioning PAH sources and pathways in a wide variety of environmental samples. This approach was demonstrated in the contrasting depositional environments of St. John's Harbour and Conception Bay.

6.0 LITERATURE CITED

Abrajano, T.A. and Holt, B. (1992) GC/C/IRMS $\delta^{13}C$ calibration and analysis of hydrocarbons. Proceedings of the 203rd American Chemical Society Meeting, San Francisco, Ca., abstract # 93.

Afghan, B.K. and Chau A.S.Y. (1989) Analysis of trace organics in the aquatic environment, CRC press Inc., 205-241.

Alsberg, T. and Stenburg, U. (1979) Capillary GC-MS analysis of PAH emissions from combustion of peat and wood in a hot water boiler. Chemosphere, 7, 487-496.

Alsberg, T., Stenburg, U., Westerholm, R., Strandell, M., Rannug, U., Sundvall, A., Romert, L., Bernson, V., Pettersson, B., Toftgard, R., Franzen, B., Jansson, M., Gustafsson, J.A., Egeback, K.E. and Tejle, G. (1985) Chemical and biological characterization of organic material from gasoline exhaust particles. Environmental Science and Technology, 19, 43-49.

Anderson, J.W., Neff, J.M., Cox, B.A., Tatem, H.E. and Hightower, G.M. (1974) Effects of oil on estuarine animals: toxicity, uptake, and depuration and respiration. In "Pollution and Physiology of Marine Organisms" F.J. Vernberg and W.B. Vernberg (eds.), New York, Academic Press, 285-310.

Arey, J., Zielinska, B., Atkinson, R., Winter, A., Ramdahl, T. and Pitts, Jr., J.N. (1986) The formation of nitro-PAH from the gas phase reactions of fluoranthene and pyrene with OH radical in the presence of NO_x. Atmospheric Environment, 20, 2339-2345.

Arneth, J.D. and Matzigkeit, U. (1986) Variations in the carbon isotope composition and production of various pyrolysis products under open and closed system conditions. Organic Geochemistry, 10, 1067-1071.

Arneth, J.D. and Matzigkeit, U. (1986a) Laboratory-simulated thermal maturation of different types of sediments from the Williston Basin, North America-effects on the production rates, the isotope and organo-geochemical composition of various pyrolysis products. Chemical Geology (Isotope Geoscience Section) 58, 339-360.

Atkinson, R. and Aschmann, S.M. (1984b) Rate constants for the reactions of O_3 and OH radicals with a series of alkynes. International Journal of Chemical Kinetics, 16, 259-268.

Atkinson, R. (1990) Gas-phase tropospheric chemistry of organic compounds: A Review. Atmospheric Environment, 24A, 1, 1-41.

Badger, G.M., Kimber, R.W.L. and Spotswood, T.M. (1960) Mode of formation of BaP in human environment. Nature, 187, 663-665.

Badger, G.M., Kimber, R.W.L. and Novotny, J. (1964) The formation of aromatic hydrocarbons at high temperatures. XXI Pyrolysis of n-butylbenzene over a range of temperatures from 300-900°C at 50°C intervals. Australian Journal of Chemistry, 17, 778-786.

Baek, S.O., Field, R.A., Goldstone, M.E., Kirk, P.W., Lester, J.N. and Perry, R. (1991a) A review of atmospheric polycyclic aromatic hydrocarbons: source fate and behaviour. Water, Air and Soil Pollution, 60, 279-300.

Baek, S.O., Goldstone, M.E., Kirk, P.W., Lester, J.N. and Perry, R. (1991b) Phase distribution and particle size dependency of polycyclic aromatic hydrocarbons in the urban environment. Chemosphere, 22, 5-6, 503-520.

Barnsley, E.A. (1975) The bacterial degradation of fluoranthene and benzo(a)pyrene. Canadian Journal of Microbiology, 21, 1004-1008.

Barnsley, E.A. (1983) Bacterial oxidation of naphthalene and phenanthrene. Journal of Bacteriology, 153, 1069-1072.

Barrere, M. (1981) Aerothermochemistry of diffusion flames. In "Soot in Combustion Systems and its Toxic Properties", J. Lahayo and G. Prado (eds.) Plenum Press, NY, 273-309.

Barrick, R.C., Hedges, J.I. and Peterson, M.L. (1980) Hydrocarbon geochemistry of the Puget Sound region -I. Sedimentary acyclic hydrocarbons. Geochimica et Cosmochimica Acta, 44, 1349-1362.

Barrick, R.C. and Prahl, F.G. (1987) Hydrocarbon geochemistry of the Puget Sound Region. III Polycyclic aromatic hydrocarbons in sediments. Estuarine, Coastal and Shelf Science, 25, 175-191.

Barrie, A., Bricout, J. and Koziet, J. (1984) Gas chromatography-stable isotope ratio analysis at natural abundance levels. Biomedical Mass Spectrometry, 11, 11, 583-588.

Bates, T.S., Hamilton, S.E. and Cline, J.D. (1984) Vertical transport and sedimentation of hydrocarbons in the central main basin of Pugent Sound, Washington. Environmental Science and Technology, 18, 299-305.

Bauer, J.E. and Capone, D.G. (1985) Degradation and mineralization of the polycyclic aromatic hydrocarbons anthracene and naphthalene in intertidal marine sediments. Applied Environmental Microbiology, 50, 81-90.

Bauer, J.E. and Capone, D.G. (1988) Effects of co-occurring aromatic hydrocarbons on the degradation of individual polycyclic aromatic hydrocarbons in marine sediment slurries. Applied Environmental Microbiology, 54, 1649-1655.

Begeman, C.R. and Burgan, J.C. (1970) Polynuclear hydrocarbon emission from automotive engines. SAE Paper 700469, Society of Automotive Engineers, Detroit, Mich.

Behymer, T.D. and Hites, R.A. (1988) Photolysis of polycyclic aromatic hydrocarbons adsorbed on fly ash. Environmental Science and Technology, 22, 1311-1319.

Benner, R., Fogel, M.L., Sprague, E.K. and Hodson, R.E. (1987) Depletion of ^{13}C in lignin and its implications for stable carbon isotope studies. Nature, 329, 708-710.

Bieri, R.H., Hein, C., Huggett, R.J., Shou, P., Slone, H., Smith, C. and Su, C.W. (1986) Polycyclic aromatic hydrocarbons in the surface sediments from the Elizabeth river estuary. International Journal of Environmental Analytical Chemistry, 26, 97-113.

Bittner, J.D., Howard, J.B. and Palmer, H.B. (1981) Chemistry of intermediate species in the rich combustion of benzene. In "Soot in Combustion Systems and its Toxic Properties", J. Lahayo and G. Prado (eds.), Plenum Press, NY, 95-126.

Bjorseth, A. and Ramdahl, T. (1983) Sources and emissions of PAH. In "Handbook of Polycyclic Aromatic Hydrocarbons (Vol.2) Emission Sources and Recent Progress in Analytical Chemistry", Marcel Dekker, Inc., 1-20.

Blumer, M. (1957) Removal of elemental sulfur from hydrocarbon fractions. Analytical Chemistry, 29, 7, 1039-1041.

Blumer, M., Blumer, W. and Reich, T. (1977) Polycyclic aromatic hydrocarbons in soils of a mountain valley: Correlation with highway traffic and cancer incidence. Environmental Science and Technology, 11, 12, 1082-1084.

Boehm, P.D. and Farrington, J.W. (1984) Aspects of the polycyclic aromatic hydrocarbons geochemistry of recent sediments in the Georges Bank region. Environmental Science and Technology, 18, 11, 840-845.

Boehm, P.D. and Requejo, A.G. (1986) Overview of the recent sediment hydrocarbon geochemistry of Atlantic and Gulf Coast outer continental shelf environments. Estuarine, Coastal and Shelf Science, 23, 29-58.

Boldrin, B., Tiehm, A. and Fritzsche, C. (1993) Degradation of phenanthrene, fluorene, fluoranthene and pyrene by a *Mycobacterium sp.*. Applied and Environmental Microbiology, 59, 6, 1927-1930.

Bonfanti, L., Cioni, M., Belli, R. and Cappiello, A. (1988) Determination of trace organic compounds in effluents from a coal-fired power plant. Biomedical and Environmental Mass Spectrometry, 16, 175-178.

Boom, A. and Marsalek, J. (1988) Accumulation of polycyclic aromatic hydrocarbons (PAH's) in an urban snowpack. Science of the Total Environment, 74, 133-148.

Borneff, J., Selenka, F., Kunte, H. and Maximos, A. (1968) Experimental studies on the formation of polycyclic aromatic hydrocarbons in plants. Environmental Research, 2, 22-29.

Bossert, I., Kachel, W.M. and Bartha, R. (1984) Fate of hydrocarbons during oily sludge disposal in soils. Applied Environmental Microbiology, 47, 763-767.

Broddin, G., Van Vaeck, L. and Van Cauwenberghe, K. (1977) The size and distribution of polycyclic aromatic hydrocarbon-containing particles from a coke emission source. Atmospheric Environment, 11, 1061-1064.

Broman, D., Coimsjo, A., Naf, C. and Zebuhr, Y. (1988) A multi-sediment trap study on the temporal and spatial variability of polycyclic aromatic hydrocarbons and lead in an anthropogenic influenced Archipelago. Environmental Science and Technology, 22, 10, 1219-1228.

Brooks, J.M., Kennicutt II, M.C., Wade, T.L., Hart, A.D., Denoux, G.J. and McDonald, T.J. (1990) Hydrocarbon distribution around a shallow water multiwell platform. Environmental Science and Technology, 24, 7, 1079-1085.

Brorstroem-Lundun, E. and Loevblad, G. (1991) Deposition of soot related hydrocarbons during long-range transport of pollution to Sweden. Atmospheric Environment, 25A, 10, 2251-2257.

Brown, D.W., Ramos, L.S., Uyeda, M.Y., Friedman, A.J., and McLeod, W.D. (1980) Ambient-temperature extraction of hydrocarbons from marine-sediment-comparison with boiling-solvent extraction. Advances Chemistry Series, 185, 313-326.

Brown, G. and Maher, W. (1992) The occurrence, distribution and sources of polycyclic aromatic hydrocarbons in the sediments of the Georges River estuary, Australia. Organic Geochemistry, 18, 5, 657-658.

Brun, G.L., Howell, G.D., and O'Neill H.J. (1991) Spatial and temporal patterns of organic contaminants in wet precipitation in Atlantic Canada. Environmental Science and Technology, 27, 7, 1249-1253

Brunnemann, K.D. and Hoffman, D. (1976) Analysis of polynuclear aromatic hydrocarbons in the respiratory environment. In "Carcinogenesis-A Comprehensive Survey (Vol. 1) Polynuclear aromatic hydrocarbons, Chemistry, Metabolism, and Carcinogenesis", R.I. Freudenthal and P.W. Jones (eds.) Raven Press, 209-223.

Bunce, N.J. and Dryfhout, H.G. (1992) Dinurnal and seasonal modelling of the tropospheric half-lives of polycyclic aromatic hydrocarbons. Canadian Journal of Chemistry, 70, 1966-1970.

Butler, J.D. and Crossley, P. (1981) Reactivity of polycyclic aromatic hydrocarbons adsorbed on soot particles. Atmospheric Environment, 15, 91-94.

Canton L. and Grimalt J.O. (1992) Gas chromatographic-mass spectrometric (GC-MS) characterization of polycyclic aromatic hydrocarbon mixtures in polluted coastal sediments. Journal of Chromatography, 607, 279-286.

Cerniglia, C.E. (1978) Metabolism of naphthalene by cell extracts of *Cunninghamella elegans*. Archives of Biochemistry and Biophysics. 186, 121-127.

Cerniglia, C.E. and Gibson, D.T. (1979) Oxidation of benzo(a)pyrene by the filamentous fungus *Cunninghamella elegans*. Journal of Biology and Chemistry 254, 12174-12180.

Cerniglia, C.E. (1984) Microbial metabolism of polycyclic aromatic compounds. Advances Applied Microbiology. 30, 31-71.

Cerniglia, C.E. and Yang, S.K. (1984) Stereoselective metabolism of anthracene and phenanthrene by the *Cunninghamella elegans*. Applied Environmental Microbiology, 47, 119.

Cerniglia, C.E. and Heitkamp, M.A. (1989) Microbial degradation of polycyclic aromatic hydrocarbons (PAH) in the aquatic environment. In "Metabolism of Polycyclic Aromatic Hydrocarbons in the Aquatic Environment", U. Varanasi (ed.) CRC Press, Inc., 41-68.

Cerniglia, C.E. (1991) Biodegradation of organic contaminants in sediments: Overview and examples with polycyclic aromatic hydrocarbons. In "Organic Substances and Sediments in Water" (Vol 3) R.A. Baker (ed.) Lewis Publishers, 267-281.

Chung, H.M., Rooney, M.A., Toon, M.B. and Claypool, G.E. (1992) Carbon isotope composition of marine crude oils. The American Association of Petroleum Geologists Bulletin, 76, 7, 1000-1007.

Chung, H.M. (1992) Origin of methyl substituted naphthalenes and other hydrocarbons compounds in the Ponca City crude. Proceedings of the 203rd American Chemical Society Meeting, San Francisco, Ca., abstract #156.

Clar, E. (1964) The aromatic sextet and its significance in relation to the stability of aromatic systems. In "Polycyclic Hydrocarbon" (Vol 1) Academic Press, 32-40.

Clayton, C.J. (1991) Effects of maturity on carbon isotope ratios of oils and condensates. Organic Geochemistry, 17, 6, 887-899.

Clayton, C.J. (1992) Effects of maturity on compound-specific carbon isotope ratios in north sea oils. Proceedings of the 203rdAmerican Chemical Society Meeting, San Francisco, Ca., abstract # 158.

Colket, M.B. and Hall, R.J. (1992) Mechanistic models for soot formation Government-Reports-Announcements-and-Index-(GRA&I)-Issue 23, 1-17.

Colla, C., Biaggi, C. and Treccani, V. (1959) Richerche sul metabolismo ossidativo microbico dell'anthracene e fenanthrene. II. Isolamento e carraterizzazione del 3,4 diossifenanthrene. Annali di Microbiologia ed Enzimologia, 9, 1.

Colombo, J.C., Pelletier, E., Brochu, C., Khalil, M. and Cattoggio, J.A. (1989) Determination of hydrocarbon sources using n-alkane and polyaromatic hydrocarbon distribution indexes. Case study: Rio de La Plata Estuary, Argentina. Environmental Science and Technology, 23, 888-894.

Commins, B.T. (1969) Formation of polycyclic aromatic hydrocarbons during pyrolysis and combustion of hydrocarbons. Atmosphere Environment, 3, 565-572.

Conkright, M.E. (1989) Stable carbon isotope compositions during the thermal alteration of organic matter. Ph.D. thesis, University of South Florida, 1-18.

Coutant, R.W., Brown, L. and Chuang, J.C. (1988) Phase distribution and artifact formation in ambient air sampling for polynuclear aromatic hydrocarbons. Atmospheric Environment, 22, 2, 403-409.

Cretney, W. J., Green D. R., Fowler B. R., Humphrey B., Fiest D. L. and Boehm P.D. (1987) Hydrocarbon biogeochemical setting of the baffin island oil spill experimental sites. I. Sediments. Arctic, 40, Supp 1:51-65.

Crittenden, B.D. and Long, R. (1976) The mechanisms of formation of polynuclear aromatic compounds in combustion systems. In "Carcinogenesis-A Comprehensive Survey (Vol. 1) Polynuclear Aromatic Hydrocarbons, Chemistry, Metabolism, and Carcinogenesis", R.I. Freudenthal and P.W.Jones, (eds.) Raven Press, 209-223.

Daisey, J.M., Cheney, J.L. and Lioy, P.J. (1986) Profiles of organic particulate emissions from air pollution sources: Status and needs for receptor source apportionment modeling. Journal of the Air Pollution Control Association, 36, 1, 17-33.

Dastillung, M. and Albrecht, P. (1976) Molecular test for oil pollution in surface sediments. Marine Pollution Bulletin, 7, 13-15.

Davies, J.I. and Evans, W.C. (1964) Oxidative metabolism of naphthalene by soil pseudomonads. Biochemical Journal, 91, 251-261.

DeAngelis, D.G., Ruffin, D.S. and Beznik, R.B. (1980) Preliminary characterizations of emissions from woodfired residential combustion. EPA-600/7-80-040, Washington, D.C..

Deines, P. (1980) The isotopic composition of reduced organic carbon. In "Handbook of Environmental Isotope Geochemistry" (Vol.1) P. Fritz, and J. Fontes, (eds.) Elsevier, 329-406.

DesMarais, D. and Hayes, J.M. (1976) Tube cracker for opening glass-sealed ampoules under vacuum. Analytical Chemistry, 48, 1651-1652.

De Wiest, F. and Della-Fiorentina H. (1975) Suggestion for a relative definition of an air quality index, relative to hydrocarbonaceous matter associated with air-borne particulates. Atmospheric Environment, 9, 951-954.

Di Lorenzo, A. and Polletta, A. (1987) Emissions of PAH from a light-duty diesel car as a function of the engine operating conditions: A possible approach for investigating the parameters affecting formation of toxic components in soot. In "Polynuclear Aromatic Hydrocarbons: Measurements, Means and Metabolism", M. Cooke, K. Loening and J. Merrit (eds.), Eleventh International Symposium, Battelle Press, 239-258.

Dunstan, T.D. J., Mauldin, R.F., Jinxian, Z., Hipps, A.D., Wehry, E.L. and Mamantov, G. (1989) Adsorption and photodegradation of pyrene on magnetic carbonaceous and mineral sub-fractions of coal stack ash. Environmental Science and Technology, 23, 303-313.

Eakin, P.A., Fallick, A.E. and Gerc, J. (1992) Some instrumental effects in the determination of stable carbon isotope ratios by gas chromatography-isotope ratio mass spectrometry. Chemical Geology (Isotope Geoscience Section), 101, 71-79.

Eganhouse, R.P. and Kaplan, I.R. (1982) Extractable organic matter in municipal wastewater. 2. Hydrocarbons: molecular characterization. Environmental Science and Technology, 16, 541-551.

Ehrhardt, M.G. and Petrick, G. (1984) On the sensitized photo-oxidation of alkylbenzenes in seawater. Marine Chemistry, 15, 47-48.

Ehrhardt, M.G., Burns, K.A. and Bicego, M.C. (1992) Sunlight-induced compositional alterations in the seawater-soluble fraction of a crude oil. Marine Chemistry, 37, 53-64.

Ehrhardt, M.G., Klungsoyr, J. and Law, R.J. (1991) Hydrocarbons: Review of methods for analysis in sea water, biota, and sediments. Techniques in Marine Environmental Science, International Council for the Exploration of the Sea, 12, 1-41.

Evans, K.M., Gill, R.A. and Robotham, P.W.J. (1990) The source, composition and flux of PAH in sediments of the river Derwent, Derbyshire, U.K.. Water, Air and Soil Pollution, 51, 1-12.

Evans, W.C. (1977) Biochemistry of the bacterial catabolism of aromatic compounds in anaerobic environments. Nature, 270, 17-19.

Fangmark, I., Van Bavel, B., Marklund, S., Stromberg, B., Berge, N. and Rappe, C. (1993) Influence of combustion parameters on the formation of polychlorinated dibenzo-p-dioxins, dibenzofurans, benzenes, and biphenyls and polyaromatic hydrocarbons in a pilot incinerator. Environmental Science and Technology, 27, 1602-1610.

Farrington, J.W. and Tripp, B.W. (1975) A comparison of analysis methods for hydrocarbons in surface sediments. In "Marine Chemistry in the Coastal Environment", T.M. Church (Ed.) American Chemical Society, Washington, D.C., 269-289.

Foster, G.D. and Wright, D.A. (1988) Unsubstituted polynuclear aromatic hydrocarbons in sediments, clams and clams worms from Chesapeake Bay. Marine Pollution Bulletin, 19, 459-465.

Freedman, P.A., Gillyon, E.C.P. and Jumeau, E.J. (1988) Design and application of a new instrument for GC-Isotope ratio MS. American Laboratory, 8, 114-119.

Freeman, D.J. and Cattell, F.C.R. (1990) Woodburning as a source of PAH Environmental Science and Technology, 24, 1581-1585.

Freeman, K.H., Hayes, J.M., Trendal, J.M. and Albrecht, P. (1990) Evidence from carbon isotope measurements for diverse origins of sedimentary hydrocarbons. Nature, 343, 254-255.

Freeman, K.H. (1991) The carbon isotopic composition of individual compounds from ancient and modern depositional environments. PhD thesis, Indiana University, 9-92.

Freyer, H.D. and Belacy, N. (1983) $^{13}C/^{12}C$ records in Northern Hemispheric trees during the past 500 years-anthropogenic impact and climatic superpositions. Journal of Geophysical Research, 88, C11, 6844-6852.

Fuex, A.N. (1977) The use of stable isotopes in hydrocarbon exploration. Journal of Geochemical Exploration, 7, 155-188.

Fusey, P. and Oudot, J. (1984) Relative influence of physical removal and biodegradation in the depuration of petroleum-contaminated seashore sediments. Marine Pollution Bulletin, 15, 136-141.

Gearing, J.N., Buckley, D.E. and Smith, J.N. (1991) Hydrocarbon and metal contents in a sediment core from Halifax harbour: A chronology of contamination. Canadian Journal of Fisheries and Aquatic Science, 48, 2344-2354.

Gearing, P.J., Gearing, J.N., Pruell, R.J., Wade, T.L., Quinn, J.G., (1980). Partitioning of no.2 fuel oil in controlled estuarine ecosystems, sediments and suspended particulate matter. Environmental Science and Technology, 14, 1129-1136.

GESAMP (1993) Impact of oil and related chemicals on the marine environment. IMO/FAO/UNESCO/WMO/WHO/IAEA/UN/UNEP/ Joint Group of Experts on the Scientific Aspects of Marine Pollution, Report and Studies No. 50, 66-82.

Ghosh, D.K. and Mishra, A.K. (1983) Oxidation of phenanthrene by a strain of *Micrococcus*: evidence of protoacechuate pathway. Current Microbiology, 9, 219-224.

Gibson, D.T., Mahadevan, V., Jerina, D.M., Yagi, H. and Yeh, H.J. (1976) Oxidation of the carcinogens benzo(a)pyrene and benz(a)anthracene to didihydrodiols metabolites of phenanthrene. Science, 189, 295-297.

Giger, W. and Schaffner, C. (1978) Determination of polycyclic aromatic hydrocarbons in the environment by glass capillary gas chromatography. Analytical Chemistry, 50, 2, 243-249.

Gleason, J.D. and Kyser, T.K. (1984) Stable isotope compositions of gases and vegetation near naturally burning coal. Nature, 307, 254-257.

Goldstein, I.S. (1991) Overview of the chemical composition of wood. In "Wood structure and composition ", M. Lewin, and I.S. Goldstein, (eds.) Marcel Dekker Inc., 1-8.

Goni, M.A., Eglinton, T.I. and Boon, J.J. (1993) Compound-specific isotope analysis of lignin-derived phenols from plant tissues and sediments. In "Organic Geochemistry, Poster sessions from the 16th International Meeting on Organic Geochemistry, Stavanger", K. Oygard (ed.) 539-543.

Goodman, K.J. and Brenna, T.J. (1992) High sensitivity tracer detection using high-precision gas chromatography-combustion isotope ratio mass spectrometry and highly enriched [U-^{13}C]-labeled precursors. Analytical Chemistry, 64, 1088-1095.

Gordon, R.J., (1976). Distribution of airborne polycyclic aromatic hydrocarbons throughout Los Angeles. Environmental Science and Technology, 10, 370 - 373.

Grimalt, J., Marfil, C. and Ablaiges, J. (1984) Analysis of hydrocarbons in aquatic sediments, I. Sampling, handling and extraction. International Journal of Analytical Chemistry, 18, 183-194.

Grimmer, G. and Duevel, D. (1970) Biosynthetic formation of polycyclic hydrocarbons in higher plants VIII. Carcinogenic hydrocarbons in human environment, Z. Naturforsch. Wiss., 25 B, 1171-1175

Grimmer, G. and Bohnke, H. (1978) Polycyclic aromatic-hydrocarbons and heterocycles. Erdol Kolhe Erdgas Petrochemical, 31, 272-277.

Grimmer, G., Jacob, J., Naujack, K.W. and Dettbarn, G. (1983a) Determination of polycyclic aromatic compounds emitted from brown-coal-fired residential stoves by GC-MS. Analytical Chemistry, 55, 892-900.

Grimmer, G., Jacob, J., and Naujack, K.W. (1983b) Profile of the polycyclic aromatic compounds emitted from crude oils, Part 3. Inventory by GC/GC-MS.- PAH in Environmental Materials by GC-MS. Fresenius Analytical Chemistry, 314, 29-36.

Grosjean, D., Funk, K. and Harrison, J. (1983) Interactions of polycyclic aromatic hydrocarbons with atmospheric pollutants. Environmental Science and Technology, 17, 673-681.

Gross, G.P. (1974) Gasoline combustion and vehicle exhaust gas polynuclear aromatic content. Fourth Annual Report, CRC-APRAC Project CAPE-6-68, Coordinating Research Council, Inc., NY.

Grover, S.N., Pruppacher, H.R. and Hamielec, A.C. (1977) A numerical determination of the efficiency with which spherical aerosol particulates collide with spherical water drops due to intertial impaction and phoretic and electrical forces. Journal of Atmospheric Sciences, 34, 1655-1663.

Gschwend, P.M. and Hites, R.A. (1981) Fluxes of polycyclic aromatic hydrocarbons to marine and lacustrine sediments in the northeastern United States. Geochimica et Cosmochimica Acta, 45, 2359-2367.

Guerin, M.R. (1978) Energy sources of polycyclic aromatic hydrocarbons. In "Polycyclic Hydrocarbons and Cancer (Vol. 1) Environment, Chemistry and Metabolism", H.V. Gelboin & P.O. TS'O (eds.) Academic Press, 1-42.

Guerin, W.F. and Jones, G.E. (1988) Mineralization of phenanthrene by a *Mycobacterium* sp.. Applied Environmental Microbiology, 54, 937-944.

Guo, Z.K., Luke, A.H., Lee, W.P. and Scholler, D. (1993) Compound-specific carbon isotope ratio determination of enriched cholesterol. Analytical Chemistry, 65, 1954-1959.

Halaby, G.A. and Fagerson, I.S. (1971) Polynuclear aromatic hydrocarbons in heat-treated foods-pyrolysis of some lipids, beta-carotene, and cholesterol. Proceedings of the third International Congress of Food Science and Technology, 820-829.

Hallett, D.J. and Brecher, R.W. (1984) Cycling of polynuclear aromatic hydrocarbons in the great lakes ecosystem. In "Toxic Contaminant in the Great Lakes", J. Wiley & Sons, 221-237.

Hambrick, G.A., DeLaune, R.D. and Patrick, W.H. (1980) Effect of estuarine sediment pH and oxidation-reduction potential on microbial hydrocarbon degradation. Applied Environmental Microbiology, 40, 365-369.

Hangebrauck, R.P, Von Lehmden, D.J. and Meeker, J.E. (1967) Emissions of polynuclear hydrocarbons and other pollutants from heat generation and incineration processes. Journal of Air Pollution Control Association, 14, 267-278.

Hase, A. and Hites, R.A. (1976) On the origins of polycyclic aromatic hydrocarbons in recent sediments: Biosynthesis by anaerobic bacteria. Geochimica et Cosmochimica Acta, 40, 1141-1143.

Hayes, J.M., Freeman, K.H., Popp, B.N. and Hoham, C.H. (1989) Compound-specific isotopic analysis: A novel tool for reconstruction of ancient biogeochemical processes. Advances in Organic Geochemistry, 16, 4-6, 1115-1128.

Heitkamp, M.A. and Cerniglia, C.E. (1987) Effects of chemical structure and exposure on microbial degradation of polycyclic aromatic hydrocarbons in freshwater and estuarine ecosystems. Environmental Toxicology and Chemistry, 6, 535-546.

Hellou J., Upshall C., Ni I. H., Payne J. F. and Huang Y. S. (1991) Polycyclic aromatic hydrocarbons in harp seals (*Phoca groenlandica*) from the Northwest Atlantic. Archives of Environmental Contamination and Toxicology, 21, 135-140.

Herbes, S.E. and Schwall, L.R. (1978) Microbial transformation of polycyclic aromatic hydrocarbons in pristine and petroleum-contaminated sediments. Applied Environmental Microbiology, 35, 306-316.

Herrmann, R. (1981) Transport of polycyclic aromatic hydrocarbons through a partly urbanized river basin. Water, Air and Soil Pollution, 16, 445-467.

Hiereth, H. (1988) Investigation of the mechanism of soot formation in the diesel engine. Government-Reports-Announcements-and-index-(GRA&I),-Issue-02.

Hilpert, L.R., May, W.E., Wise, S.A., Chesler, S.N., and Hertz, H.S. (1978 Interlaboratory comparison of determinations of trace level petroleum hydrocarbons in marine sediment. Analytical Chemistry, 50, 458-463.

Hinga, K.R. (1984) The fate of polycyclic aromatic hydrocarbons in enclosed marine ecosystems. Ph.D thesis, University of Rhode Island.

Hoffman, E.J., Mills, G.L., Latimer, J.S. and Quinn, J.G. (1984) Urban runoff as a source of polycyclic hydrocarbons to coastal environments. Environmental Science and Technology, 18, 580-587.

Holt, B. and Abrajano, T.A. (1991) Chemical and isotopic alteration of organic matter during stepped combustion. Analytical Chemistry, 63, 2973-2978.

Howard, J.B. and Longwell, J.P. (1983) Formation mechanisms of PAH and soot in flames. In "Polynuclear Aromatic Hydrocarbons: Formation, Metabolism and Measurements", M. Cooke, A.J. Dennis (eds.), Seventh International Symposium, Battelle Press, 27-62.

Hucknall, D.J. (1985) In "Chemistry of hydrocarbon combustion", Chapman and Hall, London, 1-30.

Huggett, R.J., De Fur, P.O. and Bieri, R.H. (1988) Organic compounds in Chesapeake Bay sediments. Marine Pollution Bulletin, 19, 454-458.

Hwang, H.M., Hodson, R.E. and Lee, R.F. (1987) Photolysis of phenol and chlorophenols in estuarine waters. In "Photochemistry of Environmental Aquatic Systems". Americam Chemical Society, Washington D.C.

Jeffrey, A.M., Yeh, H.J., Jerina, D.M., Patel, T.R., Davey, J.F. and Gibson, D.T. (1975) Initial reactions in the oxidation of naphthalene by *Pseudomonas putida*. Biochemistry, 14, 575-584.

Jensen, T.E. and Hites, R.A. (1983) Aromatic diesel emissions as a function of engine conditions. Analytical Chemistry, 55, 594-599.

Jerina, D.M., Slander, H., Yagi, H., Wells, M.C., Davey, J.F., Mahadevan, V. and Gibson, D.T. (1976) Dihydrodiols from anthracene and phenanthrene. Journal American Chemical Society, 98, 5988-5994.

Johnson, A.C., Larsen, P.F., Gadbois, D.F. and Humanson, A.W. (1985) The distribution of polycyclic aromatic hydrocarbons in the surficial sediment of Penobscot Bay (Maine, USA) in relation to possible sources and to other sites worldwide. Marine Environmental Research, 15, 1-16.

Junge, C.E. (1977) Basic considerations about trace constituents in the atmosphere as related to the fate of global pollution. Advances Environmental Science and Technology, 8, 1, 7-25.

Kamens, R.M., Fulcher, J.N. and Zhishi, G. (1986) Effect of temperature on wood soot PAH decay in atmosphere with sunlight and low NO_x. Atmospheric Environment, 20, 1579-1583.

Kamens, R.M., Guo, Z., Fulcher, J.N. and Bell, D.A. (1988) Influence of humidity, sunlight, and temperature on the daytime decay of polyaromatic hydrocarbons on atmospheric soot particles. Environmental Science and Technology, 22, 1, 103-108.

Kamens, R.M., Guo, J., Guo, Z. and McDow, S.R. (1990) PAH degradation by heterogenous reactions with N_2O_5 atmospheric particles. Atmospheric Environment, 24A, 1161-1173.

Kanury, A.M. (1976) In "Introduction to Combustion Phenomena", Gordon and Breach Science Publishers, 195-216.

Karickhoff, S.W., Brown, D.S., and Scott, T.A. (1979) Sorption of hydrophobic pollutants on natural sediments, Water Research, 13, 241-248.

Kennicutt II, M.C., Denoux, G.J. and McDonald, S.J. (1992) Hydrocarbon contamination on the Antarctic Peninsula, I. Arthur Harbor-Subtidal sediments. Marine Pollution Bulletin, 24, 10, 499-506.

Kennicutt II, M.C., Brooks, J.M. and McDonald, T.J. (1991) Origins of hydrocarbons in Bering Sea sediments-I. Aliphatic hydrocarbons and fluorescence. Organic Geochemistry, 17, 1, 75-83.

Khan, A.U., Pitts, Jr., J.N. and Smith, E.B. (1967) Singlet oxygen in the environmental sciences: The role of singlet molecular oxygen in the production of photochemical air pollution. Environmental Science and Technology, 1, 656-658.

Killops, S.D. and Howell, V.J. (1988) Sources and distribution of hydrocarbons in Bridgewater Bay (Severn Estuary, U.K.) Intertidal Surface Sediments. Estuarine, Coastal and Shelf Science, 27, 237-261.

Killops, S.D. and Al-Juboori, M.A.H.A. (1990) Characterization of the unresolved complex mixture (UCM) in the gas chromatograms of biodegraded petroleums. Organic Geochemistry, 15, 2, 147-161.

Killops, S.D. and Massoud, M.S. (1992) Polycyclic aromatic hydrocarbons of pyrolytic origin in ancient sediments: evidence for Jurassic vegetation fires. Organic Geochemistry, 18, 1, 1-7.

Kirso, U., Paalme, L., Voll, M., Urbas, E. and Irha, N. (1990) Accumulation of carcinogenic hydrocarbons at the sediment-water interface. Marine Chemistry, 30, 337-341.

Kiyohara, H. and Nagao, K. (1978) The catabolism of phenanthrene and naphthalene by bacteria. Journal General Microbiology, 105, 69-75.

Kiyohara, H., Nagao, K., Kuono, K., and Yano, K. (1982) Phenanthrene degrading phenotype of *Alcaligens faecalis* AFK2. Applied Environmental Microbiology, 43, 458-464.

Klamer, J.C., Hull, R.N., Laane, R.W. and Eisma, D. (1990) The distribution of heavy metals and polycyclic aromatic hydrocarbons in the sediments of the oyster grounds (North Sea). Netherlands Journal of Sea Research, 26, 1, 83-87.

Korfmacher, W.A., Wehry, E.L., Mamantov, G. and Natusch, D.F.S. (1980) Resistance to photochemical decomposition of polycyclic aromatic hydrocarbons vapour-adsorbed on coal fly ash. Environmental Science and Technology, 14, 1094-1099.

Korte, F. and Boedefeld, E. (1978) Ecotoxicological review of global impact of petroleum industry and its products. Ecotoxicology and Environmental Safety, 2, 55-103.

Laflamme, R.E. and Hites, R.A. (1978) The global distribution of polycyclic aromatic hydrocarbons in recent sediments. Geochimica et Cosmochimica Acta., 42, 289-303.

Lake, J.L., Norwood, C., Dimock, D. and Bowen, R. (1979) Origins of polycyclic aromatic hydrocarbons in estuarine sediments. Geochimica et Cosmochimica Acta, 43, 1847-1854.

Lake, J.L., Dimock, D., and Norwood, C. (1980) A comparison of methods for the analysis of hydrocarbons in marine sediments, Advance Chemistry Series, 185, 343-360.

Lane, D.A. (1989) The fate of polycyclic aromatic compounds in the atmosphere during sampling. In "Chemical Analysis of Polycyclic Aromatic Compounds", Chemical Analysis Series (Vol. 101) T. Vo-Dinh (ed) A Wiley-Interscience Publication, 31-58.

Lang, K.F., Buffleb, H. and Zander, M. (1963) Pyrolysis of polycyclic aromatic hydrocarbons. Erdol Und Kohle, 16, 944-946.

Langmuir, C.H., Vocke, Jr, R.D., Hanson, G.N. and Hart, S.R. (1978) A general mixing equation with applications to Icelandic basalts. Earth and Planetary Science Letters, 37, 380-392.

Larsen, P.F., Gadbois, D.F., Johnson, A.C. and Dogget, L.F. (1983) Distribution of polycyclic aromatic hydrocarbons in the surficial sediment of Casco Bay Maine. Bulletin of Environmental Contamination and Toxicology, 30, 530-535.

Latimer, J.S., Hoffman, E.J., Hoffman., G., Fasching, J.L. and Quinn, J.G. (1990) Sources of petroleum hydrocarbons in urban runoff. Water, Air and Soil Pollution, 52, 1-21.

Leahy, J.G. and Colwell, R.R. (1990) Microbial degradation of hydrocarbons in the environment. Microbiological Reviews, 54, 3, 305-315.

Leavitt, S.W. and Long, A. (1986) Stable-carbon isotope variability in tree foliage and wood. Ecology, 67, 4, 1002-1010.

Leavitt, S.W. (1993) Seasonal $^{13}C/^{12}C$ changes in tree rings: species and site coherence, and a possible drought influence. Canadian Journal for Research, 23, 210-218.

Lee, R.F. and Ryan, C. (1976) Biodegradation of petroleum hydrocarbons by marine microbes. In "Proceeding of the Third International Biodegradation Symposium", J.M. Sharpley and A.M. Kaplan (eds.), Applied Science Publishers, 119-125.

Lee, R.F. and Anderson, J.W. (1977) Fate and effects of naphthalenes: controlled ecosystem pollution experiment. Bulletin Marine Science, 27, 127-134.

Lee, R.F., Gardner, W.S., Anderson, J.W., Blaylock, J.W. and Barwell, C.J. (1978) Fate of polycyclic aromatic hydrocarbons in controlled ecosystems enclosures. Environmental Science and Technology, 12, 832-838.

Lee, M.L., Novotny, M.V. and Bartle, K.D. (1981). Analytical Chemistry of Polycyclic Aromatic Compounds. Academic Press, NY, London.

Leuenberger, C., Czuczwa, J., Heyerdahl, E. and Giger, W. (1988) Aliphatic and polycyclic aromatic hydrocarbons in urban rain, snow and fog. Atmosphere Environment, 22, 4, 695-705.

Lichtenthaler, R.G., Oreld, F. Sporstol, S. and Vogt, N.B. (1986) Comparison of extraction methods for the analysis of oily drill cuttings. Proc. Conf. on oil based drilling fluids: Cleaning and Environmental Effects of Oil Contaminated Drill Cuttings. Trondheim, Norway, 24-26, 100-102.

Lima-Zanghi, C. (1968) Bilan des acides gras du Plancton marin et pollution par le benzo-3,4 pyrene. Cah. Oceanographic, 20, 203-216.

Lipiatou, E. and Saliot, A. (1991) Fluxes and transport of anthropogenic and natural polycyclic aromatic hydrocarbons in the western Mediterranean Sea. Marine Chemistry, 32, 51-71.

Lipiatou, E. and Saliot, A. (1992) Biogenic aromatic hydrocarbon geochemistry in the Rhone River Delta and in surface sediments from the open North-Western Mediterranean Sea. Estuarine, Coastal and Shelf Science, 34, 515-531.

Liverovskii, A.A., Shmulevskaya, E.I., Romanovskaya, L.S., Pankina, E.I., Kun, NV, Dikun, P.P. and Kostenko, L.D. (1972) Formation of 3,4-benzopyrene during the pyrogenic decomposition of lignins and terpenes. Izv. Vyssh. Uchebn. Zaved. Lesn. Zh., 15, 99-103.

Low, G.K.C., Batley, G.E. and Brockbank, C.I. (1987) Solvent-induced photodegradation as a source of error in the analysis of polycyclic aromatic hydrocarbons. Journal of Chromatography, 392, 199-210.

Lowdon, J.A. and Dyck, W. (1974) Seasonal variations in the isotope ratios of carbon in maple leaves and other plants. Canadian Journal Earth Science, 11, 79-88.

Ludwig, B., Hussler, G., Wehrung, P. and Albrecht, P. (1981) C_{26}-C_{29} Triaromatic steroid derivatives in sediments and petroleums. Tetrahedron Letters, 22, 34, 3313-3316.

Mackenzie, A.S. (1984) Application of biological markers in petroleum geochemistry. Advances in Petroleum Geochemistry, 1, 115-214.

Macko, S.A., Leskey, T., Ryan, M. (1992) Carbon isotopic analysis of individual carbohydrates by GC/IRMS. Proceedings of the 203rd American Chemical Society Meeting, San Francisco, Ca., abstract # 107.

MacLeod, Jr., W.D., Prohaska, P.G., Gennero, D.D. and Brown, D.W. (1982) Interlaboratory Comparisons of selected trace hydrocarbons in Marine sediments. Analytical Chemistry, 54, 386-392.

MacLeod, Jr.,W.D., Friedman, J. and Brown, D.W. (1988) Improved interlaboratory comparisons of polycyclic aromatic hydrocarbons in marine sediments. Marine Environmental Research 26, 209-221.

Maher, W.A. and Aislabie, J. (1992) Polycyclic aromatic hydrocarbons in nearshore marine sediments of Australia. Science of the Total Environment, 112, 143-164.

Mair, B.J. and Martinez-Pico, J.L. (1962) Composition of trinuclear aromatic portion of the heavy gas oil and lubricating distillate. Proceedings of the American Petroleum Institute. 42, Section 3, 173-185.

Mair, B.J. (1964) Terpenoids, fatty acids and alcohols as source materials for petroleum hydrocarbons. Geochimica et Cosmochimica Acta, 28, 1303-1321.

Maja, J.A. (1986) Polycyclic aromatic hydrocarbons (PAH) composition of mesquite (*Prosopis fuliflora*) smoke and grilled beef. Journal of Agriculture, Food and Chemistry, 34, 2, 249-250.

Martel, L., Gagon, M.J., Masse, R., Leclerc, A. and Tremblay, L. (1986) Polycyclic aromatic hydrocarbons in sediments from the Saguenay Fjord, Canada. Bulletin of Environmental Contamination and Toxicology, 37, 133-140.

Masclet, P., Mouvier, G. and Nikolaou, K. (1986) Relative decay index and sources of polycyclic aromatic hydrocarbons. Atmosphere Environment, 20, 439-447.

Masuda, Y., Mori, K., and Kuratsune, M. (1967) Polycyclic aromatic hydrocarbons formed by pyrolysis of carbohydrates, amino acids, and fatty acids. Gann, 58, 69-74.

Matthews, D.E. and Hayes, J.M. (1978) Isotope-ratio-monitoring gas chromatography mass spectrometry. Analytical Chemistry, 50, 1465-1473.

May, W.E., Wasik, S.P. and Freeman, D.H. (1978) Determination of the solubility behaviour of some polycyclic aromatic hydrocarbons in water. Analytical Chemistry, 50, 997-1000.

McCarty, P.L., Rittmann, B.E. and Bouwer, E.J. (1984) Microbial processes affecting chemical transformations in groundwater. In "Groundwater Pollution Microbiology", G. Bitton and C.P. Gerba (eds.), John Wiley & Sons, NY., 89-115.

McCrillis, R.C., Watts, R.R. and Warren, S.H. (1992) Effects of operating variables on PAH emissions and mutagenicity of emissions from woodstoves. Journal of Air and Waste Management Association, 42, 5, 691-694.

McElroy, A.E., Farrington, J.W. and Teal, J.M. (1985) Bioavailability of polycyclic aromatic hydrocarbons in the aquatic environment. In "Metabolism of Polycyclic Aromatic Hydrocarbons in the Aquatic Environment", U. Varanasi (ed.) CRC Press, Inc., 2-33.

McVeety, B.D. and Hites, R.A. (1988) Atmospheric deposition of polycyclic aromatic hydrocarbons to water surfaces: A mass balance approach. Atmospheric Environment, 22, 3, 511-536.

Means, J.C. and Wijayaratne, R. (1982) Role of natural colloids in the transport of hydrophobic pollutants. Science, 215, 968-970.

Melander, L. and Saunders, Jr. W.H. (1980) Carbon isotope effects. In "Reaction Rates of Isotopic Molecules", A Wiley-Interscience Publication, John Wiley & Sons, NY., 225-255.

Merritt, D.A., Ricci, M.P. and Hayes, J.M. (1992) Compound-specific isotopic analysis: isotopic calibration, background correction and peak deconvolution. Proceedings of the 203rd American Chemical Society Meeting, San Francisco, Ca., abstract # 92.

Mille, G., Mulyono, M., Eljammal, T. and Bertrand, J.C. (1988) Effects of oxygen on hydrocarbon degradation studies *in vitro* in surficial sediments. Estuarine Coastal and Shelf Science, 27, 283-295.

Mitra, S. and Wilson, N.K. (1992) Pattern of polycyclic aromatic hydrocarbons in indoor air: Exploratory principal component analysis. Environment International, 16, 5, 477-487.

Morel, G., Samhan, O., Literathy, P., Al-Hashash, H., Moulin, L., Saeed, T., Al-Matourk, K., Martin-Bouyer, M., Saber, A., Paturel, L., Jarosz, J., Vial. M., Combet, E., Fachinger, C. and Suptil, J. (1991) Evaluation of chromatographic and spectroscopic methods for the analysis of petroleum-derived compounds in the environment. Fresenius Journal of Analytical Chemistry, 339, 699-715.

Mueller, J.G., Chapman, P.J. and Pritchard, P.H. (1988) Action of a fluoranthene-utilizing bacterial community on polycyclic aromatic hydrocarbons components of Creosote. Applied Environmental Microbiology 55, 12, 3085-3090.

Mueller, J.G., Chapman, P.J., Blattmann, B.O. and Pritchard, P.H. (1990) Isolation and characterization of a fluoranthene-utilizing strain of *Pseudomonas paucimobilis*. Applied Environmental Microbiology, 56, 4, 1079-1086.

Naf, C., Broman, D., Pettersen, H., Rolff, C. and Zebuhr, Y. (1992) Flux estimates and pattern recognition of particulate aromatic hydrocarbons, polychlorinated dibenzo-p-dioxins, and dibenzofurans in the waters outside various emissions sources on the swedish baltic coast. Environmental Science and Technology, 26, 7, 1444-1457.

National Research Council (1985) Oil in the sea Inputs, Fates and Effects, National Academy Press, Washington, D.C..

Neff, J.M. (1979) Polycyclic Aromatic Hydrocarbons in the Aquatic Environment. Sources, Fates and Biological Effects. Applied Science Publishers, London.

Newfoundland Design Associates Ltd. (1987-1988) St. John's Harbour water quality study, 4, Government of NFLD & Labrador, Dept., of Municipal Affairs, 1-14.

Niaussat, P., Auger, C. and Mallet, L. (1970) Appearance of carcinogens hydrocarbons in pure *Bacillus bandius* cultures relative to the presence of certain compounds in the medium. C.R. Acad. Science, Paris, 270 D, 1042-1045.

Nielsen, T. (1984) Reactivity of polycyclic aromatic hydrocarbons toward nitrating species. Environmental Science and Technology, 18, 157-163.

Nielsen, T. and Ramdahl, T. (1986) Discussion on "Determination of nitrofluoranthene and 2-nitropyrene in ambient particulate matter: evidence for atmospheric reactions". Atmospheric Environment, 20, 1507-1514.

Novotny, V., Sung, H.M., Bannerman, R. and Baum, K.J. (1985) Estimating non-point pollution from small watersheds. Water Pollution Control Federation, 57, 339-348.

Officer, C.B. and Lynch, D.R. (1989) Bioturbation, sedimentation and sediment-water exchanges. Estuarine Coastal Shelf Science, 28, 1-12.

O'Malley, V.P., Abrajano, Jr., T.A. and Hellou, J. (1994) Determination of the $^{13}C/^{12}C$ ratios of individual PAH from environmental samples: Can PAH sources be apportioned?. Organic Geochemistry (in press).

Ostman, C.E. and Colmsjo, A.L.0 (1988) A laboratory method for the assessmeent of polycyclic aromatic hydrocarbons emissions from heated bitumen. Proceeding of the 10th International Symposium on PAH. Battelle Press, Columbus Ohio, 673-685.

Ostrom, N.E. (1992) Biogeochemical cycling of carbon and nitrogen in Conception Bay, Newfoundland. PhD thesis, Memorial University of Newfoundland, 89-113.

Ostrom, P.H. and Bakel, A. (1992) Maintenance of isotopic integrity during isolation of individual alkanes and during addition of a background signal from the maltene fraction of an oil. Proceedings of the 203rd American Chemical Society Meeting, San Francisco, Ca., abstract # 94.

Paalme, L., Irha, N., Urbas, E., Tsyban, A. and Kirso, U. (1990) Model studies of photochemical oxidation of carcinogenic polyaromatic hydrocarbons. Marine Chemistry, 30, 105-111.

Page, E.B. (1963) Ordered hypotheses for multiple treatments: A significant test for multiple ranks. Journal of the American Statistical Association, 58, 216-230.

Pancirov, R.J. and Brown, R.A. (1975) Analytical methods for PAH in crude oils, heating oils and marine tissues. Conference Proceedings on prevention and control of oil pollution, Washington, D.C., API., 103-113.

Payne, J.R. and Phillips, C.R. (1985) Photochemistry of petroleum in water. Environmental Science and Technology, 19, 569-579.

Pedersen, P.S., Ingwersen, J., Nielsen, T. and Larsen, E. (1980) Effects of fuel, lubricant, and engine operating parameters on the emission of polycyclic aromatic hydrocarbons. Environmental Science and Technology, 14,1, 71-79.

Petrasek, A.C., Kugelman, I.J., Austern, B.M., Pressley, T.A., Winslow, L.A. and Wise, R.H. (1983) Fate of toxic organic compounds in wastewater treatment plants. Journal of Water Pollution Control Federation, 55, 1286-1296.

Pham, T., Lum, K. and Lemieux, C. (1993) Sources of PAH in the St. Lawrence River (Canada) and their relative importance. Chemosphere, 27, 7, 1137-1149.

Pierce, R.C. and Katz, M. (1975) Dependency of polynuclear aromatic hydrocarbon content on size distribution of atmospheric aerosols. Environmental Science and Technology, 9, 347-353.

Pitts, Jr., J.N., Khan, A.U., Smith, B.E. and Wayne, R.P. (1969) Singlet molecular oxygen and photochemical air pollution. Environmental Science and Technology, 3, 3, 241-247.

Pomeroy, L.R., Wiebe, W.J., Diebel, D., Thompson, R.J., Rowe, G.T. and Pakulski, J.D. (1991) Bacterial responses to temperature and substrate concentrations during the Newfoundland spring bloom. Marine Ecology Progress Series, 75, 143-159.

Prahl, F.G. and Carpenter, R. (1979) The role of zooplankton fecal pellets in the sedimentation of polycyclic aromatic hydrocarbons in Dabob Bay, Washington. Geochimica et Cosmochimica Acta, 43, 1959-1972.

Prahl, F.G. and Carpenter, R. (1983) Polycyclic aromatic hydrocarbons (PAH) phase associations in Washington Coastal sediments. Geochimica et Cosmochimica Acta, 47, 1013-1023.

Prahl, F.G. and Carpenter, R. (1984) Polycyclic aromatic hydrocarbons in Washington Coastal sediments. Estuarine, Coastal and Shelf Science, 18, 703-720.

Pruell, J.R., Hoffman E.J. and Ouinn J.G. (1984) Total hydrocarbons, polycyclic aromatic hydrocarbons and synthetic organic compounds in the hard shell clam, *Mercenaria mercenaria*, purchased at commercial seafood stores. Marine Environmental Research, 11, 163-181.

Pruell, J.R. and Quinn, J.G. (1985) Polycyclic Aromatic Hydrocarbons in surface sediments held in experimental mesocosms. Toxicological Environmental Science, 10, 183-200.

Pruell, J.R. and Quinn, J.G. (1988) Accumulation of Polycyclic Aromatic Hydrocarbons in Crankcase Oil. Environmental Pollution, 49, 89-97.

Pruell, J.R., Norwood, C.B., Bowen, R.D., Boothman, W.S., Rogerson, P.F., Hackett, M. and Butterworth, B.C. (1990) Geochemical study of sediment contamination in New Bedford Harbour, Mass. Marine Environmental Research, 29, 77-101.

Radding, S.B., Mill, T., Gould, C.W., Liu, D.H., Johnson, H.L., Bomberger, D.C. and Fojo, C.V. (1976) The environmental fate of selected polynuclear aromatic hydrocarbons. EPA560/5-75-009. US Environmental Protection Agency.

Radke, M. (1987) Organic geochemistry of aromatic hydrocarbons. Advances in Petroleum Geochemistry, 2, 141-207.

Ramdahl, T. (1983a) Retene-a molecular marker of wood combustion in ambient air. Nature, 306, 580-582.

Ramdahl, T. (1983b) PAH emissions from combustion of biomass. In "Handbook of Polycyclic Aromatic Hydrocarbons (Vol.2) Emission Sources and Recent Progress in Analytical Chemistry", A. Bjorseth and T. Ramdahl, (eds.) Marcel Dekker, Inc. 61-85.

Ramos, L.S. and Prohaska, P.G. (1981) Sephadex LH-20 chromatography of extracts of marine sediments and biological samples for the isolation of PAH. Journal of Chromatography, 21, 284-289.

Readman, J.W., Mantoura, R.F.C., Rhead, M.M. and Brown, L. (1982) Aquatic distribution and heterotrophic degradation of polycyclic aromatic hydrocarbons (PAH) in the Tamer Estuary. Estuarine Coastal Shelf Science, 14, 369-389.

Readman, J.W., Mantoura, R.F.C. and Rhead, M.M. (1986) A record of polycyclic aromatic hydrocarbons (PAH) pollution obtained from accreting sediments of the Tamer estuary, U.K. Evidence for non-equilibrium behaviour of PAH. Science of the Total Environment, 66, 73-94.

Rieley, G., Collier, R.J., Jones, D.M., Eglinton, G., Eakin, P.A. and Fallick, A.E. (1991) Sources of sedimentary lipids deduced from stable carbon-isotope analysis of individual compounds. Nature, 352, 426-428.

Rogge, W.F., Hildeman, L.M., Mazurek, M.A. and Cass, G.R. (1993) Sources of fine organic aerosol. 2. Noncatalyst and catalyst-equipped automobiles and heavy-duty diesel trucks. Environmental Science and Technology, 27, 636-651.

Rontani, J.F., Bonin, P. and Giusti, G. (1987) Mechanistic study of interactions between photo-oxidations and biodegradation of n-nonylbenzene in seawater. Marine Chemistry, 22, 1-12.

Rowland, S.J. and Robson, J.N. (1990) The widespread occurrence of highly branched acyclic C_{20}, C_{25} and C_{30} hydrocarbons in recent sediments and biota-A review. Marine Environmental Research, 30, 191-216.

Rudling, L. Ahling, B. and Lofroth, G. (1982) In "Residential Solid Fuels" J.A. Cooper and D. Malek (eds.) Oregen Graduate Center, Beaverton, Oreg., 34.

Sackett, W.M. (1978) Carbon and hydrogen isotope effects during the thermocatalytic production of hydrocarbons in laboratory simulation experiments. Geochimica et Cosmochimica Acta, 42, 571-580.

Saliot, A., Tronczynski, J., Scribe, P. and Letolle, R. (1988) The application of isotopic and biogeochemical markers to the study of the biochemistry of organic matter in a macrotidal estuary, the Loire, France. Estuarine, Coastal and shelf Science, 27, 645-669.

Sanders, G., Jones, K.C. and Taylor, J.H. (1993) A simple method to assess the susceptibility of polynuclear aromatic hydrocarbons to photolytic decomposition. Atmospheric Environment, 27A, 2, 139-144.

Sano, M., Yotsui, Y., Abe, H. and Sasaki, S. (1976) A new technique for the detection of metabolites labelled by the isotope ^{13}C using mass fragmentography. Biomedical Mass Spectrometry, 3, 1-3.

Santschi, P., Hohener, P., Benoit, G. and Buchholtz-ten Brink, M. (1990) Chemical processes at the sediment-water interface. Marine Chemistry, 30, 269-315.

Scheibe, S. (1991) The benthic macrofauna of the deep sublitoral in Conception Bay, Newfoundland, Canada. MSc. thesis, Kiel University, Germany, 1-37.

Schmeltz, I. and Hoffman, D. (1976) Formation of polynuclear aromatic hydrocarbons from combustion of organic matter. In "Carcinogenesis-A Comprehensive Survey (Vol. 1) Polynuclear aromatic hydrocarbons, Chemistry, Metabolism, and Carcinogenesis", R.I. Freudenthal and P.W. Jones (eds.) Raven Press, 225-239.

Schoendorf, T. and Harrmann, R. (1987) Transport and chemodynamics of organic micropollutants and ions during snowmelt. Nordic Hydrology, 18,4-5, 259-278.

Sherrill, T.W. and Sayler, G.S. (1980) Phenanthrene biodegradation in freshwater environments. Applied Environmental Microbiology, 39, 172-178.

Shiaris, M.P. and Jambard-Sweet, D. (1986) Polycyclic aromatic hydrocarbons in surficial sediments of Boston Harbour Mass. USA. Marine Pollution Bulletin, 17, 469-472.

Shiaris, M.P. (1989) Seasonal biotransformation of naphthalene, phenanthrene and benzo(a)pyrene in surficial estuarine sediments. Applied Environmental Microbiology, 55, 1391-1399.

Sicre, M.A., Marty, J.C. and Saliot, A. (1987) Aliphatic and aromatic hydrocarbons in different sized aerosols over the Mediterranean Sea: Occurrence and Origin. Atmospheric Environment, 22, 10, 2247-2259.

Simoneit, B.R.T. and Kaplan, I.R. (1980) Triterpenoids as molecular indicators of paleoseepage in recent sediments of the southern Califorina Bight. Marine Environmental Research, 3, 113-128.

Simoneit, B.R.T. and Mazurek, M.A. (1982) Organic matter of the troposphere-II. Natural background of biogenic lipid matter in aerosols over the rural western United States. Atmospheric Environment, 16, 9, 2139-2159.

Simoneit, B.R.T. (1985) Application of molecular marker analysis to vehicular exhaust for source reconciliations. International Journal Environmental Analytical Chemistry, 22, 203-233.

Simoneit, B.R.T. (1986) Characterization of organic constituents in aerosols in relation to their origin and transport: a review: International Journal of Environmental Analytical Chemistry, 23, 207-237.

Smith, J.N. and Levy, E.M. (1990) Geochronology for polycyclic aromatic hydrocarbon contamination in sediments of the Saguenay Fjord. Environmental Science and Technology, 24, 874-879.

Smith, M.R. (1990) The biodegradation of aromatic hydrocarbons by bacteria. Biodegradation, 1, 191-206.

Smith, M.R., Ewing, M. and Ratledge, C. (1991) The interactions of various aromatic substrates degraded by *Pseudomonas* sp. NCIB 10643: Synergistic inhibition of growth by two compounds which serve as growth substrates. Applied Microbiology Biotechnology, 34, 536-538.

Socha, S.B. and Carpenter, R. (1987) Factors affecting pore water hydrocarbon concentrations in Puget Sound Sediments. Geochimica et Cosmochimica Acta, 51, 1273-1284.

Sofer, Z. (1980) Preparation of carbon dioxide for stable carbon isotope analysis of petroleum fractions. Analytical Chemistry, 52, 1389-1391.

Sofer, Z. (1984) Stable carbon isotope compositions of crude oils: Application to source depositional environments and petroleum alteration. The American Association of Petroleum Geologists Bulletin, 68, 1, 31-48.

Speers, G.C. and Whitehead, E.V. (1969) Crude Petroleum. In "Organic Geochemistry", G. Eglinton and M.T.J. Murphy (eds.) Springer-Verlag NY-Heidelberg-Berlin, 638-667.

Spies, R.B., Andresen, B.D. and Rice, D.W. (1987). Benzthiazoles in estuarine sediments as indicators of street runoff. Nature, 327, 697-699.

Sporstol, S., Gjos, N., Lichtenthaler, R.G., Gustavsen, K.O., Urdal, K., Oreld, F. and Skel, J. (1983) Source identification of aromatic hydrocarbons in sediments using GC-MS. Environmental Science and Technology, 17, 5, 282-286.

Stahl, W.J. (1980) Compositional changes and $^{13}C/^{12}C$ fractionations during the degradation of hydrocarbons by bacteria. Geochimica et Cosmochimica Acta 44, 1903-1907.

Standley, L.J. and Simoneit, B.R.T. (1987) Characterization of extractable plant wax, resin, and thermally matured components in smoke particles from prescribed burns. Environmental Science and Technology, 21, 163-169.

Stenberg, U.R. (1983) PAH Emissions from Automobiles. In "Handbook of Polycyclic Aromatic Hydrocarbons (Vol.2) Emission, Sources and Recent Progress in Analytical Chemistry", A. Bjorseth and T. Ramdahl, (eds.) Marcel Dekker, Inc., 87-111.

Steinhauer, M.S. and Boehm, P.D. (1992) The composition and distribution of saturated and aromatic hydrocarbons in nearshore sediments, river sediments, and coastal peat of the Alaskan Beaufort Sea; Implication for detecting anthropogenic hydrocarbon inputs. Marine Environmental Research, 33, 223-253.

Streuli, C.A. (1971) The effects of solvent change on the separation processes of Sephadex LH-20 modified dextran. Journal of Chromatography, 56, 225-229.

Suess, M.J. (1976) The environmental load and cycle of polycyclic aromatic hydrocarbons. Science of the Total Environment, 6, 239-250.

Takada, H., Onda, T. and Ogura, N. (1990) Determination of polycyclic aromatic hydrocarbons in urban street dusts and their source materials by capillary gas chromatography. Environmental Science and Technology, 24, 8, 1179-1186.

Talarico, P.C., Albaugh, E.W. and Snyder, R.E. (1965) Separation of paraffinic classes in petroleum distillates on a cross-linked dextran. Analytical Chemistry, 3 7 , 2192-2194.

Tan, Y.L. and Heit, M. (1981) Biogenic and abiogenic polynuclear aromatic hydrocarbons in sediments from two remote Adirondack lakes. Geochimica et Cosmochimica Acta, 45, 2267-2279.

Tan, Y.L., Quanci, J.F., Borys, R.D. and Quanci, M.J. (1992) Polycyclic aromatic hydrocarbons in smoke particles from wood and duff burning. Atmosphere Environment, 26A, 6, 1177-1181.

Tissier, M.J. and Saliot, A. (1983) Pyrolytic and naturally occurring polycyclic aromatic hydrocarbons in the marine environment. Advances in Organic Geochemistry, John Wiley & Sons Ltd., 268-278.

Tuominen, J., Salomaa, S., Pyysalo, H., Skytta, E., Tikkanen, L., Nurmela, T., Sorsa, M., Pohojla, V., Sauri, M. and Himberg, K. (1988) Polynuclear aromatic compounds and genotoxicity in particulate and vapor phases of ambient air: Effects of traffic, season and meteorological conditions. Environmental Science and Technology, 22, 1228-1234.

Uthe, J.F. (1991) Polycyclic Aromatic Hydrocarbons in the Environment. Canadian Chemical News, 45, 7, 25-27.

Valerio, F. and Lazzarotto, A. (1985) Photochemical degradation of PAH in real and laboratory conditions. International Journal of Environmental Analytical Chemistry, 23, 135-156.

Van Cauwenberghe, K.A.V. (1983) Atmospheric Reactions of PAH. In "Handbook of Polycyclic Aromatic Hydrocarbons (Vol.2) Emission Sources and Recent Progress in Analytical Chemistry", A. Bjorseth and T. Ramdahl (eds.) Marcel Dekker, Inc., 351-384.

Van Hook, W.A. (1969) Isotope separation by gas chromatography. In "Isotope effects in Chemical Processes", R.F. Gould (ed.) Advances in Chemical Series, ACS Publications, 99-118.

Van Vaeck, L., Broddin, G. and Van Cauwenberghe, K. (1979) Differences in particle size distributions of major organic pollutants in ambient aerosols in urban, rural and seashore areas. Environmental Science and Technology, 13, 1494-1502.

Van Vaeck, L. and Van Cauwenberghe, K. (1985) Characteristic parameters of particle size distribution of primary organic constituents of ambient aerosols. Environmental Science and Technology, 19, 707-716.

Vazquez-Duhalt, R. (1989) Environmental impact of used motor oil. Science of the Total Environment, 79, 1-23.

Venkatesan, M.I. and Kaplan, I.R. (1982) Distribution and transport of hydrocarbons in surface sediments of the Alaskan Outer Continental Shelf. Geochimica et Cosmochimica Acta, 46, 2136-2149.

Venkatesan, M.I. (1988) Occurrence and possible sources of perylene in Marine sediments-a Review. Marine Chemistry, 25, 1-27.

Vo-Dinh, T. (1989) Significance of chemical analysis of polycyclic aromatic compounds in related biological systems. In: "Chemical Analysis of Polycyclic Aromatic Compounds", Chemical Analysis Series (Vol.101) T. Vo-Dinh (ed) A Wiley-Interscience Publication, 1-25.

Volkman, J.K., Holdsworth, D.G., Neill, G.P. and Bavor H.J. (1992) Identification of natural, anthropogenic and petroleum hydrocarbons in aquatic sediments. The Science of the Total Environment, 112, 203-219.

Wachs, B., Wagner, H. and Van Donkelaar, P. (1992) Two-stroke lubricant emissions in a body of water subjective to intensive outboard motor operations. The Science of the Total Environment, 116, 59-81.

Wakeham, S.G. (1977) Synchronous fluorescence spectroscopy and its application to indigenous and petroleum-derived hydrocarbons in lacustrine sediments. Environmental Science and Technology, 11, 272-276.

Wakeham, S.G., Schaffner, C. and Giger, W. (1980a) Polycyclic aromatic hydrocarbons in recent lake sediments - I, Compounds having anthropogenic origins. Geochimica et Cosmochimica Acta, 44, 403-413.

Wakeham, S.G., Schaffner, C. and Giger, W. (1980b) Polycyclic aromatic hydrocarbons in recent lake sediments - II, Compounds derived from biogenic precursors during early diagenesis. Geochimica Cosmochimica Acta, 44, 415-429.

Wallcave, L., Garica, H., Feldman, R., Lijinsky, W. and Shubik, P. (1971) Skin tumorigenesis in mice by petroleum asphalts and coal-tar pitches of known polynuclear aromatic hydrocarbon content. Toxicology and Appied Pharmacology, 18, 41-52.

Warman, K. (1983) PAH Emissions from Coal-Fired Plants. In "Handbook of Polycyclic Aromatic Hydrocarbons (Vol.2) Emission, Sources and Recent Progress in Analytical Chemistry", A. Bjorseth, and T. Ramdahl (eds.) Marcel Dekker, Inc., 21-59.

Wehner, H., Tehschner, M. and Bosecker, K. (1985) Chemical reactions and stability of biomarkers and stable isotope ratios during *in-vitro* biodegradation of petroleum. Organic Geochemistry, 10, 463-471.

Weinstein, N.J. (1974). Waste Oil Recycling and Disposal. National Environmental Research Center, Office of Research and Development, US EPA, Report No. EPA-670/2-74-052.

Weissenfels, W.D., Beyer, M. and Klein, J. (1990) Degradation of phenanthrene, fluorene and fluoranthene by pure bacterial cultures. Applied Microbiology Biotechnology, 32, 470-484.

Westell, J.C., Leuenberger, C., and Schwarzenbach, R.P. (1985) Influence of pH and ionic strength on the aqueous and the nonaqueous distribution of chlorinated phenols. Environmental Science and Technology, 19, 193.

Westerholm, R., Stenburg, U. and Alsberg, T. (1988) Some aspect of the distribution of polycyclic aromatic hydrocarbons (PAH) between particles and gas phase from diluted gasoline exhausts generated with the use of a dilution tunnel, and its validity for measurement in air. Atmospheric Environment, 22, 5, 1005-1010.

Whitehouse, B.G. (1984) The effects of temperature and salinity on the aqueous solubility of polynuclear aromatic hydrocarbons. Marine Chemistry, 14, 319-332.

Whitly, K.T. and Sverdrup, G.M., (1980) In "The Character and Origin of SMOG" G.M. Hidy, P.K. Mueller, D. Grosjean, B.R. Appeal and J.J. Wesolowski, (eds). J.Wiley & Sons, New York, 477-515.

Wild, S.R., McGrath, S.P. and Jones, K.C. (1990) The polycyclic aromatic hydrocarbon (PAH) content of archived sewage sludges. Chemosphere, 20, 6, 703-716.

Wild, S.R. and Jones, K.C. (1993) Biological and abiotic losses of polynuclear aromatic hydrocarbons (PAH) from soils freshly amended with sewage sludge. Environmental Toxicology and Chemistry, 12, 5-12.

Williams, P.T., Horne, P.A. and Talyor, D.T. (1993) Polycyclic aromatic hydrocarbons in polystyrene derived pyrolysis oil. Journal of Analytical and Applied Pyrolysis, 25, 325-334.

Wong, M.K. and Williams, P.J. (1980) A study of three extraction methods for hydrocarbons in marine sediments. Marine Chemistry, 9, 183-190.

Wortham, H., Nguyen, E.B., Masclet, P., and Mouvier, G. (1993) Study of heterogenous reactions of polycyclic aromatic hydrocarbons I: Weakening of PAH-Support bonds under photonic irradiation. Science of the Total Environment, 128, 1-11.

Yamasaki, H., Kuwata, K. and Miyamoto, H. (1982) Effects of ambient temperature on aspects of airborne polycyclic aromatic hydrocarbons. Environmental Science and Technology, 16, 4, 189-194.

Yokley, R.A., Garrison, A.A., Wehry, E.L. and Mamantov, G. (1986) Photochemical transformation of pyrene and benzo(a)pyrene vapour-deposited on eight coal stack ashes. Environmental Science and Technology, 20, 1, 86-92.

Youngblood, W.W. and Blumer, M. (1975) Polycyclic aromatic hydrocarbons in the environment: homologous series in soils and recent marine sediments. Geochimica et Cosmochimica Acta, 39, 1303-1314.

Zafiriou, O.C. (1977) Marine organic photochemistry previewed. Marine Chemistry, 5, 497-522.

Zander, M. (1983) Physical and chemical properties of polycyclic aromatic hydrocarbons. In "Handbook of Polycyclic Aromatic Hydrocarbons" (Vol.1) A Bjorseth and T. Ramdahl (eds.) Marcel Dekker, Inc., 1-25.

Zavarin, E. and Cool, L. (1991) Extraneous materials from wood. In "Wood Structure and Composition ", M. Lewin and I.S. Goldstein (eds.) Marcel Dekker Inc., 321-407.

Zepp, R.G. and Schlotzhauer, P.F. (1979) Photoreactivity of selected aromatic hydrocarbons in water. In "Polynuclear Aromatic Hydrocarbons", P.W. Jones and P. Leber (eds.) Ann Arbor Science Publishers.

Zylstra, G.J., Wang, P.X. and Didolkar, V.A. (1992) Manipulation of the genes for polycyclic aromatic hydrocarbon degradation. ACS Conference Proceedings Series: Harnessing biotechnology for the 21st century; 9th International Biotechnology Symposium and Exposition, 68-71.

Appendix A1. $\delta^{13}C$ of the individual PAH isolated from the single and composite fireplace soot samples.

No	PAH	Mol Wt	Sing 1	Sing 2	Sing 3	Sing 4	Sing 5	Sing 6	Sing 7	Sing 8	Sing 9	Sing 10	Comp	Comp Repeat
1	Pa	178	-25.8	-26.3	-26.3	-27.2	-26.9	-27.0	-26.7	-25.5	-25.2	-27.0	-26.7	-27.0
2	A	178	-23.5	-23.8	-24.7	-25.2	-	-24.2	-25.1	-23.3	-24.4	-	-25.7	-25.7
3	Methyl Pa	192	-25.3	-26.0	-26.7	-27.2	-27.3	-27.1	-26.4	-25.2	-25.4	-26.2	-27.2	-27.8
4	Methylene Pa-A*	190	-24.0	-24.5	-	-	-	-	-26.1	-23.6	-24.2	-	-	-
5	Methyl Pa	192	-25.1	-25.7	-25.4	-25.5	-26.3	-26.1	-26.0	-24.5	-24.7	-	-26.8	-27.1
6	Phenyl Na	204	-26.5	-27.1	-27.0	-27.5	-	-26.8	-26.9	-26.2	-25.8	-27.6		-28.2
7	Dimethyl Pa-A	206	-	-	-25.8	-25.1	-	-	-	-24.3	-24.5		-27.0	-27.1
8	Fl	202	-25.2	-25.3	-24.5	-24.4	-26.7	-26.3	-27.0	-24.7	-25.1	-27.3	-25.3	-25.0
9	Py	202	-24.9	-24.8	-23.9	-23.2	-26.9	-26.2	-27.1	-24.0	-24.7	-28.3	-25.7	-25.2
10	Unknown	218	-24.5	-24.1	-23.1	-20.7	-23.5	-22.3	-26.2	-23.6	-23.8	-	-24.6	-24.9
11	Methyl Fl-Py*	216	-24.9	-24.4	-24.2	-23.7	-26.7	-26.2	-25.5	-24.2	-24.9	-25.4		-25.4
12	Methyl Fl-Py*	216	-24.5	-24.3	-24.1	-22.9	-25.9	-25.6	-26.6	-24.6	-25.1	-		-24.8
13	Methyl Fl-Py*	216	-24.9	-24.4	-23.7	-22.9	-24.0	-24.7	-26.7	-24.8	-24.4	-		-24.8
14	Retene*	234	-	-	-26.7	-	-	-	-26.3	-	-	-	-26.5	-26.5
15	Dimethyl Fl-Py*	230	-24.8	-25.5	-23.8	-23.7	-26.1	-	-27.1	-24.5	-25.1	-24.5	-24.5	-24.1
16	B(ghi)Fl/CP(cd)Py*	226	-24.7	-24.4	-24.4	-22.7	-25.0	-24.4	-26.1	-24.9	-24.4	-24.7	-23.9	-24.2
17	BaA	228	-24.1	-24.8	-25.3	-23.4	-26.3	-23.9	-26.1	-24.3	-23.7	-26.7	-25.6	-25.2
18	Chy	228	-25.5	-24.8	-23.9	-23.4	-26.4	-25.2	-27.1	-24.6	-25.3	-26.4	-25.6	-25.2
19	BFl	252	-26.1	-25.7	-25.1	-25.8	-26.0	-25.9	-27.4	-24.6	-24.7	-	-26.8	-26.6
20	BeP	252	-26.5	-	-24.8	-25.3	-26.4	-	-26.6	-	-	-	-25.0	-25.2
21	BaP	252	-26.6	-	-24.8	-25.3	-26.4	-	-26.7	-25.4	-24.8	-	-25.1	-25.2

* = Tentatively identified by GC-MS

Appendix A2. $\delta^{13}C$ of the individual PAH isolated from the single and composite car soot samples.

No	PAH	Mol W	Comp 1 1-3	Comp 2 4-9	Comp 3 9-11	Comp 4 1-9	Comp 5 1-5	Sing 1	Sing 1 Repeat	Sing 2	Sing 3	Sing 4	Sing 5
1	Na	128	-	-	-	-25.6	-	-26.3	-26.5	-	-26.2	-	
2	Methyl Na	142	-	-	-	-25.7	-26.3	-26.3	-26.4	-26.1	-27.0	-	-26.2
3	Methyl Na	142	-	-	-	-25.2	-	-25.8	-25.5	-	-26.2	-	
4	Ay	152	-	-23.7	23.6	-23.5	-23.6	-23.1	-23.6	-23.9	-22.7	-23.9	-24.1
5	Dibenzofuran*	168	-	-	-	-	-26.6	-	-	-25.0	-26.0	-	-
6	F	166	-26.2	-	-	-	-26.0	-	-	-25.6	-26.4	-25.8	-26.0
7	Pa	178	-26.4	-26.1	-26.7	-25.9	-25.9	-23.1	-23.7	-26.4	-25.9	-26.2	-26.5
8	A	178	-24.5	-24.2	-25.5	-25.8	-24.8	-23.5	-24.4	-25.4	-25.5	-24.6	-24.4
9	Methyl Pa	192	-26.4	-27.5	-27.8	-26.3	-26.5	-27.2	-27.2	-27.4	-27.0	-25.9	-26.3
10	Methyl Pa	192	-26.1	-28.3	-	-25.6	-26.3	-	-	-26.8	-25.5	-	-26.4
11	Phenyl Na	204	-26.0	-27.0	-	-25.8	-25.6	-25.4	-25.8	-26.5	-26.4	-26.0	-26.0
12	Fl	202	-24.7	-26.3	-25.8	-25.6	-23.7	-21.8	-21.8	-25.3	-24.1	-25.4	-25.6
13	Py	202	-25.5	-25.2	-24.4	-24.8	-24.1	-20.8	-20.9	-24.5	-22.3	-25.4	-25.6
14	Methyl Fl-Py*	216	-	-	-	-26.0	-	-24.3	-23.4	-25.5	-26.3	-	-
15	B(ghi)Fl/I(cd)Py*	226	-25.2	-27.1	-26.0	-24.7	-23.3	-21.3	-21.8	-24.1	-24.4	-26.4	-26.3
16	BaA	228	-25.6	-23.6	-22.9	-25.2	-	-22.1	-21.6	-26.3	-24.0	-	-
17	Chy	228	-26.2	-27.0	-26.3	-26.8	-25.9	-24.7	-22.7	-26.3	-	-	-26.3
18	BFl	252	-25.7	-26.3	-27.4	-26.8	-	-23.5	-22.9	-25.6	-	-	-25.6
19	BeP	252	-25.1	-26.1	-	-26.9	-	-23.3	-23.6	-26.1	-	-	
20	BaP	252	-25.1	-24.2	-25.9	-28.5	-	-22.5	-22.7	-26.1	-	-	

* = Tentatively identified by GC-MS

Appendix A3. $\delta^{13}C$ of the individual PAH isolated from the single and composite crankcase oil samples.

No	PAH	Mol Wt.	Comp 1	Comp 2	Comp 3	Comp 4	Comp 5	Comp 6	Sing 1	Sing 2	Sing 3	Sing 4	Sing 5	Sing 6
1	Na	128	-	-	-	-	-	-26.5	-26.8	-	-	-	-	-
2	Methyl Na	142	-26.9	-27.8	-27.7	-26.3	-26.8	-26.8	-27.8	-	-	-26.8	-27.1	-
3	Methyl Na	142	-26.0	-27.8	-25.0	-25.6	-26.2	-26.0	-26.5	-	-	-26.0	-26.9	-
4	Dimethyl Na	156	-27.2	-	-25.7	-26.3	-26.9	-26.2	-26.6	-26.9	-26.3	-26.5	-27.1	-
5	Dibenzofuran*	168	-	-	-	-27.3	-27.9	-28.1	-27.1	-28.1	-28.3	-	-28.8	-
6	Trimethyl Na	170	-	-	-27.4	-27.2	-27.2	-26.8	-26.8	-26.8	-26.6	-	-27.3	-
7	F	166	-28.6	-29.3	-	-28.0	-28.5	-27.4	-28.1	-27.3	-28.9	-28.4	-29.0	-
8	DBT	184	-28.4	-28.1	-28.4	-27.8	-28.3	-28.2	-28.1	-28.0	-28.7	-28.4	-28.2	-28.6
9	Pa	178	-29.6	-29.0	-29.3	-28.8	-28.2	-28.8	-28.9	-29.0	-28.9	-28.6	-28.1	-28.9
10	Methyl DBT*	198	-27.2	-	-	-27.3	-	-27.1	-27.9	-27.1	-27.6	-	-27.1	-
11	Methyl Pa	192	-28.2	-27.3	-28.4	-28.0	-27.4	-28.1	-27.8	-26.8	-27.3	-27.1	-27.0	-27.3
12	Methyl Pa	192	-28.0	-27.3	-28.1	-27.1	-26.6	-26.9	-27.9	-27.1	-26.5	-26.6	-25.7	-27.8
13	Phenyl Na	204	-27.3	-25.5	-28.2	-26.5	-	-27.1	-27.9	-26.3	-	-	-28.5	-
14	Dimethyl Pa*	206	-27.5	-27.8	-26.9	-27.2	-27.3	-26.8	-26.7	-25.5	-26.5	-26.6	-26.7	-27.9
15	Dimethyl Pa*	206	-27.8	-27.4	-27.0	-26.6	-	-28.1	-26.1	-24.4	-26.4	-	-	-
16	Fl	202	-27.9	-27.1	-27.4	-27.1	-26.7	-26.9	-27.3	-29.3	-27.1	-26.8	-25.0	-
17	Py	202	-29.6	-28.8	-29.1	-27.9	-27.6	-28.6	-29.4	-29.1	-28.9	-28.1	-28.8	-28.2
18	Methyl Fl-Py*	216	-27.2	-27.5	-28.4	-26.8	-26.3	-26.8	-	-26.8	-27.6	-27.4	-26.9	-
19	Methyl Fl-Py*	216	-26.9	-26.6	-28.2	-26.3	-26.5	-26.4	-	-26.7	-26.6	-27.3	-28.1	-
20	Methyl Fl-Py*	216	-26.8	-28.9	-27.2	-26.6	-	-26.8	-	-25.3	-	-28.4	-25.2	-
21	BaA/Chy	228	-27.3	-27.2	-27.8	-27.3	-27.6	-27.4	-	-27.6	-27.3	-27.1	-28.5	-
22	BFl	252	-27.7	-27.3	-29.9	-27.0	-28.8	-27.5	-	-27.5	-	-28.1	-27.7	-
23	BeP/BaP	252	-27.6	-27.8	-	-28.8	-	-28.7	-	-25.9	-	-28.2	-26.4	-

* = Tentatively identified by GC-MS

Appendix A4. $\delta^{13}C$ of the individual PAH isolated from crude petroleum and petroleum products.

No	PAH	Mol Wt.	Arab Crude	Cal Crude	C. Case Oil	O. Board Motors	#2 Fuel Oil
1	Na	128	-27.0	-27.7	-26.8	-26.4	-27.0
2	Methyl Na	142	-27.1	-28.5	-27.2	-26.6	-27.0
3	Methyl Na	142	-26.4	-27.4	-26.5	-25.1	-25.6
4	Dimethyl Na	156	-26.0	-28.1	-	-25.4	-26.8
5	Dimethyl Na	156	-26.1	-27.6	-26.0	-25.6	-26.5
6	Dimethyl Na	156	-26.3	-27.2	-26.7	-25.7	-26.7
7	Dimethyl Na	156	-24.8	-25.7	-26.0	-25.3	-25.5
8	Dimethyl Na	156	-22.7	-25.0	-25.0	-24.5	-25.5
9	Trimethyl Na	170	-25.3	-27.2	-	-26.1	-26.7
10	Trimethyl Na	170	-25.8	-27.3	-	-26.6	-26.6
11	Trimethyl Na	170	-25.4	-26.2	-27.2	-27.3	-26.9
12	Trimethyl Na	170	-24.8	-25.9	-	-27.3	-26.9
13	DBT	184	-28.5	-31.5	-28.3	-	-26.6
14	Pa	178	-27.7	-29.4	-28.7	-28.6	-
15	Methyl DBT	198	-29.7	-32.2	-	-	-
16	Methyl DBT	198	-28.6	-30.3	-	-	-
17	Methyl DBT	198	-27.3	-29.2	-	-	-
18	Methyl Pa	192	-27.5	-29.2	-27.2	-28.4	-
19	Methyl Pa	192	-27.3	-29.2	-26.9	-	-
20	Dimethyl DBT*	212	-30.7	-31.4	-	-	-
21	Dimethyl DBT*	212	-29.5	-30.6	-	-	-
22	Dimethyl DBT*	212	-27.8	-27.6	-	-	-
23	Dimethyl Pa	206	-27.7	-29.4	-27.0	-	-
24	Trimethyl DBT*	226	-28.5	-30.4	-	-	-
25	Trimethyl DBT*	226	-28.5	-30.3	-	-	-
26	Fl	202	-	-	-27.1	-26.8	-
27	Py	202	-	-	-28.8	-27.9	-
28	Baa+Chy	228/228	-	-	-27.7	-	-
29	BFl	252	-	-	-27.8	-	-
30	BaP+BeP	252/252	-	-	-26.7	-	-

* = Tentatively identified by GC-MS

Appendix A5. $\delta^{13}C$ of the individual PAH isolated from the power generating station and domestic furnace composite soots.

No	PAH	Mol Wt	Stack Hopper	Dom. Fur. I	Dom. Fur. II
1	Pa	178	-25.6	-25.7	-25.4
2	Methyl Pa	192	-26.0	-27.9	-26.2
3	Methyl Pa	192	-	-26.4	-25.9
4	Phenyl Na	204	-	-	-27.3
5	Dimethyl Pa-A*	206	-26.5	-27.1	-26.6
6	Fl	202	-25.7	-26.3	-25.8
7	Py	202	-25.6	-	-25.9
8	Methyl Fl-Py*	216	-26.8	-	-
9	Trimethyl Pa-A*	220	-	-	-25.3
10	BaA+Chy	228	-26.5	-27.3	-27.3
11	BFl	252	-	-28.3	-
12	BeP+BaP	252	-	-26.3	-

* = Tentatively identified by GC-MS

Appendix A6. $\delta^{13}C$ of the individual PAH isolated from the open-road and enclosed car park sweeps.

No	PAH	Mol Wt	Sing 1	Sing 2	Sing 3	Sing 4	Sing 5!	Sing 6!!	Sing 7	Sing 8	Sing 9	Sing 10	Sing 11
1	Methyl Na	142	-	-	-	-	-	-29.8	-	-	-	-	-
2	Methyl Na	142	-	-	-	-	-	-27.3	-	-	-	-	-
3	Dimethyl Na	156	-	-	-	-	-	-28.4	-	-	-	-	-
4	Dibenzofuran*	168	-	-	-	-	-	-27.3	-	-	-	-	-
5	F	166	-	-	-	-	-	-29.5	-	-	-	-	-
6	Pa	178	-24.9	-25.6	-25.6	-25.3	-27.4	-29.6	-25.8	-26.1	-26.5	-25.9	-25.9
7	A	178	-	-	-	-24.1	-	-	-	-	-	-	-23.4
8	Methyl Pa	192	-	-	-26.2	-26.6	-	-30.4	-	-	-	-	-24.6
9	Methyl Pa	192	-	-	-	-25.5	-	-28.8	-	-	-	-	-24.3
10	Dimethyl-Pa/A*	206	-	-	-	-	-	-29.2	-	-	-	-	-
11	Fl	202	-25.4	-25.1	-25.9	-25.0	-27.0	-28.6	-25.3	-25.1	-26.6	-26.2	-25.7
12	Py	202	-25.7	-24.3	-23.8	-25.0	-27.2	-29.3	-25.5	-26.8	-25.4	-24.2	-25.2
13	BaA+Chy	228	-26.9	-25.7	-27.4	-27.5	-	-	-	-	-	-27.6	-24.6
14	BFl	252	-26.9	-27.4	-27.4	-27.4	-28.5	-	-	-	-	-27.0	-26.6
15	BeP+BaP	252	-	-	-	-24.8	-26.4	-	-	-	-	-26.1	-27.3

! = Cement paved car park
!! = Asphalt paved car park
* = Tentatively identified by GC-MS

Appendix A7. $\delta^{13}C$ of the individual PAH isolated from the surface and deeper St. John's Harbour sediments.

No	PAH	Mol Wt.	Top 2 cm	10 cm Deep	20 cm Deep	30 cm Deep	Top 2 cm	Top 2 cm	Top 2 cm	Top 2 cm	Top 2cm	Top 2cm	Top 2 cm	Top 2cm	Top 2 cm
1	Pa	178	-25.2	-25.6	-25.6	-25.7	-25.7	-25.9	-25.7	-25.3	-25.7	-25.4	-25.3	-25.5	-25.4
2	A	178	-24.4	-24.9	-25.2	-	-24.9	-24.9	-24.9	-24.9	-24.6	-23.5	-25.0	-24.2	-24.4
3	Methyl Pa-A	192	-26.6	-25.9	-25.9	-	-27.2	-	-	-27.2	-27.7	-26.1	-26.7	-26.5	-25.4
4	Methylene Pa-A*	190	-26.7	-	-26.3	-	-27.2	-	-	-25.4	-25.5	-25.4	-	-	-
5	Methyl Pa	192	-25.6	-	-25.9	-	-26.6	-26.7	-	-26.5	-26.6	-	-25.2	-	-24.9
6	Phenyl Na	204	-	-	-26.0	-	-26.7	-	-	-26.5	-25.8	-26.0	-26.2	-	-25.9
7	Dimethyl Pa/A	206	-26.6	-26.4	-26.4	-	-27.6	-	-	-27.4	-27.8	-25.6	-25.7	-	-25.0
8	Fl	202	-25.9	-25.9	-26.0	-24.5	-26.5	-26.2	-25.6	-25.7	-25.4	-25.9	-25.1	-24.9	-26.3
9	Py	202	-26.4	-26.1	-26.2	-25.1	-26.5	-26.5	-25.9	-25.7	-25.5	-25.8	-25.1	-25.7	-26.7
10	Methyl Fl-Py*	216	-26.5	-25.9	-26.2	-	-	-26.6	-	-25.6	-25.9	-26.0	-26.5	-	-25.5
11	Methyl Fl-Py*	216	-26.2	-26.4	-25.8	-	-26.3	-26.7	-	-26.5	-25.8	-26.2	-26.0	-	-25.6
12	Retene+	234	-26.8	-26.4	-26.6	-	-26.7	-26.8	-	-26.7	-25.8	-25.8	-25.7	-	-25.9
13	B(ghi)Fl/CP(cd)Py*	226	-26.7	-26.4	-26.6	-	-26.4	-26.5	-	-27.7	-27.0	-26.4	-27.1	-	-
14	BaA	228	-25.7	-25.4	-26.5	-	-26.0	-26.6	-25.9	-26.2	-24.9	-25.9	-25.8	-25.5	-25.5
15	Chy	228	-25.5	-26.0	-26.5	-26.6	-26.4	-26.6	-25.6	-26.4	-25.4	-26.1	-25.2	-25.8	-25.6
16	BFl	252	-26.0	-26.7	-26.3	-	-26.2	-26.8	-26.6	-26.8	-26.1	-26.3	-26.5	-26.2	-26.1
17	BaP	252	-26.1	-25.9	-25.7	-	-25.8	-26.2	-26.4	-26.0	-26.8	-25.3	-25.7	-	-26.6

* = Tentatively identified by GC-MS

Appendix A8. $\delta^{13}C$ of the individual PAH isolated from the surface and deeper Conception Bay sediments.

No	Site	Pa	Fl	Py	BaA Chy	BFl	BeP BaP	Per	Retene*
1	CTR23/2 cm	-26.0	-26.3	-26.1	-25.2	-26.6	-	-23.3	-25.6
2	CTR23/4 cm	-25.5	-26.1	-26.3	-26.3	-27.2	-	-24.5	-24.6
3	CTR23/4 cm (R)	-25.8	-26.3	-26.3	-25.6	-	-	-25.0	-25.2
4	CTR23/6 cm	-25.6	-26.2	-25.8	-25.3	-	-	-24.2	-25.0
5	CTR23/8 cm	-26.2	-26.3	-26.4	-26.5	-27.4	-26.2	-24.2	-24.8
6	CTR23/10 cm	-26.4	-26.1	-26.3		-26.9	-	-	-
7	CTR/12 cm	-25.9	-26.5	-	-25.3	-26.7	-26.4	-22.5	-24.8
8	CC4/2 cm	-25.5	-26.0	-26.3	-26.0	-26.6	-	-24.8	-25.0
9	CC4/2 cm (R)	-25.6	-26.5	-25.7	-25.3	-	-	-24.8	-25.3
10	BRLP5/2 cm	-25.8	-26.6	-26.4	-26.2	-26.8	-	-24.3	-25.5
11	BRLP5/2 cm (R)	-25.8	-26.1	-	-26.6	-28.9	-	-24.7	-26.1
12	BRLP5/4 cm	-25.6	-26.3	-26.2	-	-	-	-24.4	-24.7
13	BRLP5/6 cm	-26.1	-26.2	-25.6	-25.2	-27.8	-27.3	-24.5	-24.7
14	BRLP5/8 cm	-26.4	-25.9	-	-25.7	-27.0	-26.7	-	-24.8
15	BRLP5/10 cm	-26.1	-26.5	-	-25.8	-	-25.9	-22.4	-25.0
16	BRLP5/12 cm	-26.1	-26.8	-26.8	-26.6	-27.2	-	-25.2	-25.3
17	BRLP/14 cm	-25.9	-26.8	-26.2	-25.4	-27.0	-	-22.6	-25.8
18	BRLP5/C4/2 cm	-26.6	-26.6	-25.9	-25.4	-26.4	-	-25.2	-28.1
19	BRLP5/C4/8 cm	-25.8	-26.8	-26.1	-25.4	-27.8	-26.0	-24.1	-24.8
20	CC1/2 cm	-26.2	-26.3	-	-	-	-	-23.6	-25.7
21	CC1/4 cm	-25.9	-26.2	-26.0	-	-	-26.2	-24.5	-25.5
22	US3.5/2 cm	-26.1	-26.2	-	-26.0	-	-	-24.1	-25.0
23	CW4/2 cm	-26.1	-26.5	-26.8	-	-	-	-24.8	-
24	CC6/2 cm	-25.6	-26.4	-26.2	-26.0	-27.6	-	-24.3	-26.1

R = Repeat analysis
* = Tentatively identified by GC-MS

Appendix B. $\delta^{13}C$ of the bulk organic fraction in Conception Bay and St. John's Harbour sediments

Site	Fraction	$\delta^{13}C$ vs PDB	Duplicate
Conception Bay			
BRLP5	2 cm	-21.9	
	4 cm	-21.9	
	8 cm	-21.8	-21.9
	10 cm	-21.8	
	12 cm	-21.6	
	14 cm	-21.5	-21.6
CC1	2 cm	-21.8	
CTR 23	2 cm	-21.8	
	14 cm	-21.8	
CC6	2 cm	-21.9	-21.9
CW4	2 cm	-21.9	-21.9
CC4	2 cm	-21.9	
US3.5	2 cm	-21.8	
St. John's Harbour			
Deep Portion	2 cm	-24.9	-25.1
Adel. Rd.	2 cm	-25.3	
Quid. V. Rd.	2 cm	-25.1	-25.1

Appendix C. Metal concentrations (ppm) in the surface and deeper sediments of Conception Bay.

Sample	Pb	Ni	Cu	Zn	V	Cr	Ce	Ba	As	Sr
CC1										
2 cm	5	24	27	61	102	56	67	518	42	159
12 cm	6	22	24	61	102	60	68	546	33	151
20 cm	ND	24	25	59	105	62	80	540	25	159
BRLP 5										
2 cm	7	23	26	62	102	56	66	512	36	151
4 cm	11	22	25	66	108	57	76	548	29	144
6 cm	5	20	25	61	98	56	72	500	39	145
8 cm	8	22	27	62	111	57	86	537	29	155
10 cm	8	24	28	64	107	57	105	507	31	157
12 cm	8	23	28	63	108	57	79	530	30	149
14 cm	6	24	29	64	106	62	72	538	33	151
CTR 23										
2 cm	7	24	25	61	110	60	55	551	35	151
14 cm	ND	25	27	62	96	64	45	527	14	156
CC6	6	19	21	57	81	49	85	447	34	147
US3.5	4	20	19	51	86	47	70	492	21	150
CC4	10	22	25	61	87	47	53	320	33	140
CW4	8	15	13	43	80	50	71	541	19	149

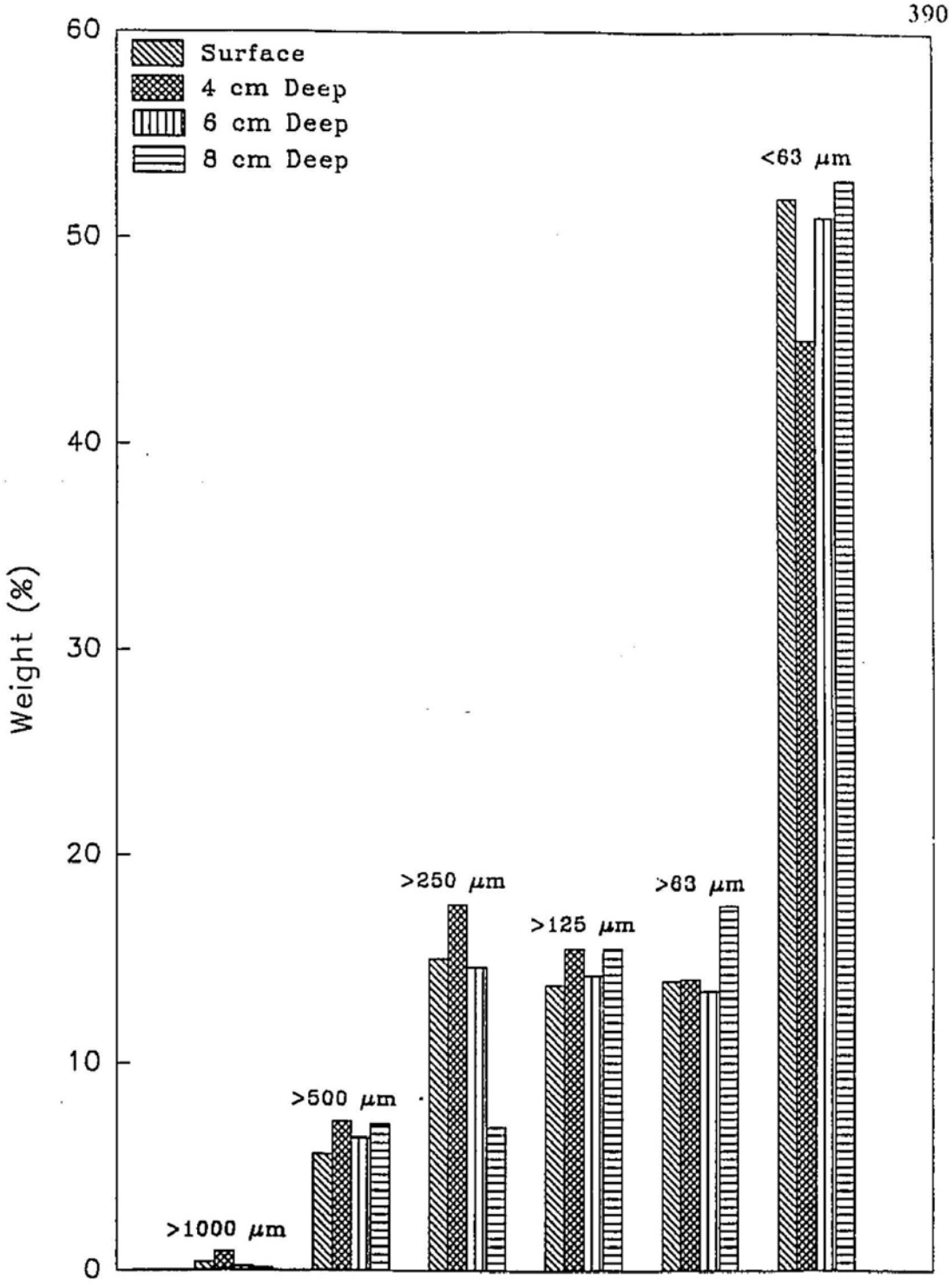

Appendix D. Summary of the grain size analysis (% dry weight) for the surface and deeper sediments of Conception Bay.

Appendix E1. Major ion trace (mass 44) of a fire soot sample with internal standards and reference gas injection.

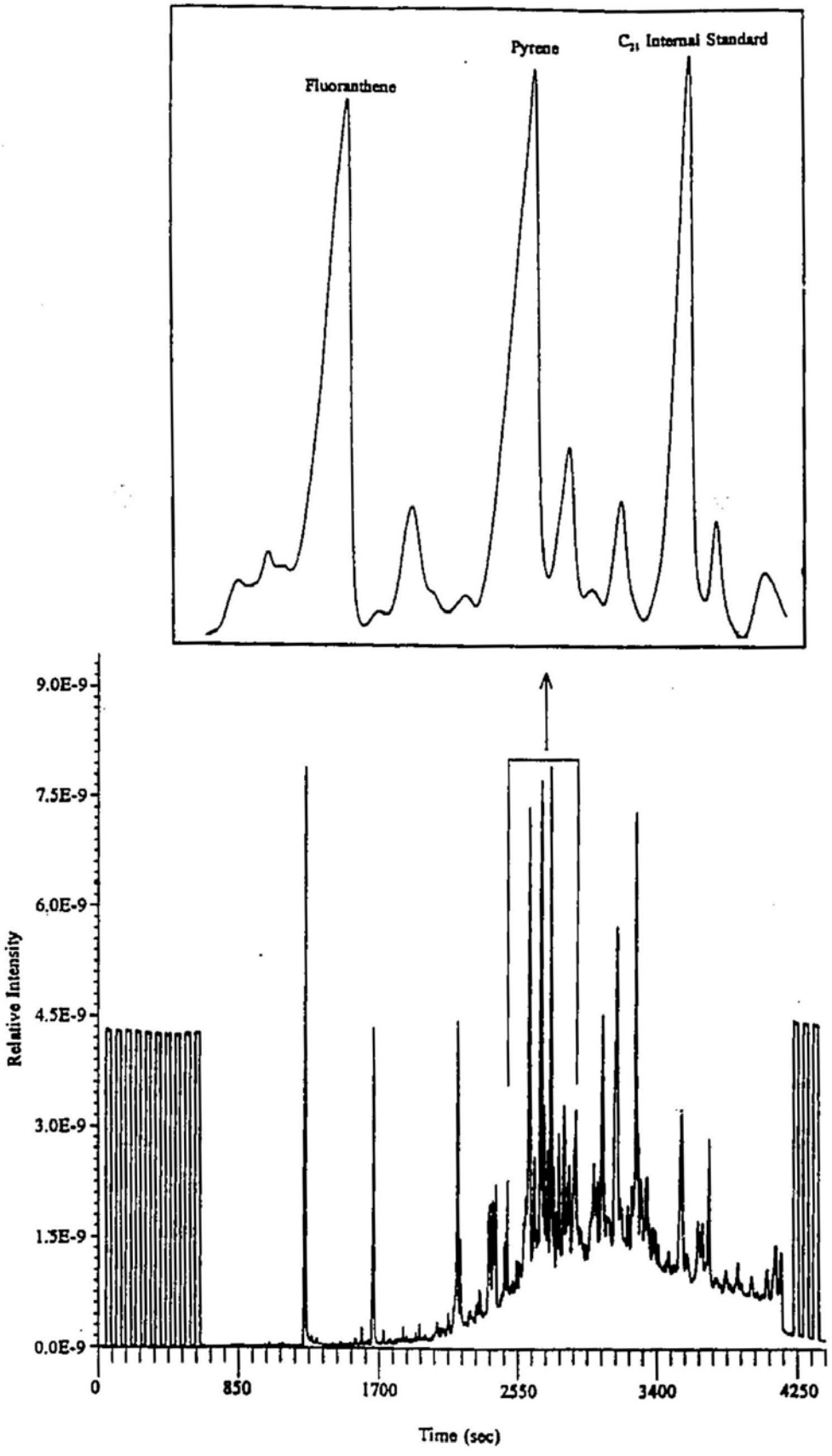
Fluoranthene
Pyrene
C_{21} Internal Standard
9.0E-9
7.5E-9
6.0E-9
4.5E-9
3.0E-9
1.5E-9
0.0E-9
Relative Intensity
0
850
1700
2550
3400
4250
Time (sec)

Appendix E2. Major ion trace (mass 44) of a car soot sample with internal standards and reference gas injection.

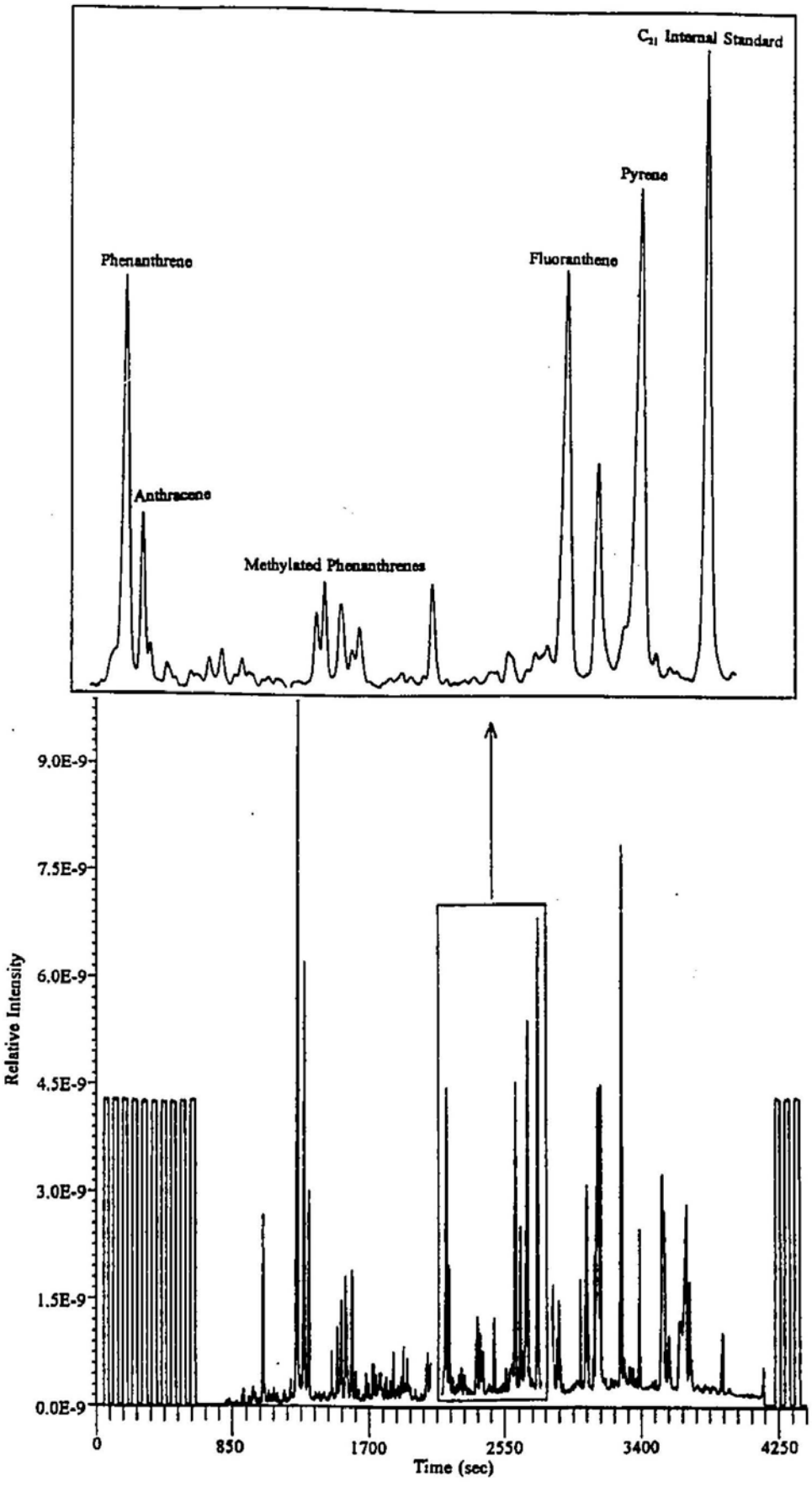
C21 Internal Standard
Pyrene
Fluoranthene
Phenanthrene
Anthracene
Methylated Phenanthrenes
9.0E-9
7.5E-9
6.0E-9
4.5E-9
3.0E-9
1.5E-9
0.0E-9
Relative Intensity
0
850
1700
2550
3400
4250
Time (sec)

Appendix E3. Major ion trace (mass 44) of a road sweep sample with internal standards and reference gas injection.

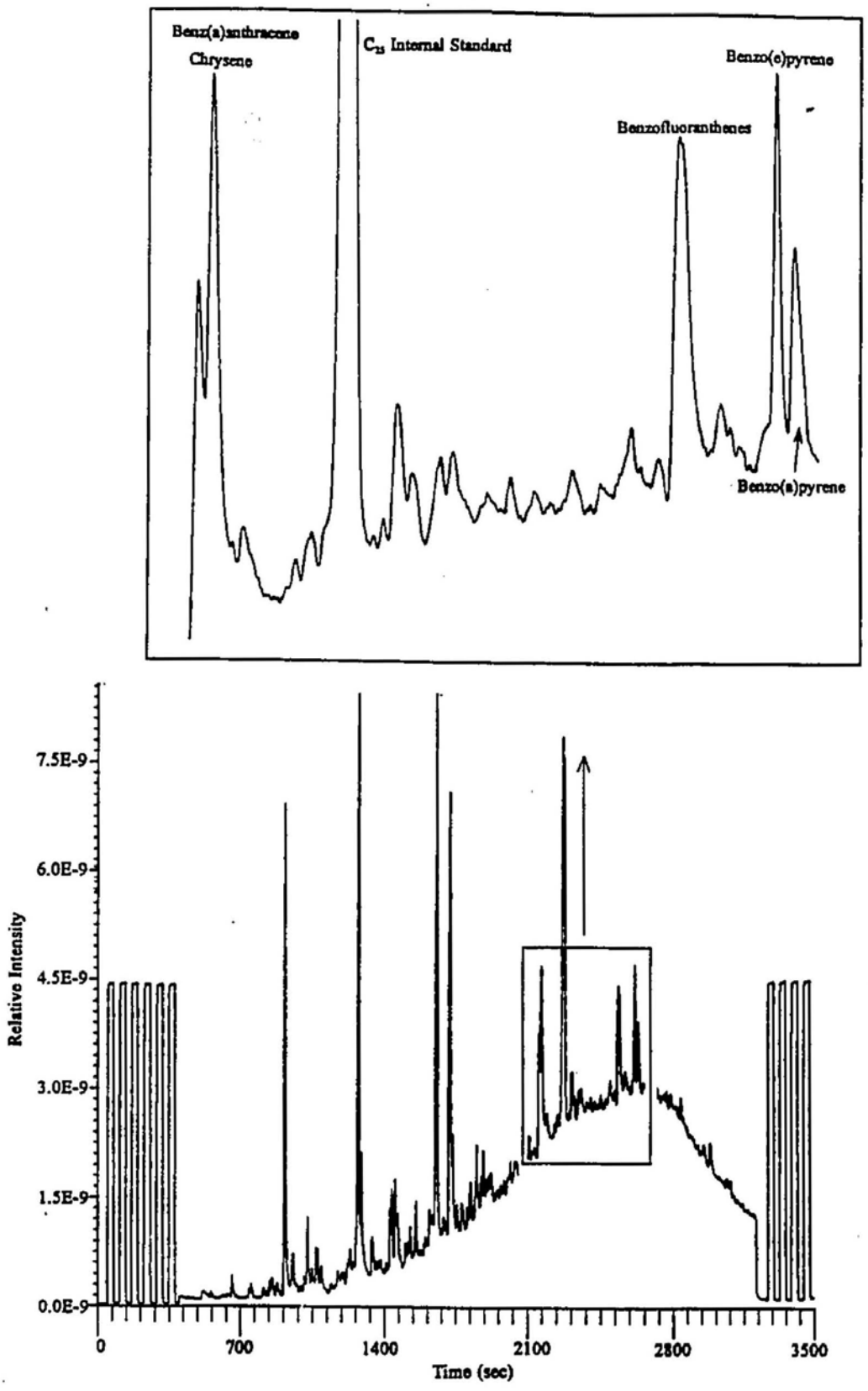
Benz(a)anthracene
Chrysene
C_{25} Internal Standard
Benzofluoranthenes
Benzo(e)pyrene
Benzo(a)pyrene
Relative Intensity
7.5E-9
6.0E-9
4.5E-9
3.0E-9
1.5E-9
0.0E-9
0
700
1400
2100
2800
3500
Time (sec)

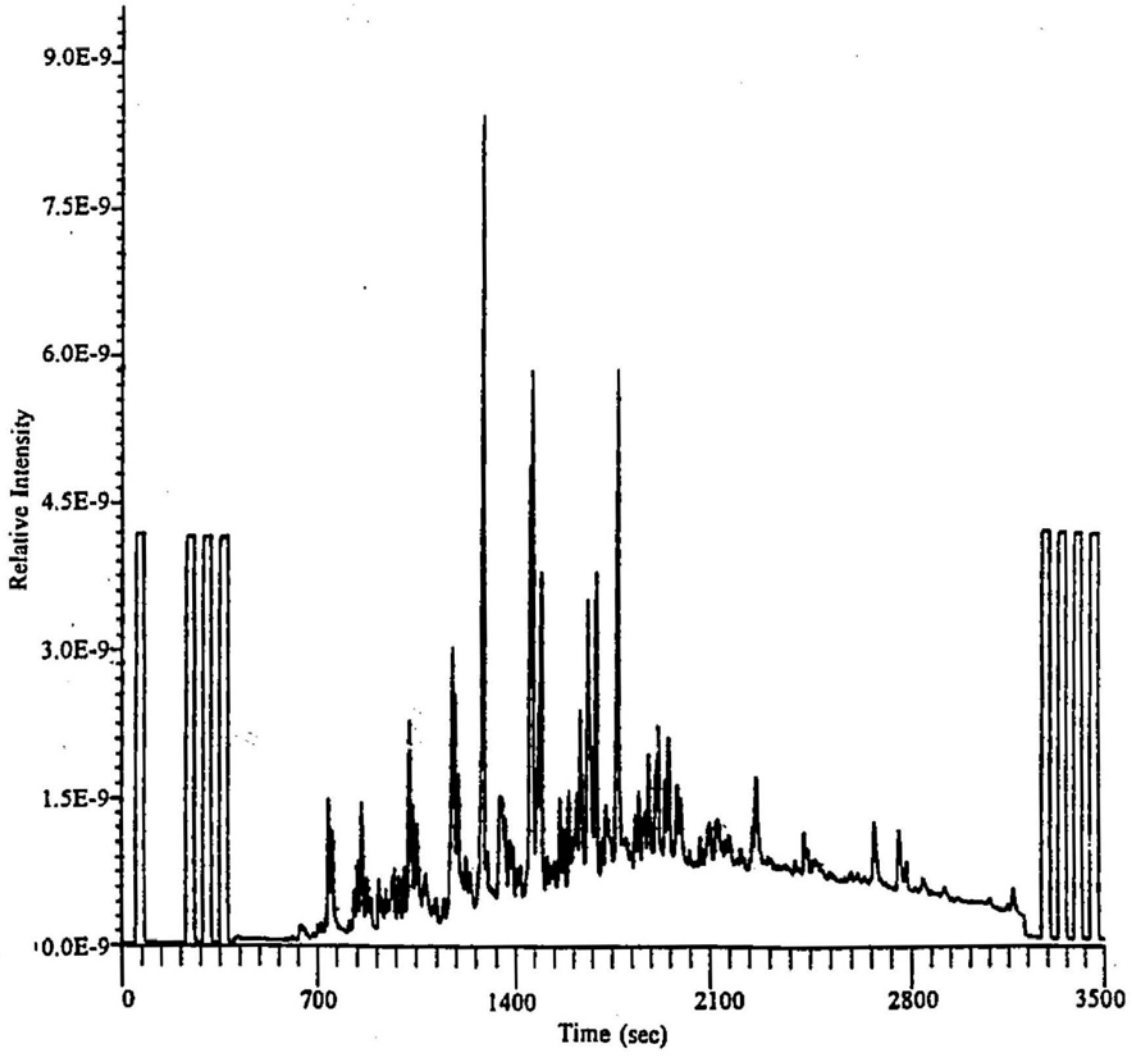

Appendix E4. Example of a major ion trace (mass 44) of a crankcase oil fraction (3)

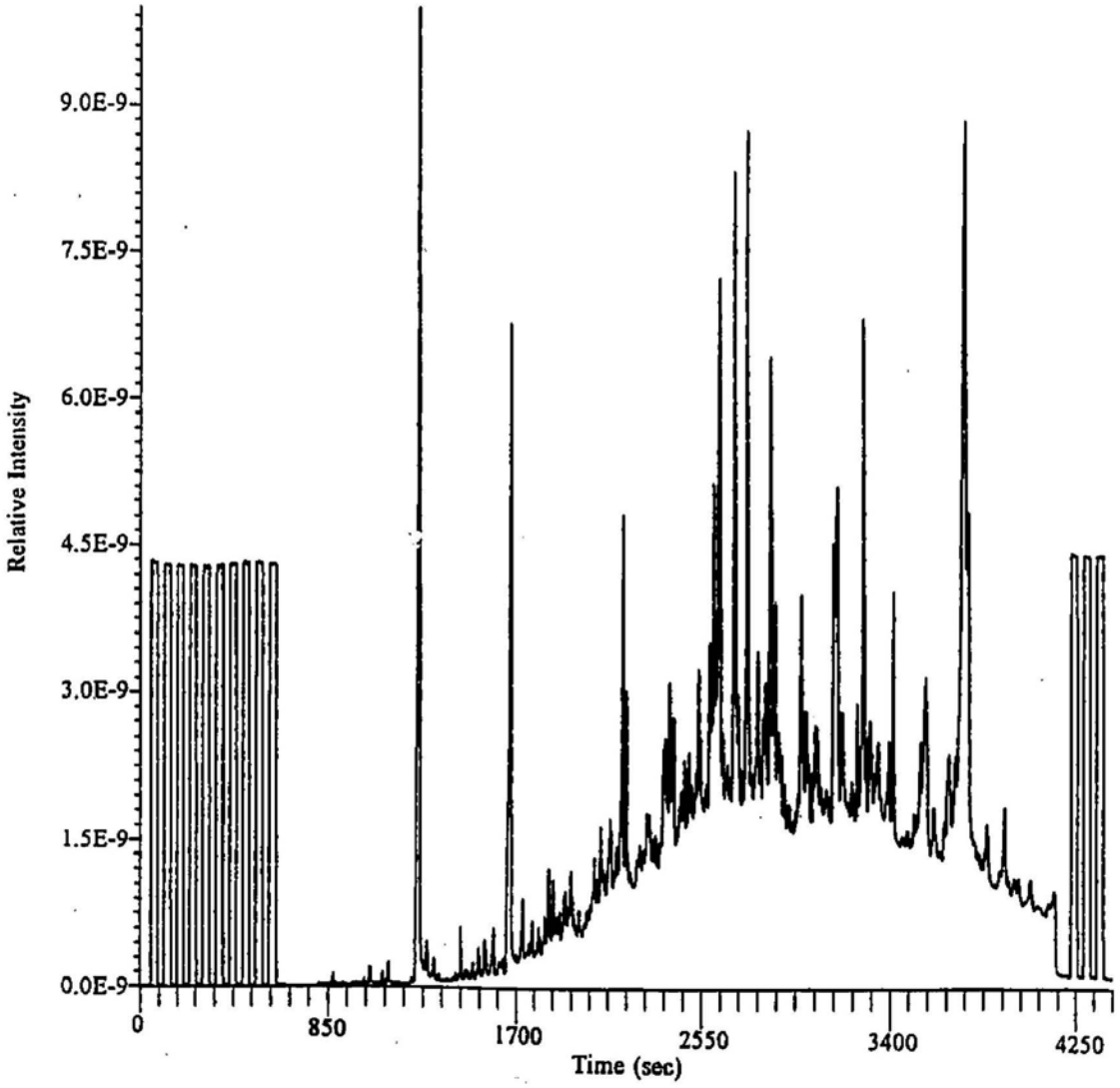

Appendix E5. Example of a major ion trace (mass 44) of a St. John's Harbour surface sediment sample.

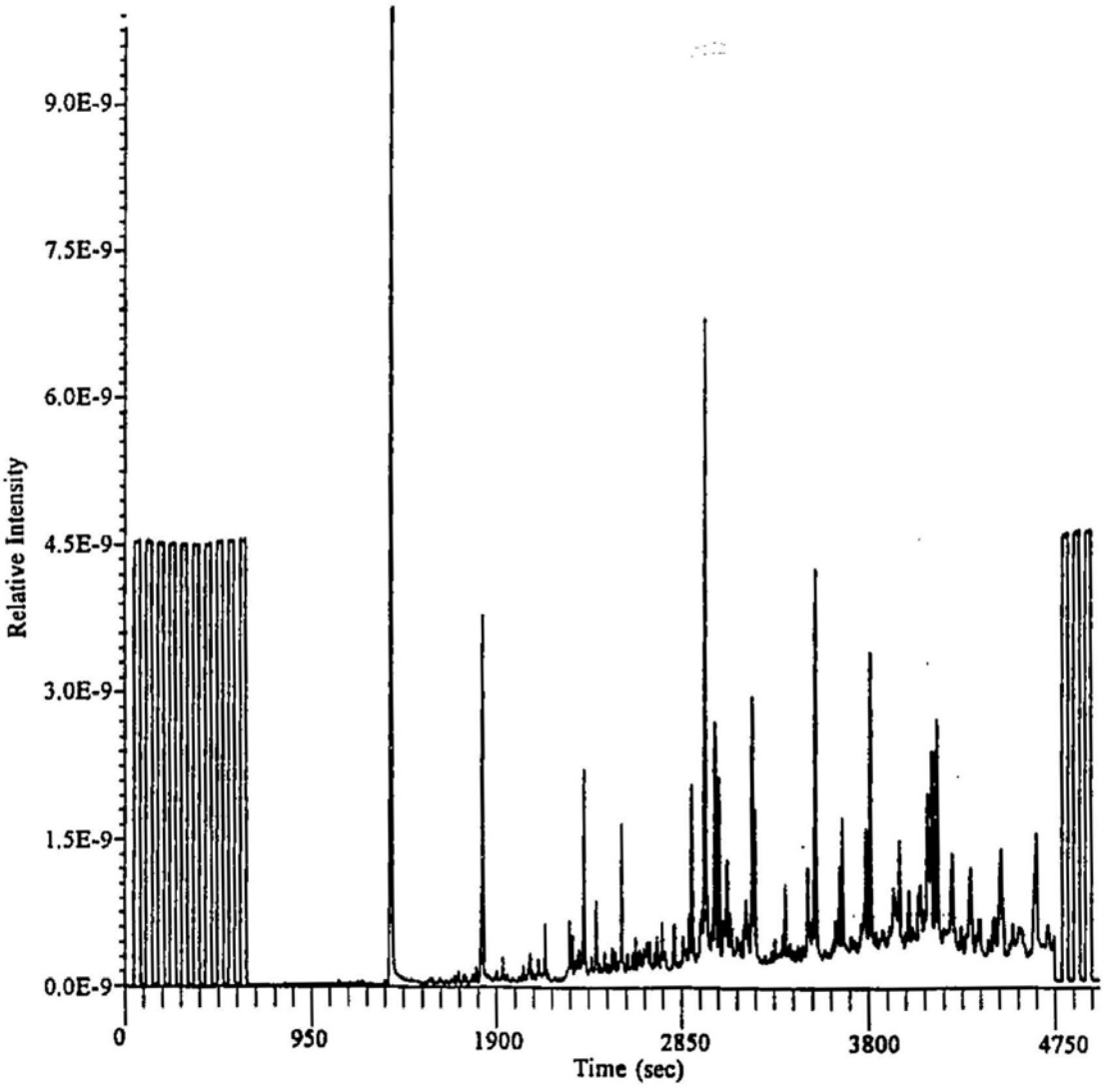

Appendix E6. Example of major ion trace (mass 44) of a Conception Bay surface sediment sample.

Appendix F1. Examples of total ion chromatograms (TIC) obtained for a fireplace and car soot sample (primary sources).

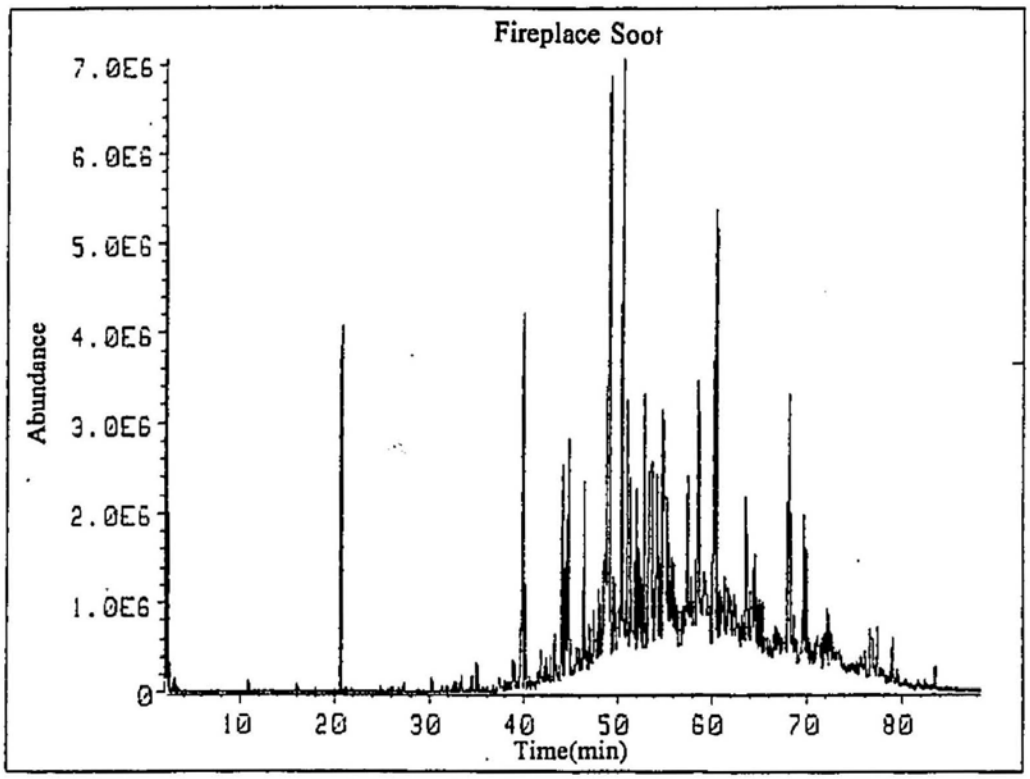
Fireplace Soot
7.0E6
6.0E6
5.0E6
4.0E6
3.0E6
2.0E6
1.0E6
0
Abundance
10
20
30
40
50
60
70
80
Time(min)

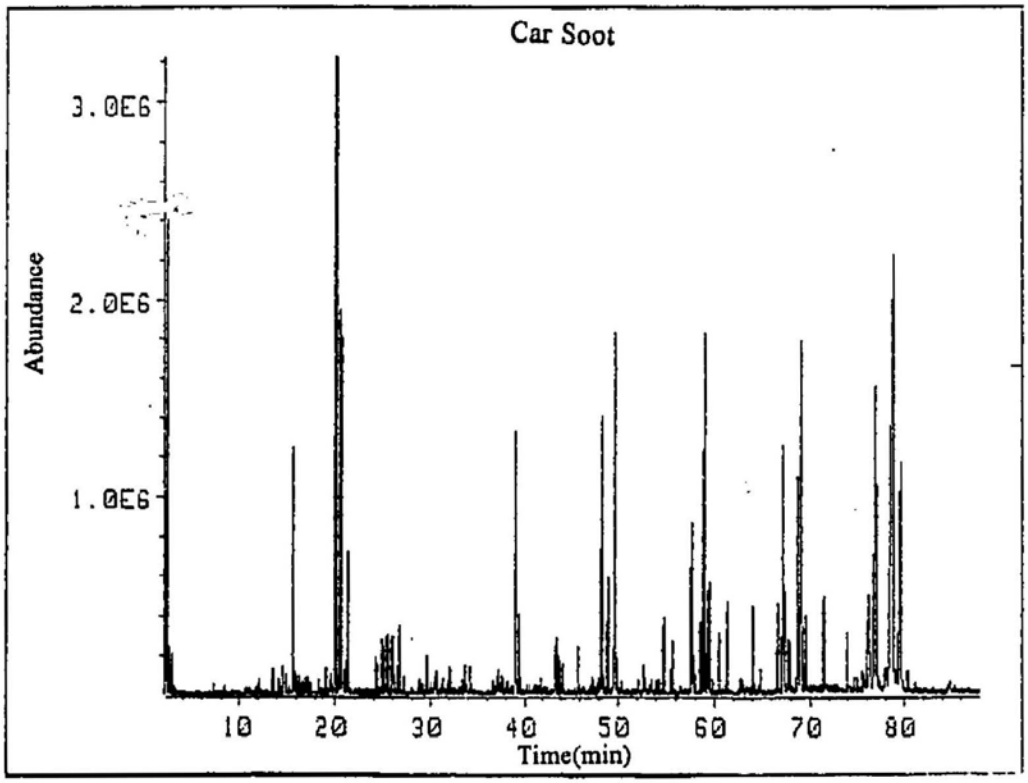
Car Soot
3.0E6
2.0E6
1.0E6
Abundance
10
20
30
40
50
60
70
80
Time(min)

Appendix F2. Examples of total ion chromatograms (TIC) obtained for a car soot (primary source) and road sweep (secondary source) sample.

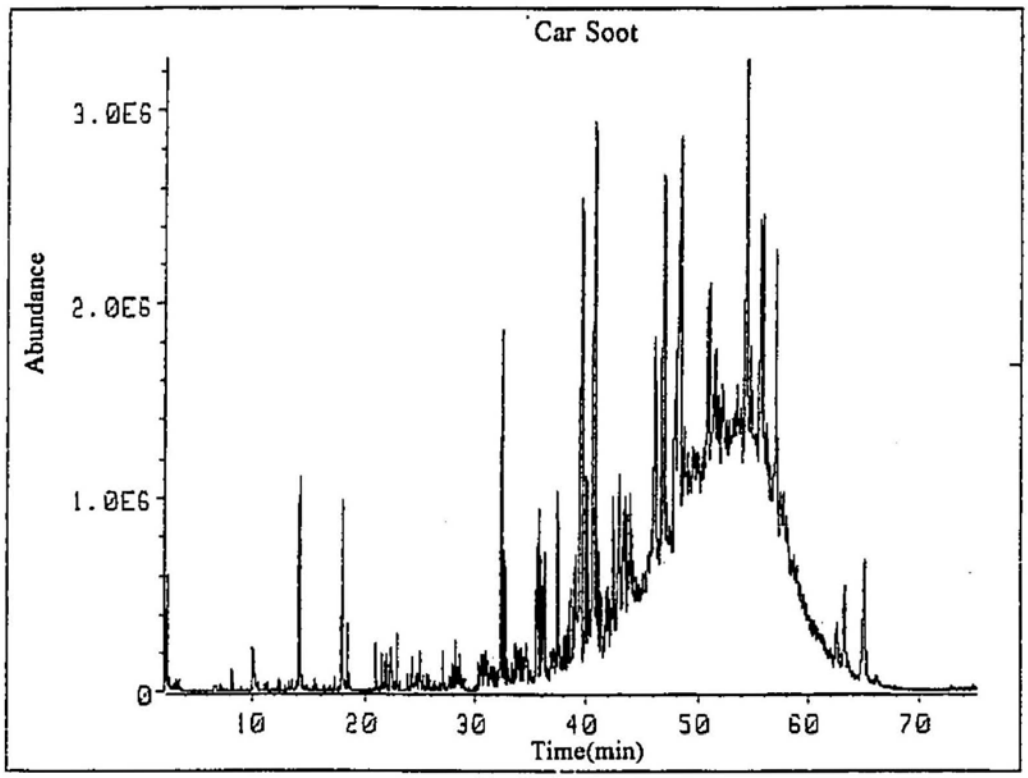
Car Soot
Abundance
3.0E6
2.0E6
1.0E6
0
10
20
30
40
50
60
70
Time(min)

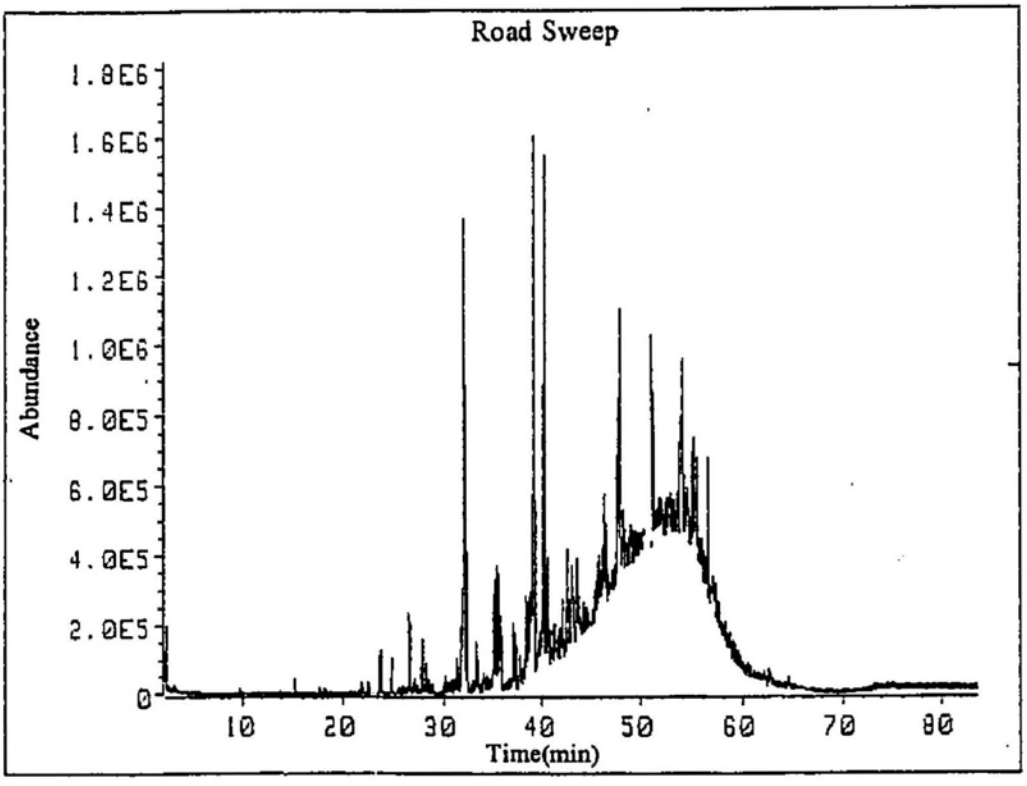
Road Sweep
Abundance
1.8E6
1.6E6
1.4E6
1.2E6
1.0E6
8.0E5
6.0E5
4.0E5
2.0E5
0
10
20
30
40
50
60
70
80
Time(min)

Appendix F3. Examples of total ion chromatograms (TIC) obtained for a St. John's Harbour and Conception Bay sediment.

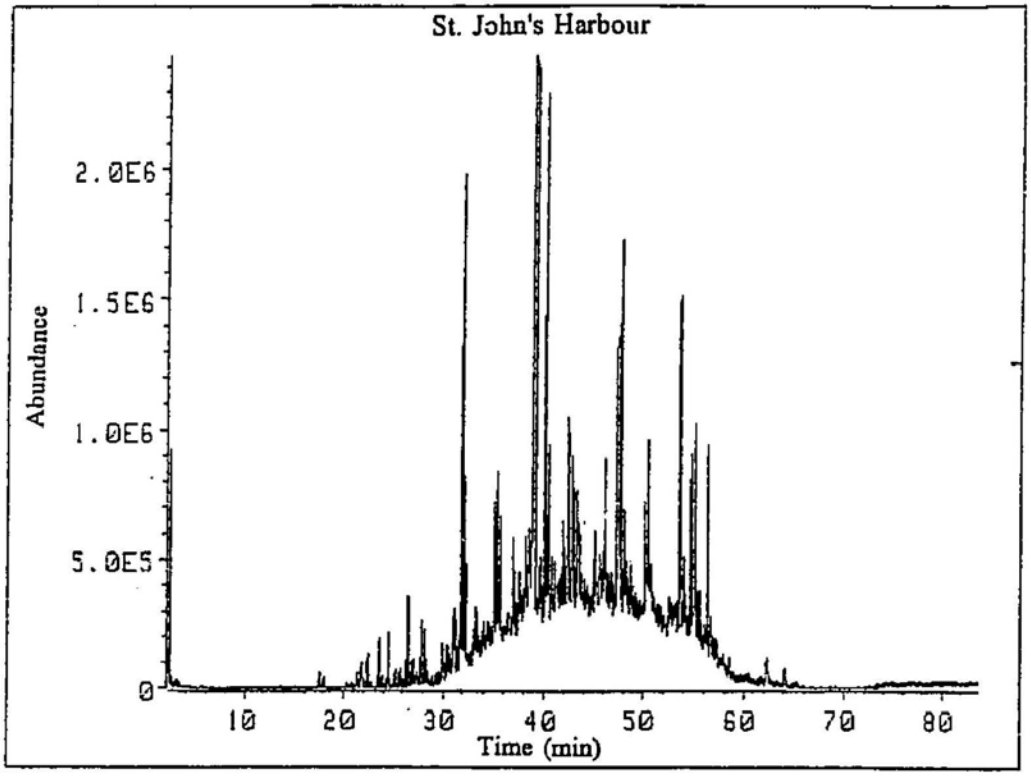
St. John's Harbour
Abundance
2.0E6
1.5E6
1.0E6
5.0E5
0
10
20
30
40
50
60
70
80
Time (min)

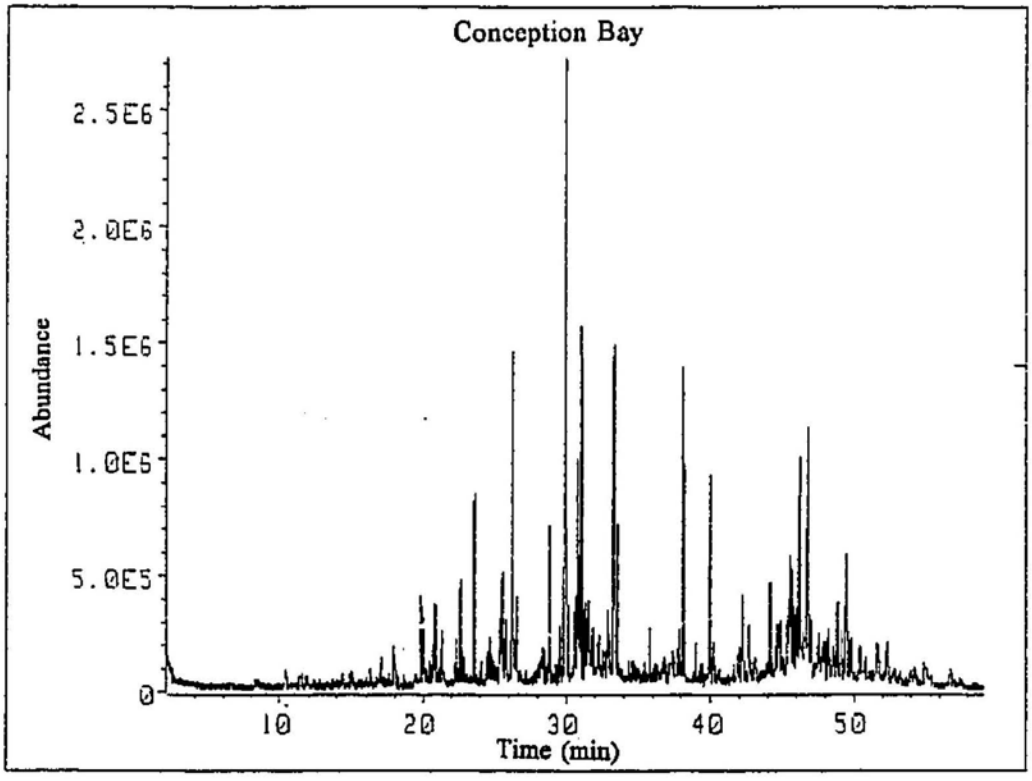
Conception Bay
Abundance
2.5E6
2.0E6
1.5E6
1.0E6
5.0E5
0
10
20
30
40
50
Time (min)

Appendix G. Location of fire soot, roadsweep and snow samples

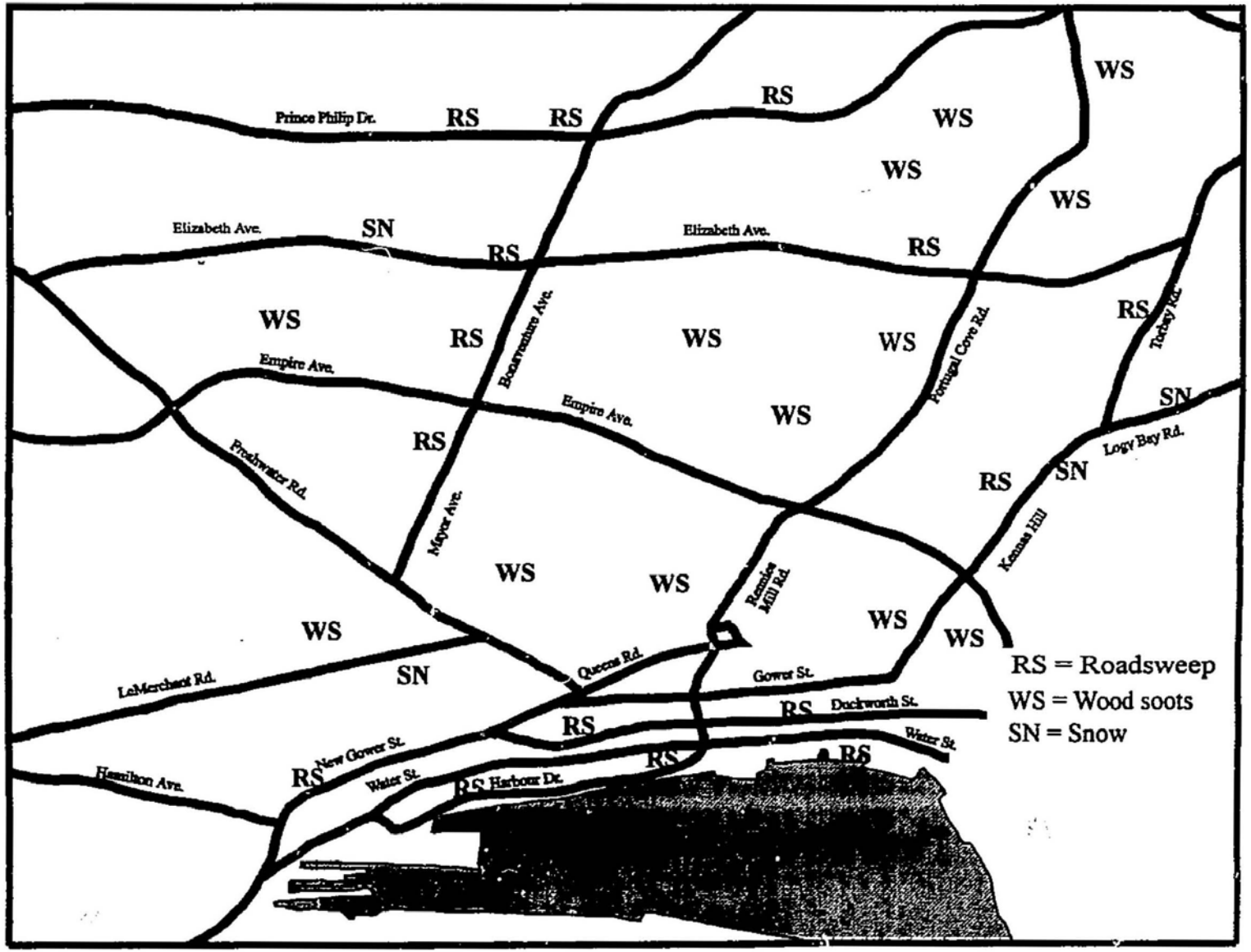

Appendix H. Laboratory experiments and samples collected